OPTIMIZING THE OUTCOMES OF RIDE-HAILING PLATFORMS: UNRESOLVED CHALLENGES AND NEW INSIGHTS

SONIA BAGHERIRAD

A DISSERTATION SUBMITTED TO THE FACULTY OF GRADUATE STUDIES IN PARTIAL FULFILLMENT OF THE REQUIREMENTS FOR THE DEGREE OF DOCTOR OF PHILOSOPHY

GRADUATE PROGRAM IN ADMINISTRATION
YORK UNIVERSITY
TORONTO, ONTARIO

APRIL 2025

Abstract

This dissertation focuses on ride-hailing platforms such as Didi, Grab, Lyft, and Uber, innovative on-demand online services that quickly match riders with drivers. Specifically, it investigates how platforms optimize their outcomes under varying internal policies and environmental factors while considering stakeholder behavior. The research is divided into two studies.

Chapter 2 reviews 89 publications published in operations and supply chain management journals about challenges that ride-hailing platforms face in day-to-day operations. An organizational framework is presented to synthesize the central research questions addressed in the existing literature, with these central research questions generally focusing on the impact that interactions among stakeholders and environmental factors have on ride-hailing platform outcomes, rider experience, and driver welfare. The organizational framework classifies the 89 publications into five main themes and identifies future research directions. One important research direction is the need for more research into mechanisms (e.g., information sharing) that encourage desired driver behavior, particularly their relocation decisions across zones to balance supply and demand.

Chapter 3 investigates how sharing information about the proportions of ride requests, drivers, and average ride distances between zones affects (i) regret-averse drivers' decisions to relocate and (ii) matching efficiency and the platform's profitability. Of particular interest is whether information sharing can substitute for monetary compensation, the extent of this effect, and the conditions under which different information is most effective. Using a two-period Stackelberg game, we compare various information-sharing strategies against a baseline model that only shares surge multipliers, with the objective of either maximizing the platform's profit or supply-demand matching efficiency. Our findings affirm that surge pricing is beneficial when there is an imbalance between supply (i.e., idle drivers) and demand (i.e., ride requests). Importantly, information can generally serve as a substitute for financial incentives, with its effectiveness depending on the degree of imbalance between idle drivers and ride requests and shared information. Higher relocation costs, moreover, can further amplify the benefit of sharing more information.

Acknowledgements

This dissertation represents a significant milestone in my Ph.D. journey and provides a wonderful opportunity to express my heartfelt gratitude. It is truly extraordinary that I have had the support, care, and encouragement of so many incredible people who have been instrumental in this achievement. This work would not have been possible without their unwavering support.

I sincerely thank my main supervisor, Professor Moren Lévesque, for her unwavering support throughout this journey. Her diligence, invaluable feedback, and insightful guidance, combined with her discipline and full support, have been instrumental in my success. I also extend my deepest gratitude to Professor M. Johnny Rungtusanatham, my former co-supervisor. I learned so much from him, both academically and in life. His patience, passion, and full support were truly remarkable and played a pivotal role in helping me find my direction during my Ph.D. pursuit. I am profoundly grateful to Professor Adam Diamant, my committee member, for his exceptional hands-on support and insightful feedback, which greatly enhanced the quality of my dissertation research results. His mentorship was pivotal in shaping my academic foundation, and his encouragement helped me get through the toughest days and guided me to keep moving forward. I also extend my heartfelt thanks to Professor Divinus Oppong-Tawiah for being a member of my committee. It has been a great pleasure to work with and learn from him. Last but not least, I am also grateful to Professor David A. Johnston for his role as my co-supervisor and for his support and encouragement throughout this process.

My family, my parents and siblings—Sima, Sara, and Saeid—stood by me during my Ph.D. journey. I am grateful for their endless love and encouragement. I am deeply appreciative of my best friends, Elnaz Asadi and Nudrat Mahmood, whose encouragement has also been a source of strength, as well as Ting Cao and Ortac Onder, whose Ph.D. journey overlapped with mine.

Lastly, I thank my husband, Saeed, who made it all possible. I am forever indebted to him for his patience, love, and steadfast support.

Table of Contents

List of Tables

List of Figures

Chapter 1

Introduction

Over the past decade, ride-hailing has emerged as a global trend (e.g., Afeche et al., 2023), with many individuals opting for it over conventional taxi services. Typically, ride-hailing platforms (e.g., Lyft and Uber) utilize GPS tracking to connect potential riders with drivers via mobile applications (or apps). These apps allow users to book rides in real time, track their drivers, and manage payments within the app's interface.

Ride-hailing services have grown significantly over the past decade, driven by several factors, including increased smartphone penetration, advancements in mobile technology, which provide a more seamless and user-friendly experience, and changing consumer preferences. The global ride-hailing market is expected to grow 11.45% from USD 53.02 billion in 2025 to USD 91.16 billion by 2030 (Mordor Intelligence Research & Advisory, 2025). Between September 2023 and 2024, Uber, for example, grew active platform users to an average of 161 million monthly, a 13.38% increase. During the same period, Uber grew its driver and courier pool by 14.7% from 6.9 to 7.8 million. The 7.8 million drivers and couriers facilitated 2.87 billion trips as of September 2024, while collectively earning $18 billion.[1]

Ride-hailing platforms offer several benefits, including promoting sustainable transport (e.g., Yu et al., 2019), reducing the number of single-occupancy vehicles (e.g., Arora et al., 2024), meeting ride requests in real time quickly and at a reasonable cost (e.g., Cachon et al., 2017), and alleviating traffic congestion (e.g., Naumov and Keith, 2023). Despite these advantages and significant growth in recent years, ride-hailing platforms face various challenges in optimizing their service and ensuring successful implementation (c.f., Benjaafar et al., 2022). One prominent and ongoing challenge for ride-hailing platforms is the efficiency of matching supply (i.e., drivers) to demand (i.e., ride requests) dynamically across geographical regions (i.e., zones).

This dissertation comprises two essays that contribute to the literature on ride-hailing platforms. The overarching question underlying both essays is the following: *How do ride-hailing platforms optimize their outcomes (e.g., services and profitability) under different internal policies*

[1] Uber statistics from https://backlinko.com/uber-users.

and environmental factors while considering stakeholders' behavioral factors? This overarching question encompasses several research questions that have garnered much research attention since 2016. Bai et al. (2019), for example, asked how ride-hailing platforms should set pricing for riders and wages for drivers when riders are price-sensitive and drivers are earnings-sensitive.

Although research on ride-hailing platforms has been reviewed as a subset of the sharing economy in some review articles (e.g., Hawlitschek et al., 2018; Wang and Yang, 2019; Tirachini, 2020; Tafreshian et al., 2020), a comprehensive and systematic review from the operations and supply chain management (OSCM) domain is missing. Chapter 2 addresses this gap and reviews the literature on ride-hailing platforms by focusing on research published in OSCM journals pertaining to the challenges ride-hailing platforms face regarding day-to-day operations. A primary focus of research on ride-hailing platforms in OSCM regards the impact that interactions among stakeholders and environmental factors have on ride-hailing platform outcomes (e.g., profit and service level maximization), riders (e.g., delay minimization), and/or drivers (e.g., labor welfare). Chapter 2 analyzes 89 relevant publications and develops an overarching framework to synthesize the five prevalent themes reflected in OSCM research on ride-hailing platforms, namely (i) ride-hailing platform's decisions affecting platform, rider, and driver outcomes; (ii) demand-side and supply-side behaviors affecting ride-hailing platform's decisions and stakeholder outcomes; (iii) ride-hailing platform's decisions affecting driver and/or rider behavior and stakeholder outcomes; (iv) environmental factors affecting ride-hailing platform's decisions and stakeholder outcomes; and (v) economic, environmental, and social impacts of ride-hailing platforms. These five themes highlight five future research directions for OSCM scholars to consider, including (i) interactions among mechanisms for desired driver behavior, (ii) competition for riders and drivers, (iii) ride-hailing collaboration with other ride-hailing platforms or car-rental companies, (iv) regulatory agencies as stakeholders, and (v) sharing untruthful information.

Chapter 3 focuses on how ride-hailing platforms can efficiently match supply (i.e., drivers) to demand (i.e., ride requests) dynamically across geographical regions (i.e., zones). Supply-demand matching in this context is challenging because drivers in the ride-hailing sector typically operate as independent contractors with flexible schedules, deciding where and when to work. Specifically, Chapter 3 asks the following related research questions: *What is the impact on drivers' relocation decisions and the platform's profitability from sharing information about (i) the demand-to-supply* *ratio in the non-surge zone, (ii) the ratio of the average ride distance for the surge zone to the average ride distance for the non-surge zone, and (iii) the proportion of drivers initially located in the non-surge zone? Which pieces of information should a platform share with drivers to encourage an adequate number of drivers to relocate to surge zones under different parameter regimes? Under what conditions can sharing of information substitute for offering of financial incentives (i.e., surge pricing) to impact drivers' relocation decisions and the platform's profitability?* Chapter 3 develops a two-stage Stackelberg game to optimize supply-demand matching efficiency and profitability for ride-hailing platforms. The platform determines the optimal surge multiplier to offer and selects specific pieces of information to share with drivers. Chapter 3 determines how information sharing, in addition to surge pricing, influences drivers' relocation decisions, as well as conditions under which surge pricing can be substituted with information sharing. The latter research findings enable ride-hailing platforms to lower their operational costs while enhancing supply-demand matching efficiency. These analytically derived research findings complement prior scholarly work on supply-demand matching via drivers' relocation decisions (e.g., Guda and Subramanian, 2019; Hu et al., 2022; Jiang et al., 2021).

Chapter 4 has a threefold objective. First, it provides a summary overview of this dissertation. Second, it discusses the contributions of the findings presented in Chapters 2 and 3. Finally, it highlights future research opportunities from Chapters 2 and 3.

Chapter 2

Ride-Hailing Platform Research in Operations and Supply Chain Management: A Review and Future Directions

Abstract

Ride-hailing platforms, innovative on-demand online services that quickly match riders with drivers, aim to provide sustainable transportation solutions and alleviate congestion. These platforms have experienced exponential growth in recent years and have significantly impacted the global economy. To explore the key aspects of this industry, we present an organizational framework that synthesizes the central research questions in the existing literature, classifies the body of work into five main themes, and identifies key directions for future research.

Keywords: Sharing economy; Ride-hailing; Operations management; Online platforms

2.1. Introduction

Ride-hailing, a prominent aspect of the sharing economy, involves a transportation mode where a ride-hailing platform promptly connects riders with available drivers. Uber, Lyft, and DiDi are among the key players in this industry. These ride-hailing platforms offer drivers the advantages of flexible, self-scheduled work while providing riders with rapid and adaptable travel options. Drivers in the ride-hailing sector typically operate as independent contractors with flexible schedules. Scholarly interest in ride-hailing platforms has markedly increased since 2014. The ride-hailing industry commands attention not only in academic research but also in practical implementation. In 2024, the global ride-hailing market was valued at USD 165.6 billion and is projected to grow to USD 190.1 billion by 2026, with an estimated value of approximately USD 216 billion by 2028 (Statista, 2025).

Research on ride-hailing platforms spans multiple disciplines, with publications in operations and supply chain management (e.g., Feng et al., 2021), economics (e.g., Angrist et al., 2021), and transportation (e.g., Haferkamp et al., 2024) journals. In reviewing the relevant literature on ride-hailing platforms, this chapter focuses on research published in operations and supply chain management journals pertaining to the challenges ride-hailing platforms face regarding day-to-day operations. Indeed, a significant portion of research on both ride-hailing platforms and the broader sharing economy focuses on operational challenges (Tafreshian et al., 2020). These operational challenges require ride-hailing platforms to make decisions to impact supply-side (i.e., driver) and demand-side (i.e., rider) behavioral factors, while considering constraints imposed on the industry from regulatory mechanisms and from competition among ride-hailing platforms or with the taxi industry.

Section 2.2 explains the identification and selection of articles to be reviewed, as well as how selected articles are reviewed. Section 2.3 presents an overarching framework about research on ride-hailing platforms published in operations and supply chain management journals that subsumes five main themes. Section 2.4 identifies and discusses five future research opportunities before concluding in Section 2.5.

2.2. Identifying, Selecting, and Reviewing Relevant Articles

2.2.1. Identifying Relevant Articles

Relevant articles are identified following three steps.

Step 1 - Primary studies: I searched for review articles in Google Scholar using the terms "ride-hailing," "ride-sharing," and "sharing economy." This search yielded nine review articles: Hawlitschek et al. (2018): 936 citations; Sutherland and Jarrahi (2018): 824 citations; Wang and Yang (2019): 473 citations; Tirachini (2020): 409 citations; Benjaafar and Hu (2020): 280 citations; Chen et al. (2020): 219 citations; Tafreshian et al. (2020): 108 citations; Klarin and Suseno (2021): 97 citations; and Rojanakit et al. (2022): 92 citations. Of the nine, the five with the highest number of citations were selected for a thorough review. This helped to identify relevant keywords related to research on ride-hailing platforms.

Step 2 - Keyword identification: I identified keywords to be used in searching for relevant articles. These included "ride-sharing," "ridesharing," "ride sharing," "ride-hailing," "ride hailing," "ride share," "rideshare," "ride-sourcing," "ride sourcing," "ride pooling," "ride-pooling," "ride matching," "ride-matching," "sharing economy," "flexible driver," "peer-to-peer," "peer to peer," and the names of the most prominent ride-hailing platforms, such as "Uber," "Lyft," and "Didi." "Car-pooling," "car pooling," "carpooling," "car pool," "car-pool," "car-sharing," "car sharing," and "carsharing," which refer to short-term auto-sharing, were excluded.

Step 3 - Search databases: I searched the Web of Science Core Collection using the keywords from Step 2. The search spanned the last 15 years from the inception of the ride-hailing industry initiated by Uber in 2009 up until 2024. The search found 6772 articles whose titles, abstracts, and/or keywords contained the specified search terms. Excluding non-English articles, conference papers, theses, and dissertations yielded a total of 4150 journal articles.

2.2.2. Selecting and Coding Relevant Articles

Research into ride-hailing emerged around 2011. Amey et al. (2011), for example, compared it with the taxi industry and delineated potential benefits and obstacles. Agatz et al. (2011), another example, focused on the scheduling and routing problem in these services. Research interest in ride-hailing within operations and supply chain management appeared later, around 2016, primarily through conference papers (e.g., Chen and Sheldon, 2016). To select relevant papers to review, the following selection criteria shown in Table 2-1 were applied:

Table 2-1. Criteria for paper selection

Selection Criterion	Reason for Criterion	Number of Articles
Being published after 2016	Research on ride-hailing platforms by operations and supply chain management disciplinary scholars can be traced back to 2016 and not before	4102
Being published in journals in the Web of Science (WOS) categories "Management", "Operations Research Management Science", "Transportation", "Business", "Engineering Manufacturing" and "Engineering Industrial"	These Using WOS categories include journals likely to publish research relevant to operations and supply chain management	198
Being published in peer-reviewed journals and/or the journals ranked A in on the Australian Business Deans Council (ABDC) list	Journals ranked A are likely to have greater requirements for research rigor	134
Being relevant to ride-hailing platforms	Research not about ride-hailing platforms, their operational challenges or decisions, and the impact of these challenges and decisions are not relevant	89

Table 2-2 shows the distribution of the 89 journal articles for review.

Table 2-2. Distribution of reviewed papers

Journal	2017	2018	2019	2020	2021	2022	2023	2024	Total
Management Science	0	0	1	1	3	4	2	0	11
Manufacturing & Service Operations Management	1	1	1	0	3	5	6	1	18
European Journal of Operational Research	0	0	1	2	2	0	1	1	7
Journal of Business Research	0	0	0	0	0	1	1	0	2
Transportation Science	0	0	1	0	1	3	1	2	8
International Journal of Production Economics	0	0	2	0	1	2	2	1	8
Production and Operations Management	0	0	0	0	2	3	2	1	8
Operations Research	0	0	2	0	0	3	1	2	8
Omega	0	0	0	0	3	0	0	2	5
Journal of the Operational Research Society	0	0	1	0	0	0	0	1	2
International Journal of Production Research	0	0	0	0	0	1	0	0	1
IEEE Transactions on Engineering Management	0	0	0	0	1	1	1	0	3
Journal of Operations Management	0	0	0	0	0	0	3	0	3
Decision Sciences	0	0	0	1	0	0	2	0	3
International Journal of Operations & Production Management	0	0	0	1	0	0	1	0	2
Total	1	1	9	5	16	23	23	11	89

The 89 articles were subsequently evaluated and coded for the following information: year of publication, journal name, research question(s), primary methodological approach (i.e., analytical, empirical, or hybrid), name of methodology used, and main insights. Appendix A in this chapter summarizes the coded information by article in order of year of publication.

2.3. Organization of Relevant Research

The 89 articles that were reviewed can be organized as shown in Figure 2-1. Ride-hailing platforms typically involve three stakeholders: the platform itself, riders (i.e., the demand side), and drivers (i.e., the supply side). A primary focus of research on ride-hailing platforms in operations and supply chain management regards the impact that interactions among stakeholders and environmental factors have on ride-hailing platform outcomes (e.g., profit and service level maximization), riders (e.g., delay minimization), and/or drivers (e.g., labor welfare). This focus can be divided into five relevant themes, denoted by combinations of the arrows shown in the legend at the bottom of Figure 2-1.

Figure 2-1. Research on Ride-Hailing Platforms

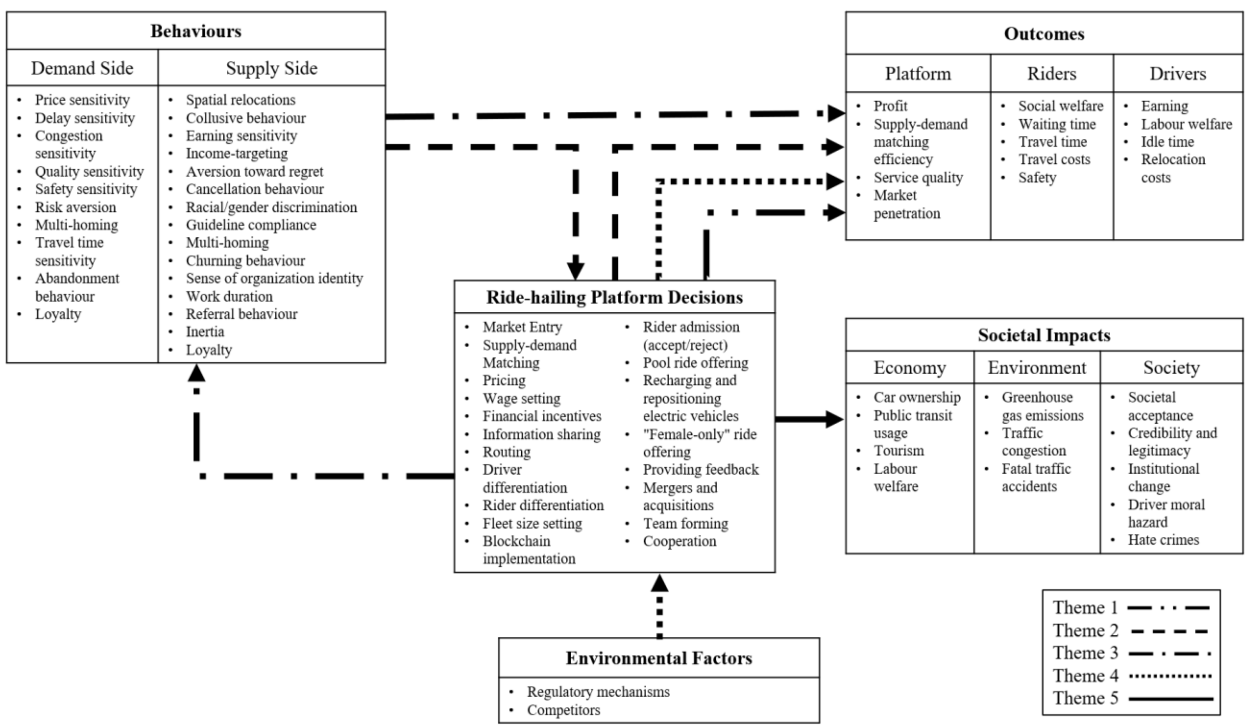

- *Theme 1: Ride-hailing platform's decisions affecting platform, rider, and driver outcomes*: This theme investigates the influences of ride-hailing platforms' decisions on achieving optimal outcomes for different stakeholders. These decisions, in this context, include pricing strategies for riders (Lee et al., 2023), wage setting for drivers (Zhong et al., 2019), incentive mechanisms for encouraging desirable behaviors (Garg and Nazerzadeh, 2022), and pool ride offering (Jacob and Roet-Green, 2021). A substantive subset within this research focuses on developing algorithms to support the ride-hailing platform's decision to optimize supply-demand matching (Afeche et al., 2023; Besbes et al., 2022).
- *Theme 2: Demand-side and supply-side behaviors affecting ride-hailing platform's decisions and stakeholder outcomes*: This theme examines the interactions between the platform, riders, and drivers, including research on the impact of demand-side behaviors (e.g., price sensitivity, delay sensitivity, safety sensitivity, and multi-homing behaviors) and/or supply-side behaviors (e.g., spatial relocations, cancellation tendencies, earnings sensitivity, and collusive behavior) on the platforms' decision-making processes (e.g., setting prices for riders and financial incentives for drivers).
- *Theme 3: Ride-hailing platform's decisions affecting driver and/or rider behavior and stakeholder outcomes*: This theme examines the impact of ride-hailing platform's decisions on demand-side and/or supply-side behaviors. Also relevant are investigations into the outcomes for ride-hailing platforms, riders, and/or drivers (Allon et al., 2023; Guda and Subramanian, 2019).
- *Theme 4: Environmental factors affecting ride-hailing platform's decisions and stakeholder outcomes*: This theme corresponds to research on the influence of external environmental factors (e.g., regulatory mechanisms and competition with public transportation or the taxi industry) on ride-hailing platform's decisions. These decisions—related to pricing, financial incentives, and fleet size—subsequently affect outcomes for stakeholders within the ride-hailing ecosystem (Nie et al., 2024; Zhang et al., 2023).
- *Theme 5: Economic, environmental, and social impacts of ride-hailing platforms*: This theme is distinct in that the research focus is on the broader impact of the emergence or existence of the ride-hailing industry on the economy, environment, and society at large (Liu et al., 2021; Barrios et al., 2023).

The sections below provide greater details for each of the five themes.

2.3.1. Theme 1: Ride-Hailing Platform's Decisions Affecting Platform, Rider, and Driver Outcomes

The central question for Theme 1 is *how ride-hailing platform's decisions influence the outcomes for the platform, riders, and drivers*. This multifaceted topic has been addressed by various seminal studies, including Cachon et al. (2017), Bimpikis et al. (2019), Guan et al. (2022), and Zhang et al. (2023). Table 2-3 summarizes the internal decisions made by ride-hailing platforms that affect stakeholder outcomes, such as ride-hailing platform's profits, labor welfare, rider surplus, and service quality. As shown in Table 2-3, two primary ride-hailing platform's decisions frequently discussed in this context are pricing and the matching of supply and demand. Al-Kanj et al. (2020), Özkan (2020), and Wang et al. (2023) examine both decisions simultaneously.

Table 2-3. Theme 1: Ride-Hailing Platform's Decisions Affecting Platform, Rider, and Driver Outcomes

Study	Ride-Hailing Platform's Decisions												
	Matching	Pricing	Wage setting	Financial incentives	Information sharing	Routing	Driver differentiation	Rider differentiation	Fleet size setting	Cooperation	Rider admission (accept/reject)	Pool ride offering	Recharging and repositioning EVs
Cachon et al. (2017)		✓	✓	✓									
Agussurja et al. (2019)	✓												
Bimpikis et al. (2019)		✓		✓									
Braverman et al. (2019)	✓					✓							
Lin & Zhou (2019)		✓	✓	✓									
Sun et al. (2019)	✓	✓											
Al-Kanj et al. (2020)	✓	✓		✓					✓				
Özkan (2020)	✓	✓											
Wang & Wu (2020)	✓												
Chakravarty (2021)			✓	✓									
Feng et al. (2021)	✓												
Guo et al. (2021)	✓					✓							
Jacob & Roet-Green (2021)		✓	✓									✓	
Lin et al. (2021)		✓	✓							✓			
Xu et al. (2021)	✓					✓							
Yu et al. (2021)	✓												✓
Besbes et al. (2022)	✓												
Beirigo et al. (2022)	✓					✓							
Chen et al. (2022b)		✓	✓	✓									
Garg & Nazerzadeh (2022)		✓	✓	✓									
Guan et al. (2022)	✓					✓							

Hu et al. (2022)	✓			✓	✓								
Hu & Zhou (2022)	✓												
Kullman et al. (2022)	✓												✓
Ma et al. (2022)		✓		✓									
Pavone et al. (2022)	✓												
Afeche et al. (2023)	✓												
De Munck et al. (2023)								✓			✓		
Lee et al. (2023)		✓		✓									
Wang et al. (2023)	✓	✓				✓							
Zhang et al. (2023)	✓					✓							
Chen et al. (2024)		✓		✓									
Krishnaprasad (2024)			✓				✓						
Lyu et al. (2024)	✓												
Wang et al. (2024a)	✓												

2.3.1.1. Price Setting Strategies

Price setting strategies for riders constitute a significant portion of research within this theme, with various methods employed to address the issue, including game theory (e.g., Ma et al., 2022), dynamic programming (e.g., Garg and Nazerzadeh, 2022), queuing models (e.g., Jacob and Roet-Green, 2021), and econometric modeling (e.g., Lee et al., 2023). Several studies focus on comparing different pricing strategies. For instance, Lin and Zhou (2019) conduct a comparative analysis of static pricing, dynamic pricing, and surge pricing, yielding notable findings: (a) static pricing is optimal when the number of riders during high-demand periods is relatively low; (b) surge pricing does not consistently outperform dynamic pricing; and (c) while dynamic pricing significantly enhances ride-hailing platform's profits, surge pricing approaches dynamic pricing in profitability when the ride-hailing platform effectively manages diverse driver types or reduces its commission rate. Chen et al. (2022b) also compare static and surge pricing, showing that surge pricing becomes more profitable with a larger number of potential participants during non-peak periods, whereas riders benefit more from static pricing when the commission rate and a drivers compensation ratio are either sufficiently low or high across both models.

Several studies concentrate specifically on surge pricing and its impact on stakeholder outcomes. Bimpikis et al. (2019) examine the relationship between demand patterns and surge pricing on ride-hailing platforms, along with its effect on profitability and rider surplus. Using an equilibrium model, their research reveals two key insights: first, optimal profits for the platform and aggregate rider surplus are achieved when demand is evenly distributed across the network's locations; second, surge pricing significantly benefits the ride-hailing platform when demand is unevenly distributed, emphasizing the importance of understanding demand dynamics for effective pricing strategies. Ma et al. (2022) propose a spatial-temporal pricing (STP) strategy that aligns incentives, ensuring subgame-perfect equilibrium by guaranteeing drivers consistently accept ride assignments. They demonstrate that, regardless of historical context, the STP strategy yields outcomes that are welfare-optimal, envy-free, individually rational, budget-balanced, and core-selective. Lee et al. (2023) explore the interaction between surge pricing and capacity decisions across space and time within a two-sided ride-hailing platform framework. Their empirical analysis of surge pricing considers the proximal capacity effect—the impact of driver availability in neighboring zones on pricing in a focal zone—and the proximal pricing effect—the influence of prices in neighboring zones on pricing in the focal zone. By examining data from Uber's San Francisco region, they show the significant and simultaneous influence of both effects on surge pricing estimates, particularly during periods of high demand. Moreover, their study highlights the importance of spatial proximity in shaping price distributions under conditions of heightened service demand.

Garg and Nazerzadeh (2022) compare two prominent pricing strategies: additive pricing and multiplicative pricing. In a single-state setting where ride requests arrive according to a Poisson process, they established that multiplicative pricing is incentive-compatible. They then examine a dynamic setting in which the market zone state stochastically transitions over time between surge and non-surge conditions, characterized by varying trip payments, demand distributions, and intensities. In this dynamic context, they find that additive pricing is incentive-compatible. Using real data from a ride-hailing platform, they numerically demonstrate that additive pricing is more compatible with incentives in practice than multiplicative pricing. Chen et al. (2024) also introduce a framework for evaluating both static and dynamic pricing strategies to maximize a ride-hailing platform’s cumulative expected profit in a nonstationary environment. They consider a setting where a firm operates with a fixed number of drivers—similar to traditional taxi companies—while facing demand fluctuations over time and across regions, as well as deterministic travel times between locations. Pricing decisions not only influence immediate ride demand between origin-destination pairs but also shape the future distribution of available drivers, as vehicles become free to serve new requests only after completing trips. Consequently, supply availability is temporally and spatially correlated, making the design of an effective dynamic pricing strategy complex. They develop a set of near-optimal heuristic strategies for dynamic pricing and demonstrate, through numerical analysis, that dynamic pricing not only increases the platform's revenue but also enhances service levels by accommodating a greater number of riders compared to static pricing approaches.

Besides pricing, several studies investigate wage or contract settings for drivers. For example, Cachon et al. (2017) explore the complex dynamics of adjusting prices and wages in response to demand fluctuations on ride-hailing platforms. Their research addresses the conditions under which different contractual strategies—such as fixed contracts, dynamic price contracts, dynamic wage contracts, commission contracts, and optimal contracts—can be implemented. Their study produce several key insights: (a) optimal contracts substantially increase ride-hailing platform's profits compared to fixed price or wage contracts; (b) surge pricing, while not always optimal, often achieves near-optimal profits; (c) when drivers become more expensive, surge pricing benefits both drivers and riders, improving driver utilization and providing riders with lower prices during periods of normal demand and increased service availability during peak times; and (d) contrary to common criticisms, all stakeholders can benefit from the prudent use of surge pricing on ride-hailing platforms with self-scheduling drivers.

Chakravarty (2021) explores the feasibility of ride-hailing platforms adopting a blended capacity model that combines full-time drivers on fixed wages with independent drivers compensated through revenue sharing. The study examined whether such a model could be sustainable. Chakravarty concludes that a blended capacity ride-hailing platform can thrive under conditions of high demand, a substantial pool of independent drivers, and moderate wage rates for full-time drivers. This research highlights the potential viability of innovative operational models within the ride-hailing industry. Similarly, Krishnaprasad (2024) studies ride-hailing platforms operating with dual capacities, consisting of full-time drivers and self-schedulers, and analyzed a non-discriminatory preferential policy to prioritize drivers. They investigate two policies: a contingency capacity policy, where self-schedulers receive higher priority in demand allocation, and a common-pool policy, where equal preference is given to both types of drivers. Their findings suggest that the contingency capacity policy can deliver optimal profits for ride-hailing platforms with a smaller full-time workforce.

Research has also examined pricing strategies alongside other ride-hailing platform's strategies (e.g., ride pooling, rental car cooperation). For example, Jacob and Roet-Green (2021) investigate the complexities associated with pooled rides, highlighting the challenges they present for both ride-hailing platforms—such as reduced profit margins per rider—and for riders, including extended travel times, despite the potential benefits they offer. They analyze how the availability of both pooled and solo ride options influences ride-hailing platform pricing strategies. Their findings reveal that the ride-hailing platform benefits from offering both solo and pooled rides when there is a balanced distribution of rider types across low and high-demand segments. However, under conditions of high congestion, the ride-hailing platform's optimal strategy may involve offering either solo or pooled rides exclusively, rather than both options simultaneously.

Lin et al. (2021) examine the problem of cooperation with car-rental companies in conjunction with pricing strategies. They explore the complex balance that ride-hailing platforms must manage as they increase cooperation with car rental companies to expand their driver pool and meet rising demand. However, this collaboration can introduce inefficiencies in supply-demand matching, potentially affecting rider and driver welfare by increasing wait times and driver idle periods. To assess this trade-off, the authors evaluate the impact of partnerships with car rental companies on ride-hailing platform's profitability and rider and driver welfare. Their findings highlight the nuanced dynamics at play: while collaboration with rental car companies can benefit the ride-hailing platform, the resulting profit and pricing dynamics do not necessarily rise in tandem with the influx of potential drivers, or the commission paid by rental car companies to the ride-hailing platform. Additionally, they demonstrate that a win-win-win outcome—benefiting the ride-hailing platform, riders, and drivers—can be achieved under specific conditions. This outcome is most attainable when the ride-hailing platform either imposes a high commission rate or adopts a low fixed payout ratio for drivers. Such conditions are favorable when the rider pool size or delay cost is significant, while the driver pool size or service rate remains modest.

2.3.1.2. Supply-Demand Matching

Another issue of substantive interest within is the ride-hailing platform's decision-making process regarding supply-demand matching. Researchers have employed various methodologies, such as the Markov decision process (Agussurja et al., 2019), fluid models (Özkan, 2020), game theory (Afeche et al., 2023), dynamic programming (Al-Kanj et al., 2020), queuing theory (Feng et al., 2021), and mixed-integer optimization (Lyu et al., 2024) to propose algorithms aimed at optimizing supply-demand matching. For example, Agussurja et al. (2019) develop a value-iteration-based approximation algorithm to identify the optimal multiperiod vehicle dispatching strategy. In this approach, the ride-hailing platform determines which subsets of demand to satisfy in the current period, considering both standby demand and uncertain future demand. When applied to a real-world public transport dataset from Singapore, their method demonstrates improved convergence and enhanced solution quality as the sample size increases. Notably, the method yields optimal results in scenarios characterized by higher distributional variability and larger planning regions. Hu and Zhou (2022) focus on formulating an optimal supply-demand matching policy to maximize the expected total discounted rewards, taking into account the carryover of unmatched demand and supply to subsequent periods. Their study establishes a priority hierarchy among potential matching pairs, with the optimal policy, determined by matching rewards and subject to specified conditions, operating efficiently down to a threshold when matching specific pairs. Pavone et al. (2022) investigate the driver-rider matching problem using hypergraphs, with both utility maximization and cost minimization objectives. They present a polynomial-time algorithm and prove that it achieves the optimal competitive ratio among deterministic algorithms.

Several studies within this stream focus on minimizing waiting times for riders. Wang and Wu (2020) address this issue by developing a data-driven system based on the Rolling Time Horizon approach, typically applied in modeling time-series problems, to tackle the driver-rider matching problem. More specifically, in the Rolling Time Horizon approach, the system redistributes driver resources by solving an off-line optimization problem in each iteration that seeks to fulfill the maximum number of both current and anticipated future ride requests. To achieve this, the off-line problem incorporates parameters derived from historical data, specifically the spatiotemporal patterns of future demand. Their results show that the proposed system significantly reduces average waiting times and improves planning efficiency as compared to the traditional request-driven dispatching method. Feng et al. (2021) extend the discussion by comparing two distinct rider-driver matching systems: an on-demand system where the ride-hailing platform coordinates driver-rider matches and a street-hailing system where drivers pick up the first rider they encounter. Their study aims to evaluate efficiency gains provided by ride-hailing platforms and to assess whether these ride-hailing platforms reduce rider waiting times as compared to traditional street-hailing mechanisms. The authors conclude that the efficiency of each approach is context-dependent. Specifically, the on-demand system proves more effective in reducing rider waiting times under conditions of low or high traffic intensity, whereas the traditional street-hailing system performs better in environments characterized by moderate traffic intensity.

Besbes et al. (2022) develop a queuing model to address the driver-rider matching problem. Although the "square root safety staffing rule" from the multi-server queueing literature (Bassamboo et al., 2010) is traditionally employed to balance driver utilization and rider wait times, their findings reveal that this rule does not achieve the desired balance between driver utilization and rider wait times in ride-hailing platforms. Instead, they argue for drivers to apply a higher safety factor, proportional to the offered load raised to the power of 2/3, to better balance utilization and waiting time. In their study, Lyu et al. (2024) develop matching algorithms that can balance competing objectives within the ride-hailing domain. These objectives encompass a spectrum ranging from revenue optimization to minimizing rider waiting times, mitigating driver idle periods, and prioritizing drivers based on their service scores. The authors propose a compromise solution closest to the ideal solution that seeks to minimize the ℓ_p-norm–based distance function, effectively aligning attained performance metrics with predetermined target benchmarks. They demonstrate that riders can anticipate heightened service quality and reduced waiting times, representing a marked improvement over existing policies that are fixated solely on pick-up distance minimization while drivers.

Some studies in this stream address both routing and matching. Braverman et al. (2019) develop a fluid model to identify the optimal rider-driver matching policy by incorporating an empty-car routing mechanism. Their findings suggest that the optimal network utility derived from fluid-based optimization establishes an upper bound on the utility in systems with a finite number of cars, irrespective of whether the routing policy is static or dynamic, as long as the closed queuing network maintains a stationary distribution. Guo et al. (2021) explore effective matching and routing algorithms, as well as decision rules for dynamic timeframe segmentation. They formally define the concepts of dynamic timeframes and commuter migration, introducing an innovative model to assess matching quality. Their study proposes decision rules for segmenting timeframes and developing an anticipation-based commuter migration method using historical matching data. Additionally, they introduce a novel local search heuristic algorithm that efficiently generates near-optimal solutions within a short computational time. Xu et al. (2021) concentrate on improving matching policies by explicitly modeling vacant trips between consecutive rider deliveries using a game-theoretic model. Their experiments, utilizing data from Didi Chuxing on both the small-scale Nguyen–Dupuis network and the more realistic Friedrichshain network, demonstrate that their model can predict ride-hailing system performance and assess its impact on network traffic conditions.

Guan et al. (2022) develop a heuristic algorithm to investigate the optimal policy for ride-matching and routing, considering riders' dynamic mode choices. Their findings demonstrate how ride-matching and routing decisions influence the outcomes for ride-hailing stakeholders. The model simulates ride-hailing decision-making behavior based on cumulative prospect theory. A series of computational experiments confirm the effectiveness and efficiency of their proposed algorithm, using actual traffic data from Beijing, China. Zhang et al. (2023) develop a scalable algorithm to support dial-a-ride routing with capacitated vehicles, time windows, and vehicle–rider coordination. Their computational results show that this algorithm outperforms state-of-the-art benchmarks, delivering significantly better solutions in shorter computational times and enabling real-time operations in large-scale systems. They suggest that the primary benefits of driver-rider coordination arise from thoroughly reoptimizing “upstream” operations rather than merely adjusting “downstream” stopping locations.

Three studies investigate matching decisions alongside operational controls over supply and demand within ride-hailing platforms. Afeche et al. (2023) analyze the impact of two operational controls on drivers and ride-hailing platform’s profitability: demand-side admission control, which enables the ride-hailing platform to accept or reject ride requests based on rider pick-up and drop-off locations, and supply-side capacity repositioning, which allows the ride-hailing platform to directly manage the timing and feasibility of drivers’ relocations from lower to higher demand areas. Their findings indicate that, under certain conditions, the ride-hailing platform may benefit from rejecting demand in low-demand zones, even when those zones have excess supply, thereby incentivizing drivers to relocate to higher-demand areas. They also identify the maximum potential benefit for both the ride-hailing platform and drivers resulting from enhanced ride-hailing platform control measures. De Munck et al. (2023) examine rider admission and driver reservation policy for later arrivals of impatient riders. They find that it offers advantages for the ride-hailing platform, riders, and drivers, significantly outperforming a policy that controls both rider admission and rider reservation. Wang et al. (2024a) consider the effect of rider abandonment and cancellations, deriving an optimality condition that leads to a policy adaptable to fluctuating demand. Their results show that as the matching policy becomes more aggressive (e.g., by enlarging the matching radius to expedite matches), the number of successful matches increases, reducing idle drivers and waiting riders (and thus, fewer abandonments). However, this approach compromises match quality (measured by pickup distance), leading to a higher rate of cancellations.

Three studies within this stream focus on the integration of autonomous vehicles in ride-hailing systems. Yu et al. (2021) optimize the matching, repositioning, and recharging operations for electric autonomous vehicles (EAVs). They develop a Markov Decision Process model and generate a vehicle pooling policy to serve ride requests and maximize the profit. Their experiments, conducted using real data from Haikou city, demonstrate the superiority of their proposed policy over the commonly used the "closest distance" policy and predetermine recharging rules in terms of increasing revenue and reducing response time. They find that performance is influenced by factors such as the number of available EAVs, request arrival rates, and the number of recharging stations, with response times decreasing as fleet size and the number of recharging stations increase. Beirigo et al. (2022) explore how to efficiently match autonomous vehicles with riders. Their proposed policy outperforms a reactive optimization approach across various vehicle availability scenarios while requiring fewer vehicles. They show that mobility services can offer stringent service-level agreements to different user groups by incorporating delay and rejection penalties. Kullman et al. (2022) examine how a third-party operator controlling a fleet of electric vehicles for ride-hailing services can optimize matching, repositioning, and recharging operations. Their most effective policy, trained using deep reinforcement learning, consistently outperforms the re-optimization approach across different instance sizes and could be scaled to larger instances without the need for retraining.

2.3.1.3. Supply-Demand Matching and Price Setting

A subset of research within this theme explores matching decisions alongside price setting strategies. This stream began with Sun et al. (2019), who investigates the optimal pricing strategy under two types of driver selection: first-to-respond or closest-to-the-rider. Their game-theoretic model demonstrates that the ride-hailing platform's pricing structure should include a fare based on ride length (relative to standard taxi fares) and an additional fee for rush hour congestion, which increases with rider waiting costs. Accordingly, ride-hailing platform pricing can fall below standard taxi rates when traffic conditions are optimal, the ride-hailing platform’s commission is sufficiently low, and drivers have modest profit expectations. Al-Kanj et al. (2020) extend this problem by incorporating electric vehicles. They address the dispatch problem, including rider-vehicle allocation, recharging, repositioning, parking, surge pricing, and determining the optimal fleet size of electric vehicles. They propose an operational dispatch strategy to determine which driver to assign to a particular trip, with their proposed strategy outperforming the myopic policy that assigns drivers to riders without accounting for future consequences of these decisions by 17%.

Özkan (2020) investigates the interplay between pricing and matching decisions. By partitioning the city into disjoint areas, the study questions whether fixing matching decisions to a simple rule while optimizing pricing decisions alone suffices for optimal performance. Their analytical results indicate that joint optimization of pricing and matching decisions significantly enhances ride-hailing platform performance, underscoring the interdependence of these two elements. Hu et al. (2022) explore ride-hailing platform’s matching decisions in the context of surge pricing dynamics, with a focus on temporal considerations and information sharing. Examining the temporal complexities inherent in ride-hailing operations, their study identifies optimal surge-pricing policies while accounting for the strategic behaviors exhibited by both riders and drivers. They demonstrate that short-lived, sharp price surges tended to incentivize high-value riders to delay their trips, leading to an influx of drivers into the region to serve riders at lower prices. Wang et al. (2023) develop an exact method to solve the first-mile ride-hailing problem. The first-mile ride-hailing problem plans routes and schedules for a fleet of identical vehicles to pick up requests from geographically dispersed riders within specified time windows and transport them to a single destination before their deadlines. The proposed exact method is based on a branch-price-and-cut (BPC) algorithm, combining state-of-the-art techniques with an innovative pricing algorithm and is capable of solving a modified Solomon benchmark instances with up to 100 riders, as well as real-world instances with up to 290 riders. The proposed method helps ride-hailing platforms arrange routes to improve the utilization of vehicles, satisfy ride requests given deadlines (e.g., delivering the riders to the airport), and earn high rider satisfaction while minimizing the routing costs.

2.3.2. Theme 2: Demand-Side and Supply-Side Behaviors Affecting Ride-Hailing Platform's Decisions and Stakeholder Outcomes

The core question for Theme 2 is *what rider and driver behaviors and attributes affect ride-hailing platform's decisions and consequently stakeholder outcomes*. Noteworthy examples include Bai et al. (2019), Jiang et al. (2021), Mejia and Parker (2021), and Wang et al. (2024b). Table 2-4 summarizes research relevant to this theme, with a main focus being the impact of demand-side and supply-side behaviors on ride-hailing platform's decisions about prices, wages for drivers, and financial incentives (i.e., surge pricing and bonuses).

Table 2-4. Theme 2: Demand-Side and Supply-Side Behaviors Affecting Ride-Hailing Platform’s Decisions and Stakeholder Outcomes

Study	**Ride-Hailing Platform’s Decisions**								**Demand-Side Behaviors**								**Supply-Side Behaviors**								
	Pricing	Wage setting	Financial incentives	Information Sharing	Driver differentiation	Blockchain implementation	Pool ride offering	"Female-only" ride offering	Price sensitivity	Delay sensitivity	Congestion sensitivity	Quality sensitivity	Safety sensitivity	Risk aversion	Multi-homing	Travel time sensitivity	Spatial relocations	Collusive behavior	Earning sensitivity	Income-targeting	Aversion toward regret	Cancellation behavior	Racial and/or gender discrimination	Intension to obey the guidelines	Multi-homing
Taylor (2018)	✓	✓								✓									✓						
Bai et al. (2019)	✓	✓							✓										✓						
Zhong et al. (2019)		✓	✓																✓						✓
Bernstein et al. (2021)	✓	✓	✓						✓		✓								✓						✓
Dong & Leng (2021)	✓	✓	✓							✓					✓										
Jiang et al. (2021)			✓	✓													✓				✓				
Mejia & Parker (2021)				✓																		✓	✓		
Tang et al. (2021)								✓	✓	✓			✓						✓						
Chen et al. (2022a)	✓	✓	✓																	✓					
Cohen et al. (2022)			✓							✓						✓									
Choi & Shi (2022)						✓								✓											
Tripathy et al. (2022)	✓		✓						✓	✓								✓	✓						
Idug et al. (2023)				✓																		✓		✓	
Wang et al. (2024b)	✓	✓			✓		✓		✓		✓	✓							✓						

Taylor (2018) investigates how rider sensitivity to delays and driver sensitivity to earnings influence the optimal pricing and wage policies of ride-hailing platforms. The study provides several key insights as follows: (a) when rider valuation uncertainty is moderate, increased delay sensitivity raises optimal prices; (b) higher driver opportunity cost uncertainty, combined with moderate expected opportunity costs, reduces optimal wages; (c) driver independence tends to lower prices under driver opportunity cost uncertainty; and (d) under rider valuation uncertainty, driver independence raises prices only if valuation uncertainty is sufficiently high. Zhong et al. (2019) concentrate on wage-setting for drivers in scenarios where ride-hailing platforms employ both permanent and temporary drivers who drive for multiple ride-hailing platforms and are sensitive to earnings. Their findings reveal that: (a) a monopoly ride-hailing platform should offer higher subsidies to attract temporary drivers, which leads to lower prices when both temporary and permanent drivers are employed, compared to relying solely on temporary drivers; (b) ride-hailing platforms can achieve higher profits, as well as increased rider surplus and social welfare, by employing a mix of temporary and permanent drivers; and (c) the employment of permanent drivers significantly alters the effect of competition on optimal strategies, rider/driver surpluses, and social welfare.

Bai et al. (2019) advance this research by addressing how ride-hailing platforms should simultaneously determine prices for riders and wages for drivers. Using two queuing models—a base model with a fixed payout ratio and an extended model with a time-based payout ratio— they recommend that ride-hailing platforms raise driver commissions when demand rises, capacity declines, or riders become more sensitive to delays. Moreover, they find that optimal ride-hailing platform pricing does not necessarily follow a monotonic trend in response to changes in driver capacity or waiting costs. Dong and Leng (2021) examine optimal strategies for setting unit wages and service prices under conditions where riders are sensitive to delays. Their analysis includes situations where riders choose when to use ride-hailing versus taxi services, while drivers retained the flexibility to accept or reject ride requests. Their study reveals several insights: (a) in response to increased rider demand, ride-hailing platforms should raise distance fares, wages, and the payout ratio to attract more drivers; (b) conversely, an influx of drivers warrants a reduction in both distance fares and wages, along with a possible decrease in the payout ratio to maximize profitability; (c) a simultaneous increase in both rider and driver numbers can significantly boost ride-hailing platform’s profits, provided these numbers remain below specific threshold levels; and (d) ride-hailing platforms benefit most when there is a balanced growth in both rider and driver numbers, highlighting a symbiotic relationship between demand and supply dynamics.

Wang et al. (2024b) explore pricing strategies for ride-hailing platforms offering two service modes: a deterministic service mode, where riders select a specific service option, and a probabilistic service mode, where riders request a service knowing that they may be assigned to one of several service classes by the ride-hailing platform. Riders are sensitive to price, quality, and congestion, while drivers are sensitive to earnings. Their findings demonstrate that ride-hailing platform’s price setting strategies and service allocations are influenced by both demand-side and supply-side behavioral factors. The decision between a deterministic or probabilistic approach depends on the riders' base valuation and its variability, and incorporating a bundled option does not always result in increased ride-hailing platform’s profits. Some research focuses on financial incentive decisions. Bernstein et al. (2021) examine surge pricing in contexts where riders are sensitive to both price and congestion and drivers multi-home across multiple ride-hailing platforms and are sensitive to earnings. Their findings suggest that surge pricing benefits both drivers and riders, particularly when drivers operate on multiple ride-hailing platforms. Tripathy et al. (2022) explore the effects of driver collusive behavior on surge pricing policies within ride-hailing platforms. Their research uncovers how drivers strategically manipulate surge pricing by coordinating to create artificial shortages, triggering higher prices. They identify the conditions under which such collusion is likely to occur and its implications for ride-hailing platform’s profitability. Notably, they suggest that in certain cases, ride-hailing platforms might actually benefit from elevated surge prices driven by rider demand persistence in the face of driver collusion, underscoring the complex dynamics between strategic behavior and pricing within ride-hailing ecosystems. Chen et al. (2022a) develop an econometric framework to analyze driver working decisions when they have income targets. They identify optimal bonus rates for maximizing peak-hour capacity and long-term profitability. By modeling data from a large sample of DiDi drivers, their study reveals insights into income-targeting behavior, the non-monotonic relationship between bonus rates and working hours, and the strategic allocation of bonus budgets by ride-hailing platforms to optimize capacity and profitability.

Jiang et al. (2021) investigate the influence of drivers' aversion to regret on their relocation decisions between surge and non-surge zones and how this affects ride-hailing platforms' financial incentives and information-sharing strategies. Through a combination of theoretical modeling and empirical experimentation, they identify key factors influencing drivers' relocation decisions, including the provision of fixed bonuses and information about demand-to-supply ratios. Their study finds that drivers are more likely to relocate to surge zones when they exhibit higher regret aversion, receive demand-to-supply ratio information, and are offered fixed bonuses, highlighting the complex interaction between psychological factors and incentive mechanisms in shaping driver behavior. Similarly, Cohen et al. (2022) focus on financial incentives from the rider's perspective. They examine the impact of targeted, proactive compensation sent to riders who experience frustration, demonstrating that compensating frustrated riders is both profitable and increases engagement. This approach is particularly effective for mitigating long wait times, though less so for long travel durations. Moreover, the study shows that compensation is more impactful when offered to frustrated riders than when provided to those who are not frustrated, with its effectiveness being influenced by rider's prior usage frequency.

Two studies examine the role of gender- and race-related characteristics in ride-hailing platforms. Mejia and Parker (2021) explore how rider characteristics, including gender, race, and attitudes toward LGBT rights, affect drivers' cancellation rates and the ride-hailing platform's decisions on sharing rider information. Through empirical analysis, they uncover persistent biases in driver behavior, particularly concerning race and LGBT-related attributes. While no biases are detected at the ride request stage, they emerge post-acceptance, though gender biases were not observed. The study also highlights moderating factors, showing lower cancellation rates for non-Caucasian riders during peak times, but no similar moderating effects are noted for riders signaling support for LGBT rights. These findings provide nuanced insights into the complexities of discrimination within the ride-hailing environment. Tang et al. (2021) conduct a comparative analysis of traditional and "hybrid" ride-hailing systems, focusing on gender-related safety concerns. They examine whether a hybrid system designed to serve only female riders could benefit all stakeholders. Their results revealed mixed outcomes, with potential disadvantages for male riders and females unconcerned with safety in a hybrid system. However, they identify conditions under which transitioning to a hybrid model could create a win-win scenario for safety-conscious female riders and the ride-hailing platform, depending on the magnitude of mismatch costs.

Choi and Shi (2022) and Idug et al. (2023) diverge from other studies within this theme by focusing on more novel ride-hailing platform's decisions. Choi and Shi (2022) examine the implementation of blockchain technology by ride-hailing platforms and analyze optimal pricing and hygiene level decisions during the COVID-19 outbreak, both with and without blockchain adoption. They conclude that while blockchain implementation increases service costs, it also improves hygiene standards. If riders have significant concerns about infection, blockchain adoption can create a win-win scenario for the ride-hailing platform, drivers, and riders. However, when drivers are responsible for maintaining hygiene standards, both the optimal service price and hygiene level tend to be lower. Additionally, the study emphasizes that reducing fluctuations in rider perceptions of service value is key to enhancing the benefits and effectiveness of blockchain adoption. Idug et al. (2023) explore the impact of driver intention to comply with ride-hailing platform's guidelines on their operational performance and the ride-hailing platform's decision regarding guideline announcements. Using survey data from 513 Uber and Lyft drivers in the United States, they find that driver intention to comply with guidelines has a positive effect on their ratings and acceptance rates while reducing cancellation rates. Moreover, adherence to the ride-hailing platform's guidelines is linked to improved operational performance. Interestingly, drivers believe that penalties for guideline violations are effective but also believe that the likelihood of being caught for ignoring the guidelines is low, revealing a complex interplay of perceived risks and incentives in the ride-hailing ecosystem.

2.3.3. Theme 3: Ride-Hailing Platform's Decisions Affecting Driver and/or Rider Behavior and Stakeholder Outcomes

The core question for Theme 3 is *how ride-hailing platform's decisions affect driver and rider behaviors and, consequently stakeholder outcomes*. Noteworthy examples include Guda and Subramanian (2019), Besbes et al. (2021), Allon et al. (2023), and Hu et al. (2024). Table 2-5 summarizes research relevant to this theme, with the main focus being the impact of ride-hailing platform's decisions about surge pricing (i.e., financial incentives) and sharing information with drivers or riders on demand-side and supply-side behaviors.

Table 2-5. Theme 3: Ride-Hailing Platform’s Decisions Affecting Driver and/or Rider Behavior and Stakeholder Outcomes

	Ride-Hailing Platform’s Decisions							Demand-Side Behaviors				Supply-Side Behaviors									
Study	Pricing	Wage setting	Financial incentives	Information Sharing	Providing feedback	Mergers and acquisitions	Team forming	Price sensitivity	Delay sensitivity	Abandonment behavior	Loyalty to the platform	Spatial relocations	Joining behavior	Churning behavior	Sense of organization identity	Income-targeting	Work duration	Cancellation behavior	Referral behavior	Inertia	Loyalty to the platform
Guda & Subramanian (2019)	✓		✓	✓								✓									
Jia et al. (2020)						✓					✓										✓
Besbes et al. (2021)	✓		✓									✓									
Miao et al. (2022)			✓														✓				
Yu et al. (2022)				✓					✓	✓											
Ai et al. (2023)							✓								✓		✓				
Allon et al. (2023)			✓													✓	✓			✓	
Bimpikis & Mantegazza (2023)													✓								
Lahiri et al. (2023)			✓		✓									✓					✓		
Haferkamp et al. (2024)				✓								✓						✓			
Hu et al. (2024)	✓	✓		✓								✓									

Four studies in this stream focus on the impact of surge pricing and information sharing on driver spatial relocation behavior. Guda and Subramanian (2019) examine the effects of surge pricing and forecast information sharing on drivers’ relocation decisions. Their subgame perfect equilibrium model challenges traditional views by suggesting that surge pricing can, in some cases, reduce demand in surge zones. Furthermore, they reveal the complexity of drivers’ relocation decisions, indicating that merely providing drivers with information on where to relocate may be insufficient. Interestingly, they find that strategic surge pricing could be advantageous even in zones with excess supply, potentially yielding higher profitability than incentivizing drivers’ relocations, highlighting the intricate dynamics between driver behavior and ride-hailing platform’s decisions on pricing and information sharing. Besbes et al. (2021) investigate the influence of surge pricing on drivers’ relocation decisions, focusing on how optimal pricing across different city locations affects driver strategies. They develop a solution aimed at balancing supply and demand, revealing a pricing strategy that varies across locations to achieve equilibrium in some areas while inducing congestion in others, effectively pricing out less profitable locations. Their optimal pricing policy divides the city into multiple regions: the origin, the inner center, and the outer center. In the origin region, surge pricing has a positive effect, encouraging some drivers to stay while others move toward this area. In contrast, drivers located in the outer center are too far from the demand surge, prompting the ride-hailing platform to strategically adjust prices to incentivize relocation toward the origin.

Haferkamp et al. (2024) examine the effects of sharing repositioning heatmaps on driver availability, cancellation rates, and earning opportunities. Their findings suggest that well-designed repositioning heatmaps can significantly reduce service cancellations, thereby minimizing revenue loss for both ride-hailing platforms and drivers. Sharing these heatmaps with drivers boosts their average earnings and helps stabilize income fluctuations across the driver pool. Additionally, heatmaps contribute to a more equitable and efficient distribution of service coverage across the city. Providing repositioning heatmaps to new and less experienced drivers can facilitate their integration into the system, creating a more level playing field. Hu et al. (2024) build on Guda and Subramanian (2019) by exploring how ride-hailing platform's decisions regarding pricing by region, cross-regional surge pricing, bonus incentives, and information sharing influence drivers' spatial relocations, ride-hailing platform's profits, and social welfare. They demonstrate that ride-hailing platforms can either implement surge pricing or offer bonus incentives in neighboring regions before demand peaks to balance supply and demand. Cross-regional demand amplifies the effectiveness of bonus incentives while diminishing the efficacy of surge pricing. Moreover, the ride-hailing platform prefers bonus incentives over surge pricing when only a small number of drivers are required to relocate. While sharing information with drivers can encourage relocation, its impact is limited, with only a portion of drivers choosing to move. Similar to Guda and Subramanian (2019), Bimpikis and Mantegazza (2023) also examine the impact of strategic disclosure of forecast demand information on drivers deciding whether to join the system. Through an information design framework, they demonstrate the existence of a Bayesian equilibrium in which the platform selectively reveals demand information to optimize its profitability. Their findings suggest that the platform benefits from disclosing only partial information—indicating whether demand is high or low—either to incentivize driver entry when participation costs are significant or to deter entry to sustain higher prices. While this approach enhances the platform's profitability compared to both non-disclosure and full disclosure (when the outside option has moderate value), it may negatively impact rider welfare by reducing the availability of idle drivers and driving up prices. Yu et al. (2022) also explore the impact of information sharing but from the demand-side perspective. They investigate how providing waiting time information—both its initial magnitude and subsequent updates—affects riders' abandonment behavior in virtual queues. Their field experiment reveals that both the initial waiting time information and the frequency of updates significantly influence rider abandonment rates. Adjusting the initial waiting time by one minute had no impact on abandonment, as the effect of this adjustment was neutralized by frequent updates. However, larger adjustments lead to abandonment rates being primarily driven by the magnitude of the waiting time information.

Miao et al. (2022) and Allon et al. (2023) examine the effects of surge pricing on other supply-side behavioral issues. Miao et al. (2022) investigate the causal relationship between surge pricing and drivers' earnings, revealing that while surge pricing increases drivers' weekly earnings, it simultaneously reduces daily earnings due to competition effects outweighing cherry-picking effects. Their study identifies surge pricing as a factor attracting more part-time drivers to the market, which in turn crowded out full-time drivers. These findings illuminate the complex dynamics between surge pricing, driver supply, and earnings distribution on ride-hailing platforms. Allon et al. (2023), through an empirical study, explore the influence of financial incentives on drivers' decisions regarding whether to work and the number of hours worked. Their results demonstrate a significant positive impact of financial incentives on both the decision to work and the number of hours worked. Furthermore, they identify behavioral theories, such as income-targeting behavior and inertia, and stress the importance of incorporating behavioral factors when designing incentive schemes to prevent understaffing and maintain optimal service levels.

Three studies examine driver loyalty behaviors. Jia et al. (2020) investigate the impact of ride-hailing platform's decisions on mergers and acquisitions on supply network readiness and how these decisions contribute to ride-hailing platform loyalty through enhanced driver and enhanced rider satisfaction. They suggest that ride-hailing platforms can pursue mergers and acquisitions strategies to integrate resources and reduce excessive competition within their industries. By attracting more stakeholders to enhance supply network readiness and operational capacity, ride-hailing platforms can better meet driver, as well as rider, expectations, thereby fostering satisfaction and promoting ride-hailing platform loyalty. Ai et al. (2023) explore how ride-hailing platform-led team formations influence the creation of team identity among drivers and drivers' earnings. Their field experiment demonstrates that ride-hailing platforms can leverage team identity to boost both revenue and driver engagement in the gig economy. In their experiment, drivers working in teams exhibited a 12% increase in earnings and put in more hours, with the effect persisting for two weeks after the experiment, though at a diminished rate. Additionally, drivers from the same hometown were more likely to communicate with each other, while drivers in teams of similar ages continued to work longer hours and earn more even after the experiment concluded. Lahiri et al. (2023) focus on ride-hailing platform's feedback mechanisms and effects on driver referral and churn behaviors, as well as the resulting operational effectiveness. They find that goal-oriented feedback enhances various operational metrics, leading to improved resource availability, increased driver referrals, and reduced driver turnover. Ride-hailing platforms can enhance their operational efficiency and resource availability by combining targeted feedback with a flexible commission structure for drivers.

2.3.4. Theme 4: Environmental Factors Affecting Ride-Hailing Platform's Decisions and Stakeholder Outcomes

The central question for Theme 4 is *how environmental factors influence ride-hailing platform's decisions and, consequently, the outcomes for ride-hailing platforms, drivers, and riders*. Of particular interest are regulatory mechanisms and market competition, with notable contributions from Yu et al. (2020), Benjaafar et al. (2022), Siddiq and Taylor (2022), and Fan et al. (2024). Table 2-6 identifies relevant research for this theme, with all but two studies not focusing on ride-hailing platform's pricing.

Table 2-6. Theme 4: Environmental Factors Affecting Ride-Hailing Platform's Decisions and Stakeholder Outcomes

Study	Environmental Factors		Ride-Hailing Platform's Decisions				
	Regulatory mechanisms	Competitors	Pricing	Wage setting	Financial incentives	Fleet size	Cooperation
Yu et al. (2020)	Regulatory policies controlling the maximum number of registered drivers	Traditional taxi industry	✓				
Li et al. (2021)		Customized bus services	✓				
Zhang et al. (2021)	Government regulation on taxi fares	Traditional taxi industry	✓		✓		
Benjaafar et al. (2022)	Wage-floor regulations		✓				
Cohen & Zhang (2022)		Two cooperative ride-hailing platforms	✓				✓
Siddiq & Taylor (2022)	Regulatory policies for platform's accessing to autonomous vehicles (Avs)		✓				
Wei et al. (2022)		Public transit ridership	✓				

Zhong et al. (2022)	Regulatory policies on pricing	Traditional taxi industry	✓				
Diao et al. (2023)		Traditional taxi industry	✓				
Hu &Liu (2023)	Regulatory policies on wage and price	Two non-cooperative ride-hailing platforms	✓	✓			
Zeng & He (2023)	Regulatory policies for upper bounds on price surges		✓		✓		
Zhao et al. (2023)	Government subsidies for peak carbon dioxide emissions	Two non-cooperative ride-hailing platforms	✓			✓	
Fan et al. (2024)	Government intervention on expanding the dedicated areas to automated vehicles					✓	
Nie et al. (2024)	Government regulation on rider information collection (Privacy regulations)		✓				

Several studies within this theme explore the effects of regulatory mechanisms on ride-hailing platform's decisions and stakeholder outcomes in monopolistic environments. For example, Benjaafar et al. (2022) examine how wage-floor regulations and an expanding driver pool impact ride-hailing platform's pricing and stakeholder welfare, finding that driver welfare initially rises then falls as the driver pool grows and that an effective wage floor improves both driver and rider welfare despite higher prices. Similarly, Siddiq and Taylor (2022) investigate the influence of autonomous vehicle access on ride-hailing platform's pricing and welfare, concluding that while driver welfare declines with high-cost autonomous vehicles, social welfare increases with individually owned autonomous vehicles, and ride-hailing platform's profit depends on the ownership structure and vehicle costs. Zeng and He (2023) explore how regulatory caps on price surges influence ride-hailing platform's surge pricing and the welfare of riders and drivers. Their findings reveal a backward-bending demand curve, where rising prices initially boost demand due to perceived convenience but later decrease it as price effects dominate. They argue that capping price surges can align the financial interests of ride-hailing platforms with rider and driver welfare. Fan et al. (2024) focus on how government expansion of AVs-only zones influences a ride-hailing platform's fleet size decisions for automated and non-automated vehicles. Their study reveals that as the size of AVs-only zones increases, the fleet of automated vehicles grows nonlinearly, while the fleet of conventional vehicles decreases due to shifting demand. Initially, AVs-only zones might cause detours for human-driven vehicles, but as the zones expand, they significantly reduce congestion, providing substantial benefits. Similarly, Nie et al. (2024) study the impact of privacy regulations, which control rider information collection and usage, on ride-hailing platform's pricing strategies and data collection. They find that privacy regulations push ride-hailing platforms towards partial-coverage pricing, enhancing information security but potentially reducing benefits for all stakeholders. Thus, privacy regulation involves a trade-off between economic benefits and information security.

A significant portion of research within this theme explores competitive environments where ride-hailing platforms set policies while considering competition from public transportation and other ride-hailing services. Yu et al. (2020) analyze the effects of regulating the maximum number of registered drivers on ride-hailing platforms in competition with the taxi industry, finding that without intervention, ride-hailing platforms can potentially displace traditional taxis, while balanced regulatory policies and fare adjustments in the taxi industry can improve social welfare. Similarly, Zhang et al. (2021) investigate dual-fairness concerns in the ride-hailing industry which refers to (1) taxi driver concerns about unfair competition with ride-hailing drivers and (2) ride-hailing driver concerns regarding lack of fairness in their job due to rating system and commission schemes. They propose incentive strategies, such as revenue and demand sharing, to mitigate these concerns. Their research demonstrates that government regulation of taxi fares could reduce fairness-related issues and enhance ride-hailing platform's profitability and social welfare, highlighting the complex interplay of fairness, incentives, and regulation in the ride-hailing sector. Zhong et al. (2022) study pricing strategies for ride-hailing platforms in competition with traditional taxis under various government regulatory scenarios. They find that unregulated pricing leads to higher rates and profits for ride-hailing platforms, while regulatory interventions should focus on promoting competition by adjusting taxi supply based on demand levels. Diao et al. (2023) explore conditions for coexistence between ride-hailing platforms and taxi companies, showing that equilibrium pricing depends on the ratio of rider inconvenience costs and the demand for long-distance rides. Inconvenience costs refer to all hassle costs that the riders incur (e.g., hailing the ride, walking, waiting, paying, etc.). Surprisingly, higher taxi inconvenience costs lead to increased taxi fares, and reducing these costs can either benefit or harm both industries, depending on ride distance distributions.

Other forms of public transportation have also been analyzed as competitors to ride-hailing platforms. Li et al. (2021) study pricing strategies when ride-hailing platforms compete with customized bus services, finding that optimal pricing for both services depends on their strategies, with ride-hailing prices being a quadratic function of bus unit prices when the bus unit price is known to ride-hailing platforms. Wei et al. (2022) examine conditions for coexistence between public transit and ride-hailing platforms, demonstrating that coordinated scheduling can reduce systemwide costs, saving millions of dollars daily during rush hours while benefiting riders, operators, and the overall system by reallocating public transit recourses to where they align with rider preferences which leads to congestions reduction.

Competition between ride-hailing platforms has also been explored. Hu and Liu (2023) analyze how regulatory policies that impose precommitments on ride-hailing platforms regarding rider prices and/or driver wages affect equilibrium outcomes between competing platforms. They find that regulatory policies on the more competitive side, whether on the demand or the supply side, lead to lower outcomes compared to the absence of such policies. Therefore, platforms benefit more from precommitments on the less competitive side. When competition is nearly equal, pre-committing to commission rates is less profitable than avoiding commitment; however, this reverses when competition levels are uneven. Zhao et al. (2023) focus on the impact of government subsidies and environmental preferences of riders on ride-hailing platform's pricing, fleet size, and competitive equilibrium. They find that ride-hailing platforms using self-operated new energy vehicles (NEVs) benefit more from government subsidies and green preferences than those using franchised, driver-owned vehicles. However, higher government subsidies lead to lower optimal ride prices for both types of platforms. They also highlight how capturing riders' green preferences can help franchised ride-hailing platforms expand NEV fleets, supporting carbon peak goals. Cohen and Zhang (2022) investigate the dynamics of competition and coopetition between ride-hailing platforms, showing that competition for riders and drivers creates a unique equilibrium. Their study reveals that coopetition can be mutually beneficial when demand-side competition is intense but can harm one ride-hailing platform when competition is stronger on the supply side.

2.3.5. Theme 5: Economic, Environmental, and Social Impacts of Ride-Hailing Platforms

The central question for Theme 5 is *how ride-hailing services impact the economy, environment, and society*. Tseng and Chan (2019) initiate research interest related to this theme by examining how ride-hailing platforms like Uber influence societal acceptance of the sharing economy. Their case study reveals that Uber uses *framing, aggregating*, and *bridging* strategies to build credibility, gain legitimacy, and drive institutional change. Offering a vision to the public, hosting charitable events, and soliciting celebrity endorsements are examples of *framing* strategies to shape a positive brand image for Uber. Establishing links with potential drivers, holding frequent briefings, providing discount codes, and signing petitions are *aggregating* strategies to increase legitimacy. Securing more resources and partnering with car rental companies, allying with shops and events, opening its API on the website, and sharing data with the government are examples of *bridging* strategies to enhance legitimacy and drive institutional change.

A primary concern within this theme is the environmental impact of the ride-hailing industry. Yu et al. (2019) propose a model to minimize carbon emissions and maximize average driver profit for the Bilinear Geometric Ride-Sharing Problem (BGRSP). They develop an exact method by eliminating most of the non-Pareto-optimal solutions, which can effectively reduce emissions while maintaining driver satisfaction. Naumov and Keith (2023) examine the effects of ride pooling on traffic congestion and greenhouse gas emissions in US cities by determining optimal pricing strategies for both individual and pooled rides to bolster ride-hailing platform's revenue while incentivizing riders to opt for pooling. Doing so curbs vehicle miles traveled and mitigates the environmental impact of urban transportation. Their study reveals that lowering driving costs and offering uniform price reductions across both individual and pooled rides might decrease rider preference for pooling. They highlight the need for differential pricing strategies, where prices for pooled rides should be reduced, prices for individual rides should be maintained or increased, especially as automated vehicle technologies lower service costs. Arora et al. (2024) investigate the impact of promoting pooled transportation and reducing the number of ride-hailing drivers on traffic congestion and greenhouse gas emissions. Their findings indicate that reducing walking distances for pooled services can substantially reduce the commutes and decrease the number of ride-hailing drivers, resulting in an annual reduction of up to 4.8 thousand tonnes of emissions and cost savings exceeding one million dollars.

Several studies examine the safety-related impacts of the ride-hailing industry. Liu et al. (2021) investigate moral hazard, which is measured by driver detour or the extra distance a driver adds to the fastest route and service quality, finding that taxi drivers cover 8% more distance than Uber drivers on metered airport routes, especially for nonlocal riders. Longer routing leads to increased travel times, highlighting the need for ride-hailing platforms to mitigate driver moral hazard. Barrios et al. (2023) conduct an empirical examination into the ramifications of the introduction of ride-hailing platforms on fatal traffic accidents within US cities. Their findings reveal a 2%-4%

rise in fatal accidents involving pedestrians and cyclists, linked to increased vehicle miles traveled and traffic delays. Moreover, fatal accidents and fatalities exhibit an upward trajectory in tandem with indicators of heightened driver adoption of ride-hailing platforms. They recommend enhanced driver certifications and navigation algorithms that prioritize safety. Qiu et al. (2024) study the effect of ride-hailing services on hate crimes, reporting a 5.75% decrease, likely due to increased interactions between diverse groups as ride-hailing services foster positive environments and interactions that promote mutual understanding among different groups.

Several studies investigate traffic congestion due to ride-hailing services. Li et al. (2022b) find that ride-hailing services exacerbate (alleviate) traffic congestion in compact urban areas (sprawling cities). The impact on traffic congestion is influenced by both the efficiency-enhancing and demand-inducing effects of ride-hailing services, with the overall effect varying based on the level of urban compactness. Agarwal et al. (2023) observe that during periods of strikes or ride-hailing platform unavailability, travel times consistently decrease. This effect is most pronounced in heavily congested regions during peak hours. The authors posit that ride-hailing platforms are substantial contributors to urban congestion. Benjaafar et al. (2022) investigate the impact of the ride-hailing industry on traffic and car ownership and show that while ride-hailing services might decrease the number of car owners, they can also lead to increased traffic. As ownership costs rise, both traffic and car ownership may increase. A revenue-maximizing ride-hailing platform might prefer a scenario where vehicles are frequently driven with only a few riders, resulting in higher traffic congestion. Gong et al. (2023) also find that Uber's entry into a market correlates with a short-term rise in vehicle ownership, particularly for small vehicles eligible for ride-hailing platform use, driven by consumers seeking to capitalize on excess rents. This effect, however, depends on vehicle size, with small vehicles experiencing a more significant increase in sales compared to larger vehicles. Liu et al. (2024) explore the congestion effect due to ride-hailing pick-ups and drop-offs, demonstrating that ride-hailing pick-ups and drop-offs reduce traffic speed significantly. Their experiments in Manhattan reveal that redirecting these trips from curb space can lower system-wide travel time by up to 2.44%. Curb space refers to a multi-purpose space to be used for vehicular parking, loading and unloading, and rider pick-ups and drop-offs.

Besides concerns related to the environment, safety, and traffic congestion, researchers have also investigated the impact of ride-hailing services on public transit usage (e.g., Pan and Qiu, 2022), tourism (e.g., Tan et al., 2022), and sustainability more broadly (e.g., Guo et al., 2023). Pan and Qiu (2022) reveal that Uber's entry into a market decreases bus ridership significantly while having little influence on public demand-response transit. Demand-response transit, often referred to as paratransit, consists of services where vehicles operate without a fixed route or schedule, except possibly for temporary accommodations, picking up and dropping off passengers at designated locations based on individual service requests. Tan et al. (2022) note that consumption habits, peer-to-peer consumption spillover, and taxi availability significantly shape tourist use of ride-hailing services, with cost savings diminishing in importance over time. Moreover, safety reputation and familiarity with the destination are not significant determinants of tourist behavior. Guo et al. (2023) find that when ride-hailing services focus solely on economic objectives, environmental and social outcomes are negatively impacted. Substantial reductions in carbon emissions are, however, achievable with minimal economic sacrifices through pricing adjustments or increases in driver commissions. Prioritizing travel time over travel distance also improved economic, environmental, and social outcomes.

2.4. Future Research Directions

Appendix A highlights the dominance of analytical modeling in research on ride-hailing platforms within the field of operations and supply chain management. While analytical models offer a theoretical approach and insights to support decision-making, the complex dynamics of the ride-hailing industry—shaped by ride-hailing platform, demand-side, and supply-side behaviors, as well as external factors such as government interventions—may necessitate empirical research to validate these analytical insights. For instance, theoretical results regarding the impact of ride-hailing platform sharing with drivers on their relocation decisions (e.g., Guda and Subramanian, 2019; Hu et al., 2022) could be strengthened through empirical validation. Similarly, the findings reported by Zhao et al. (2023) concerning the effect of government subsidies and riders' environmental preferences on ride-hailing platform pricing, fleet size, and competitive equilibrium could benefit from empirical evidence. Beyond the suggestion for empirical validation of theoretical findings, this literature review identifies five future research opportunities for operations and supply chain management researchers to undertake in order to advance understanding of ride-hailing platform's operations.

2.4.1. Interactions among Mechanisms for Desired Driver Behavior

Research in Theme 3 examines the impact of ride-hailing platform's decisions on driver behavior, demonstrating that platforms can strategically implement various measures to influence driver actions in alignment with their objectives. Financial incentives and information sharing are two important ride-hailing platform's decisions to manage driver availability across zones and enhance supply-demand matching efficiency. Research on financial incentives shows that surge pricing can motivate idle drivers to relocate from non-surge zones to surge zones (Bimpikis et al., 2019; Cachon et al., 2017). Likewise, research shows that information sharing with drivers can also motivate desired drivers' relocation behaviors (e.g., Guda and Subramanian, 2019; Hu et al., 2024; Haferkamp et al., 2023), with investigations analyzing the effects of sharing different pieces of information with drivers, including market forecasts (Guda and Subramanian, 2019; Hu et al., 2024); forecasts of ride requests, current and expected fleet distribution, and driver specific locations (Haferkamp et al., 2023); and real-time demand (i.e., ride requests) and supply (i.e., availability of drivers) information for non-surge zones (Jiang et al., 2021) and surge zones (Hu et al., 2022). Whether, and to what extent, these mechanisms complement or substitute for one another in influencing desired drivers' relocation behaviors and enhancing supply-demand matching efficiency are interesting avenues for future research. More specifically:

a) Under what conditions would information sharing with drivers substitute for or strengthen financial incentives to motivate desired drivers' relocation behavior for a specific level of supply-demand matching efficiency?
b) Do different types of information being shared impact desired drivers' relocation behaviors in varying ways?

These research questions are addressed in Chapter 3 of this dissertation.

2.4.2. Competition for Riders and Drivers

Research insights from Themes 2 and 3 are generally derived by assuming monopolistic conditions. Ride-hailing platforms are frequently assumed to operate without direct competition (e.g., Bai et al., 2019; Deng and Leng, 2021; Guda and Subramanian, 2019; Jiang et al., 2021; Tripathy et al., 2022; Allon et al., 2023; Wang et al., 2024), with models typically assuming that drivers work exclusively for a single ride-hailing platform and that riders are loyal and do not switch across different ride-hailing platforms (e.g., Jiang et al., 2021). Theme 4, on the other hand, includes a few studies (Hu and Liu, 2023; Zhao et al., 2023) exploring competition for riders and drivers and examining win-win scenarios and sustainability outcomes for competing ride-hailing platforms. Since multiple ride-hailing platforms often serve the same market, drivers often "multi-home" and work for more than one ride-hailing platform, and riders typically have more than one ride-hailing app on their mobile devices, assumptions of monopolistic conditions do not mimic reality, with ride-hailing platforms necessarily competing for both drivers and riders. Research relaxing assumptions of monopolistic conditions is thus encouraged to derive additional insights on competitive dynamics among ride-hailing platforms serving the same markets and behavioral aspects of demand-side and supply-side participants in these competitive settings. Of particular interest are investigations into supply-side and demand-side behavioral factors that affect or are affected by pricing decisions among competing ride-hailing platforms. More specifically:

a) Does information sharing by a ride-hailing platform adequately motivate desired drivers' relocation behaviors when competitors offer surge pricing, and riders are not loyal?
b) When competing ride-hailing platforms serve the same market, are financial incentives effective in discouraging drivers from working for more than one ride-hailing platform?

2.4.3. Ride-Hailing Collaboration with Other Ride-Hailing Platforms or Car-Rental Companies

Ride-hailing platforms do collaborate with one another or with car-rental companies. Cohen and Zhang (2022) from Theme 4, for example, explore the dynamics of coopetition (i.e., cooperation and competition) between two ride-hailing platforms. Lin et al. (2021) from Theme 1 demonstrate the benefits of ride-hailing platform's collaboration with car-rental companies under monopolistic conditions. Research on such collaborations, besides these two exceptions, is limited. The prevalence of such collaborations calls for more research to explore the nature of such collaborations and their advantages and disadvantages. More specifically:

a) How are collaborations between ride-hailing platforms structured? Between ride-hailing platforms and car-rental companies?

b) When ride-hailing platforms compete to partner with car-rental companies, are there win-win-win solutions where both ride-hailing platforms and car-rental companies enjoy higher profits from cooperating?
c) How does ride-hailing platform's collaboration with one another affect drivers' relocation behaviors and/or cancellation behavior? Rider behavior?

2.4.4. Regulatory Agencies as Stakeholders

For ride-hailing platforms, drivers and riders are not the only stakeholders with conflicting interests; regulatory agencies also play a significant role. Theme 4 includes research exploring the impact that local government or municipal agencies have on internal ride-hailing platform's decisions and outcomes via such regulations as the maximum number of registered drivers (Yu et al., 2020), taxi fares (Zhang et al., 2021), wage floors for drivers and prices for riders (Benjaafar et al., 2022; Hu and Liu, 2023; Zeng and He, 2023; Zhong et al., 2022), access to autonomous vehicles (Fan et al., 2024; Siddiq and Taylor, 2022), and peak carbon dioxide emissions (Zhao et al., 2023). The impact of these regulations on supply-side and demand-side behavioral factors, however, has yet to be investigated. More specifically:

a) Under what conditions do regulations ensure the availability and fair treatment of all transportation choices? For ride-hailing platforms competing for drivers and riders?
b) How and why do regulations influence driver loyalty to ride-hailing platforms or their churning behavior?

2.4.5. Sharing Untruthful Information

Research from Theme 3 highlights the value of ride-hailing platform sharing information with drivers. Anecdotal evidence, however, suggests that drivers often distrust the information given to them by ride-hailing platforms.[2] This distrust may be valid since ride-hailing platforms may have an incentive to share misleading market information with drivers (Guda and Subramanian, 2019). Distrust of information has also been investigated in a manufacturer-retailer setting as this relates to conditions under which truthful information is revealed by either party (e.g., Berman et al., 2019; Wei et al., 2023; Lu, 2024). Wei et al. (2023), for instance, investigate the relationship

[2] https://www.forbes.com/sites/lensherman/2024/01/16/will-2024-be-a-year-of-reckoning-for-ubers-driver-relations/

between inventory sharing and demand learning to mitigate supply-demand mismatches, examining how the incentive for untruthful information sharing changes by learning demand over time. Given the similar power dynamic between ride-hailing platforms and drivers, the extent to which ride-hailing platforms share untruthful information with drivers, the impact of sharing such untruthful information on driver behaviors, and how this practice of sharing untruthful information changes as drivers learn via repeated interactions with the ride-hailing platform are intriguing research opportunities. More specifically:

a) Under what conditions would ride-hailing platforms share untruthful information?
b) What impact does untruthful information sharing have on driver behaviors initially and over time?

2.5. Conclusions

This chapter provides a review of 89 academic research articles on ride-hailing platforms published in operations and supply chain management journals. The publications coalesce around five themes seeking to address the following questions: a) how do ride-hailing platform's decisions influence the outcomes for the platform, riders, and drivers?, b) how do rider and driver behaviors and their attributes affect ride-hailing platform's decisions and consequently stakeholder outcomes?, c) how do ride-hailing platform's decisions affect driver and rider behaviors and consequently stakeholder outcomes?, d) how do environmental factors influence ride-hailing platform's decisions and, consequently, the outcomes for ride-hailing platforms, drivers, and riders?, and e) what are the impacts of ride-hailing services on the economy, environment, and society? Over 60 percent of the academic research on ride-hailing platforms are analytical modeling papers. Empirical research is encouraged to validate the analytically derived theoretical findings.

This chapter also identifies and encourages five future research directions. One is for research on interactions between mechanisms deployed to incentivize desired drivers' relocation behaviors, particularly in assessing conditions under which information sharing can substitute for or augment surge pricing. Another is for research into ride-hailing platform's decisions, antecedents, and consequences while relaxing assumptions of monopolistic conditions. A third encourages research into the nature of ride-hailing platform's collaborations with one another or with car-rental companies, as well as the advantages and disadvantages of such collaborations. The fourth is for research focusing on the impact of regulations by regulatory agencies on ride-hailing platform's decisions and effects on drivers and riders. Finally, the fifth calls for more research into when ride-hailing platforms share untruthful information with drivers and its impact on driver behaviors.

Chapter 3

Managing Supply-Demand Imbalance in Ride-Hailing: The Impact of Diverse Information on Surge Prices

Abstract

The ride-hailing market continues to grow, yet efficiently redistributing drivers amid fluctuating demand remains a challenge. While platforms primarily use surge pricing to encourage relocation, sharing relevant information—such as the proportion of ride requests and drivers in each zone or the relative average ride distance—can also influence driver decisions. This study examines whether information sharing can substitute for monetary incentives, the extent of this effect, and the conditions under which different types of information are most effective. Using a two-period Stackelberg game, we compare various information-sharing strategies against a baseline model that only shares surge multiplier values, with the objective of either maximizing platform profit or supply-demand matching efficiency. Our findings indicate that information can serve as a substitute for financial incentives, with its effectiveness depending on the degree of imbalance between idle drivers and ride requests. Higher relocation costs further amplify the benefit of sharing more information. Thus, the study contributes to the ride-hailing literature by clarifying how surge pricing and information interact and identifying what types of information are most valuable and when.

Keywords: ride-hailing, surge pricing, on-demand platforms, information sharing, supply-demand matching

3.1. Introduction

Over the past decade, the proliferation of internet access and smartphones has fostered the growth of the sharing economy. Ride-hailing, a prominent aspect of this industry, involves a transportation model where a platform promptly connects riders with available drivers. Scholarly interest in ride-hailing platforms has markedly increased, driven in part by the rapid expansion of companies like Uber and Lyft. In 2014, for instance, there were 700,000 active Uber drivers, three times the number of taxi drivers (Jiang et al., 2021). From 2009 to 2019, Uber and Lyft tripled the number of U.S. drivers (Griswold and Kopf, 2019). Recent statistics indicate that Uber and Lyft, respectively, have 7.8 million and almost 2 million active drivers globally (Uber Statistics, 2024; Lyft Statistics, 2024). Furthermore, the ride-hailing market continues to see significant increases, with the customer-base projected to grow to 2.31 billion by 2029 (Statista, 2025).

Ride-hailing platforms offer drivers the advantage of flexible and self-scheduled work while providing riders with rapid and adaptable travel options. To compete, ride-hailing platforms must match available drivers (i.e., supply) to riders (i.e., demand) within a particular area or zone, in real time and on short notice. How efficient Uber or Lyft is in matching drivers to riders impacts its service quality, profits, and competitiveness. A key challenge faced by all ride-hailing platforms is managing driver availability amid fluctuating and unpredictable demand. Drivers for ride-hailing platforms are independent contractors who decide their own working hours and the areas where they prefer to pick up riders. Hence, at any time, some zones may experience fewer drivers than ride requests—a "supply-shortage" or surge zone—while other zones face the opposite—a "supply-overage" or non-surge zone. Supply-demand mismatches, on average, increase driver idle time while reducing driver earnings and, similarly, increase rider waiting time while decreasing rider satisfaction (Cachon et al., 2017; Guda and Subramanian, 2019; Jiang et al., 2021).

Although many algorithms exist to match idle drivers to ride requests (e.g., Taylor, 2018; Özkan and Ward, 2020), these solutions alone are typically unable to resolve persistent supply-demand mismatches. Consequently, with no direct control over driver availability, ride-hailing platforms must continually incentivize idle drivers to relocate from non-surge to surge zones. Developing and implementing policies to efficiently redistribute drivers, with the goal of maximizing supply-demand matching efficiency (i.e., the percentage of fulfilled ride requests), remains a key challenge (Besbes et al., 2021). To this end, most ride-hailing platforms like Uber and Lyft use *surge pricing*, which is a financial incentive to encourage drivers to relocate to areas experiencing a surge in demand. Cachon et al. (2017) and Bimpikis et al. (2019) suggest that surge pricing is generally effective at motivating idle drivers to move to areas with a high number of ride requests. However, conflicting anecdotal evidence from Uber drivers suggests that dynamic pricing may not always be strategically appropriate. For instance, one driver writes, "*I'm pretty sure chasing surge [driving to a surge zone] is pretty pointless like chasing smoke in the sky*." Another driver contends "*I have come to the conclusion that hunting surge does not get me more money in most days. It gets me the same money or even less than accepting base but with significant less effort.*" More than 100 similar quotes can be found in Uber drivers' forums (https://www.uberpeople.net/). Further, concerns about exorbitant fares (Reilly, 2014; Lynley, 2024) have led to increased government scrutiny, with regulations increasingly focused on capping surge multipliers (Willingham, 2017). In fact, a competitive advantage for ride-hailing platforms is finding ways to reduce their reliance on surge pricing altogether (Ngila, 2023), as it has been shown that more loyal, full-time drivers can be hurt by surge pricing in the long term (Miao et al., 2023).

These issues raise important questions about the effectiveness of relying on surge pricing as the sole mechanism for incentivizing drivers to relocate, and whether other operational levers could be used in tandem. For instance, several scholars propose that platforms, in addition to offering financial incentives, should share information relevant to a driver's decision regarding whether to relocate from a non-surge zone to a surge zone. In particular, Guda and Subramanian (2019) examine how sharing market forecasts—that is, predicting which areas are likely to become surge zones in the next few hours or days—affect drivers' decisions to relocate. Jiang et al. (2021) suggest that providing information on the demand-to-supply ratio can effectively encourage idle drivers to relocate. Similarly, Hu et al. (2022) propose sharing information on both supply (available drivers) and demand (number of ride requests) within surge zones.

We extend this research by proposing several models in which, alongside the surge multiplier, different information is shared with drivers who, we assume, are regret averse. We focus on the impact of information sharing on drivers' relocation decisions, as well as the platform's matching efficiency and profit. Specifically, in a two-zone model, we analyze the effect of sharing: the proportions of (i) ride requests and (ii) drivers that are initially located in each (surge vs. non-surge) zone, as well as (iii) the average ride distance in one zone relative to the other. We theoretically and numerically compare various combinations of these information combinations with a baseline model that shares only the surge multiplier. This allows us to investigate whether information can substitute for monetary compensation, the extent of this substitution effect, and which types of information are most effective at encouraging drivers to relocate.

To address these research questions, we develop a two-period Stackelberg game with a fixed number of drivers dispersed between each of the two zones. Before the first stage, the platform observes the locations of both riders and drivers. We assume there are sufficient drivers to meet all ride requests, and thus, the platform must focus on effectively balancing supply and demand. In the first stage, the platform sets the surge multiplier value and decides what information to share with the drivers. In the second stage, drivers observe the surge multiplier and the information disclosed by the platform. They then independently maximize their regret-averse utility function by deciding whether to stay in their current zone or relocate. After making this decision, they are matched with customers requesting rides in their chosen zone. Eight models are developed based on the information the platform chooses to share with drivers, and the assumption that the platform can also set the surge multiplier value. For each model, we derive closed-form expressions for the equilibrium, which in our case, represents the proportion of drivers who relocate from their original zone. Based on these equilibrium values, we determine the optimal surge multiplier and derive closed-form solutions for the platform's maximal matching efficiency and profit.

By comparing these eight models in numerical analysis, we find that not only does information act as a substitute for monetary compensation (i.e., a lower surge multiplier with equal matching efficiency and platform profit) over a wide range of scenarios, but the type of information the platform discloses depends on the degree of imbalance between idle drivers and ride requests. For instance, if the average ride distance in the surge zone exceeds its expectation, sharing this information improves supply-demand matching efficiency and reduces the surge multiplier as compared to withholding it. However, we also observe that when the relocation cost is negligible, sharing additional information provides no added benefit, and the platform can rely solely on the surge multiplier. These findings align with prior research on the benefits of sharing information to motivate driver relocation (e.g., Guda and Subramanian, 2019; Hu et al., 2022, 2024; Jiang et al., 2021) and extend it by demonstrating how different information can impact outcomes.

Another body of research on ride-hailing investigates how surge-pricing strategies benefit platforms since these policies can increase the number of drivers who relocate to a surge zone (e.g., Cachon et al., 2017; Bimpikis et al., 2019; Bernstein et al., 2021; Dong and Leng, 2021). We refine this work by examining how sharing different information can affect surge pricing, revealing a nonlinear relationship between information disclosure and the optimal surge multiplier. For instance, with a fixed number of drivers, the proportion of ride requests in the surge zone generally exhibits a monotonic relationship, with the optimal surge multiplier being bimodal when the platform is completely transparent. However, this pattern does not always hold. For example, if the platform shares the proportion of ride requests but not the proportion of drivers, the relationship is non-monotonic due to the interplay between known and assumed information. This insight adds nuance to the understanding of how surge pricing and information interact.

Lastly, while our focus is not primarily on how drivers' aversion to regret impacts supply-demand matching efficiency, as in Jiang et al. (2021), we extend their findings by examining how such aversion may influence the effectiveness of information sharing. We find that as drivers become more regret-averse, supply-demand matching efficiency increases and information sharing becomes increasingly valuable in preventing a significant rise in the surge multiplier. Our numerical study also indicates that, as we decrease the upper bound on the surge multiplier value, maximizing platform profit becomes equivalent to maximizing matching efficiency. The speed of this convergence, however, depends on the shared information. While Hu et al. (2022) also compare these objectives when the platform shares supply and demand data, they do not examine the differences in the associated optimal surge multiplier. We complement their work by reinforcing the idea that information sharing can act as a substitute for surge pricing regardless of whether a platform aims for profitability or by maximizing the number of matches.

3.2. Literature Review

Research on ride-hailing platforms span multiple disciplines, including economics (e.g., Cramer and Krueger, 2016; Dills and Mulholland, 2018; Alvarez and Argente, 2022), information systems (e.g., Guo et al., 2019; Hong et al., 2020; Cheng et al., 2023), logistics and transportation (e.g., Urata et al., 2021; Li et al., 2022a; Haferkamp et al., 2023), and operations management (e.g., Bimpikis et al., 2019; Özkan and Ward, 2020; Afeche et al., 2023). Two themes are of particular interest. The first is to effectively match riders and drivers within a geographic area (Feng et al., 2021; Hu and Zhou, 2022; Lyu et al., 2024). The second theme studies the benefits of different pricing policies on platforms, drivers, and riders (Cachon et al., 2017; Taylor, 2018; Zhong et al., 2019; Bernstein et al., 2021; Li et al., 2022b). Our research addresses both topics by analytically examining how driver relocation decisions are influenced by two platform policies: (i) surge pricing as a financial incentive and (ii) the sharing of *accurate*, real-time operational information with drivers. Table 3-1 categorizes the relevant literature associated with these themes.

The upper-left quadrant of Table 3-1 highlights research on driver relocation decisions made without platform intervention; there are no financial incentives, nor is there information sharing. This research typically focuses on developing competitive games aimed at maximizing matching efficiency or deriving optimal policies under the assumption of centralized control by the platform. For instance, Yang et al. (2018) model driver relocation decisions as a function of the dynamics of a spatiotemporal demand process (riders) and the number of other drivers that are present in the same region. Using a mean-field game with competitive agents (drivers), they show that the equilibrium strategy follows a threshold structure: it is optimal for a driver to leave an area when the number of other drivers exceeds a threshold given by a function of the number of riders in that region. Viewing the ride-hailing system as a closed queueing network where drivers roam with empty cars in search of a ride, Braverman et al. (2019) propose a routing mechanism through which the platform centrally manages network flow to maximize driver availability. Simulation results—based on data from Didi Chuxing, a ridesharing platform operating in China—confirm the benefits of the optimal routing policy, which is derived using a fluid approximation of system dynamics.

Table 3-1. Ride-haling platform research on driver relocation decisions

	Does not emphasize financial incentives	**Emphasizes financial incentives**
Does not share information with drivers	Afeche et al. (2023) Urata et al. (2021) Braverman et al. (2019) Yang et al. (2018)	Chen et al. (2024) Lee et al. (2023) Besbes et al. (2021) Ong et al. (2021) Özkan and Ward (2020) Bimpikis et al. (2019)
Shares information with drivers	Haferkamp et al. (2023) Yu et al. (2022)	Hu et al. (2024) Bimpikis & Mantegazza (2023) Ma et al. (2022) Hu et al. (2022) Jiang et al. (2021) Guda & Subramanian (2019)

Urata et al. (2021) model driver relocation decisions as an absorbing Markov decision process, which they calibrate using a large dataset from Didi Chuxing. They find that idle drivers typically remain stationary during the day but become more mobile late at night, actively seeking out matching opportunities. Additionally, while drivers generally exhibit an aversion to repositioning, when they choose to relocate, they show a preference for moving to more distant areas. In contrast, Afeche et al. (2023) develop a game-theoretic fluid model for a two-location, four-route network and examine system profitability by controlling two operational levers: ride request acceptances and driver repositioning. They show that decentralized control over rider acceptances and repositioning leads to inefficiencies, while increased platform control over the handling of ride requests benefits drivers and the platform. Specifically, their model demonstrates that strategically refusing ride requests from non-surge zones can boost system profitability. Furthermore, they find that greater platform control over driver relocation decisions can also benefit both stakeholders.

The upper-right quadrant of Table 3-1 includes studies that focus exclusively on the role of surge pricing in driver relocation decisions without any other information being shared with drivers. Considering a network of zones across which drivers decide to relocate to maximize their earnings, Bimpikis et al. (2019) formulate an infinite-horizon, discrete-time model of a ride-hailing network. Their findings indicate that, in equilibrium, profits for both the platform and drivers are maximized when demand across the network is balanced. However, in the presence of an imbalance between idle drivers and ride requests, surge pricing is the optimal strategy and using a fixed commission rate may even result in profit losses for the platform. Özkan and Ward (2020) challenge the approach of fixing a pricing or matching policy, such as pairing riders with the closest available driver. By analyzing a queueing control problem, they prove the asymptotic optimality of a joint policy derived from a linear program which maximizes the number of matches while determining favorable driver-rider assignments. Alternatively, using a measure-theoretic Stackelberg game, Besbes et al. (2021) show that the platform's revenue-maximizing pricing policy incentivizes drivers to relocate from neighboring zones, while higher prices in distant non-surge zones are needed to encourage driver movement.

Ong et al. (2021) discuss the development of Lyft's Personalized Power Zone product, which replaces heatmaps to dynamically adjust driver compensation. They model the problem as a multiagent dynamic program and propose an approximate solution approach that first selects which drivers to incentivize and where they should relocate and then determines how each driver should be compensated. They evaluate their technical approach using real-world data from 320 cities to show that their methodology can increase incremental bookings by 0.5%, generating millions in additional revenue. It also has the potential to reduce pick-up times and ride cancellations as well as enhance the experience for drivers and riders alike. Lee et al. (2023) use a combination of empirical analysis and simulation to demonstrate how ride requests, driver distributions, and pricing dynamically interact. Finally, Chen et al. (2024) propose a framework for evaluating both static and dynamic pricing policies with the goal of maximizing a platform's cumulative expected profit in a nonstationary environment. They develop a set of near-optimal dynamic heuristic strategies and confirm their theoretical findings by numerically demonstrating that dynamic pricing outperforms static pricing by boosting both revenue and the number of riders that are served.

The lower-left quadrant of Table 3-1 features studies that explore how platform-controlled information disclosure shapes driver decisions. By performing a large-scale, randomized field experiment, Yu et al. (2022) empirically examine the impact of sharing information about waiting time—both its initial magnitude and subsequent updates over time—on riders' abandonment behavior. They identify a complex trade-off between the magnitude of the initial waiting time estimate and the frequency of updates, with riders' abandonment behavior influenced by the relationship between pessimistic and neutral waiting time information. Haferkamp et al. (2023) propose a stochastic dynamic programming model and study the platform's ability to share a "repositioning heatmap"—a forecast of ride requests, current and expected fleet distributions, and driver locations—with drivers. Using a simulation based on New York City ride-hailing data, they find that well-designed heatmaps can significantly reduce rider cancellations, increase platform revenue, and promote a fairer distribution of earnings among drivers.

The fourth quadrant in the lower right of Table 3-1 includes research on driver relocation decisions in the presence of both financial incentives and information sharing. Guda and Subramanian (2019) develop a two-period, two-zone, signaling game and find that sharing forecasts with drivers (i.e., which zones are expected to become surge zones in the next hours/days) without surge pricing fails to motivate enough drivers to relocate. However, using surge pricing alone can reduce the platform's profit if demand in the surge zone is not sufficiently high. Thus, combining surge pricing with forecast information enables truthful communication between the platform and its drivers, improving platform profitability. Hu et al. (2024) extend Guda and Subramanian (2019) by examining surge pricing, bonus incentives, and information sharing when riders can request service within or across regions. They find that cross-regional demand enhances the attractiveness of bonus strategies and reduces the effectiveness of surge pricing, while their findings on information align with Guda and Subramanian (2019). Jiang et al. (2021) propose a two-stage Stackelberg game involving regret-averse drivers who incur a relocation cost for moving between regions and receive a fixed bonus for successful matches in surge zones. They examine a setting where the platform can share the demand-to-supply ratio with drivers. Laboratory experiments confirm their analytical findings showing that when relocation costs exceed the bonus, too few drivers relocate to the surge zone, while when relocation costs are lower than the bonus, too many drivers relocate. Additionally, they find that incorporating drivers' behavioral biases can increase platform profits, enhance worker utility, and improve matching efficiency, provided the platform offers both a bonus and shares the demand-to-supply ratio. This is because regret-averse drivers are more likely to relocate to surge zones as compared to rational drivers.

Using a two-period, game-theoretical model, Hu et al. (2022) demonstrate the superiority of the "penetration surge pricing" policy—a low initial price followed by a high price—over the "skimming surge pricing" policy—a short-lived, sharp price surge followed by a low price—to motivate relocations when the platform shares information with drivers on supply and demand for the surge zone. Ma et al. (2022) develop a multi-period, multi-location planning game to determine the optimal sequence of matches and routes in a setting where both the platform and drivers have full knowledge of all network information (e.g., supply, demand, travel times, trip costs, and rider types) over the entire horizon. They identify a subgame-perfect dynamic equilibrium strategy (i.e., the spatio-temporal pricing mechanism) in which drivers always accept trip assignments and prove that this policy exhibits several desirable properties, including being temporally consistent, welfare-optimal, envy-free, and core-selecting. Finally, Bimpikis and Mantegazza (2023) study strategic information disclosure in a setting where a ride-hailing platform has private knowledge of future demand and interacts with potential drivers who decide whether to join the system. Using an information design approach, they establish the existence of a Bayesian equilibrium in which the platform selectively shares demand information to maximize profit. They show that the platform should disclose only partial information (i.e., demand is either high or low) to encourage driver entry when joining is costly or to discourage driver entry to induce higher prices. While this strategy enhances platform profitability as compared to not disclosing any information (and full disclosure for moderate values of the outside option), it can also reduce rider welfare by limiting the number of idle drivers and increasing prices.

Our study fits into the lower right quadrant of Table 3-1. We model the relocation decisions of regret-averse drivers moving to/from a non-surge to a surge zone when the platform offers a financial incentive (surge multiplier) in addition to sharing different types of information.

Specifically, building on the modeling framework of Jiang et al. (2021), we develop a two-period, two-region Stackelberg game that accounts for drivers' regret aversion, relocation costs, matching uncertainty, and the financial incentives provided by the platform to encourage relocation. Our model, however, introduces several novel features: (1) allows either zone to be the surge zone; (2) permits drivers to relocate to either region; (3) defines drivers' earnings as a function of ride distances rather than a fixed amount per ride; (4) replaces an additive bonus by a surge multiplier; and (5) as a complement to surge pricing, evaluates the impact of the platform sharing up to three pieces of information with the drivers: the distribution of riders, the average ride distance in one zone relative to the other, and the initial spatial distribution of drivers. These modifications substantially increase the complexity of the mathematical analysis—notably, deriving equilibrium solutions and the optimal surge multiplier value—and allow us to study the extent to which information can substitute for monetary incentives and what information is most effective at encouraging drivers to relocate. Furthermore, the added dynamics and emphasis on comparing information offer new operational insights.

3.3. Model Formulations

3.3.1. Initial Setting

In this section, we develop a two-period, two-region, game-theoretic model, which is a commonly used approach to study the problem of matching riders with self-interested, utility-maximizing drivers (e.g., Guda and Subramanian, 2019; Jiang et al., 2021; Afeche et al., 2023). For simplicity, we consider a setting with two zones, A and B, each with a different number of ride requests and idle drivers. Our Stackelberg game begins with the platform deciding on what information to share with the drivers. After observing the distribution of riders (demand) and drivers (supply), the platform sets a surge multiplier value and shares it, along with zone-based information, with all drivers. We assume that all drivers obtain this information and then immediately decide whether to remain in their current zone or relocate to maximize their utility. Once all relocation decisions are made, idle drivers are matched with riders in their selected zone, while any excess riders or drivers go unmatched. Table 3-2 provides an overview of the model notation.

Table 3-2. Notation summary

Notation	Description
Parameters	
$\boldsymbol{n}$	Total number of riders (or drivers) over both zones
$\boldsymbol{D_i}$	§ Number of riders in Zone $i, i \in \{A, B\}$
$\boldsymbol{S_i^0}$	§ Initial number of drivers in Zone $i, i \in \{A, B\}$
$\boldsymbol{S_i^1}$	§ Final number of drivers in Zone $i, i \in \{A, B\}$ after all relocations have taken place
$\boldsymbol{p}$	Price per kilometer (km)
$\boldsymbol{x_i}$	Average ride distance in Zone $i, i \in \{A, B\}$
$\boldsymbol{\theta}$	Drivers' commission on each ride where $0 < \theta \leq 1$
$\boldsymbol{c}$	§ Relocation cost
$\boldsymbol{\eta}$	§ The degree of drivers' aversion toward regret
Information to share	**Description**
$\boldsymbol{\rho}$	The proportion of ride requests in Zone A, which follows a uniform distribution on $(0,1)$ when it is unknown to drivers
$\boldsymbol{\lambda}$	The average ride distance in Zone B relative to Zone A, or $\lambda = \frac{x_B}{x_A}$, which follows a uniform distribution on $(0, Z)$ when it is unknown to drivers
$\boldsymbol{\alpha}$	The proportion of drivers initially located in Zone A, which follows a uniform distribution on $(0,1)$ when it is unknown to drivers
Outcomes	**Description**
$\boldsymbol{m}$	Surge multiplier on each ride
$\boldsymbol{\gamma_i}$	The proportion of drivers who relocate from Zone $i \in \{A, B\}$ to the other zone
$\boldsymbol{\pi_{k,i}^j}$	§ Driver earning initially located in Zone $k \in \{A, B\}$ and ends up in Zone $i \in \{A, B\}$, if a ride is available ($j = 1$) or not ($j = 0$)
$\boldsymbol{u_{A,i}}$	The expected regret-averse utility for a driver initially located in Zone A who ends up in Zone $i \in \{A, B\}$
$\boldsymbol{u_{B,i}}$	The expected regret-averse utility for a driver initially located in Zone B who ends up in Zone $i \in \{A, B\}$
$\widehat{\boldsymbol{M}}$	Supply-demand matching efficiency
$\widehat{\boldsymbol{\Pi}}$	Platform's profit

§ These parameters and assumptions are analogous to Jiang et al. (2021).

We assume there are exactly n drivers and riders in the system located in zones S_i^0 and D_i, respectively, for $i \in \{A, B\}$. Thus, there is enough supply ($S_A^0 + S_B^0 = n$) to fulfill demand ($D_A + D_B = n$); the platform must focus on incentivizing drivers to make decisions that balance drivers and riders across the regions. While Jiang et al. (2021) make a similar assumption, a key difference is that we do not assume all drivers are initially located in Zone A. Thus, depending on the distribution of drivers and riders, each zone can have a supply-shortage (*surge zone*) or a supply-overage (*non-surge zone*). This is important as it implies that drivers are unaware of supply-demand imbalances unless the platform shares this information.

Denoting the proportion of ride requests in Zone A as ρ, the demand in Zone A and Zone B is $D_A = \rho n$ and $D_B = (1 - \rho)n$, respectively. Consistent with Jiang et al. (2021), we assume ρ

follows a uniform distribution on $(0,1)$. This ensures that initial demand is random, zonal demands are negatively correlated, and drivers have no prior knowledge of which zone has higher demand. Similarly, denoting the proportion of drivers initially located in Zone A as α, which also follows a uniform distribution on $(0,1)$, we can write the initial supply for Zone A and Zone B as $S_A^0 = \alpha n$ and $S_B^0 = (1-\alpha)n$, respectively. This also ensures that the spatial distribution of drivers is negatively correlated and that they have no prior knowledge of which zone has higher supply. As the value of ρ (respectively, α) tends toward 0 or 1, all riders (respectively, drivers) are initially concentrated in a single zone. Since this scenario is somewhat unrealistic, and to simplify the mathematical analysis, we assume that these edge cases are inadmissible. Thus, Zone A is denoted as the "surge zone" when $\rho > \alpha$, whereas Zone B is a "surge zone" when $\rho < \alpha$.

Drivers earn income by matching with riders, while the platform collects a commission from each ride leaving the driver with an expected earning of $px_i\theta$. That is, a driver can expect to earn the product of the price p per kilometer (km) multiplied by the average ride distance x_i for $i \in \{A, B\}$ and commission rate θ. Parameters p and θ are set by the platform and known to all drivers (Boudreau, 2019) while x_i is not known until after a driver chooses to relocate or remain in the current zone. We define λ as the average ride distance in Zone B relative to Zone A; that is, $\lambda = \frac{x_B}{x_A}$. When a demand surge occurs, the platform implements a multiplicative surge pricing scheme where the price per km is increased by a surge multiplier, m, to mp for some $m \geq 0$; for instance, drivers see the value of the surge multiplier m for the surge zone on their heatmap (Haferkamp et al., 2023). This setting differs from Jiang et al. (2021) in which a fixed bonus is added to a driver's earning if the driver chooses to relocate and finds a ride. The multiplicative functional form is more realistic since it has been the most popular surge pricing policy of companies like Uber, Lyft, and DiDi (Zha et al., 2017; Chen et al., 2022; Abedinpour, 2024). Finally, riders exhibit price insensitivity up to a threshold below which they remain relatively indifferent to price changes (Chen et al., 2022). Thus, we assume that once this threshold is exceeded, the demand for ride requests naturally decreases because outside (alternative) options like walking, waiting, or using taxi services are more competitive.

Assumption 1. The surge multiplier m does not exceed the threshold m_{max}; that is, $m \leq m_{max}$.

Since all ride requests are registered through the platform, information for all supply- and demand-related parameters are unknown to drivers unless the platform decides to share this data. Thus, the game starts by having the platform observe the realized spatial distribution of riders and drivers in the two-zone system. They then decide (i) what information to share with the drivers to encourage them to relocate—that is, whether (or not) to share the proportion ρ of ride requests in Zone A, the average ride distance λ in Zone B relative to Zone A, and/or the proportion α of drivers initially located in Zone A. Notice that once drivers receive information about one zone, they can immediately infer the same parameter for the other zone due to the two-zone structure of the problem. The platform also determines (ii) the value of the surge multiplier m. In the second stage of the game, drivers observe m as well as any combination of ρ, λ, and α based on what has been shared by the platform. Drivers then decide whether to stay in their current zone or relocate to the other zone. Drivers who relocate to the other zone incur a penalty c representing a fixed relocation cost (Jiang et al., 2021). Once all relocations are complete, the platform matches riders with drivers located in the *same* zone. Unmet ride requests are assumed to be lost, and any excess supply of drivers remains unmatched. To account for the different combinations of information the platform may choose to share with drivers, we analyze eight models, as shown in Table 3-3. Each model specifies which piece(s) of information, in addition to the surge multiplier, the platform shares with drivers.

Table 3-3. Information the platform can share with the drivers (beside the surge multiplier m)

	Proportion of ride requests in Zone A (ρ)	The average ride distance in Zone B relative to Zone A (λ)	Proportion of drivers initially located in Zone A (α)
Model 1	Not shared	Not shared	Not shared
Model 2	Not shared	Shared	Not shared
Model 3	Not shared	Not shared	Shared
Model 4	Not shared	Shared	Shared
Model 5	Shared	Not shared	Not shared
Model 6	Shared	Shared	Not shared
Model 7	Shared	Not shared	Shared
Model 8	Shared	Shared	Shared

3.3.2. Driver Earning and Utility

The earnings for drivers who are initially located in Zone $k \in \{A, B\}$ and end up in Zone $i \in \{A, B\}$, denoted as $\pi_{k,i}^{j}$, depend on whether they are matched with a ride request ($j = 1$) or not ($j = 0$). Without loss of generality, we normalize the average ride distance in Zone B relative to Zone A by setting $x_A = 1$; this now gives $\lambda = x_B$. Hence, a driver who is initially located in Zone A and chooses to stay in Zone A earns

$$\pi_{A,A}^{j=1} = px_A\theta = p\theta, \tag{1}$$

if the driver is matched with a ride request in the same zone. Otherwise,

$$\pi_{A,A}^{j=0} = 0. \tag{2}$$

A driver who is initially located in Zone A, relocates to Zone B, and is matched with a rider in Zone B earns

$$\pi_{A,B}^{j=1} = mpx_B\theta - c = mp\lambda\theta - c. \tag{3}$$

Notice that because $m \geq 0$, Zone B is a surge zone if $m > 1$ and a non-surge zone otherwise. If such a driver is not matched with a rider, then the fixed cost associated with relocating is lost. That is,

$$\pi_{A,B}^{j=0} = -c. \tag{4}$$

To entice relocation, m must be suitably chosen such that $\pi_{A,B}^{j=1} > 0$, which implies that:

> **Assumption 2.** To ensure that drivers in Zone B are appropriately compensated for a match, either $mp\lambda\theta - c > 0$ if the average ride distance λ (in Zone B relative to zone A) is shared with (i.e., known to) drivers, or $mp\frac{Z}{2}\theta - c > 0$ if λ is not shared with (i.e., unknown to) drivers.

If a driver is initially located in Zone B and chooses to stay in Zone B, the driver earns

$$\pi_{B,B}^{j=1} = mp\lambda\theta, \tag{5}$$

if matched with a ride request in Zone B. Otherwise,

$$\pi_{B,B}^{j=0} = 0. \tag{6}$$

Finally, a driver who is initially in Zone B, relocates to Zone A, and is matched with a rider in Zone A earns

$$\pi_{B,A}^{j=1} = px_A\theta - c = p\theta - c. \tag{7}$$

Otherwise, if the driver is not matched, then again, the fixed cost associated with relocating is lost and

$$\pi_{B,A}^{j=0} = -c. \tag{8}$$

Here too, to entice relocation, we require $\pi_{B,A}^{j=1} > 0$, which gives:

Assumption 3. To ensure drivers in Zone A are appropriately compensated for a match, $p\theta - c > 0$.

We denote the proportion of drivers initially in Zone A and Zone B who choose to relocate as $\gamma_A \in [0,1]$ and $\gamma_B \in [0,1]$, respectively. Thus, the number of drivers in Zone A and Zone B after all relocations have taken place are $S_A^1 = (1-\gamma_A)\alpha n + \gamma_B(1-\alpha)n$ and $S_B^1 = (1-\gamma_B)(1-\alpha)n + \gamma_A \alpha n$, respectively. As a consequence of our setup, a driver who ends up in Zone A will be matched to a rider with probability $\min\left(1, \frac{D_A}{S_A^1} = \frac{\rho}{(1-\gamma_A)\alpha + \gamma_B(1-\alpha)}\right)$. This occurs if the demand for rides (D_A) is below the supply of drivers (S_A^1). A driver who ends up in Zone A will not be matched with probability $1 - \min\left(1, \frac{D_A}{S_A^1} = \frac{\rho}{(1-\gamma_A)\alpha + \gamma_B(1-\alpha)}\right)$. On the other hand, a driver who ends up in Zone B will be matched to a rider with probability $\min\left(1, \frac{D_B}{S_B^1} = \frac{1-\rho}{(1-\gamma_B)(1-\alpha) + \gamma_A \alpha}\right)$—which occurs if the demand for rides (D_B) is below the supply of drivers (S_B^1)—and will not be matched with probability $1 - \min\left(1, \frac{D_B}{S_B^1} = \frac{1-\rho}{(1-\gamma_B)(1-\alpha) + \gamma_A \alpha}\right)$.

Drivers may experience a sense of loss when they are not matched with a rider. This arises from counterfactual thinking, where individuals compare the outcome of their chosen actions with the potential outcome of an action they chose not to take. If the unchosen action would have led to a more favorable result, they may feel regret over their decision (Roese, 1994; Jiang et al., 2021). Thus, we consider utility functions that incorporate a regret-averse parameter which can augment the penalty for unfavorable outcomes, that is, relocation decisions that fail to result in a match. This parameter captures the psychological cost of regret experienced by drivers when their chosen action leads to a less desirable outcome as compared to an alternative they could have taken. Specifically, for drivers initially located in Zone $k \in \{A, B\}$ and who end up in Zone $i \in \{A, B\}$, we denote their utility as $u_{k,i}^j$, where $j \in \{0,1\}$ captures whether a driver is matched with a rider ($j = 1$) or not ($j = 0$). When $j = 1$, a driver feels no regret and the regret-averse utility is identical to the monetary payoff of the outcome, that is, $u_{k,i}^{j=1} = \pi_{k,i}^{j=1}$. In contrast, unmatched drivers feel regret and will perceive losses in the form of a foregone surplus impacted by the regret parameter. Following Özer and Zheng (2016) and Jiang et al. (2021), we consider a regret-averse parameter $\eta \geq 0$ and express the forgone surplus as the difference between the foregone payoff of the unchosen action and the realized payoff of the chosen action. Thus, the regret-averse utility for drivers who feel regret is $u_{k,i}^{j=0} = \pi_{k,i}^{j=1} - \eta(\pi_{k,i}^{j=1} - \pi_{k,-i}^{j=0})$, where the subscript "$-i$" refers to the unchosen zone. Note that if drivers are not regret-averse, then $\eta = 0$ and their utility $u_{k,i}^{j}$ is identical to their payoff $\pi_{k,i}^{j}$. Tables 3-4 and 3-5 summarize the regret-averse utilities along with the probabilities of finding a ride in that region.

Table 3-4. Drivers' regret-averse utility and matching probabilities (initially located in Zone A)

	Staying in Zone A		Relocating to Zone B	
	Available ride ($j = 1$)	Unavailable ride ($j = 0$)	Available ride ($j = 1$)	Unavailable ride ($j = 0$)
Utility ($u_{A,i}^{j}$)	$p\theta$	$0 - \eta(mp\lambda\theta - c)$	$mp\lambda\theta - c$	$-c - \eta(p\theta + c)$
Prob. of finding a ride	$\min\left\{1, \frac{\rho}{(1-\gamma_A)\alpha + \gamma_B(1-\alpha)}\right\}$	$1 - \min\left\{1, \frac{\rho}{(1-\gamma_A)\alpha + \gamma_B(1-\alpha)}\right\}$	$\min\left\{1, \frac{1-\rho}{(1-\gamma_B)(1-\alpha) + \gamma_A\alpha}\right\}$	$1 - \min\left\{1, \frac{1-\rho}{(1-\gamma_B)(1-\alpha) + \gamma_A\alpha}\right\}$

Table 3-5. Drivers' regret-averse utility and matching probabilities (initially located in Zone B)

	Staying in Zone B		Relocating to Zone A	
	Available ride ($j = 1$)	Unavailable ride ($j = 0$)	Available ride ($j = 1$)	Unavailable ride ($j = 0$)
Utility ($u_{B,i}^{j}$)	$mp\lambda\theta$	$0 - \eta(p\theta - c)$	$p\theta - c$	$-c - \eta(mp\lambda\theta + c)$
Prob. of finding a ride	$\min\left\{1, \frac{1-\rho}{(1-\gamma_B)(1-\alpha) + \gamma_A\alpha}\right\}$	$1 - \min\left\{1, \frac{1-\rho}{(1-\gamma_B)(1-\alpha) + \gamma_A\alpha}\right\}$	$\min\left\{1, \frac{\rho}{(1-\gamma_A)\alpha + \gamma_B(1-\alpha)}\right\}$	$1 - \min\left\{1, \frac{\rho}{(1-\gamma_A)\alpha + \gamma_B(1-\alpha)}\right\}$

From Tables 3-4 and 3-5, the expected regret-averse utility for a driver who is initially located in Zone A and who ends up in Zone $i \in \{A, B\}$, denoted by $\mathbb{E}[u_{A,i}(\eta|\mathcal{F})]$, is given by the following functions:

$$\mathbb{E}[u_{A,A}(\eta|\mathcal{F})] = p\theta \min\left\{1, \frac{\rho}{(1-\gamma_A)\alpha + \gamma_B(1-\alpha)}\right\} - \eta(mp\lambda\theta - c)\left(1 - \min\left\{1, \frac{\rho}{(1-\gamma_A)\alpha + \gamma_B(1-\alpha)}\right\}\right)$$

$$\mathbb{E}[u_{A,B}(\eta|\mathcal{F})] = (mp\lambda\theta - c)\min\left\{1, \frac{1-\rho}{(1-\gamma_B)(1-\alpha) + \gamma_A\alpha}\right\} - (c + \eta(p\theta + c)).\left(1 - \min\left\{1, \frac{1-\rho}{(1-\gamma_B)(1-\alpha) + \gamma_A\alpha}\right\}\right), \quad (9)$$

where $\mathcal{F}$ represents the shared information that is known by the drivers immediately before making their relocation decisions. Alternatively, the expected regret-averse utility for a driver who is initially located in Zone B and who ends up in Zone $i \in \{A, B\}$, denoted by $\mathbb{E}[u_{B,i}(\eta|\mathcal{F})]$, is given by the following functions:

$$\mathbb{E}[u_{B,A}(\eta|\mathcal{F})] = (p\theta - c)\min\left\{1, \frac{\rho}{(1-\gamma_A)\alpha + \gamma_B(1-\alpha)}\right\} - (c + \eta(mp\lambda\theta + c))\left(1 - \min\left\{1, \frac{\rho}{(1-\gamma_A)\alpha + \gamma_B(1-\alpha)}\right\}\right)$$

$$\mathbb{E}[u_{B,B}(\eta|\mathcal{F})] = mp\lambda\theta \min\left\{1, \frac{1-\rho}{(1-\gamma_B)(1-\alpha)+\gamma_A\alpha}\right\} - \eta(p\theta - c)\left(1 - \min\left\{1, \frac{1-\rho}{(1-\gamma_B)(1-\alpha)+\gamma_A\alpha}\right\}\right). \quad (10)$$

For (9) and (10), the expectation operator $\mathbb{E}[\cdot]$ is taken over the joint distribution of all uncertain parameters, which depends on what information $\mathcal{F}$ the platform chooses to share with drivers.

3.3.3. Platform Objectives and Equilibrium Solutions

We focus on two objectives: maximizing the (i) platform's profit; and (ii) supply-demand matching efficiency, which is defined as the number of ride requests that are successfully matched by drivers across both zones (Besbes et al., 2022; Afeche et al., 2023). While profitability is crucial for ride-hailing platforms survival, considering matching efficiency is also an important objective, because it can reduce the drivers' idle time, enhance the earnings of both drivers and platforms, and increase service quality through meeting more ride requests and faster (e.g., Chen et al., 2022; Hu and Zhou, 2022; Hu et al., 2024). Denoting the platform's profit function as $\widehat{\Pi}$ and the matching efficiency as $\widehat{M}$, the platform wishes to maximize:

$$\widehat{\Pi} = p(1-\theta)\min\{S_A^1, D_A\} + mp\lambda(1-\theta)\min\{S_B^1, D_B\} \quad (11)$$

and

$$\widehat{M} = \frac{\min\{S_A^1, D_A\} + \min\{S_B^1, D_B\}}{n} = \frac{\min\{(1-\gamma_A^*)\alpha n + \gamma_B^*(1-\alpha)n, \rho n\} + \min\{(1-\gamma_B^*)(1-\alpha)n + \gamma_A^*\alpha n, (1-\rho)n\}}{n}. \quad (12)$$

In our context, drivers act strategically by using the information provided to them and the observed surge multiplier to maximize their expected regret-averse utility. Therefore, the platform must offer adequate incentives and data transparency to maximize (11) or (12). To this end, let γ_i^* be the equilibrium solution associated with the proportion of drivers who relocate from Zone $i \in \{A, B\}$ and end up in the other zone, given the information available to them and the surge multiplier value set by the platform. To find γ_A^* and γ_B^*, we compare drivers' expected regret-averse utilities in (9) and (10) to find their intersection points. More specifically, over the joint distribution of all uncertain parameters, we solve $\mathbb{E}[u_{k,i}(\eta|\mathcal{F})] = \mathbb{E}[u_{k',i'}(\eta|\mathcal{F})]$ for any $k, k', i, i' \in \{A, B\}$ such that $(k, i) \neq (k', i')$. These equilibrium points allow us to identify the range of surge multiplier values for which a proportion of (potentially all) drivers will relocate (stay) to maximize their utilities. Nevertheless, the equilibrium points and surge multiplier ranges are functions of the information shared with drivers. Thus, they will differ depending on the model in Table 3-3.

3.3.3.1. Equilibria for Models 1-4

In Model 1 (Table 3-3), the platform does not share any information with drivers. Thus, the proportion ρ of ride requests in Zone A, the average relative ride distance λ in Zone B, and the proportion α of drivers initially located in Zone A, are unknown to them. Under this joint distribution, we explicitly derive the equilibrium values for γ_A^* and γ_B^*, noting that those for Models 2-4 closely mirror these solutions.

From (9), the expected regret-averse utilities of a driver initially located in Zone A, who either stays in Zone A or relocates to Zone B are, respectively,

$$\mathbb{E}[u_{A,A}(\eta|m)] = p\theta - \tfrac{1}{4}\left(p\theta + \eta\left(mp\tfrac{Z}{2}\theta - c\right)\right)(1 - \gamma_A + \gamma_B)$$

$$\mathbb{E}[u_{A,B}(\eta|m)] = mp\tfrac{Z}{2}\theta\,\tfrac{3+\gamma_B-\gamma_A}{4} - c - \eta(p\theta + c)\tfrac{1-\gamma_B+\gamma_A}{4}. \tag{13}$$

Similarly, from (10), the expected regret-averse utilities of a driver initially located in Zone B, who either relocates to Zone A or stays in Zone B are, respectively,

$$\mathbb{E}[u_{B,A}(\eta|m)] = p\theta - c - \tfrac{1}{4}\left(p\theta + \eta\left(mp\tfrac{Z}{2}\theta + c\right)\right)(1 - \gamma_A + \gamma_B)$$

$$\mathbb{E}[u_{B,B}(\eta|m)] = mp\tfrac{Z}{2}\theta - \left(mp\tfrac{Z}{2}\theta + \eta(p\theta - c)\right)\tfrac{1+\gamma_A-\gamma_B}{4}. \tag{14}$$

We consider nine different scenarios to find γ_A^* and γ_B^*: (i) $\gamma_A^* = \gamma_B^* = 0$; (ii) $\gamma_A^* = 1$ and $\gamma_B^* = 0$; (iii) $\gamma_A^* = 0$ and $\gamma_B^* = 1$; (iv) $\gamma_A^* = \gamma_B^* = 1$; (v) $0 < \gamma_A^* < 1$ and $0 < \gamma_B^* < 1$; (vi) $\gamma_A^* = 1$ and $0 < \gamma_B^* < 1$; (vii) $0 < \gamma_A^* < 1$ and $\gamma_B^* = 1$; (viii) $\gamma_A^* = 0$ and $0 < \gamma_B^* < 1$; and (ix) $0 < \gamma_A^* < 1$ and $\gamma_B^* = 0$. For instance, if $\gamma_A^* = \gamma_B^* = 1$, all drivers relocate from their original zones. For this to occur, the utility of moving to Zone B must exceed the utility of staying in Zone A for drivers initially located in Zone A, that is, $\mathbb{E}[u_{A,A}(\eta|m)] \le \mathbb{E}[u_{A,B}(\eta|m)]$, and the utility of moving to Zone A must exceed the utility of staying in Zone B for drivers who are initially located in Zone B, that is, $\mathbb{E}[u_{B,B}(\eta|m)] \le \mathbb{E}[u_{B,A}(\eta|m)]$. We use these inequalities to determine the range of surge multiplier values (m) that induce this behavior amongst the drivers. Theorem 1 summarizes the results of this derivation (*note:* all proofs appear in the online supplementary material).

Theorem 1. *For Model 1, the proportion of drivers relocating in equilibrium are:*

Table 3-6. Result summary (Theorem 1)

Region	% of drivers γ_A^* initially located in Zone A relocating to Zone B	% of drivers γ_B^* initially located in Zone B relocating to Zone A	Range for the surge multiplier m
1	0	1	$0 \le m \le \frac{2}{Z}\left(\frac{1}{2+\eta} - \frac{c}{p\theta}\right)$
2	0	$0 < \gamma_B < 1$	$\frac{2}{Z}\left(\frac{1}{2+\eta} - \frac{c}{p\theta}\right) \le m \le \frac{2}{Z}\left(1 - \frac{c(4+2\eta)}{p\theta(3+\eta)}\right)$

		$\gamma_B^* = \frac{p\theta(3+\eta)(2-mZ)-4c(2+\eta)}{p\theta(1+\eta)(mZ+2)}$	
3	0	0	$\frac{2}{Z}\left(1-\frac{c(4+2\eta)}{p\theta(3+\eta)}\right) \le m \le \frac{2}{Z}\left(1+\frac{c(4+2\eta)}{p\theta(3+\eta)}\right)$
4	$0<\gamma_A<1$ $\gamma_A^* = \frac{(3+\eta)\left(mp\frac{Z}{2}\theta - p\theta\right)-c(4+2\eta)}{(1+\eta)\left(p\theta+mp\frac{Z}{2}\theta\right)}$	0	$\frac{2}{Z}\left(1+\frac{c(4+2\eta)}{p\theta(3+\eta)}\right) \le m \le \frac{2}{Z}\left(1+\frac{c}{p\theta}\right)(2+\eta)$
5	1	0	$\frac{2}{Z}\left(1+\frac{c}{p\theta}\right)(2+\eta) \le m \le m_{max}$

When the platform sets a sufficiently low surge multiplier (Region 1), all drivers are incentivized to relocate from Zone B to Zone A, that is, Zone A becomes the *surge zone*. However, as m increases, the opposite occurs (Region 5). Note that it is never optimal for drivers in both regions to simultaneously relocate. Thus, out of the nine original scenarios, four of them are omitted from Table 3-6: (i) all drivers relocate from their original zones, $\gamma_A^* = \gamma_B^* = 1$; (ii) all drivers from one zone relocate to the other, while only some drivers from the second zone relocate, $\gamma_A^* = 1$ and $0 < \gamma_B^* < 1$ or $0 < \gamma_A^* < 1$ and $\gamma_B^* = 1$; and (iii) some drivers from one zone relocate to the other zone, $0 < \gamma_A^* < 1$ and $0 < \gamma_B^* < 1$. In this setting, because no information is shared, the platform's only operational lever is to signal that there is a demand imbalance by setting the surge multiplier value. For a sufficiently small value of m, drivers discern that demand in Zone A is much higher than in Zone B. Consequently, all or a portion of drivers initially located in Zone B relocate to Zone A (i.e., $\gamma_B^* = 1$ or $0 < \gamma_B^* < 1$ and $\gamma_A^* = 0$). Alternatively, if m is large enough, drivers ascertain that demand in Zone B is much higher than Zone A. Hence, all or a portion of drivers initially located in Zone A relocate to Zone B (i.e., $\gamma_A^* = 1$ or $0 < \gamma_A^* < 1$ and $\gamma_B^* = 0$). Finally, for some interval m, $\gamma_A^* = \gamma_B^* = 0$ as the supply-demand imbalance is insufficient to justify the cost of switching. Thus, all drivers stay in their original zones as the compensation is insufficient to incentivize relocation.

The equilibria for Models 2–4 are similar to Model 1. In Model 2, the platform shares with drivers the average ride distance λ in Zone B relative to Zone A, while ρ and α are unknown. Since λ follows a uniform distribution, the expected regret-averse utilities $\mathbb{E}[u_{A,A}(\eta|m,\lambda)]$, $\mathbb{E}[u_{A,B}(\eta|m,\lambda)]$, $\mathbb{E}[u_{B,A}(\eta|m,\lambda)]$, and $\mathbb{E}[u_{B,B}(\eta|m,\lambda)]$ are identical to, respectively, $\mathbb{E}[u_{A,A}(\eta|m)]$, $\mathbb{E}[u_{A,B}(\eta|m)]$, $\mathbb{E}[u_{B,A}(\eta|m)]$, and $\mathbb{E}[u_{B,B}(\eta|m)]$, except λ replaces $\frac{Z}{2}$. Hence, for Model 2, the equilibria in Theorem 1 hold with λ replacing $\frac{Z}{2}$. Similarly, for Model 3, the platform shares the proportion α of drivers initially located in Zone A, while ρ and λ are unknown. Again, the expected regret-averse utilities $\mathbb{E}[u_{A,A}(\eta|m,\alpha)]$, $\mathbb{E}[u_{A,B}(\eta|m,\alpha)]$, $\mathbb{E}[u_{B,A}(\eta|m,\alpha)]$, and $\mathbb{E}[u_{B,B}(\eta|m,\alpha)$ are similar to (13) and (14), except that $\left((1-\gamma_A)\alpha+\gamma_B(1-\alpha)\right)$ replaces $(1-\gamma_A+\gamma_B)$. Thus, for Model 3, the equilibria in Theorem 1 hold while γ_A^* and γ_B^* are multiplied by $\frac{1+\alpha+\alpha\eta}{(3+\eta)(1-\alpha)}$. Lastly, for Model 4, the platform shares the proportion α of drivers initially located in Zone A and the average ride distance λ in Zone B relative to Zone A; ρ remains unknown. As before, the drivers' expected regret-averse utilities are similar to (13) and (14) while Model 4's equilibria are identical to those in Theorem 1, except λ replaces $\frac{Z}{2}$ while γ_A^* and γ_B^* are multiplied by $\frac{1+\alpha+\alpha\eta}{(3+\eta)(1-\alpha)}$.

3.3.3.2. Equilibria for Models 5 and 6

In Model 5, the platform shares with drivers the proportion ρ of ride requests in Zone A, while α and λ are unknown. The drivers' expected regret-averse utilities are now given by $\mathbb{E}[u_{A,A}(\eta|m,\rho)]$, $\mathbb{E}[u_{A,B}(\eta|m,\rho)]$, $\mathbb{E}[u_{B,A}(\eta|m,\rho)]$, and $\mathbb{E}\left[u_{B,B}(\eta|m,\rho)\right]$. Although the general approach for deriving equilibrium values remains the same as in Theorem 1—that is, by identifying the intersection points—γ_A^* and γ_B^* are considerably more complex as they involve composite functions of logarithms. This arises because the platform chooses to share ρ, which means that drivers know the exact number of drivers in each zone (as defined in Tables 3-4 and 3-5). Consequently, deriving the equilibrium values and the corresponding surge multiplier ranges for which they are valid becomes significantly more intricate. However, using the Lambert function, these values can still be expressed in closed form. Theorem 2 summarizes the results.

Theorem 2. *For Model 5, defining $W(.)$ as the Lambert function and h(m), f(m), g(m), and j(m) linear fractional functions of m, the proportion of drivers relocating in equilibrium are:*

Table 3-7. Result summary (Theorem 2)

Region	% of drivers γ_A^* initially located in Zone A relocating to Zone B	% of drivers γ_B^* initially located in Zone B relocating to Zone A	Range for the surge multiplier m
1	0	1	$0 \le m \le \frac{2}{Z}\left(\frac{\rho}{1-\eta\rho+\eta}-\frac{c}{p\theta}\right)$
2.1	0	1 when $\rho-\gamma_B<0$	$0 \le m \le \frac{\frac{1+\eta}{1-\rho}(p\theta\rho-c)+\eta(p\theta-c)\,log[1-\rho]-\frac{\rho}{1-\rho}(c\eta+p\theta)\,log[\rho]}{\frac{1}{2}pZ\theta\left((1+\eta)-log[1-\rho]+\frac{\rho}{1-\rho}\eta log[\rho]\right)}$
2.2	0	$0<\gamma_B<1$	$\frac{2}{Z}\left(\frac{\rho}{1-\eta\rho+\eta}-\frac{c}{p\theta}\right) \le m \le \frac{\frac{1+\eta}{1-\rho}(p\theta\rho-c)+\eta(p\theta-c)\,log[1-\rho]-\frac{\rho}{1-\rho}(c\eta+p\theta)\,log[\rho]}{\frac{1}{2}pZ\theta\left((1+\eta)-log[1-\rho]+\frac{\rho}{1-\rho}\eta log[\rho]\right)}$

	$1-h(m)W\left(\frac{1}{h(m)}e^{j(m)}\right)$[3] when $\rho-\gamma_B \geq 0$		
3	0	0	$\frac{\frac{1+\eta}{1-\rho}(p\theta\rho-c)+\eta(p\theta-c)\,log[1-\rho]-\frac{\rho}{1-\rho}(c\eta+p\theta)\,log[\rho]}{\frac{1}{2}pZ\theta\left((1+\eta)-log[1-\rho]+\frac{\rho}{1-\rho}\eta log[\rho]\right)} \leq m \leq \frac{\frac{1+\eta}{1-\rho}(c+p\theta\rho)+\eta(c+p\theta)\,log[1-\rho]+\frac{\rho}{1-\rho}(c\eta-p\theta)\,log[\rho]}{\frac{1}{2}pZ\theta\left((1+\eta)-log[1-\rho]+\eta\frac{\rho}{1-\rho}log[\rho]\right)}$
4.1	$0<\gamma_A<1$ $1-f(m)W\left(\frac{1}{f(m)}e^{g(m)}\right)$[4] when $\rho \leq 1-\gamma_A$	0	$\frac{\frac{1+\eta}{1-\rho}(c+p\theta\rho)+\eta(c+p\theta)\,log[1-\rho]+\frac{\rho}{1-\rho}(c\eta-p\theta)\,log[\rho]}{\frac{1}{2}pZ\theta\left((1+\eta)-log[1-\rho]+\eta\frac{\rho}{1-\rho}log[\rho]\right)} \leq m \leq \frac{2}{Z}\left(1+\frac{c}{p\theta}\right)\left(\frac{1+\eta\rho}{1-\rho}\right)$
4.2	1 when $\rho > 1-\gamma_A$	0	$\frac{\frac{1+\eta}{1-\rho}(c+p\theta\rho)+\eta(c+p\theta)\,log[1-\rho]+\frac{\rho}{1-\rho}(c\eta-p\theta)\,log[\rho]}{\frac{1}{2}pZ\theta\left((1+\eta)-log[1-\rho]+\eta\frac{\rho}{1-\rho}log[\rho]\right)} \leq m \leq m_{max}$
5	1	0	$\frac{2}{Z}\left(1+\frac{c}{p\theta}\right)\left(\frac{1+\eta\rho}{1-\rho}\right) \leq m \leq m_{max}$

Notice that the ranges of the surge multipliers differ significantly as compared to Theorem 1. First, the proportion ρ of ride requests in Zone A appears in these equations since this information is shared with drivers. Second, the equilibrium points are solutions to a transcendental equation and by sharing ρ, logarithmic expressions are introduced into the regret-averse utility functions. Nevertheless, as in Theorem 1, there is no solution where (i) all drivers relocate from their original zones (i.e., $\gamma_A^* = \gamma_B^* = 1$); (ii) all drivers from one zone relocate to the other, while only some drivers from the second zone relocate (i.e., $\gamma_A^* = 1$ and $0 < \gamma_B^* < 1$ or $0 < \gamma_A^* < 1$ and $\gamma_B^* = 1$); and (iii) only some drivers from one zone relocate to the other zone (i.e., $0 < \gamma_A^* < 1$ and $0 < \gamma_B^* < 1$). For Model 6, the platform shares with drivers the proportion ρ of ride requests in Zone A as well as the average ride distance λ in Zone B relative to Zone A; α remains unknown. The resulting equilibria are similar to those in Table 3-7, except λ replaces $\frac{Z}{2}$ in Theorem 2.

3.3.3.3. Equilibria for Models 7 and 8

For Model 7, only the average ride distance λ in Zone B relative to Zone A is unknown. Because the platform shares both α and ρ, the calculation of the probabilities of finding a ride are known

---

3 $h(m) = \frac{-(1-\rho)\left(mp\frac{Z}{2}\theta+\eta(p\theta-c)\right)}{(\eta+1)(p\theta-c)}$ and $j(m) = \frac{1}{-(1-\rho)\left(mp\frac{Z}{2}\theta+\eta(p\theta-c)\right)}\Big(-(1-\rho)\log[1-\rho]\left(mp\frac{Z}{2}\theta+\eta(p\theta-c)\right)-\rho(p\theta-c)+\rho\log[\rho]\left(p\theta+\eta\left(mp\frac{Z}{2}\theta+c\right)\right)+\left(c+\eta\left(mp\frac{Z}{2}\theta+c\right)\right)(1-\rho)-\rho\left(mp\frac{Z}{2}\theta+\eta(p\theta-c)\right)+mp\frac{Z}{2}\theta+(\eta+1)(p\theta-c)\Big)$.

4 $f(m) = \frac{-\rho\left(p\theta+\eta\left(mp\frac{Z}{2}\theta-c\right)\right)}{(1+\eta)\left(mp\frac{Z}{2}\theta-c\right)}$ and $g(m) = \frac{1}{-\rho\left(p\theta+\eta\left(mp\frac{Z}{2}\theta-c\right)\right)}\Big(p\theta\rho-\rho\log[\rho]\left(p\theta+\eta\left(mp\frac{Z}{2}\theta-c\right)\right)+\rho\eta\left(mp\frac{Z}{2}\theta-c\right)+(1-\rho)\log[1-\rho]\left(mp\frac{Z}{2}\theta+\eta(p\theta+c)\right)+\rho\left(mp\frac{Z}{2}\theta+\eta(p\theta+c)\right)\Big)$.

to the drivers (see Tables 3-4 and Table 3-5). In particular, subcases in the derivations of the equilibrium solutions emerge, and they depend on whether $\frac{\rho}{(1-\gamma_A)\alpha+\gamma_B(1-\alpha)} \leq 1$, which implies $\alpha \geq \max\left(0, \frac{\rho-\gamma_B}{1-\gamma_A-\gamma_B}\right)$, or $\frac{1-\rho}{(1-\gamma_B)(1-\alpha)+\gamma_A\alpha} \leq 1$, which implies $\alpha \leq \max\left(0, \frac{\rho-\gamma_B}{1-\gamma_A-\gamma_B}\right)$. Theorem 3 summarizes the findings.

Theorem 3. *For Model 7, the proportion of drivers relocating in equilibrium are:*

Table 3-8. Result summary (Theorem 3) when $\alpha \leq max\left(0, \frac{\rho-\gamma_B^*}{1-\gamma_A^*-\gamma_B^*}\right)$

Region	% of drivers γ_A^* initially located in Zone A relocating to Zone B	% of drivers γ_B^* initially located in Zone B relocating to Zone A	Range for the surge multiplier m
1	0	$0 < \gamma_B < 1$ $\gamma_B^* = 1 - \frac{\left(mp\frac{Z}{2}\theta + \eta(p\theta - c)\right)(1-\rho)}{(p\theta - c)(1-\alpha)(1+\eta)}$	$\frac{2}{Z}\left(1 - \frac{c}{p\theta}\right) \leq m \leq \frac{2}{Z}\left(1 - \frac{c}{p\theta}\right)\frac{1-\alpha+\eta(\rho-\alpha)}{1-\rho}$
2	0	0	$\frac{2}{Z}\left(1 - \frac{c}{p\theta}\right)\left(\frac{1-\alpha+\eta(\rho-\alpha)}{1-\rho}\right) \leq m \leq \frac{2}{Z}\left(1 + \frac{c}{p\theta}\right)\left(\frac{1-\alpha+\eta(\rho-\alpha)}{1-\rho}\right)$
3	$0 < \gamma_A < 1$ $\gamma_A^* = \frac{(1-\rho)mp\frac{Z}{2}\theta - (p\theta + c)\left(1-\alpha+\eta(\rho-\alpha)\right)}{\alpha(p\theta + c)(1+\eta)}$	0	$\frac{2}{Z}\left(1 + \frac{c}{p\theta}\right)\frac{1-\alpha+\eta(\rho-\alpha)}{1-\rho} \leq m \leq \frac{2}{Z}\left(1 + \frac{c}{p\theta}\right)\left(\frac{1+\eta\rho}{1-\rho}\right)$
4	1	0	$\frac{2}{Z}\left(1 + \frac{c}{p\theta}\right)\left(\frac{1+\eta\rho}{1-\rho}\right) \leq m \leq m_{max}$

Table 3-9. Result summary (Theorem 3) when $\alpha \geq max\left(0, \frac{\rho-\gamma_B^*}{1-\gamma_A^*-\gamma_B^*}\right)$

Region	% of drivers γ_A^* initially located in Zone A relocating to Zone B	% of drivers γ_B^* initially located in Zone B relocating to Zone A	Range for the surge multiplier m
1	0	1	$0 \leq m \leq \frac{2}{Z}\left(\frac{\rho}{1-\eta\rho+\eta} - \frac{c}{p\theta}\right)$
2	0	$0 < \gamma_B < 1$ $\gamma_B^* = \frac{\rho p\theta + \left(mp\frac{Z}{2}\theta + c\right)(\eta(\rho-\alpha)-\alpha)}{\left(mp\frac{Z}{2}\theta + c\right)(1-\alpha)(1+\eta)}$	$\frac{2}{Z}\left(\frac{\rho}{1-\eta\rho+\eta} - \frac{c}{p\theta}\right) \leq m \leq \frac{2}{Z}\left(\frac{\rho}{\alpha+\eta(\alpha-\rho)} - \frac{c}{p\theta}\right)$
3	0	0	$\frac{2}{Z}\left(\frac{\rho}{\alpha+\eta(\alpha-\rho)} - \frac{c}{p\theta}\right) \leq m \leq \frac{2}{Z}\left(\frac{\rho}{\alpha+\eta(\alpha-\rho)} + \frac{c}{p\theta}\right)$
4	$0 < \gamma_A < 1$ $\gamma_A^* = 1 - \frac{\rho\left(p\theta + \eta\left(mp\frac{Z}{2}\theta - c\right)\right)}{\alpha(1+\eta)\left(mp\frac{Z}{2}\theta - c\right)}$	0	$\frac{2}{Z}\left(\frac{\rho}{\alpha+\eta(\alpha-\rho)} + \frac{c}{p\theta}\right) \leq m \leq \frac{2}{Z}\left(1 + \frac{c}{p\theta}\right)$

Once again, there is no solution where $\gamma_A^* = \gamma_B^* = 1$, $\gamma_A^* = 1$ and $0 < \gamma_B^* < 1$, $0 < \gamma_A^* < 1$ and $\gamma_B^* = 1$, and $0 < \gamma_A^* < 1$ and $0 < \gamma_B^* < 1$. If the proportion α of drivers initially located in Zone A satisfies $\alpha \geq \max\left\{0, \frac{\rho-\gamma_B^*}{1-\gamma_A^*-\gamma_B^*}\right\}$, no surge multiplier exists where $\gamma_A^* = 1$ and $\gamma_B^* = 0$. Conversely, when $\alpha \leq \max\left\{0, \frac{\rho-\gamma_B^*}{1-\gamma_A^*-\gamma_B^*}\right\}$, no surge multiplier exists where $\gamma_A^* = 0$ and $\gamma_B^* = 1$. These cases arise in the limit where $\alpha = 0$ or $\alpha = 1$ (singleton sets), respectively, which as previously mentioned, signifies that all drivers are initially concentrated in a single zone. This is observed in the proof of this result, where we also derive the closed-form solutions for all equilibrium values under each of the subcases. Finally, we remark that Model 8's equilibria closely mirror those of Model 7 such that Theorem 3 remains valid except that λ replaces $\frac{Z}{2}$.

3.3.4. Structure of the Optimal Solution

3.3.4.1. Optimal Supply-Demand Matching Efficiency

Given the optimal relocation behavior of drivers, we next explore how the platform should set the surge multiplier to maximize the matching efficiency. Using a property of the minimum function, $\widehat{M}$ is given by

$$\widehat{M} = \frac{\min\{S_A^1, D_A\} + \min\{S_B^1, D_B\}}{n} = \frac{1}{n}\left(\frac{1}{2}(S_A^1 + D_A) - \frac{1}{2}|S_A^1 - D_A| + \frac{1}{2}(S_B^1 + D_B) - \frac{1}{2}|S_B^1 - D_B|\right)$$
$$= 1 - |\rho - \alpha(1-\gamma_A^*) - (1-\alpha)\gamma_B^*|. \quad (15)$$

To determine the m^* that maximizes (15), we identify optimal surge multiplier values that are conditional on m^* existing within each of the regions specified in Theorems 1 to 3. We compare these surge multipliers to identify a set of *candidate solutions* of which one is guaranteed to be globally optimal. Theorem 4 outlines the general structure of the candidate solution set and properties of the matching efficiency.

Theorem 4. *For each of the eight models in Table 3-3:*

(a) *The optimal surge multiplier* m^* *is either at one of the endpoints of its corresponding interval, equals zero, or solves* $|\rho - \alpha(1-\gamma_A^*) - (1-\alpha)\gamma_B^*| = 0$.

(b) *A closed-form or analytic expression exists for all candidate surge multipliers and their corresponding matching efficiency values.*

(c) *The set of candidate optimal surge multipliers is non-empty and finite.*

For all eight models, the optimal surge multiplier is located at the endpoints of the corresponding interval when either all drivers from one zone relocate to the other while no drivers relocate in the reverse direction, or no relocation occurs between the zones. This is because, in these scenarios, matching efficiency is a linear function of the surge multiplier. However, when only a portion of drivers relocate between zones, the optimal surge multiplier depends on multiple factors such as whether a zone's demand exceeds its supply (i.e., whether $\alpha > \rho$ or $\alpha \leq \rho$) and the cost-to-earnings ratio (i.e., $\frac{c}{p\theta}$). In these cases, the optimal surge multiplier lies within a finite set of interval endpoints, $m = 0$, or when $|\rho - \alpha(1-\gamma_A^*) - (1-\alpha)\gamma_B^*| = 0$. Note that although $m = 0$ might seem counterintuitive, it indicates that the surge multiplier should be set so small that drivers are highly motivated to relocate from Zone B to Zone A.

3.3.4.2. Optimal Profit

Similar to Section 3.3.4.1, we explore how the platform should set the surge multiplier to maximize the profit. For tractability, (12) can be simplified to:

$$\begin{aligned}
\widehat{\Pi} &= p(1-\theta)\min\{S_A^1, D_A\} + mp\lambda(1-\theta)\min\{S_B^1, D_B\} \\
&= \frac{1}{2}p(1-\theta)(S_A^1 + D_A - |S_A^1 - D_A|) + \frac{1}{2}mp\lambda(1-\theta)(S_B^1 + D_B - |S_B^1 - D_B|) \\
&= \frac{1}{2}np(1-\theta)\Big(\big(\rho + \alpha(1-\gamma_A^*) + \gamma_B^*(1-\alpha)\big)(1-m\lambda) + 2m\lambda\Big) \\
&\quad -\frac{1}{2}np(1-\theta)(1+m\lambda)|\rho - \alpha(1-\gamma_A^*) - (1-\alpha)\gamma_B^*|. \qquad (16)
\end{aligned}$$

To determine the m^* that maximizes $\widehat{\Pi}$, we again identify optimal surge multiplier values that are conditional on m^* existing within each of the regions specified in Theorems 1 to 3. We then compare these surge multipliers to derive a set of candidate solutions of which one is guaranteed to be globally optimal. Theorem 5 summarizes the general structure of the candidate set and the corresponding platform profit.

Theorem 5.

(a) *For all models in Table 3-3, a closed-form or analytic expression exists for all candidate surge multiplier values and their corresponding profit values.*

(b) *The set of candidate optimal surge multipliers is non-empty and finite.*

We, interestingly, observe similar properties for the profit function as we do for matching efficiency. However, in some cases, we can eliminate a greater number of candidate solutions. For instance, in Models 1–4 as well as Models 7 and 8, when $\alpha \geq \max\left\{0, \frac{\rho - \gamma_B^*}{1-\gamma_A^*-\gamma_B^*}\right\}$, the optimal surge multiplier is either at the upper bound of its corresponding interval, equals zero, or solves $|\rho - \alpha(1-\gamma_A^*) - (1-\alpha)\gamma_B^*| = 0$. The lower bound is never optimal. Similarly, for Models 5 and 6 as well as Models 7 and 8, when $\alpha \leq \max\left\{0, \frac{\rho - \gamma_B^*}{1-\gamma_A^*-\gamma_B^*}\right\}$, the optimal surge multiplier is either at one of the endpoints of its corresponding interval, equals zero, or solves $|\rho - \alpha(1-\gamma_A^*) -$

$(1-\alpha)\gamma_B^*| = 0$. This occurs because setting a higher m allows the platform to earn greater profits, which aligns with drivers' motivation to maximize earnings. Thus, the selection of m_{max} is a critical component of our approach. Indeed, because the model does not account for outside opportunities, it assumes that matches will still occur even if m_{max} is set unrealistically high. In practice, setting m_{max} to be large would reduce riders' demand, violating the assumptions of our model.

3.4. Numerical Study

Building on the theoretical results from the previous section, we conduct a numerical analysis to evaluate how information sharing affects the platforms matching efficiency and profitability. We do so by manipulating six parameters: (a) the average ride distance in Zone B relative to Zone A, λ; (b) the proportion of drivers initially located in Zone A, α; (c) the proportion of riders in Zone A, ρ; (d) the relocation cost, c; (e) the degree of drivers' aversion to regret, η; and (f) the maximum possible surge multiplier, m_{max}. In what follows, we focus on presenting key numerical insights and relegate all tables to the online supplementary material.

For our experiments, the price p per km and the driver commission θ per ride are set to \$0.81 and 0.75, respectively, reflecting Uber's price per km in Canada (Uber Blog, 2019) and driver commission (Uber, 2019). From Assumption 3 (i.e., $p\theta - c > 0$), the relocation cost c is initially set to 0.30 but can range from 0.01 to 0.60. Drivers' degree of aversion to regret takes two values: $\eta = 0.699$ as estimated in Jiang et al.'s (2021) experiment; and $\eta = 1.2$ as used in these authors' numerical analysis. However, we also perform a sensitivity analysis with respect to η. The maximum possible surge multiplier m_{max} is initially set to 5, although we experiment with how varying this parameter affects the solution structure. Note that while Uber does not reveal a range for the surge multiplier, Özdemir (2024) mentions that it "can vary from 1.1× to 3× or more". The total number of drivers (n) is set to 100 following Jiang et al. (2021), although its value does not impact our findings. When known to drivers, the average ride distance λ in Zone B relative to Zone A follows a uniform distribution on $(0, Z)$ with Z set to 2 or 4 as ride patterns can vary throughout the day. When a sensitivity analysis is not with respect to λ, we set λ to its expected value of $\frac{Z}{2}$. Finally, the proportion of riders (ρ) and drivers (α) follow uniform distributions between on (0,1). Thus, unless this information is provided to the drivers by the platform, drivers' expectation of these values are 0.5. The numerical results are presented in Appendix B.

3.4.1. Optimizing Supply-Demand Matching Efficiency

3.4.1.1. Should Information Be Shared?

We find that sharing information with drivers can reduce the reliance on surge pricing as the primary mechanism for matching supply and demand. Specifically, Model 8 (sharing all information) outperforms Models 4, 6, and 7 (sharing two pieces of information) in terms of having higher matching efficiencies or lower surge multiplier values for the same efficiency. Similarly, Models 4, 6, and 7 outperform Models 1, 2, 3, and 5, where either no information or one piece of information is shared. This leads to the first insight.

Insight 1. *Sharing information with drivers can be a substitute for monetary compensation.*

Figure 3-1 illustrates **Insight 1.** We focus on even-numbered models because the optimal matching efficiencies and surge multipliers are identical to the odd-numbered models by setting $\lambda = \mathbb{E}[\lambda] = \frac{Z}{2}$. The proportion ρ of ride requests in Zone A is set to 0.4, while the proportion α of drivers located in Zone A varies from 0.45 to 0.99. In these scenarios, Zone B is the surge zone, and thus, the surge multiplier exceeds 1.0. However, over the entire interval, the matching efficiency equals 1.0. For $\alpha > 0.6$, sharing all three pieces of information outperforms sharing one or two such pieces, or sharing no information at all. Consequently, sharing more information lowers the optimal surge multiplier, with the substitution effect being more pronounced when the imbalance $|\rho - \alpha|$ between available drivers and ride requests is large.

Figure 3-1. The optimal surge multiplier vs. the proportion of drivers in Zone A

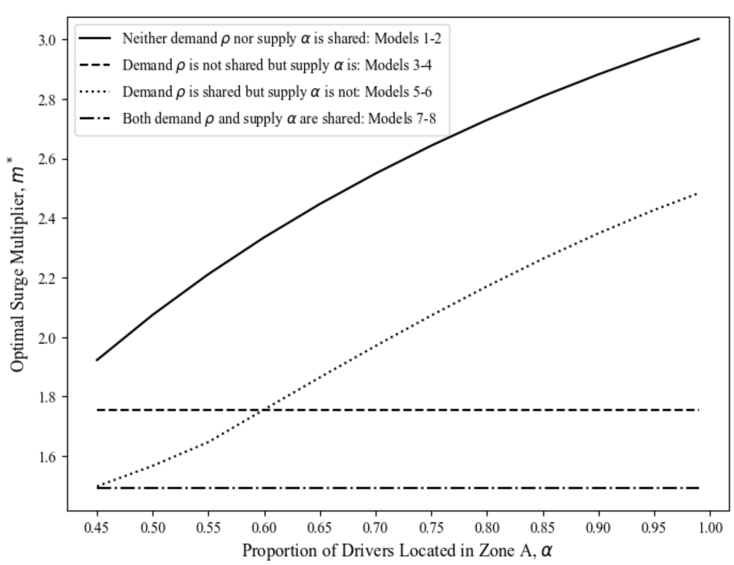

$\rho = 0.4$
$c = 0.3$
$\eta = 1.2$
$p = 0.81$
$\theta = 0.75$
$n = 100$
$m_{max} = 5$
$Z = 2$
$\lambda = 1$

Nevertheless, as illustrated in the bottom left of Figure 3-1, the type of information that is shared can be important. In fact, in some cases, information sharing may be unnecessary. For instance, when the relocation cost c is small, the matching efficiency can be maximized via the surge multiplier alone; there is no additional benefit (i.e., reducing the multiplier) to sharing information. This leads to the second insight.

Insight 2. *When the relocation cost is negligible, there is no additional value in sharing information. This effect is amplified when the imbalance between idle drivers and ride requests is small.*

Figure 3-2 illustrates **Insight 2**. We again vary Zone A's proportion α of drivers between 0.45 and 0.99 while fixing $\rho = 0.4$, which ensures that all models achieve a matching efficiency of 1.0. As in Figure 3-1, Zone B is the surge zone. However, in contrast to Figure 3-1, the relocation cost in Figure 3-2 is $c = 0.01$, which is 30 times lower. Model 1 now has the lowest surge multiplier, with a more pronounced effect for small imbalances between idle drivers and ride requests. This suggests that when the relocation cost is negligible, the surge multiplier alone can be used to incentivize driver relocation behavior.

Figure 3-2. The optimal surge multiplier vs. the proportion of drivers located in Zone A

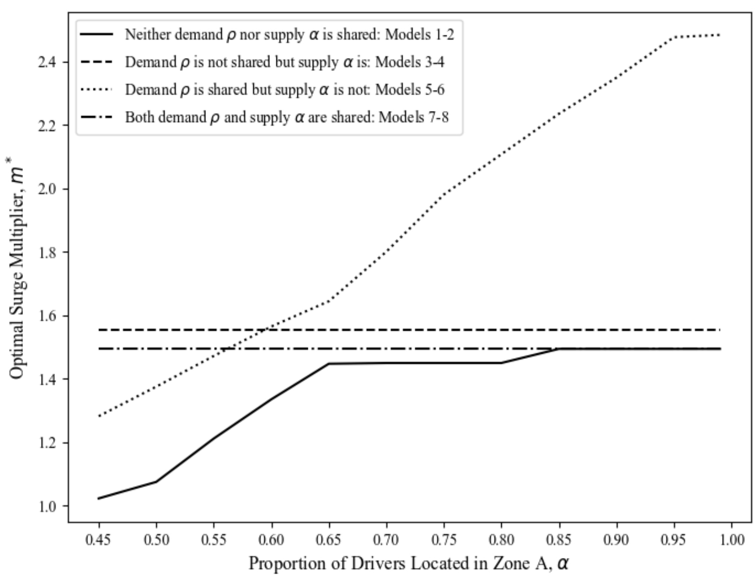

$\rho = 0.4$
$c = 0.01$
$\eta = 1.2$
$p = 0.81$
$\theta = 0.75$
$n = 100$
$m_{max} = 5$
$Z = 2$
$\lambda = 1$

Figure 3-2 also indicates that the optimal surge multiplier does not always vary predictably, and this behavior can depend on the type of information that is shared with drivers. Specifically, in this setting, the matching efficiency is maximized when m^* solves $|\rho - \alpha(1-\gamma_A^*) - (1-\alpha)\gamma_B^*| = 0$. When the proportion α of drivers initially located in Zone A is not shared with drivers (i.e., Models 1–2 and 5–6), the optimal surge multiplier is dependent on α. Alternatively, when α is shared with drivers (i.e., Models 3–4 and 7–8), m^* does not depend on α and the optimal surge multiplier remains fixed as α is varied. This dichotomy highlights how information sharing can alter the optimal surge multiplier's functional form and, consequently, influence the stability of the pricing relationship between m^* and supply/demand.

Insight 3. *The optimal surge multiplier value varies nonlinearly with the magnitude of the imbalance between idle drivers and ride requests as well as what information is shared with drivers.*

Figure 3-3 further illustrates **Insight 3** for scenarios where the proportion ρ of ride requests in Zone A varies from 0.01 to 0.95 and the supply of drivers is set to $\alpha = 0.2$. Note that while most drivers are in Zone B (since $1 - \alpha = 0.8$), high values of ρ indicates a surge in Zone A, while low values of ρ indicates a surge in Zone B. When ρ is not shared (Models 1–4), the surge multiplier varies with respect to the imbalance $|\rho - \alpha|$. That is, for large values of ρ, the optimal surge multiplier is below 1.0 as most of the ride requests are in Zone A. As ρ decreases, the surge multiplier increases until its value approaches m_{max}. This monotonic relationship occurs because drivers believe that demand in Zone A equals $\mathbb{E}[\rho] = 0.5$. Therefore, to correct drivers' misperception about the number of ride requests, a higher surge multiplier is used. Nevertheless, as is observed in Figure 3-3, the change in the surge multiplier over the range is nonlinear.

Alternatively, when demand ρ is shared with drivers (Models 5–8), the behavior of the surge multiplier depends on whether α is known. If it is (Models 7–8), two optimal surge multiplier values exist, one above and below 1.0, depending on whether Zone A has more riders or drivers. Since drivers are directly informed about the exact supply-demand imbalance, less financial incentive is needed to motivate relocation, as it already aligns with their best interest. If α is not known (Models 5–6), then the surge multiplier is used to correct drivers' misperception about the number of drivers is Zone A. That is, drivers assume $\mathbb{E}[\alpha] = 0.5$. Because $\alpha = 0.2$, Zone A is the surge zone when $\rho \geq 0.2$, which requires that $m^* < 1$ to incentivize drivers to relocate to Zone A. As ρ approaches α (i.e., decreases from 0.95 to 0.2), drivers' perceived that the supply shortage diminishes, reducing their motivation to relocate. Consequently, the platform lowers the surge multiplier in Zone B to incentivize movement to Zone A, even when $\rho < \mathbb{E}[\alpha]$. When $\rho < 0.2$, Zone B becomes the surge zone necessitating $m^* \geq 1$ to make it more attractive. In this case, drivers overestimate the actual supply shortage based on the perceived gap between ρ and $\mathbb{E}[\alpha]$. As ρ decreases, ride requests increasingly concentrate in Zone B. Since $\alpha = 0.2$, most drivers are already in Zone B and the platform aims to ensure they do not relocate. Therefore, while $m^* \geq 1$, it gradually decreases because the imbalance $|\rho - \mathbb{E}[\alpha]|$ alone is enough for the remaining drivers in Zone A to be incentivized to relocate to Zone B.

Figure 3-3. The optimal surge multiplier vs. the proportion of ride requests in Zone A

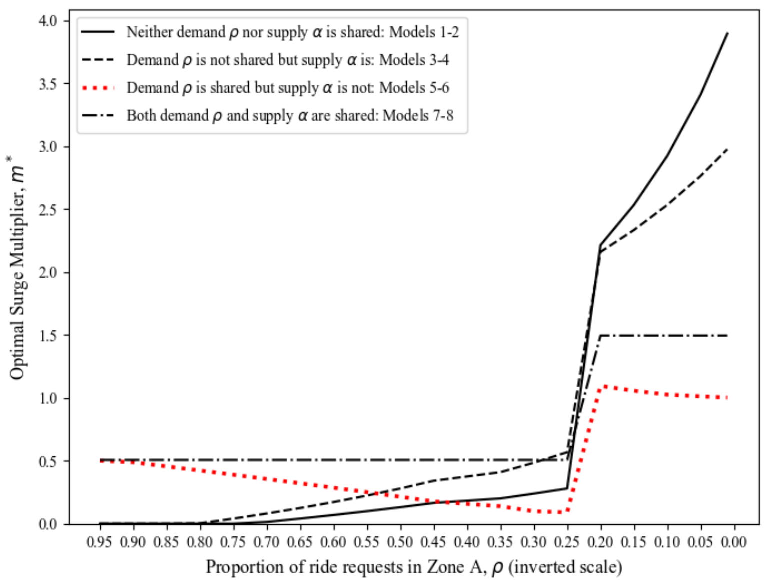

$\alpha = 0.2$
$c = 0.3$
$\eta = 0.699$
$p = 0.81$
$\theta = 0.75$
$n = 100$
$m_{max} = 5$
$Z = 2$
$\lambda = 1$

3.4.1.2. What Information Should Be Shared and When?

We next analyze the effect of sharing the average ride distance ratio λ with drivers. We find that sharing λ is beneficial (i.e., greater matching efficiency and smaller surge multiplier) provided $\lambda > \mathbb{E}[\lambda]$ in the surge zone. Specifically, if Zone B is the surge zone and $\lambda > \mathbb{E}[\lambda]$, sharing λ encourages drivers to relocate to Zone B and reduces the need for a high surge multiplier. In contrast, if Zone B is the surge zone but $\lambda < \mathbb{E}[\lambda]$, then Zone B becomes less attractive, requiring the platform to raise the surge multiplier to compensate. A similar effect is observed when Zone A is the surge zone. This leads to the fourth insight.

Insight 4. *When the average ride distance in a surge zone exceeds its expectation, sharing this information yields greater matching efficiency and smaller surge multiplier values.*

Figure 3-4 illustrates **Insight 4** by plotting the optimal surge multiplier as a function of the average ride distance ratio λ (in Zone B relative to Zone A), which varies between 0.1 and 3.9. Because the supply $\alpha = 0.9$ and the demand $\rho = 0.2$, Zone B is the surge zone. In these scenarios, the optimal matching efficiency across all eight models is 1.0. Since $\mathbb{E}[\lambda] = \frac{Z}{2} = 2$, when $\lambda < 2$, m^* is lower for the odd-numbered models (where λ is not shared). Conversely, when $\lambda > 2$, m^* is lower for the even numbered models which shares λ with drivers. These findings suggest that sharing λ can act as a direct substitute to the surge multiplier.

Figure 3-4. The optimal surge multiplier vs. average ride distance in Zone B relative to Zone A

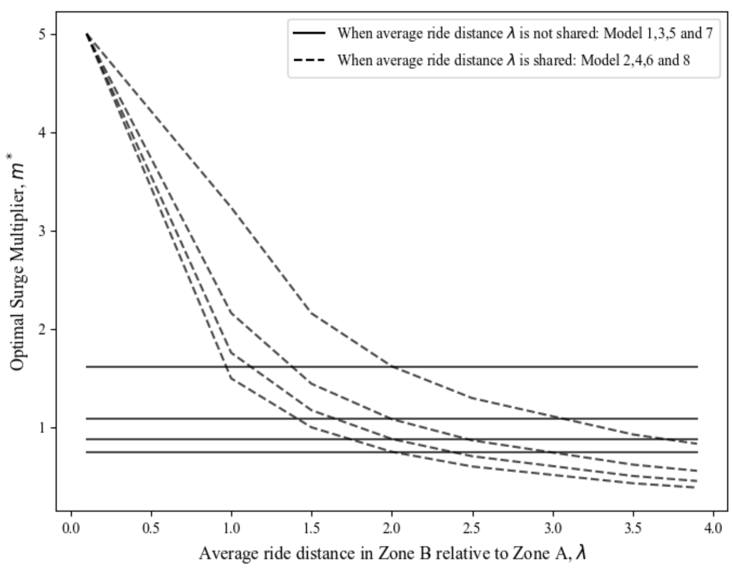

$\alpha = 0.9$
$\rho = 0.2$
$c = 0.3$
$\eta = 0.699$
$p = 0.81$
$\theta = 0.75$
$n = 100$
$m_{max} = 5$
$Z = 4$

We next consider the effect of sharing supply α and demand ρ information with drivers. We find that the benefit depends on the magnitude of the imbalance $|\rho - \alpha|$. Figure 3-5 illustrates this for scenarios where $\rho = 0.2$ and $0.2 \leq \alpha \leq 0.99$ (note the inverted scale for $|\rho - \alpha|$). In these cases, all models achieve a matching efficiency of 1.0. However, when $|\rho - \alpha|$ is sufficiently high, Models 7–8 have the lowest optimal surge multiplier values followed by Models 5–6. As $|\rho - \alpha|$ decreases (e.g., $\alpha \leq 0.3$ and $0 \leq |\rho - \alpha| \leq 0.1$), Models 1–2 have the smallest m^* as compared to the other models. Models 1–2 then become the preferred choice when the system is fully balanced, meaning $|\rho - \alpha| = 0$. This leads to a fifth insight.

Insight 5. *Information sharing is beneficial when there are large supply-demand imbalances.*

Figure 3-5. The optimal surge multiplier vs. the supply-demand imbalance

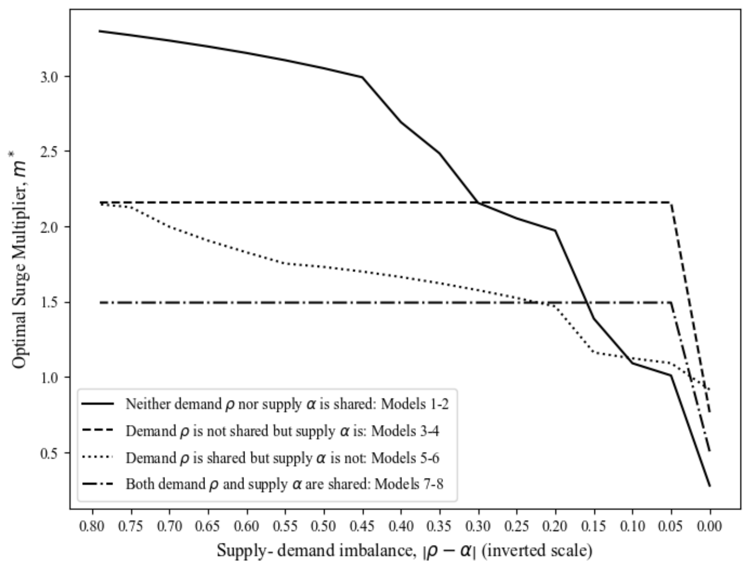

$c = 0.3$
$\eta = 1.2$
$p = 0.81$
$\theta = 0.75$
$n = 100$
$m_{max} = 5$
$Z = 2$
$\lambda = 1$

3.4.1.3. How Do Key Model Parameters Affect the Outcomes?

Jiang et al. (2021) show that the relocation cost c influences the drivers' relocation decisions, with high financial incentives (e.g., large bonuses) being necessary when c is high. We now explore how the information shared with drivers may impact this finding. Our experiments indicate that higher relocation costs negatively affect all models, primarily by increasing the optimal surge multiplier. However, the ordering of the models remain unchanged as the relocation cost varies: Models 7–8 (where both supply α and demand ρ are shared) exhibit lower surge multipliers than Models 3–4 (where α is shared but not ρ), which then exhibit lower surge multipliers than Models 5–6 (where ρ is shared but not α). Models 1–2 (where neither supply α nor demand ρ is shared) have the highest m^*. Figure 3-6(a) illustrates this finding when all models achieve a matching efficiency of 1.0 and Zone B is the surge zone (i.e., $\alpha > \rho$).

As illustrated in Figure 3-6(b) where Zone A is the surge zone (i.e., $\alpha < \rho$), increasing the relocation cost reduces the matching efficiency for Models 1–4, whereas Models 5–8 maintain a matching efficiency of 1.0 over the entire range. Furthermore, the difference between Models 3–4 and Models 5–6 in Figures 3-6(a) and 3-6(b) is entirely driven by which region is the surge zone. Overall, the impact of relocation costs on outcomes reinforces the notion that information sharing serves a similar role as surge pricing; higher relocation costs require more information to improve matching efficiency. This leads to a sixth insight.

Insight 6. *The benefits of information sharing increase as the relocation cost rises.*

Figure 3-6. The optimal surge multiplier or matching efficiency vs. the cost of driver relocation

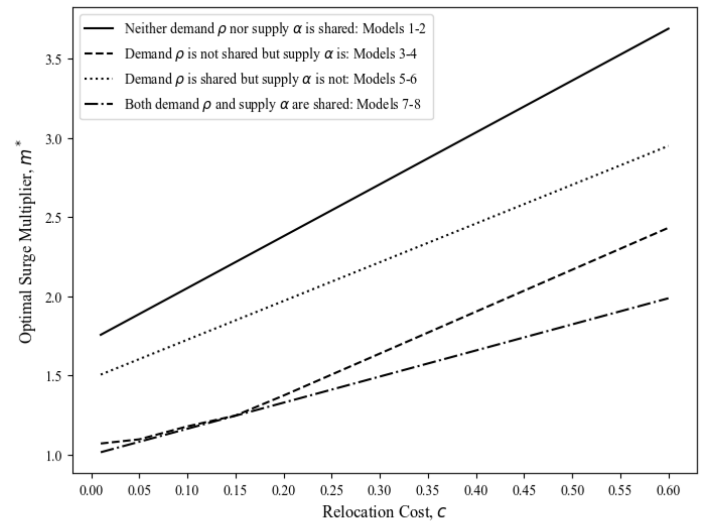

(a) Trend in the optimal surge multiplier when Zone B's demand exceeds supply: $\alpha = 0.95 > \rho = 0.4$

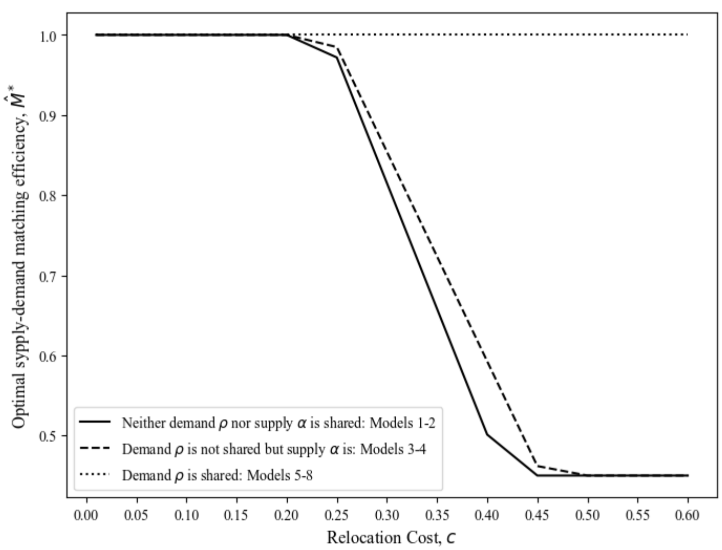

(b) Trend in the matching efficiency when Zone B's supply exceeds demand: $\alpha = 0.4 < \rho = 0.95$

$p = 0.81$	$\theta = 0.75$	$\eta = 0.699$	$n = 100$	$m_{max} = 5$	$Z = 2$	$\lambda = 1$

We next analyze the impact of the regret aversion parameter η on information sharing. Our findings indicate that the benefits of information sharing persist across a broad range of values, with its effectiveness increasing as drivers become more regret averse. That is, to overcome their reluctance and ensure adequate numbers relocate to the surge zone, providing information on both supply α and demand ρ (i.e., Models 7–8) results in the lowest value of the optimal surge multiplier m^*. This leads to a seventh insight.

Insight 7. *The more regret averse drivers are, the more effective information sharing becomes.*

Figure 3-7. The optimal surge multiplier vs. drivers' aversion to regret

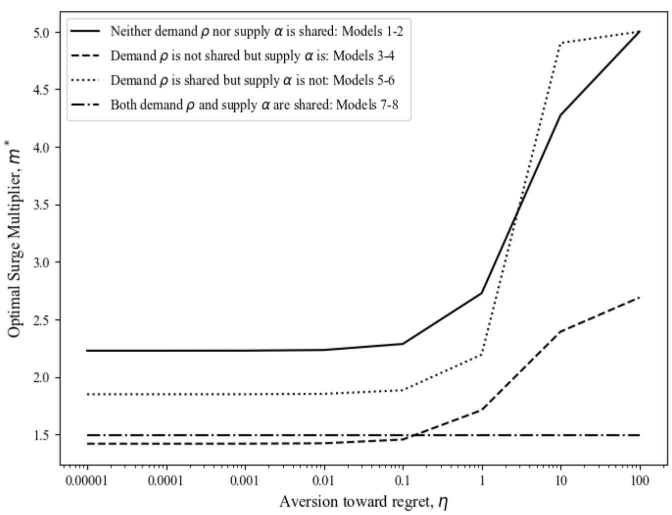

$\alpha = 0.85$
$\rho = 0.4$
$c = 0.3$
$p = 0.81$
$\theta = 0.75$
$n = 100$
$m_{max} = 5$
$Z = 2$
$\lambda = 1$

Figure 3-7 illustrates **Insight 7** where $\eta = 0.00001$ signifies that drivers are rather rational and $\eta = 100$ represents drivers that are highly averse to regret. In all cases, the models achieve an optimal matching efficiency of 1.0. However, Models 3–4 and 7–8, which share the proportion α of drivers in Zone A, consistently yield the lowest optimal surge multiplier. While these models exhibit similar performance for small values of η, Models 7–8 give the lowest optimal surge multiplier when $\eta > 0.1$. In contrast, Models 1–2 and 5–6 (which do not share α), have the highest surge multiplier values over the entire interval.

3.4.2. Optimizing Platform Profit

By maximizing profit rather than supply-demand matching efficiency, we observe that when the maximum surge multiplier (m_{max}) is sufficiently large, the optimal surge multiplier is consistently set to this value. This occurs for all models and numerical scenarios, and aligns with the platform's incentive structure, since an increase in m^* also increases the commission drivers earn per ride. Nevertheless, a large value for m_{max} introduces practical limitations. Specifically, excessive ride costs undermine the model's insights, as in reality, riders will opt for cheaper transportation alternatives (outside options). However, as m_{max} decreases, the optimal surge multipliers for both objectives converge. Further, by varying m_{max} across $\{5, 10, 15, 25, 50, 100\}$, we observe in Figure 3-8 that the profit-maximizing surge multiplier converges more quickly to the efficiency-maximizing value when more information is shared. This leads to a final insight.

Insight 8. *As the largest possible surge multiplier m_{max} decreases, the optimal surge multipliers associated with maximizing profit and supply-demand matching efficiency converge, with the rate dependent on what information is shared.*

Figure 3-8. Convergence of the optimal surge multiplier when maximizing matching efficiency

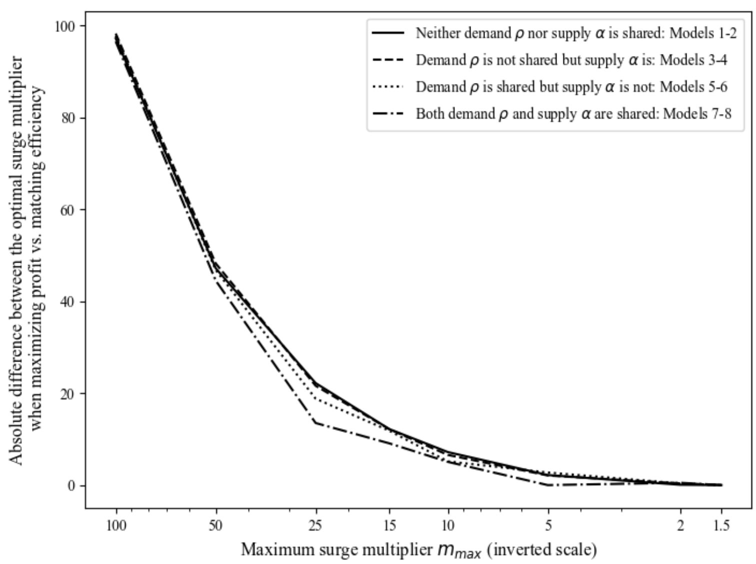

$\alpha = 0.85$
$\rho = 0.4$
$c = 0.3$
$\eta = 1.2$
$p = 0.81$
$\theta = 0.75$
$n = 100$
$Z = 2$
$\lambda = 1$

3.5. Concluding Remarks

Financial incentives, such as surge pricing, are commonly employed mechanisms to encourage ride-hailing drivers to relocate from non-surge to surge zones. However, the excessive use of this operational lever to influence idle drivers' behavior has been a persistent concern for regulators, customers, and even ride-hailing platforms themselves (e.g., Willingham, 2017; Miao et al., 2023; Ngila, 2023; Lynley, 2024). This study examines how sharing information about the proportions of ride requests, drivers, and average ride distances between zones affects (i) regret-averse drivers' decisions to relocate and (ii) matching efficiency and platform profitability. Of particular interest is whether information sharing can substitute for monetary compensation, the extent of this effect, and the conditions under which different information is most effective. Using a two-period Stackelberg game, we compare various information-sharing strategies against a baseline model that only shares the surge multiplier value.

Our findings are consistent with Bimpikis et al. (2019), Özkan (2020), Besbes et al. (2021), and Lee et al. (2023) in showing that surge pricing is particularly beneficial when supply (idle drivers) and demand (ride requests) are imbalanced. Importantly, we find that selecting a reasonable upper bound for the surge multiplier enables the platform to simultaneously optimize matching efficiency and profit. This result aligns with Zeng and He (2023), who advocate for imposing regulatory interventions to cap surge multiplier values. Indeed, our analysis indicates that information can generally serve as a substitute for financial incentives, with greater information disclosure resulting in a larger reduction in the surge multiplier. However, we also find that the impact of shared information—the proportion of ride requests across zones, the proportion of drivers across zones, and the average ride distance in one zone relative to the other—is not solely determined by the imbalance between idle drivers and ride requests. Instead, it is also shaped by critical factors such as relocation costs, drivers' degree of regret aversion, and their expectations about information that has been withheld. Thus, our study advances ride-hailing research by clarifying how surge pricing and information interact and identifying what types of information are most valuable and when.

Despite its contributions to theory and practice, this study has several limitations. Our models do not account for temporal dynamics, which can capture the different response timescales of riders and drivers to surge pricing and shared information. While incorporating multiple time periods would better reflect real-world conditions, it would also introduce significant complexity and reduce tractability. For instance, ride requests may be canceled due to price changes, or drivers may enter or exit zones before completing trips, altering the zone's surge status before matching occurs. Our models also assume that drivers accept assigned rides after relocating, whereas in practice, they can still accept or reject a ride request after relocating. Accounting for this decision-making could offer deeper insights into the value and timing of information sharing. While we assume that platforms share credible information—as noted by Hu et al. (2024) and Guda and Subramanian (2019)—platforms may have an incentive to share false data. Future models could explore how drivers perceive and respond to potentially biased information and whether a driver can glean additional insight from repeated interactions with a platform that varies the information it discloses. Furthermore, our models assume information is shared symmetrically with all drivers. In reality, platforms like Uber can modify what to disclose based on factors such as market conditions, driver ratings, and shift history. Examining how information should be tailored to drivers could refine strategies for optimizing platform performance. Finally, our analysis focuses on platform profit and matching efficiency. These are, however, not the only relevant objectives to consider. Driver welfare, rider surplus, and environmental impact are also important factors, especially when they conflict with efficiency-based outcomes tied to profit. Incorporating these considerations into future models would deepen appreciation for the positive and negative externalities of surge pricing and information sharing on supply-side (i.e., drivers), demand-side (i.e., riders), and societal metrics, as well as their complex trade-offs.

Chapter 4

Conclusions

4.1. Overview

Ride-hailing platforms have witnessed rapid growth in recent years. The profitability of these platforms hinges on their ability to efficiently match supply (i.e., drivers) with demand (i.e., ride requests) over time and across geographic zones. However, optimizing supply-demand matching efficiency remains an ongoing challenge since drivers independently determine when and where to work. Ensuring sufficient supply availability across zones poses a persistent difficulty. This dissertation comprises two essays that contribute to the literature on ride-hailing platforms.

Chapter 2 reviews research published in OSCM journals pertaining to challenges ride-hailing platforms face regarding day-to-day operations. A primary focus of research on ride-hailing platforms in OSCM regards the impact that interactions among stakeholders and environmental factors have on ride-hailing platform's outcomes (e.g., profit and service level maximization), riders (e.g., delay minimization) and/or drivers (e.g., labor welfare). Chapter 2 systematically identifies 89 relevant articles published in OSCM journals. Analysis of these 89 publications led to the development of an overarching framework to categorize OSCM research on ride-hailing platforms into five prevalent themes (i.e., ride-hailing platform's decisions affecting platform, rider, and driver outcomes; demand-side and supply-side behaviors affecting ride-hailing platform's decisions and stakeholder outcomes; ride-hailing platform's decisions affecting driver and/or rider behavior and stakeholder outcomes; environmental factors affecting ride-hailing platform's decisions and stakeholder outcomes; and economic, environmental, and social impacts of ride-hailing platforms. Chapter 2 concludes by offering five future research directions for OSCM scholars to consider (i.e., interactions among mechanisms for desired driver behavior; competition for riders and drivers, ride-hailing collaboration with other ride-hailing platforms or car-rental companies, regulatory agencies as stakeholders, and sharing untruthful information).

Focusing on how ride-hailing platforms can efficiently match supply (i.e., drivers) to demand (i.e., ride requests) dynamically across geographical regions (i.e., zones), Chapter 3 develops a two-stage Stackelberg game to optimize supply-demand matching efficiency and profitability for ride-hailing platforms. The platform determines the optimal surge multiplier to offer and selects specific pieces of information to share with drivers. Chapter 3 determines how information sharing, in addition to surge pricing, influences drivers' relocation decisions and, more importantly, conditions under which surge pricing can be substituted with information sharing. The latter research findings enable ride-hailing platforms to lower their operational costs while enhancing supply-demand matching efficiency. These analytically derived research findings complement prior scholarly work on supply-demand matching via drivers' relocation decisions (e.g., Guda and Subramanian, 2019; Hu et al., 2022; Jiang et al., 2021).

4.2. Discussion of Contributions

A primary contribution of Chapter 2 is the development of an organizing framework that categorizes the existing OSCM literature on ride-hailing platforms into five main themes, addressing the following five corresponding questions: a) How do ride-hailing platform's decisions influence outcomes for platforms, riders, and drivers?; b) How do rider and driver behaviors and attributes affect platform's decisions and stakeholder outcomes?; c) How do platform's decisions impact rider and driver behaviors, subsequently influencing stakeholder outcomes?; d) How do environmental factors shape platform's decisions and their effects on platforms, drivers, and riders?; e) What are the economic, environmental, and societal impacts of ride-hailing services?

This framework benefits established OSCM researchers by summarizing the research questions addressed in this context, highlighting areas where significant work has been done, and identifying themes of ride-hailing operational challenges that require further attention. It also reveals new parameters recently introduced in the literature that were previously overlooked. New OSCM researchers interested in studying ride-hailing platforms can benefit from this framework in multiple ways. Primarily, it saves time by providing a summarized and organized schematic of existing literature, helping them not only identify previously explored research questions but also the relative attention that prior work has levied on these research questions. Additionally, the framework facilitates the positioning of emerging research findings within the identified themes. Practitioners can also leverage this framework to enhance decision-making. It helps ride-hailing platforms identify key stakeholders and their objectives while recognizing that their decisions are influenced by various factors, including supply- and demand-side behavioral dynamics and regulatory mechanisms. Last, the framework demonstrates how the internal platform's decisions impact broader outcomes such as public transit usage (economic), hate crime prevalence (social), and greenhouse gas emissions (environmental), which policymakers may wish to take into consideration as new legislation is enacted.

A major contribution of Chapter 3 is the role that supply, demand, and ride-distance information play in drivers' relocation decisions from non-surge to surge zones and, importantly, the conditions under which the sharing of these pieces of information is beneficial to the ride-hailing platform, its drivers, and riders. This contribution reveals that information sharing in a ride-hailing context is not always beneficial, as prior research highlights. It also pinpoints a new piece of information (i.e., ride distance) that can be shared to improve supply-demand matching efficiency and platform's profitability while reducing both driver idle time and rider waiting time. A second major and related contribution is delineating conditions under which information sharing can effectively substitute for surge pricing in drivers' relocation decisions from non-surge to surge zones. This novel contribution can reduce operational costs for ride-hailing platforms and the fares that riders in surge zones pay. A third and final contribution is the magnitude of the surge multiplier that can optimize both supply-demand matching efficiency and platform's profitability simultaneously, with and without information sharing. This contribution extends prior work, deeming supply-demand matching efficiency and platform's profitability as desirable outcomes that are trade-offs.

4.3. Future Research

This dissertation highlights several broad considerations for future research on drivers' relocation decisions from non-surge to surge zones.

One is the need for more empirical confirmations of theoretical insights derived from prior analytical modeling studies. The literature review in Chapter 2 reveals that 76 percent of research on ride-hailing platforms published in operations and supply chain management journals derive insights from developing analytical models. These theoretical insights deserve empirical attention not only to determine the real-world conditions that bound their applicability and validity but also to assess real-world complexities necessitating alterations of their explanatory and predictive value. Case-based research, survey research, archival secondary data research, and experiments are likely to be useful methodological approaches for empirical investigations. For example, algorithms for matching ride requests to drivers (cf., Besbes et al., 2022; Feng et al., 2021) can be evaluated via case-based or field experiments to determine their effectiveness across cities varying in size (e.g., medium-sized cities like Calgary versus large metropolitan areas like Toronto). The influence of pricing on the behavior of earnings-sensitive drivers or price-sensitive riders (cf., Bai et al., 2019; Bernstein et al., 2021) may also be empirically assessed by surveying drivers. Archival data from Uber may delve into incentive schemes that have been analytically shown to moderate driver or rider cancellation behavior (cf., Haferkamp et al., 2024; Mejia and Parker, 2021). Last, the analytical results from Chapter 3 may, likewise, be assessed in field or laboratory experiments to evaluate the value of different pieces of information in relocation decisions from surge to non-surge zones.

The focus of this dissertation has been the impact of sharing specific pieces of information on drivers' relocation decisions and ride-hailing platform performance from a game theory perspective (Kumar et al., 2018). A second consideration for future research is to augment this theoretical perspective with theories and insights from other disciplines. For example, information asymmetry theory (cf., Aboody and Lev, 2000), with one party having more private information than another, may be a useful theoretical lens to investigate whether and when ride-hailing platforms may benefit from selectively sharing either accurate or misleading information to influence driver behavior. Signaling theory (cf. Connelly et al., 2011) may be another useful theoretical lens to investigate how ride-hailing platforms (as signal senders) strategically communicate information to drivers (as signal recipients) and influence their behavior. Signals sent via heatmaps versus text alerts may, for example, be interpreted and perceived differently by drivers.

Finally, insights from prior research, as well as from this dissertation, are typically generated while assuming monopolistic conditions. A third consideration is to relax this assumption, modeling and analyzing the practice of information sharing in tandem with or separate from surge pricing under competitive conditions (e.g., multiple ride-hailing platforms in the same market, ride-hailing platforms competing with traditional transportation options for drivers and riders, or ride-hailing platforms performing logistic activities other than passenger transport such as product delivery). Drivers and riders, for example, can multi-home (i.e., use multiple platforms).

Understanding how drivers make relocation decisions or prioritize one platform over another and whether there exists a win-win scenario for competing platforms sharing information with drivers would extend the extant knowledge.

References

Abedinpour, P. (2024). How Uber Calculates Your Ride Fare: The Inside Scoop on Their Pricing Strategy! https://medium.com/@peymaan.abedinpour/how-uber-calculates-your-ride-fare-the-inside-scoop-on-their-pricing-strategy-bee21e050a2f (Accessed on 22 January 2025).

Aboody, D., & Lev, B. (2000). Information asymmetry, R&D, and insider gains. *The journal of Finance*, *55*(6), 2747-2766.

Afeche, P., Liu, Z., & Maglaras, C. (2023). Ride-Hailing Networks with Strategic Drivers: The Impact of Platform Control Capabilities on Performance. *Manufacturing & Service Operations Management*, *25*(5), 1890–1908.

Agarwal, S., Mani, D., & Telang, R. (2023). The impact of ride-hailing services on congestion: Evidence from indian cities. *Manufacturing & Service Operations Management, 25(3),* 862-883.

Agatz, N.A.H., Erera, A.L., Savelsbergh, M.W.P., & Wang, X. (2011). Dynamic ride-sharing: a simulation study in Metro Atlanta. *Transportation Research Part B 45* (9), 1450–1464.

Agussurja, L., Cheng, S. F., & Lau, H. C. (2019). A state aggregation approach for stochastic multiperiod last-mile ride-sharing problems. *Transportation Science*, *53*(1), 148-166.

Ai, W., Chen, Y., Mei, Q., Ye, J., & Zhang, L. (2023). Putting teams into the gig economy: A field experiment at a ride-sharing platform. *Management Science, 69*(9), 5336-5353.

Al-Kanj, L., Nascimento, J., & Powell, W. B. (2020). Approximate dynamic programming for planning a ride-hailing system using autonomous fleets of electric vehicles. *European Journal of Operational Research*, *284*(3), 1088-1106.

Allon, G., Cohen, M. C., & Sinchaisri, W. P. (2023). The impact of behavioural and economic drivers on gig economy workers. *Manufacturing & Service Operations Management, 25*(4), 1376-1393.

Alvarez, F., & Argente, D. (2022). On the effects of the availability of means of payments: The case of uber. *The Quarterly Journal of Economics*, *137*(3), 1737-1789.

Amey, A., Attanucci, J., & Mishalani, R. (2011). Real-time ridesharing: opportunities and challenges in using mobile phone technology to improve rideshare services. *Transportation Research Record, 2217*(1), 103-110.

Angrist, J. D., Caldwell, S., & Hall, J. V. (2021). Uber versus taxi: A driver's eye view. *American Economic Journal: Applied Economics, 13*(3), 272-308.

Arora, K., Zheng, F., & Girotra, K. (2024). Private vs. pooled transportation: Customer preference and design of green transport policy. *Manufacturing & Service Operations Management*, *26*(2), 594-611.

Bai, J., So, K. C., Tang, C. S., Chen, X. (Michael), & Wang, H. (2019). Coordinating Supply and Demand on an On-Demand Service Platform with Impatient Customers. *Manufacturing & Service Operations Management*, *21*(3), 556–570.

Barrios, J. M., Hochberg, Y. V., & Yi, H. (2023). The cost of convenience: Ride-hailing and traffic fatalities. *Journal of Operations Management, 69(5)*, 823-855.

Bassamboo, A., Randhawa, R. S., & Zeevi, A. (2010). Capacity sizing under parameter uncertainty: Safety staffing principles revisited. *Management Science*, *56*(10), 1668-1686.

Beirigo, B. A., Schulte, F., & Negenborn, R. R. (2022). A learning-based optimization approach for autonomous ridesharing platforms with service-level contracts and on-demand hiring of idle vehicles. *Transportation Science*, *56*(3), 677-703.

Benjaafar, S., & Hu, M. (2020). Operations management in the age of the sharing economy: What is old and what is new?. *Manufacturing & Service Operations Management, 22*(1), 93-101.

Benjaafar, S., Bernhard, H., Courcoubetis, C., Kanakakis, M., & Papafragkos, S. (2022). Drivers, Riders, and Service Providers: The Impact of the Sharing Economy on Mobility. *Management Science*, *68*(1), 123-142.

Benjaafar, S., Ding, J.-Y., Kong, G., & Taylor, T. (2022). Labor Welfare in On-Demand Service Platforms. *Manufacturing & Service Operations Management*, *24*(1), 110–124.

Berman, O., Fazel-Zarandi, M. M., & Krass, D. (2019). Truthful cheap talk: Why operational flexibility may lead to truthful communication. *Management Science, 65*(4), 1624-1641.

Bernstein, F., DeCroix, G. A., & Keskin, N. B. (2021). Competition Between Two-Sided Platforms Under Demand and Supply Congestion Effects. *Manufacturing & Service Operations Management*, *23*(5), 1043–1061.

Besbes, O., Castro, F., & Lobel, I. (2021). Surge Pricing and Its Spatial Supply Response. *Management Science*, *67*(3), 1350–1367.

Besbes, O., Castro, F., & Lobel, I. (2022). Spatial capacity planning. *Operations Research*, *70*(2), 1271-1291.

Bimpikis, K., & Mantegazza, G. (2023). Strategic release of information in platforms: Entry, competition, and welfare. *Operations Research*, *71*(5), 1619-1635.

Bimpikis, K., Candogan, O., & Saban, D. (2019). Spatial Pricing in Ride-Sharing Networks. *Operations Research*, *67*(3), 744–769.

Boudreau, M. (2019). Changes to time and distance rates for Uber Black, SUV, Select. https://www.uber.com/en-CA/blog/time-distance-rates-black-canada/ (Accessed on 26 January 2025).

Braverman, A., Dai, J. G., Liu, X., & Ying, L. (2019). Empty-car routing in ridesharing systems. *Operations Research*, *67*(5), 1437-1452.

Cachon, G. P., Daniels, K. M., & Lobel, R. (2017). The Role of Surge Pricing on a Service Platform with Self-Scheduling Capacity. *Manufacturing & Service Operations Management*, *19*(3), 368–384.

Chakravarty, A. K. (2021). Blending capacity on a rideshare platform: Independent and dedicated drivers. *Production and Operations Management, 30(8)*, 2522-2546.

Chen, M. K., & Sheldon, M. (2016). Dynamic pricing in a labor market: Surge pricing and flexible work on the Uber platform. *EC '16: Proc. 2016 ACM Conference on Economics and Computation*. (ACM, New York), 455.

Chen, M., Zhao, D., Gong, Y., & Rekik, Y. (2022b). An on-demand service platform with self-scheduling capacity: Uniform versus multiplier-based pricing. *International Journal of Production Economics*, *243*, 108329.

Chen, Q., Lei, Y., & Jasin, S. (2024). Real-time spatial–intertemporal pricing and relocation in a ride-hailing network: Near-optimal policies and the value of dynamic pricing. *Operations Research*, *72*(5), 2097-2118.

Chen, X., Li, Z., Ming, L., & Zhu, W. (2022a). The Incentive Game Under Target Effects in Ridesharing: A Structural Econometric Analysis. *Manufacturing & Service Operations Management*, *24*(2), 972–992.

Chen, Y. J., Dai, T., Korpeoglu, C. G., Körpeoğlu, E., Sahin, O., Tang, C. S., & Xiao, S. (2020). Om forum—innovative online platforms: Research opportunities. *Manufacturing & Service Operations Management, 22*(3), 430-445.

Cheng, X., Fu, S., Sun, J., Zuo, M., & Meng, X. (2023). Trust in online ride-sharing transactions: Impacts of heterogeneous order features. *Journal of Management Information Systems*, *40*(1), 183-207.

Chod, J., Trichakis, N., & Yang, S. A. (2022). Platform tokenization: Financing, governance, and moral hazard. *Management Science*, *68*(9), 6411-6433.

Choi, T. M., & Shi, X. (2022). On-demand ride-hailing service platforms with hired drivers during coronavirus (COVID-19) outbreak: Can blockchain help?. *IEEE Transactions on Engineering Management*, *71*, 737-752.

Cohen, M. C., & Zhang, R. (2022). Competition and coopetition for two-sided platforms. *Production and Operations Management, 31(5)*, 1997-2014.

Cohen, M. C., Fiszer, M. D., & Kim, B. J. (2022). Frustration-based promotions: Field experiments in ride-sharing. *Management Science, 68*(4), 2432-2464.

Connelly, B. L., Certo, S. T., Ireland, R. D., & Reutzel, C. R. (2011). Signaling theory: A review and assessment. *Journal of management*, *37*(1), 39-67.

Cramer, J., & Krueger, A. B. (2016). Disruptive change in the taxi business: The case of Uber. *American Economic Review*, *106*(5), 177-182.

De Munck, T., Chevalier, P., & Tancrez, J. S. (2023). Managing priorities on on-demand service platforms with waiting time differentiation. *International Journal of Production Economics*, *266*, 109053.

Diao, W., Jiang, B., & Tian, L. (2023). Competition between P2P ride-sharing platforms and traditional taxis. *Production and Operations Management, 32(12)*, 3801-3815.

Dills, A. K., S. E. Mulholland. 2018. Ride-Sharing, Fatal Crashes, and Crime. *Southern Economic Journal*, 84(4), 965–991.

Dong, Z., & Leng, M. (2021). Managing on-demand ridesharing operations: Optimal pricing decisions for a ridesharing platform. *International Journal of Production Economics, 232*, 107958.

Fan, Q., van Essen, J. T., & Correia, G. H. (2024). A bi-level framework for heterogeneous fleet sizing of ride-hailing services considering an approximated mixed equilibrium between automated and non-automated traffic. *European Journal of Operational Research*, *315*(3), 879-898.

Feng, G., Kong, G., & Wang, Z. (2021). We Are on the Way: Analysis of On-Demand Ride-Hailing Systems. *Manufacturing & Service Operations Management*, *23*(5), 1237–1256.

Garg, N., & Nazerzadeh, H. (2022). Driver Surge Pricing. *Management Science*, *68*(5), 3219–3235.

Gong, J., Greenwood, B. N., & Song, Y. (2023). An empirical investigation of ridesharing and new vehicle purchase. *Manufacturing & Service Operations Management*, *25*(3), 884-902.

Griswold, A., & Kopf, D. (2019). The number of American taxi drivers has tripled in a decade https://qz.com/1647247/more-americans-are-driving-taxis-thanks-to-uber-and-lyft (Accessed on 26 January 2025).

Guan, L., Pei, J., Liu, X., Zhou, Z., & Pardalos, P. M. (2022). Ridesharing in urban areas: Multi-objective optimisation approach for ride-matching and routeing with commuters' dynamic mode choice. *International Journal of Production Research*, *60*(5), 1439-1457.

Guda, H., & Subramanian, U. (2019). Your Uber Is Arriving: Managing On-Demand Workers Through Surge Pricing, Forecast Communication, and Worker Incentives. *Management Science*, *65*(5), 1995–2014.

Guo, Y., Li, X., & Zeng, X. (2019). Platform competition in the sharing economy: Understanding how ride-hailing services influence new car purchases. *Journal of Management Information Systems*, *36*(4), 1043-1070.

Guo, Y., Zhang, Y., & Boulaksil, Y. (2021). Real-time ride-sharing framework with dynamic timeframe and anticipation-based migration. *European Journal of Operational Research, 288*(3), 810-828.

Guo, Y., Zhang, Y., Boulaksil, Y., Qian, Y., & Allaoui, H. (2023). Modelling and analysis of online ride-sharing platforms–A sustainability perspective. *European Journal of Operational Research, 304*(2), 577-595.

Haferkamp, J., Ulmer, M. W., & Ehmke, J. F. (2024). Heatmap-based decision support for repositioning in ride-sharing systems. *Transportation Science, 58*(1), 110-130.

Hawlitschek, F., Notheisen, B., & Teubner, T. (2018). The limits of trust-free systems: A literature review on blockchain technology and trust in the sharing economy. *Electronic commerce research and applications*, *29*, 50-63.

Hong, S. J., Bauer, J. M., Lee, K., & Granados, N. F. (2020). Drivers of supplier participation in ride-hailing platforms. *Journal of management information systems*, *37*(3), 602-630.

Hu, B., Hu, M., & Zhu, H. (2022). Surge Pricing and Two-Sided Temporal Responses in Ride Hailing. *Manufacturing & Service Operations Management*, *24*(1), 91–109.

Hu, M., & Liu, Y. (2023). Precommitments in two-sided market competition. *Manufacturing & Service Operations Management*, *25*(2), 704-718.

Hu, M., & Zhou, Y. (2022). Dynamic Type Matching. *Manufacturing & Service Operations Management*, *24*(1), 125–142.

Hu, X., Zhou, S., Luo, X., Li, J., & Zhang, C. (2024). Optimal pricing strategy of an on-demand platform with cross-regional passengers. *Omega*, *122*, 102947.

Idug, Y., Niranjan, S., Manuj, I., Gligor, D., & Ogden, J. (2023). Do ride-hailing drivers' psychological behaviors influence operational performance?. *International Journal of Operations & Production Management, 43(12),* 2055-2079.

Jacob, J., & Roet-Green, R. (2021). Ride solo or pool: Designing price-service menus for a ride-sharing platform. *European Journal of Operational Research, 295(3)*, 1008-1024.

Jia, F., Li, D., Liu, G., Sun, H., & Hernandez, J. E. (2020). Achieving loyalty for sharing economy platforms: an expectation–confirmation perspective. *International Journal of Operations & Production Management*, *40*(7/8), 1067-1094.

Jiang, Z.-Z., Kong, G., & Zhang, Y. (2021). Making the Most of Your Regret: Workers' Relocation Decisions in On-Demand Platforms. *Manufacturing & Service Operations Management*, *23*(3), 695–713.

Kaal, W. A. (2021). Blockchain solutions for agency problems in corporate governance. In *Information for efficient decision making: Big data, blockchain and relevance* (pp. 313-329).

Klarin, A., & Suseno, Y. (2021). A state-of-the-art review of the sharing economy: Scientometric mapping of the scholarship. *Journal of Business Research*, *126*, 250-262.

Krishnaprasad, S. (2024). Non-discriminatory operating policies for ridesharing platforms with dual capacities. *Journal of the Operational Research Society*, *75*(5), 874-887.

Kullman, N. D., Cousineau, M., Goodson, J. C., & Mendoza, J. E. (2022). Dynamic ride-hailing with electric vehicles. *Transportation Science*, *56*(3), 775-794.

Kumar, S., Mookerjee, V., & Shubham, A. (2018). Research in operations management and information systems interface. *Production and Operations Management*, *27*(11), 1893-1905.

Lahiri, A., Doğan, O. B., & Kumar, V. (2023). Nurturing resource availability of ridesharing platforms by priming goal-oriented operational effectiveness. *Journal of Business Research*, *168*, 114121.

Lee, K., Bellamy, M. A., & Joglekar, N. R. (2023). Distributed service with proximal capacity and pricing on a two-sided sharing economy platform. *Journal of Operations Management, 69*(5), 742-763.

Li, X., Li, X., Wang, H., Shi, J., & Aneja, Y. P. (2022a). Supply regulation under the exclusion policy in a ride-sourcing market. *Transportation Research Part B: Methodological*, *166*, 69-94.

Li, Y., Li, X., & Zhang, S. (2021). Optimal pricing of customized bus services and ride-sharing based on a competitive game model. *Omega, 103*, 102413.

Li, Z., Liang, C., Hong, Y., & Zhang, Z. (2022b). How do on-demand ridesharing services affect traffic congestion? The moderating role of urban compactness. *Production and Operations Management*, *31*(1), 239-258.

Lin, X., & Zhou, Y.-W. (2019). Pricing policy selection for a platform providing vertically differentiated services with self-scheduling capacity. *Journal of the Operational Research Society*, *70*(7), 1203–1218.

Lin, X., Sun, C., Cao, B., Zhou, Y. W., & Chen, C. (2021). Should ride-sharing platforms cooperate with car-rental companies? Implications for consumer surplus and driver surplus. *Omega, 102*, 102309.

Liu, M., Brynjolfsson, E., & Dowlatabadi, J. (2021). Do digital platforms reduce moral hazard? The case of Uber and taxis. *Management Science*, *67*(8), 4665-4685.

Liu, X., Qian, S., Teo, H. H., & Ma, W. (2024). Estimating and Mitigating the Congestion Effect of Curbside Pick-ups and Drop-Offs: A Causal Inference Approach. *Transportation Science*, *58*(2), 355-376.

Lu, T. (2024). Can a Supplier's Yield Risk Be Truthfully Communicated via Cheap Talk?. *Manufacturing & Service Operations Management.*

Lyft Statistics (2024). Lyft Statistics by Revenue, Active Riders, Drivers, Country, Demographics, Device and Social Media. https://www.coolest-gadgets.com/lyft-statistics/#:~:text=As%20of%20August %202022%2C%20the,USD%20112.2%20million%20in%202023 (Accessed on 26 January 2025).

Lynley, M. (2024). Uber apologizes for "confusion" at JFK during immigration protest. *TechCrunch*. https://techcrunch.com/2017/01/29/uber-apologizes-for-confusion-at-jfk-during-immigration-protest/ (Accessed on 5 February 2025).

Lyu, G., Cheung, W.C., Teo, C-P., Wang, H. (2024). Multiobjective Stochastic Optimization: A Case of Real-Time Matching in Ride-Sourcing Markets. *Manufacturing & Service Operations Management*, *26*(2), 500-518.

Ma, H., Fang, F., & Parkes, D. C. (2022). Spatio-temporal pricing for ridesharing platforms. *Operations Research*, *70*(2), 1025-1041.

Mejia, J., & Parker, C. (2021). When transparency fails: Bias and financial incentives in ridesharing platforms. *Management Science, 67(1)*, 166-184.

Miao, W., Deng, Y., Wang, W., Liu, Y., & Tang, C. S. (2023). The effects of surge pricing on driver behavior in the ride-sharing market: Evidence from a quasi-experiment. *Journal of Operations Management*, *69*(5), 794-822.

Mordor Intelligence Research & Advisory (2025). Ride Sharing Market Size & Share Analysis - Growth Trends & Forecasts (2025 - 2030). https://www.mordorintelligence.com/industry-reports/ridesharing-market (Accessed on 20 January 2025).

Naumov, S., & Keith, D. (2023). Optimizing the economic and environmental benefits of ride-hailing and pooling. *Production and Operations Management, 32(3),* 904-929.

Ngila, F. (2023). Lyft's end to surge pricing means drivers will earn less—and Lyft doesn't mind. *Quartz*. https://qz.com/lyft-drivers-car-hailing-taxi-uber-low-pay-1850720424. (Accessed on 2 January 2025).

Nie, F., Li, X., & Zhou, C. (2024). Impact of privacy regulation involving information collection on the ride-hailing market. *Omega*, *126*, 103077.

Ong, H. Y., Freund, D., & Crapis, D. (2021). Driver positioning and incentive budgeting with an escrow mechanism for ride-sharing platforms. *INFORMS Journal on Applied Analytics*, *51*(5), 373-390.

Özdemir, T. (2024). Understanding the Surge Multiplier. https://tolgaozdemir.medium.com/understanding-the-surge-multiplier-05788c6361a7 (Accessed on 23 January 2025).

Özer, Ö., & Zheng, Y. (2016). Markdown or everyday low price? The role of behavioral motives. *Management Science*, *62*(2), 326-346.

Özkan, E. (2020). Joint pricing and matching in ride-sharing systems. *European Journal of Operational Research, 287*(3), 1149-1160.

Özkan, E., & Ward, A. R. (2020). Dynamic matching for real-time ride sharing. *Stochastic Systems*, *10*(1), 29-70.

Pan, Y., & Qiu, L. (2022). How ride-sharing is shaping public transit system: A counterfactual estimator approach. *Production and Operations Management, 31*(3), 906-927.

Pavone, M., Saberi, A., Schiffer, M., & Tsao, M. W. (2022). Online hypergraph matching with delays. *Operations Research*, *70*(4), 2194-2212.

Qiu, L., Qiao, D., Tan, B. C., & Whinston, A. B. (2024). Leading the Horse to Water? Investigating the Impact of Ride-hailing Services on Hate Crimes. *Production and Operations Management*, *33*(1), 342-363.

Reilly, C. (2014). Uber admits “wrong decision” in Sydney surge pricing. *CNET*. https://www.cnet.com/roadshow/news/uber-apologises-wrong-decision-sydney-surge-pricing/ (Accessed on 5 February 2025).

Roese, N. J. (1994). The functional basis of counterfactual thinking. *Journal of personality and Social Psychology*, 66(5), 805.

Rojanakit, P., de Oliveira, R. T., & Dulleck, U. (2022). The sharing economy: A critical review and research agenda. *Journal of Business Research*, *139*, 1317-1334.

Siddiq, A., & Taylor, T. A. (2022). Ride-Hailing Platforms: Competition and Autonomous Vehicles. *Manufacturing & Service Operations Management*, *24*(3), 1511–1528.

Statista (2025). https://www.statista.com/outlook/mmo/shared-mobility/ridehailing/worldwide#:~:text=In%20terms%20of%20user%20numbers,to%20reach%2028.6%25%20by%20202 (Accessed on 15 January 2025).

Steiner, K., & Irnich, S. (2020). Strategic planning for integrated mobility-on-demand and urban public bus networks. *Transportation Science, 54*(6), 1616-1639.

Stockburger, L., Kokosioulis, G., Mukkamala, A., Mukkamala, R. R., & Avital, M. (2021). Blockchain-enabled decentralized identity management: The case of self-sovereign identity in public transportation. *Blockchain: Research and Applications*, *2*(2), 100014.

Sun, L., Teunter, R. H., Babai, M. Z., & Hua, G. (2019). Optimal pricing for ride-sourcing platforms. *European Journal of Operational Research*, *278*(3), 783-795.

Sutherland, W., & Jarrahi, M. H. (2018). The sharing economy and digital platforms: A review and research agenda. *International Journal of Information Management, 43*, 328-341.

Tafreshian, A., Masoud, N., & Yin, Y. (2020). Frontiers in service science: Ride matching for peer-to-peer ride sharing: A review and future directions. *Service Science, 12*(2-3), 44-60.

Tan, K. P. S., Yang, Y., & Li, X. R. (2022). Catching a ride in the peer-to-peer economy: Tourists' acceptance and use of ridesharing services before and during the COVID-19 pandemic. *Journal of Business Research*, *151*, 504-518.

Tang, Y., Guo, P., Tang, C. S., & Wang, Y. (2021). Gender-related operational issues arising from on-demand ride-hailing platforms: Safety concerns and system configuration. *Production and Operations Management, 30(10)*, 3481-3496.

Taylor, T. A. (2018). On-Demand Service Platforms. *Manufacturing & Service Operations Management*, *20*(4), 704–720.

Tirachini, A. (2020). Ride-hailing, travel behaviour and sustainable mobility: an international review. *Transportation*, *47*(4), 2011-2047.

Tripathy, M., Bai, J., & Heese, H. S. (2022). Driver collusion in ride-hailing platforms. *Decision Sciences*, 2022, 1–13.

Tseng, Y. C., & Chan, C. L. (2019). When the sharing economy meets established institutions: Uber and Airbnb in Taiwan. *IEEE Transactions on Engineering Management*, *68*(6), 1895-1906.

Uber Blog (2019). Changes to time and distance rates for Uber Black, SUV, Select. https://www.uber.com/en-CA/blog/time-distance-rates-black-canada/ (Accessed on 3 January 2025).

Uber Statistics (2024). Uber Statistics: How Many People Ride with Uber? https://backlinko.com/uber-users (Accessed on 26 January 2025).

Uber (2019). Understanding Uber's variable service fee. https://help.uber.com/driving-and-delivering/article/understanding-ubers-variable-service-fee?nodeId=7448ffcc-ab98-4a32-b7fc-e9c17a58bb41&_csid=sx3exSssm96y6O5YIMiLwA&state=u9fHE9vQpHTIZ1ut3DpXVMSl3PlCNWpCx-75afOe6Gc%3D&effect= (Accessed on 10 January 2025).

Urata, J., Xu, Z., Ke, J., Yin, Y., Wu, G., Yang, H., & Ye, J. (2021). Learning ride-sourcing drivers' customer-searching behavior: A dynamic discrete choice approach. *Transportation research part C: emerging technologies*, *130*, 103293.

Wang, G., Zhang, H., & Zhang, J. (2024a). On-demand ride-matching in a spatial model with abandonment and cancellation. *Operations Research*, *72*(3), 1278-1297.

Wang, H., & Yang, H. (2019). Ridesourcing systems: A framework and review. *Transportation Research Part B: Methodological*, *129*, 122-155.

Wang, L., Yuan, J., Hu, L., & Du, S. (2024b). Deterministic and probabilistic service-hailing mode choice for on-demand service platforms. *International Journal of Production Economics*, *269*, 109156.

Wang, S., Baldacci, R., Yu, Y., Zhang, Y., Tang, J., Luo, X., & Sun, W. (2023). An Exact Method for a First-Mile Ridesharing Problem. *Transportation Science*, *57*(6), 1581-1604.

Wang, T., & Wu, D. (2020). Data-driven driver dispatching system with allocation constraints and operational risk management for a ride-sharing platform. *Decision Sciences*, *51*(6), 1490-1520.

Wei, K., Vaze, V., & Jacquillat, A. (2022). Transit planning optimization under ride-hailing competition and traffic congestion. *Transportation Science*, *56*(3), 725-749.

Wei, L., Wei, W., Liu, Y., Zhang, J., & Xu, X. (2023). Mitigating supply-demand mismatch: The relationship between inventory sharing and demand learning. *Decision Sciences.*

Willingham, R. (2017). *Uber surge pricing to be capped by Victorian Government after Metro chaos*. ABC News. https://www.abc.net.au/news/2017-07-18/victorian-government-to-ban-uber-surge-pricing/8719700 (Accessed on 8 December 2024).

Xu, Z., Chen, Z., Yin, Y., & Ye, J. (2021). Equilibrium analysis of urban traffic networks with ride-sourcing services. *Transportation science*, *55*(6), 1260-1279.

Yang, P., Iyer, K., & Frazier, P. (2018). Mean field equilibria for resource competition in spatial settings. *Stochastic Systems*, *8*(4), 307-334.

Yu, G., Liu, A., Zhang, J., & Sun, H. (2021). Optimal operations planning of electric autonomous vehicles via asynchronous learning in ride-hailing systems. *Omega*, *103*, 102448.

Yu, J. J., Tang, C. S., Max Shen, Z.-J., & Chen, X. M. (2020). A Balancing Act of Regulating On-Demand Ride Services. *Management Science*, *66(7),* 2975–2992.

Yu, Q., Zhang, Y., & Zhou, Y. P. (2022). Delay information in virtual queues: A large-scale field experiment on a major ride-sharing platform. *Management Science*, *68*(8), 5745-5757.

Yu, Y., Wu, Y., & Wang, J. (2019). Bi-objective green ride-sharing problem: Model and exact method. *International Journal of Production Economics*, *208*, 472-482.

Zeng, S., & He, Y. (2023). Blessing or curse? Sharing economy and its impact on the community of customers and suppliers. *Decision Sciences*, *54*(5), 514-534.

Zhang, W., Jacquillat, A., Wang, K., & Wang, S. (2023). Routing optimization with vehicle–customer coordination. *Management Science*, *69*(11), 6876-6897.

Zhang, Y., Li, X., & Ma, H. (2021). Can ride-hailing platforms be immune to dual-fairness concerns?. *IEEE Transactions on Engineering Management, 70(3)*, 1124-1146.

Zhao, M., Li, B., Ren, J., & Hao, Z. (2023). Competition equilibrium of ride-sourcing platforms and optimal government subsidies considering customers' green preference under peak carbon dioxide emissions. *International Journal of Production Economics, 255*, 108679.

Zhong, Y., Lin, Z., Zhou, Y.W., Cheng, T.C.E., Lin, X., (2019). Matching supply and demand on ride-sharing platforms with permanent agents and competition. *International Journal of Production Economics*, *218*(2019), 363–374.

Zhong, Y., Yang, T., Cao, B., & Cheng, T. C. E. (2022). On-demand ride-hailing platforms in competition with the taxi industry: Pricing strategies and government supervision. *International Journal of Production Economics*, *243*, 108301.

Appendix A. Summary of reviewed papers

Number	Author (s)	Publication Year	Journal	Approach	Research Question(s)	Method	Insights
1	Cachon et al.	2017	Manufacturing & Service Operations Management	Analytical modeling	1. How can prices and wages be adjusted in response to demand in a ride-hailing platform? 2. What are the conditions under which any strategy among five possible contracts can be implemented? These include *fixed contracts*, *dynamic price contracts, and dynamic wage contracts*. *Commission contract, optimal contract*— could be implemented on a ride-hailing platform?	Game-theoretic Model	• An optimal contract significantly boosts the ride-hailing platform's profit compared to contracts with either a fixed price, fixed wage, or both. • While surge pricing may not be perfectly optimal, it typically delivers nearly optimal profit. • As driver costs increase, surge pricing becomes more advantageous for both drivers and riders. Drivers are utilized more effectively, and riders enjoy lower prices during regular demand periods and better access to services during peak times. • Contrary to common criticism, all stakeholders can benefit from surge pricing on a ride-hailing platform that allows for self-scheduling.
2	Taylor	2018	Manufacturing & Service Operations Management	Analytical modeling	How does riders' sensitivity to delay affect the ride-hailing platform's optimal price for riders and wage for drivers?	Game-theoretic Model and Queueing Model	• When rider valuation uncertainty is moderate, greater sensitivity to delays leads to a higher optimal price. • Increased sensitivity to delays lowers the optimal wage when driver opportunity cost uncertainty is high, and the expected opportunity cost is moderate. • In the presence of uncertainty regarding driver opportunity costs, driver independence results in a lower price. • When rider valuation uncertainty is present, driver independence raises the price only if the uncertainty in valuation is sufficiently high.
3	Agussurja et al.	2019	Transportation Science	Hybrid	What is the optimal multiperiod vehicle dispatching strategy, that is, given both standby and uncertain future demands, the ride-hailing platform decides which subsets of demands to satisfy in the current period?	Markov Decision Process and Secondary Data Collection	• The method shows improved convergence and enhanced solution quality with an increase in sample size. • The method yields optimal results, particularly when the distribution is more varied and the planning region is extensive. • Implementing this approach in parallel can further boost its performance.

(continued)

Number	Author (s)	Publication Year	Journal	Approach	Research Question(s)	Method	Insights
4	Bai et al.	2019	Manufacturing & Service Operations Management	Analytical modeling	How should a ride-hailing platform set its price rate for the riders and its wage rate for the drivers?	Queueing Model	• Ride-hailing platforms should raise their commission to drivers in response to increased demand, reduced capacity, or greater rider sensitivity to delays. • While it is ideal for the ride-hailing platform to raise prices as demand grows, the optimal price may not follow a consistent pattern when driver capacity or waiting costs rise.
5	Bimpikis et al.	2019	Operations Research	Analytical modeling	How does demand pattern affect the ride-hailing platform's spatial pricing, profit and rider surplus?	Game-theoretic Model	• The ride-hailing platform's profits and overall rider surplus are highest when demand is evenly distributed throughout the network's locations. • When demand is unevenly distributed across the network, surge pricing becomes the optimal strategy for the ride-hailing platform.
6	Braverman et al.	2019	Operations Research	Hybrid	What is the optimal rider-driver matching policy using empty-car routing mechanism by which we control car flow in the network to optimize system-wide utility functions?	Fluid Model and Secondary Data Collection	• The optimal network utility derived from fluid-based optimization serves as an upper limit on utility in a finite car system, regardless of whether the routing policy is static or dynamic, as long as the closed queuing network maintains a stationary distribution. • This upper limit is asymptotically attainable when the optimal routing policy is based on fluid-based optimization.
7	Guda & Subramanian	2019	Management Science	Analytical modeling	How do surge-pricing and forecast information hailing affect drivers' relocation decisions?	Game-theoretic Model	• Contrary to common belief, surge pricing can be effective even in areas where supply surpasses demand. • Merely notifying drivers of where they should position themselves may not guarantee that sufficient drivers will relocate to those areas. • Strategic use of surge pricing can boost overall ride-hailing platform profit across different zones and may be more lucrative than providing bonuses to drivers for relocating.

(continued)

Number	Author (s)	Publication Year	Journal	Approach	Research Question(s)	Method	Insights
8	Lin & Zhou	2019	Journal of the Operational Research	Analytical modeling	1. "How does the ride-hailing platform set the wages and prices under each pricing policy? 2. Instead of the dynamic pricing policy, whether or when the ride-hailing platform can apply the surge(static) pricing policy? 3. Compared with the dynamic pricing policy, how is the ride-hailing platform's profit performance of the surge(static) pricing policy?" (p.1204)	Dynamic Programming	• Surge pricing does not consistently yield strong results, which may explain why some on-demand ride-hailing platforms opt for static pricing policies in practice. • While dynamic pricing typically enhances the ride-hailing platform's profitability, static (surge) pricing can approach the profitability of dynamic pricing if the ride-hailing platform effectively balances different driver types and/or lowers the commission rate.
9	Sun et al.	2019	European Journal of Operational Research	Hybrid	What is the optimal pricing strategy under two types of driver selection: first to respond or closest to the rider?	Game-theoretic Model and Secondary Data Collection	• The ride-hailing platform's pricing includes a fare based on ride length (relative to standard taxi fares) and an additional fee for rush hour congestion, which rises with the rider's waiting costs. • When traffic conditions are favorable, drivers have modest profit expectations, and the ride-hailing platform's commission is low, the ride-hailing platform's price will be lower than that of regular taxis.
10	Tseng & Chan	2019	IEEE Transactions on Engineering Management	Empirical	How do Uber and Airbnb draw on a set of strategic actions to overcome institutional obstacles, gain legitimacy, and justify their new activities?	Case Study	• Uber employed strategies of framing, aggregating, and bridging to build credibility, gain legitimacy, and drive potential institutional changes. These strategies work together, each enhancing the effectiveness of the others. • Through framing, Uber shapes a favorable brand image, while aggregating helps consolidate internal resources. Bridging is used to garner new support for their emerging initiatives. • Uber implemented these strategies by using blueprints to strengthen their brand, aggregating to foster mutual aid relationships, and collaborating with suppliers and governments to secure additional support. • A thorough understanding of framing, aggregating, and bridging is essential for resolving conflicts among economic actors and overcoming institutional challenges, especially in the sharing economy.

(continued)

Number	Author (s)	Publication Year	Journal	Approach	Research Question(s)	Method	Insights
11	Yu et al.	2019	International Journal of Production Economics	Analytical modeling	How do we minimize ride-hailing carbon emissions while optimizing driver welfare?	Non-linear Programming	• They introduce the concept of Pareto-optimal rides and demonstrate that each Pareto-optimal solution of the BGRSP (Bilinear Geometric Ride-Sharing Problem) consists of these optimal rides. Consequently, the solution space can be streamlined by eliminating non-Pareto-optimal rides. • They also define the Pareto-optimal partition and show that every Pareto-optimal solution of the BGRSP is made up of these optimal partitions within each submatrix. This approach significantly narrows the solution space by excluding non-Pareto-optimal partitions, achieving up to (1-5.5E-42)*100% reduction. • The proposed model and methodology are effective in simultaneously reducing carbon emissions and ensuring driver satisfaction.
12	Zhong et al.	2019	International Journal of Production Economics	Analytical modeling	1. “Does employing permanent drivers really enhance the service level? 2. Is it beneficial for ride-hailing platforms to employ permanent drivers? 3. How do the employment of permanent drivers and competition between ride-hailing platforms affect the strategies of the ride-hailing platforms, the corresponding riders' / drivers' surpluses, and social welfare?” (p.364)	Game-theoretic Model	• To maximize profits, a monopolistic ride-hailing platform should provide higher subsidies to attract more temporary drivers, resulting in lower prices when it employs both temporary and permanent drivers compared to using only temporary drivers. • This approach can lead to increased ride-hailing platform profit, as well as greater rider surplus and overall social welfare. • In a two-sided market, a monopoly ride-hailing platform may sometimes offer more benefits to both riders and drivers than a duopoly. • The use of permanent drivers can significantly influence how competition affects the ride-hailing platform's optimal strategies, as well as the surpluses for drivers and riders and overall social welfare.

(continued)

Number	Author (s)	Publication Year	Journal	Approach	Research Question(s)	Method	Insights
13	Al-Kanj et al.	2020	European Journal of Operational Research	Analytical modeling	How do we decide on the dispatch problem, including rider-car allocation, recharging, repositioning, and parking, along with surge pricing and the fleet size of electric vehicles?	Approximate Dynamic Programming	• The performance outcomes of their model indicated that hierarchical aggregation in value function approximation leads to superior results and significantly faster convergence. • The proposed VFA policy was highly effective in guiding dispatch decisions, outperforming the myopic policy by 17%. • The VFA policy generated realistic patterns in car repositioning and recharging during off-peak times, ensuring readiness for peak-period rider demand. • The adaptive learning framework for surge pricing exhibited operational behavior akin to real-world scenarios, where prices rise with demand, resulting in a 13% revenue increase.
14	Jia et al.	2020	International Journal of Operations & Production Management	Empirical	How do ride-hailing platform companies adjust their operational strategies to foster loyalty among drivers and riders?	Case Study	• Ride-hailing platform companies could pursue mergers and acquisitions to integrate resources and minimize excessive competition within their respective industries. • To enhance supply network readiness and boost operational capacity, ride-hailing platform companies should attract more stakeholders. Meeting user expectations in this way fosters user satisfaction and, in turn, promotes ride-hailing platform loyalty. • Ride-hailing platform firms should be mindful of the externalities their operations generate. By aiming to create positive externalities and mitigate negative ones, they can better foster ride-hailing platform loyalty.
15	Özkan	2020	European Journal of Operational Research	Analytical modeling	1. "Is matching optimization necessary? 2. Is fixing the matching decisions to a simple rule and optimizing only the pricing decisions enough to achieve the optimal performance?" (p.1149)	Fluid Model	• Optimizing pricing decisions while keeping matching decisions fixed generally does not maximize the number of matches. • Optimizing matching decisions while holding pricing decisions constant is generally not optimal. • Under certain conditions, optimizing in just one dimension—whether pricing or matching—offers no advantage to the ride-hailing platform, whereas jointly optimizing both can result in substantial performance gains.

(continued)

Number	Author (s)	Publication Year	Journal	Approach	Research Question(s)	Method	Insights
16	Wang & Wu	2020	Decision Science	Analytical modeling	How can we develop a data-driven driver dispatching system for a control center to minimize riders' waiting time?	Rolling-time-horizon	• They demonstrate that the NP-hard nature of the offline problem is rooted in the allocation constraints. • The system significantly reduces average waiting times and improves planning efficiency compared to the request-driven dispatching method. • In typical scenarios, the dispatch system identifies an acceptable solution that nearly meets allocation constraints while ensuring only a slight increase in waiting time.
17	Yu et al.	2020	Management Science	Analytical modeling	What is the impact of a class of regulatory policy that controls the maximum number of registered drivers in a ride-hailing platform on: • Different stakeholders (platform, riders, drivers, and taxi drivers) • Traffic conditions • The underlying competition between the on-demand ride service and taxis	Game-theoretic Model	• In the absence of government intervention, the ride-hailing platform might potentially displace the traditional taxi industry under specific conditions. • A well-crafted regulatory policy can achieve a more effective balance among various competing objectives. • If the government can reform the taxi industry by modifying taxi fares, lowering these fares rather than enforcing stringent regulations on on-demand ride services could enhance overall social welfare.
18	Bernstein et al.	2021	Manufacturing & Service Operations Management	Analytical modeling	1. How do supply and demand in the market respond to changes in ride-hailing platform prices considering both "single-homing," where the drivers work through a single ride-hailing platform and "multihoming" where drivers deliver their service through both ride-hailing platforms? 2. What types of supply and demand outcomes can arise at equilibrium prices? 3. How do various underlying cost and market parameters influence the relationships between supply and demand and how much of the rider market gets served at equilibrium?	Game-theoretic Model	• Increasing prices during a demand surge benefits both drivers and riders compared to a scenario where ride-hailing platforms are forced to maintain the same prices as under normal demand conditions. • While individual drivers might be tempted to operate across multiple ride-hailing platforms, overall, all participants are worse off if every driver chooses to multi-home.

(continued)

Number	Author (s)	Publication Year	Journal	Approach	Research Question(s)	Method	Insights
19	Besbes et al.	2021	Management Science	Analytical modeling	“How should a ride-hailing platform optimally set prices across locations in a city and what is the impact of those prices on the strategic repositioning of drivers?” (p.1350)	Game-theoretic Model	• In the optimal strategy, the ride-hailing platform customizes its approach based on location. Prices are adjusted to perfectly align supply and demand in some areas, while congestion is intentionally created in others. Additionally, less profitable locations are indirectly excluded through pricing. • They develop a quasi-closed form for the optimal solution applicable to a range of models affected by demand shocks. Interestingly, while the optimal solution improves the balance of supply and demand around the shock, it also inadvertently causes a shift away from the shock area. • The optimal pricing strategy divides the city into several zones centered around the origin. The area experiencing the demand shock is served by three subregions: the immediate origin, the inner center, and the outer center. In the origin zone, locations benefit from the shock, attracting some drivers to remain there while others head toward the origin. In contrast, the outer center, being too distant from the shock, is purposefully penalized through pricing to encourage drivers to move closer to the origin.
20	Chakravarty	2021	Production and Operations Management	Analytical modeling	Can a ride-hailing platform with a blended capacity (full time employees with a fixed wage rate, and independent drivers who are paid a share of revenue) be viable?	Game-theoretic Model	• A mixed ride-hailing platform capacity is feasible when the wage rate is moderate, there is a substantial pool of independent drivers, and the market for ride-seekers is large.

(continued)

Number	Author (s)	Publication Year	Journal	Approach	Research Question(s)	Method	Insights
21	Dong & Leng	2021	International Journal of Production Economics	Analytical modeling	"What is the ride-hailing platform's optimal decisions on both the unit wage and the service price?" (p.2)	Choice Model	• As the number of riders grows, the ride-hailing platform should simultaneously increase both the distance fare and wages while also boosting the payout ratio to attract more drivers. • Conversely, when the number of drivers rises, the ride-hailing platform should reduce both the distance fare and wages, and it may lower the payout ratio to enhance profitability. • An increase in either the number of drivers or riders can boost the ride-hailing platform's profits, provided the numbers remain below their respective thresholds. • If the number of riders or drivers exceeds its threshold, the ride-hailing platform's profit will continue to increase, but the effect becomes less pronounced if the other group does not also expand. • The ride-hailing platform benefits most when both the number of riders and drivers are high.
22	Feng et al.	2021	Manufacturing & Service Operations Management	Analytical modeling	1. "How much increased efficiency, if any, ride hailing platforms bring to the transportation system? 2. Whether the ride-hailing platform can reduce riders' average waiting times comparing to street-hailing system where arriving riders are picked up by the first available taxi passing by?" (p.1237)	Queuing Model	• The on-demand mechanism is more effective in reducing rider waiting times when traffic intensity is either low or high, while the traditional mechanism may be more efficient when traffic intensity falls within the mid-range. • The on-demand matching mechanism may be less efficient than the traditional street-hailing approach when system utilization is moderate, and road lengths are extended.
23	Guo et al.	2021	European Journal of Operational Research	Hybrid	1. "What is a realistic matching plan evaluation method and decision rules for dynamic timeframe segmentation? 2. What is an adaptive profit-based threshold for the generated value of driver-rider pairs? 3. What is an effective matching and routing algorithm for solving large-scale instances?" (p.811)	Dynamic Programming and Secondary Data Collection	• Formally defining a dynamic timeframe and commuter migration and presenting an innovative model to assess matching quality. • Proposing decision rules for segmenting dynamic timeframes and a method for achieving anticipation-based commuter migration using historical matching data. • Introducing a new multi-strategy local search heuristic algorithm capable of producing near-optimal solutions to the problem in a short computational time.

(continued)

Number	Author (s)	Publication Year	Journal	Approach	Research Question(s)	Method	Insights
24	Jacob & Roet-Green	2021	European Journal of Operational Research	Analytical modeling	1. "How the pool and solo options affect a strategic rider's ride choice, an independent driver's decision to drive, and the ride-hailing platform's revenue? 2. How congestion and driver endogeneity affect the ride-hailing platform's optimal pricing strategies in equilibrium?" (p.1009)	Queuing Model	• The ride-hailing platform gains from providing both solo and pooled rides when rider types are evenly distributed, and congestion levels are low. • In high-congestion scenarios, the ride-hailing platform should opt to offer either solo or pooled rides, but not both. • When the number of drivers is determined within the system, the ride-hailing platform's revenue per driver can decline as the rate of rider arrivals increases.
25	Jiang et al.	2021	Manufacturing & Service Operations Management	Hybrid	1. "How does the presence of regret affect workers' relocation decisions? In other words, are regret-averse workers more or less likely to leave their current, oversupplied zone and go to the high demand zone? 2. How should a ride-hailing platform leverage this behavior and design an optimal level of compensation to encourage an adequate number of workers to move to the supply-shortage zone? Should the ride-hailing platform offer a higher or lower compensation when workers are regret averse as opposed to regret neutral? 3. Do the ride-hailing platform, workers, and riders benefit or suffer from workers' regret behavior under the ride-hailing platform's optimal level of compensation?" (p.696)	Game-theoretic Model and Experiment	• Regret aversion significantly influences workers' decisions to relocate. • Workers who are regret-averse tend to be more inclined to move to areas experiencing a shortage of supply compared to rational workers. • Despite this heightened relocation tendency, it does not necessarily result in better system performance. • Ride-hailing platform measures, such as sharing demand information and offering dynamic wage bonuses, can enhance system effectiveness. • Regret-aversion among workers can lead to increased ride-hailing platform profits, higher worker surplus, and improved demand-supply alignment, benefiting the overall on-demand system.
26	Li et al.	2021	Omega	Analytical modeling	What is the optimal price for ride-hailing services when the ride-hailing platform provides both ride-hailing and customized bus services?	Game-theoretic Model	• If the ride-hailing provider is aware of the pricing strategy for customized buses, the optimal ride-hailing price follows a quadratic relationship with the customized bus price. • When the customized bus provider knows the pricing strategy of ride-hailing, the optimal price for customized buses becomes a non-decreasing function of both the fixed factor and the linear coefficient of ride-hailing services.

(continued)

Number	Author (s)	Publication Year	Journal	Approach	Research Question(s)	Method	Insights
27	Lin et al.	2021	Omega	Analytical modeling	What is the impact of cooperating with car-rental companies on ride-hailing platforms' profit and riders' and drivers' welfare?	Game-theoretic Model	• The optimal price and the ride-hailing platform's profit do not always increase with the potential number of drivers without cars or the commission received from the company. • High commission rates paid to the ride-hailing platform by the car-rental company or a low fixed payout ratio can result in a mutually beneficial outcome for the ride-hailing platform, riders, and drivers.
28	Liu et al.	2021	Management Science	Empirical	"How do these innovations affect moral hazard and service quality?" (p.4665)	Secondary Data Collection	• On average, taxi drivers cover 8% more distance than matched Uber drivers on metered airport routes, with nonlocal riders on these routes experiencing even longer travel distances. • This extended routing is not observed for short trips in dense areas, such as within-Manhattan trips, or for airport trips with a fixed fare. • Generally, longer routing results in increased travel time rather than time savings for riders. • These observations align with the idea that digital ride-hailing platform designs mitigate driver moral hazard, contrasting with alternative explanations like driver selection or variations in navigation technologies.
29	Mejia & Parker	2021	Management Science	Empirical	To what extent do a rider's gender, race, and perception of support for lesbian, gay, bisexual, and transgender (LGBT) rights impact the drivers' cancelation rates in ride-hailing platforms?	Field Experiment	• Biases at the ride request stage have been addressed, but racial and LGBT biases persist after ride acceptance, with no evidence of gender biases. • Peak times moderate biases, showing lower cancellation rates for non-Caucasian riders, while no similar effect is observed for LGBT-supportive riders. • Despite recent adjustments to rider transparency timing, biases continue to be an unintended outcome of ride-hailing platforms.

(continued)

Number	Author (s)	Publication Year	Journal	Approach	Research Question(s)	Method	Insights
30	Tang et al.	2021	Production and Operations Management	Analytical modeling	Will a "hybrid" system with a "female-only" option result in a win-win-win outcome for riders, drivers, and the ride-hailing platform?	Queuing Model and Game-theoretic Model	• If the mismatch cost for safety-conscious female users exceeds a specific threshold, transitioning from a pooling system to a hybrid system can create a beneficial outcome for both these users and the ride-hailing platform. • However, this shift may negatively impact male users and female users who are less concerned about safety.
31	Xu et al.	2021	Transportation Science	Hybrid	How can matching policies be improved by explicitly modeling the vacant trips from the end of one rider delivery trip to the start of the next, which include cruising for riders and deadheading for picking them up?	Game-theoretic Model and Secondary Data Collection	• The numerical examples involving both the small-scale Nguyen–Dupuis network and the realistic Friedrichshain network show that the suggested model is capable of predicting ride-hailing system performance and understanding its effects on network traffic conditions.
32	Yu et al.	2021	Omega	Hybrid	How do we optimize matching, repositioning and recharging operations for electric autonomous vehicles?	Markov Decision Process and Secondary Data Collection	• Their experiments, conducted with real data from Haikou city, highlight the advantages of the proposed policy over the commonly used CD policy and predetermined recharging rules in terms of increasing revenue and reducing response time. • Performance is influenced by factors such as the number of available electric autonomous vehicles (EAVs), request arrival rate, and the number of recharging stations. • Response time decreases as fleet size and the number of recharging stations increase.
33	Zhang et al.	2021	IEEE Transactions on Engineering Management	Analytical modeling	1. "What is the impact of horizontal and vertical fairness concerns on the ride-hailing platform? 2. How can the ride-hailing platform design incentive strategies to relieve the impact of fairness concerns? 3. How can the government use taxi fares as a lever to relieve the impact of fairness concerns?" (p.1125)	Game-theoretic Model	• Both vertical and horizontal fairness issues tend to decrease the utility of the ride-hailing platform. • Implementing strategies such as revenue and demand-based hailing and fare subsidies can improve the ride-hailing platform's utility by mitigating the adverse effects of horizontal and vertical fairness concerns, respectively. • Government regulation of taxi fares can alleviate the negative effects of dual-fairness concerns and lead to higher overall social welfare.

(continued)

Number	Author (s)	Publication Year	Journal	Approach	Research Question(s)	Method	Insights
34	Besbes et al.	2022	Operations Research	Analytical modeling	"How should capacity thinking be adapted to spatial settings where drivers need to reach riders before service can start?" (p.1272)	Markov Decision Process	• The square root safety rule fails to achieve a balance between driver utilization and rider wait times in spatial systems. • In spatial settings, pick-up times contribute to the system's load and serve as an internal source of additional workload, making the system operate efficiently only when there is a significant imbalance between supply and demand. • To achieve a balance between utilization and wait times, the platform should apply a higher safety factor proportional to the offered load raised to the power of 2/3.
35	Beirigo et al.	2022	Transportatio n Science	Analytical modeling	How do we hire on-demand autonomous vehicles and match them with riders?	Approximate Dynamic programming and Mixed Integer Optimization	• The proposed policy surpasses a reactive optimization approach across various vehicle availability scenarios while requiring fewer vehicles. • Mobility services can provide stringent service-level agreements to different user groups, incorporating both delay and rejection penalties.
36	Benjaafar et al. (1)	2022	Manufacturing & Service Operations Management	Analytical modeling	1. "Are drivers indeed hurt by an expansion in the driver pool size in on-demand ride-hailing platforms? 2. Which type of wage-floor regulation is preferable? 3. Are riders hurt by the imposition of a wage floor?" (p.110)	Game-theoretic Model	• Average driver welfare first increases and then decreases as the driver pool size grows; specifically, drivers only experience negative effects from a larger driver pool when it becomes sufficiently large. • The effective wage floor is more effective than the nominal wage floor for maximizing driver welfare. • Contrary to the traditional belief that riders suffer from an effective wage floor due to higher prices, riders actually gain from it.
37	Benjaafar et al. (2)	2022	Management Science	Analytical modeling	What is the impact of the ride-hailing industry on traffic and car ownership?	Game-theoretic Model	• When the ratio of ownership costs to usage costs is low, ride-hailing is typically provided as a peer-to-peer (P2P) service. Conversely, when this ratio is high, ride-hailing is offered as a business-to-consumer (B2C) service. • While ride-hailing services might decrease the number of car owners, they can also lead to increased traffic. • As ownership costs rise, both traffic and car ownership may increase. A revenue-maximizing ride-hailing platform might prefer a scenario where vehicles are frequently driven with only a few riders, resulting in higher traffic congestion.

(continued)

Number	Author (s)	Publication Year	Journal	Approach	Research Question(s)	Method	Insights
38	Chen et al. (a)	2022	Manufacturing & Service Operations Management	Hybrid	1. "How can an econometric framework be designed to link the theoretical model that describes drivers working and quitting decisions under the target effect to data? 2. What targets do a group of hetero-generous rideshare drivers set? 3. What are the optimal bonus rates the ride-hailing platform should set to achieve the short-term objective of maximizing peak-hour capacity or the long-term objective of maximizing profit?" (p.973)	Game-theoretic Model and Secondary Data Collection	• Drivers exhibit behavior aimed at reaching specific income targets. • The drivers' working hours do not necessarily rise in a straightforward manner with increases in bonus rates due to the target effect, and the ride-hailing platform might not allocate its entire bonus budget to maximize capacity or profit.
39	Chen et al. (b)	2022	International Journal of Production Economics	Analytical modeling	1. "Which pricing scheme is more suitable for an on-demand ride-hailing platform, uniform or multiplier-based pricing? 2. What are the applicable regions of the different pricing schemes?" (p.2)	Game-theoretic Model	• In the multiplier-based pricing scheme, the price during non-peak times is set lower compared to the uniform price. • The multiplier-based pricing model becomes more profitable with a larger number of potential participants during non-peak periods, especially if either the compensation ratios in both models are high or the compensation ratio in the multiplier-based model is low. • Participants are more likely to benefit from a ride-hailing platform that uses uniform pricing under the following conditions: a lower commission ratio in both models, a lower compensation ratio in the multiplier-based model, or higher commission and compensation ratios in both models. • Riders will find the uniform pricing model more advantageous if the proportion of non-peak periods, their sensitivity to surge multiplier changes, and the ratio of potential participants between peak and non-peak periods are higher.

(continued)

Number	Author (s)	Publication Year	Journal	Approach	Research Question(s)	Method	Insights
40	Choi & Shi	2022	IEEE Transactions on Engineering Management	Analytical modeling	1. "For the ODR ride-hailing platform: What are the optimal pricing and hygiene level decisions under the CoV outbreak with and without implementing blockchain? 2. When will the implementation of blockchain help the ride-hailing platform? What will be the situation in which deploying blockchain becomes an all-win solution (i.e., riders, drivers, and ODR ride-hailing platform all get benefited)? 3. How robust are the findings when we generalize the models to different settings such as a) the case when the special hygiene level is the decision made by the drivers, and b) riders are risk averse?" (p.739)	Queueing Model	• Implementing blockchain technology results in higher service costs and improved hygiene standards. • If riders have a significant concern about infection, blockchain adoption can create a win-win situation for the on-demand ride (ODR) platform, drivers, and riders. • When drivers are responsible for maintaining special hygiene standards, both the optimal service price and hygiene level are generally lower. • Reducing fluctuations in rider perceptions of service value is crucial to enhancing the benefits and effectiveness of blockchain implementation.
41	Cohen et al.	2022	Management Science	Empirical	1. "How can we design the process of sending targeted proactive compensation to riders experiencing a frustration in the context of ride-hailing? 2. What is the impact of such a practice?" (p.2433)	Field Experiment	• Offering proactive compensation to frustrated riders proves to be profitable and enhances their engagement, particularly effective for addressing long wait times but less so for long travel durations. • This approach is more effective than providing the same compensation to riders who are not frustrated. • The effectiveness of this strategy is influenced by the rider's past usage frequency. • The most effective strategy is to provide credit for future use.
42	Cohen & Zhang	2022	Production and Operations Management	Analytical modeling	What is the impact of competition and coopetition for two-sided ride-hailing platforms on platforms' profits, rider surplus and driver welfare?	Game-theoretic Model	• Given that a driver's behavior is influenced not only by the price or wage set by the ride-hailing platform but also by the strategic interactions between both sides of the ride-hailing platform, their model lacks differentiability. Nevertheless, they demonstrated that a unique equilibrium exists for the ride-hailing platforms. • Coopetition or competitive partnerships can provide advantages to both ride-hailing platforms, riders, and drivers if supported by a well-structured profit-sharing agreement. • While coopetition proves advantageous when demand-side competition is high, it may disadvantage at least one ride-hailing platform when supply-side competition is intense.

(continued)

Number	Author (s)	Publication Year	Journal	Approach	Research Question(s)	Method	Insights
43	Garg & Nazerzadeh	2022	Management Science	Analytical modeling	1. What is the impact of surge pricing on driver earnings? 2. Which one is more beneficial? Additive surge pricing or multiplicative surge pricing?	Stochastic Dynamic Programming	• In a dynamic system where the world transitions stochastically between surge and non-surge states, with varying ride distances and driver distributions, multiplicative pricing fails to align with incentive compatibility. • They identify the conditions under which additive pricing provides greater benefits compared to multiplicative pricing.
44	Guan et al.	2022	International Journal of Production Research	Hybrid	What is the optimal policy for ride-matching and routing considering riders' dynamic mode choice?	Mixed Integer Optimization and Secondary Data Collection	• Their findings illustrate how ride-matching and routing affect ride-hailing decisions, highlighting the significant contribution to the practical implementation of ride-hailing systems. • They determine the most effective model for small-scale versus large-scale scenarios.
45	Hu et al.	2022	Manufacturing & Service Operations Management	Analytical modeling	1. "Accounting for salient temporal elements of ride hailing, what is a ride-hailing platform's optimal/equilibrium surge-pricing policy? 2. Can the ride-hailing platforms' current pricing practices be explained? 3. How may such ride-hailing platforms improve their surge-pricing policies? 4. What impact would there be if a ride-hailing platform neglects riders' and drivers' strategic behavior in their surge-pricing practice?" (p.92)	Game-theoretic Model	• A brief, steep increase in prices often leads high-value riders to wait out the initial surge period, which in turn attracts more drivers to the area who serve these riders at significantly reduced rates compared to the initial surge price. • The theoretically optimal penetration surge pricing strategy (starting with a low price and then increasing it) indicates that adopting a different approach could enhance surge pricing effectiveness, underscoring the potential benefits for ride-hailing platforms to share demand-supply information with drivers.
46	Hu & Zhou	2022	Manufacturing & Service Operations Management	Analytical modeling	What is the optimal supply-demand matching policy to maximize the expected total discounted rewards, given that unmatched demand and supply may incur waiting or holding costs, and will be fully or partially carried over to the next period? (p.125)	Stochastic Dynamic Programming	• They establish sufficient conditions for matching rewards that ensure the optimal matching policy adheres to a priority hierarchy among potential matching pairs. • This priority property streamlines the matching decision within a given period, reducing the trade-off to a choice between matching in the current period versus in the future. • For matching a specific pair, the optimal policy continues to match until a predefined threshold is reached.

(continued)

Number	Author (s)	Publication Year	Journal	Approach	Research Question(s)	Method	Insights
47	Kullman et al.	2022	Transportation Science	Analytical modeling	How does an operator controlling a fleet of electric vehicles for use in a ride-hailing service optimize matching, repositioning and recharging operations?	Markov Decision Process	• Their most effective policy, trained using deep reinforcement learning, consistently outperforms the re-optimization approach across different instance sizes and can be scaled and applied to larger instances without the need for retraining.
48	Li et al. (b)	2022	Production and Operations Management	Empirical	1. "What is the impact of Uber on traffic congestion? 2. How does urban compactness moderate the impact of Uber on traffic congestion? What are plausible underlying mechanisms?" (p.240)	Difference-in-differences	• In compact urban areas, ride-hailing services notably exacerbate traffic congestion, whereas, in sprawling cities, they tend to reduce congestion. • The impact on traffic congestion is influenced by both the efficiency-enhancing and demand-inducing effects of ride-hailing services, with the overall effect varying based on the level of urban compactness.
49	Ma et al.	2022	Operations Research	Analytical modeling	How to optimally set prices that are appropriately smooth in space and time, so that drivers will nevertheless choose to accept their dispatched trips rather than drive to another area or wait for higher prices or a better trip? (p.1025)	Game-theoretic Model	• They propose a spatio-temporal pricing (STP) strategy that aligns incentives, ensuring that it forms a subgame-perfect equilibrium where drivers consistently accept their ride assignments. • Regardless of the historical context, the STP strategy guarantees outcomes that are optimal for overall welfare, free from envy, individually rational, balanced in budget, and core-selective. • Compared to a short-sighted mechanism, the STP strategy offers significant enhancements in both social welfare and earnings fairness.

(continued)

Number	Author (s)	Publication Year	Journal	Approach	Research Question(s)	Method	Insights
50	Miao et al.	2022	Journal of Operations Management	Empirical	What is the impact of surge pricing on driver earnings and driver availability?	Difference-in-differences	• Surge pricing results in higher weekly earnings for drivers. • Analyzing weekly earnings through the lens of "intensive margin" and "extensive margin" reveals two competing effects: a cherry-picking effect and a competition effect. The daily earnings decrease because the competition effect outweighs the cherry-picking effect. • The rise in weekly earnings can be attributed to the extensive margin, where drivers compensate for lower daily earnings by increasing their number of working days. • Surge pricing incentivizes more part-time drivers to enter the market, which crowds out full-time drivers, and the overall increase in weekly earnings is predominantly due to these part-time drivers.
51	Pan & Qiu	2022	Production and Operations Management	Empirical	"Has Uber siphoned riders from public transit, or has it made public transit feasible for more riders?" (p.907)	Secondary Data Collection	• The introduction of Uber has led to a notable decrease in rider trips on buses. • However, Uber's entry has had little impact on public demand response transportation, suggesting that Uber does not directly compete with services addressing the "last-mile problem." • The influence of Uber's entry varies across different urban areas.
52	Pavone et al.	2022	Operations Research	Analytical modeling	How to optimally match riders and drivers using hypergraph with delays?	Hypergraph Matching	• They present a thresholding algorithm and demonstrate that it achieves the optimal competitive ratio for deterministic algorithms. • For k > 2, they identify both the optimal competitive ratio and the optimal polynomial-time competitive ratio, up to a factor of 2 – 1/d.

(continued)

Number	Author (s)	Publication Year	Journal	Approach	Research Question(s)	Method	Insights
53	Siddiq & Taylor	2022	Manufacturing & Service Operations Management	Analytical modeling	1. "Are competing ride-hailing platforms helped or harmed by ride-hailing platforms' obtaining access to autonomous vehicles? 2. How do the conditions under which access to autonomous vehicles reduces ride-hailing platform profits, driver welfare, and social welfare depend on the autonomous vehicles' ownership structure (i.e., whether ride-hailing platforms or individuals own autonomous vehicles)?" (p.1511)	Game-theoretic Model	• Driver welfare only declines if the cost of autonomous vehicles is high. Conversely, the impact of having access to autonomous vehicles on ride-hailing platform profit depends on the ownership of these vehicles. • For ride-hailing platform profit to decrease due to access to autonomous vehicles, it is necessary and sufficient that the cost is high for ride-hailing platform-owned vehicles and low for individually-owned vehicles. • The effect of autonomous vehicle access on social welfare is influenced by who owns the vehicles. • Social welfare increases with individually-owned autonomous vehicles but decreases with ride-hailing platform-owned autonomous vehicles, provided that the cost of these vehicles is high.
54	Tan et al.	2022	Journal of Business Research	Empirical	1. What is the impact of ride-hailing industry on tourism? 2. What are tourists' choices between ride-hailing and taxi services? 3. Is using rideshares during their trip affects tourists' satisfaction, trip value, and views on local friendliness?	Econometric Model	• Factors such as consumption competency, peer-to-peer consumption spillover, and the availability of taxi services have a significant impact on tourists' use of ride-hailing services, whereas safety reputation and destination familiarity do not significantly influence this behavior. • Over time, cost savings have become less relevant in explaining ride-hailing demand. During the pandemic, the severity of local outbreaks has influenced tourists' use of ride-hailing services. • The use of ride-hailing by tourists had a notable effect on their trip or destination evaluations in 2020, but this was not the case in 2016.
55	Tripathy et al.	2022	Decision Sciences	Analytical modeling	What is the impact of the driver's collusive behavior on the ride-hailing platform's surge pricing policy?	Game-theoretic Model	• Collusive behavior among drivers is more probable in situations where riders have moderate sensitivity to waiting times. • In certain scenarios, if riders persist in requesting services despite driver collusion, the ride-hailing platform may profit from elevated surge prices.

(continued)

Number	Author (s)	Publication Year	Journal	Approach	Research Question(s)	Method	Insights
56	Wei et al.	2022	Transportation Science	Hybrid	"Can public transit and ride-hailing coexist and thrive in a way that enhances the urban transportation ecosystem as a whole?" (p.725)	Mixed Integer Optimization and Case Study	• Their model resulted in significant systemwide cost reductions, translating to rush-hour savings of millions of dollars daily while also lowering expenses for both riders and drivers. • These findings remain consistent despite variations in assumptions about rider demand, transit service levels, ride-hailing dynamics, and transit fare structures. • By taking into account ride-hailing competition, rider preferences, and traffic congestion, transit agencies can create schedules that reduce costs for riders, operators, and the overall system, achieving a rare win-win-win scenario.
57	Yu et al.	2022	Management Science	Empirical	How does providing waiting time information, both its initial magnitude and its subsequent progress over time, impact riders' abandonment behavior in virtual queues?	Field Experiment	• The extent of initial waiting time information and how often it is updated greatly influence the rate at which riders abandon their requests. • Adjusting the initial waiting time by one minute does not affect rider abandonment, as the impact of this adjustment is neutralized by the frequency of updates. However, changes of more than one minute lead to abandonment rates being influenced primarily by the magnitude of the waiting time information. • Comparable but contrasting effects are observed when evaluating optimistic versus neutral waiting time information.
58	Zhong et al.	2022	International Journal of Production Economics	Analytical modeling	1. "How should the on-demand ride-hailing platform design its pricing strategy in competition from the traditional taxi industry under different pricing-regulating scenarios? 2. Are there specific pricing scenarios under which the government can achieve its ultimate goals? 3. What measures should the government take and how should it implement such measures to maximize the overall social welfare and profit under different pricing-regulating scenarios?" (p.2)	Game-theoretic Model	• In an unregulated pricing scenario, the price rates and profits of a monopolistic on-demand ride-hailing platform are generally higher compared to a regulated pricing scenario. • The government should promote competition between on-demand ride-hailing services and the traditional taxi industry. • If the number of taxis is insufficient relative to rider demand, increasing the total number of taxis is the most effective regulatory measure. However, when taxi supply exceeds demand, the optimal regulatory approach varies depending on the specific circumstances. • The government should implement relevant supervisory policies tailored to the current situation to enhance overall social welfare and profitability.

(continued)

Number	Author (s)	Publication Year	Journal	Approach	Research Question(s)	Method	Insights
59	Afeche et al.	2023	Manufacturing & Service Operations Management	Analytical modeling	How do two operational controls, demand-side admission control and supply-side capacity repositioning affect the matching performance?	Game-theoretic Model	• They offer insights into how managing demand-side admissions and supply-side capacity repositioning impacts equilibrium performance. • Ride-hailing platforms might strategically reject ride requests in low-demand areas to incentivize relocations to high-demand zones. • They present upper bounds on the benefits gained by ride-hailing platforms and drivers due to enhanced control.
60	Agarwal et al.	2023	Manufacturing & Service Operations Management	Empirical	How do ride-hailing services affect congestion?	Difference-in-differences	• When ride-hailing services are unavailable due to driver strikes, there is a noticeable reduction in travel time. • The most significant effects are observed in the most congested areas during peak hours. • Ride-hailing platforms are increasingly replacing more sustainable transportation options and are substantially contributing to urban congestion.
61	Ai et al.	2023	Management Science	Empirical	1. What is the impact of the creation of a team identity on individual driver revenue? 2. How do different team formations impact team member communication and productivity?	Field Experiment	• Drivers working in teams tend to put in more hours and see a 12% increase in earnings. • This effect persists for two weeks following the contest, though it is reduced by half. • Drivers in teams from similar hometowns are more likely to engage in communication, while those in teams of similar age continue to work longer hours and earn more revenue even after the contest. • Ride-hailing platform designers can utilize team identity and team-based contests to boost revenue and worker engagement in the gig economy.

(continued)

Number	Author (s)	Publication Year	Journal	Approach	Research Question(s)	Method	Insights
62	Allon et al.	2023	Manufacturing & Service Operations Management	Empirical	1. How do drivers make decisions about whether to work and work duration? 2. How do they react to incentives? 3. What are the factors that shape each driver's decision? 4. Are their decisions rational, or do they exhibit behavioral biases? 5. How can ride-hailing platforms design incentives to entice drivers? 6. How can they meet their desired service level by offering the right incentives?	Econometric Model	• Monetary incentives greatly affect both the decision to engage in work and the total hours worked, aligning with the expected positive income elasticity observed in standard economic theory. • The study supports behavioral theories like income-targeting behavior (where workers reduce hours upon reaching a financial target) and inertia (where continued work persists after extended periods of work). • Neglecting these behavioral aspects could result in a staffing shortfall of up to 10.17% below the optimal level. • Inertia may indicate a level of driver loyalty to the ride-hailing platform.
63	Barrios et al.	2023	Journal of Operations Management	Empirical	Do ride-hailing platforms impose negative safety externalities?	Difference-in-differences	• The emergence of ride-hailing platforms has led to a 3% rise in fatal accidents. • There has been an increase in indicators of traffic congestion and new car registrations following the introduction of ride-hailing services. • The authors recommend several regulatory measures for ride-hailing platforms to mitigate these safety-related externalities.
64	De Munck et al.	2023	International Journal of Production Economics	Analytical modeling	1. What is the impact of service differentiation on the ride-hailing platform, riders and drivers? 2. How can the ride-hailing platform optimally decide whether to admit or reject riders with different waiting time, and whether to allocate drivers to them or rather reserve drivers for more profitable arrivals?	Markov Decision Process	• A policy that regulates both rider admission and driver reservations can offer advantages to the ride-hailing platform, riders, and drivers. • This optimal policy is defined by two admission thresholds that vary depending on the state of the system, specifically the number of riders waiting in the opposing queue. • The proposed approach, known as the Admission and Reservation Policy (ARP), significantly outperforms three simpler alternative policies.
65	Diao et al.	2023	Production and Operations Management	Analytical modeling	"How can ride-hailing platforms and taxis profitably coexist in the market?" (p.3801)	Game-theoretic Model	• The pricing strategies of both ride-hailing platforms and taxi companies are heavily influenced by the costs of rider inconvenience and variability in ride distances. • A rise in the inconvenience cost for taxis can lead to reduced profits for both ride-hailing platforms and taxi companies. • Both types of firms can see advantages from implementing a distance-based unit pricing model under specific conditions.

(continued)

Number	Author (s)	Publication Year	Journal	Approach	Research Question(s)	Method	Insights
66	Gong et al.	2023	Manufacturing & Service Operations Management	Empirical	"Does the entry of ride-hailing platforms yield a material short-term change in the rate of durable goods (viz., automobile) purchase?" (p.885)	Difference-in-differences	• Uber's entry correlates with a notable short-term rise in private new vehicle ownership, suggesting that riders adjust their resource holdings to benefit from the ride-hailing platform's excess rents. • This effect is specific to vehicle brands that are eligible for use on the ride-hailing platform. • Smaller displacement vehicles see a more significant increase in sales compared to larger displacement vehicles, indicating that Uber's impact varies by vehicle type. • The effects are more pronounced in areas with less robust public transportation options.
67	Guo et al.	2023	European Journal of Operational Research	Hybrid	What is the optimal dispatching strategy to balance the triple-bottom-line of sustainability, i.e., economic, social and environmental perspective?	Holistic Multi-objective Model and Case Study	• Focusing solely on economic objectives leads to a significant decline in environmental and social outcomes across all scenarios considered. • In many cases, substantial reductions in carbon emissions can be achieved with only a minor impact on economic performance. • The most effective method for reducing carbon emissions involves lowering prices or increasing the commission charged to drivers. Although this reduces driver income, it can be offset by a fixed commission structure. • Environmental and social metrics generally improve (and economic metrics mostly improve) when greater emphasis is placed on travel time over travel distance.

(continued)

Number	Author (s)	Publication Year	Journal	Approach	Research Question(s)	Method	Insights
68	Hu & Liu	2023	Manufacturing & Service Operations Management	Analytical modeling	"What is the impact of precommitments in a variety of practically motivated instruments on the equilibrium outcomes of competing ride-hailing platforms?" (p.704)	Game-theoretic Model	• A precommitment made on the less competitive side (whether in terms of demand or supply) regarding price or wage results in a less severe outcome compared to no commitment at all (i.e., competing on spot-market prices and wages). • When the levels of competition on both sides are nearly equal, committing to commission rates—where platforms first compete to set these rates before setting prices—tends to be less profitable than not making any precommitments. The opposite holds true when competition levels are not closely aligned. • The capacity precommitment strategy, where ride-hailing platforms first commit to a certain matching capacity and then simultaneously set prices and wages within the constraints of that pre-committed capacity, produces the most profitable results among all competition approaches and extends the Kreps-Scheinkman equivalency to two-sided markets (assuming no demand uncertainty).
69	Idug et al.	2023	International Journal of Operations & Production Management	Empirical	1. "How do ride-hailing company drivers' intention to comply with the company guidelines affect their operation performance? 2. What factors impact ride-hailing company drivers' intention to comply with the company guidelines?" (p.2057)	Survey	• When ride-hailing drivers adhere to company guidelines, their operational performance improves. • Drivers perceive that ride-hailing companies have effective penalties to discourage guideline violations. • Despite this, drivers also believe that the likelihood of being caught for disregarding these guidelines is relatively low.

(continued)

Number	Author (s)	Publication Year	Journal	Approach	Research Question(s)	Method	Insights
70	Lahiri et al.	2023	Journal of Business Research	Empirical	1. "Do operational effectiveness indicators translate to value for the ride-hailing platform in the form of higher resource availability of drivers? 2. Jointly governing rider and driver interests, what is the quantified operational effectiveness which ride-hailing platforms can derive from a change in feedback mechanism? 3. How do perceived organizational justice elements moderate the link between the ride-hailing platform's feedback mechanism and the operational effectiveness measures?" (p.2)	Field Experiment	• Feedback that focuses on specific goals enhances various operational effectiveness metrics. • These improvements lead to better resource availability on the ride-hailing platform, resulting in more driver referrals and reduced driver turnover. • Ride-hailing platforms can boost their operational efficiency and resource availability by combining goal-oriented feedback with a flexible commission structure for drivers.
71	Lee et al.	2023	Journal of Operations Management	Empirical	1. "What is the relationship between surge pricing and capacity decisions distributed across space and time in a two-sided ride-hailing platform context? 2. Under what conditions do spatially distributed service design pricing strategies align profit maximization and welfare maximization goals?" (p.743)	Econometric Model	• They identify two key effects related to surge pricing: the proximal capacity effect, which refers to how driver availability in nearby areas influences pricing in a focal zone, and the proximal pricing effect, which involves how current prices in adjacent zones affect the pricing in the focal zone. • Their findings indicate that both the proximal capacity and proximal pricing effects have a significant and simultaneous impact on surge price estimation when demand is substantial. • Spatial proximity plays a crucial role in determining price distribution, especially when service demand is notably high.
72	Naumov & Keith	2023	Production and Operations Management	Empirical	1. "Can ride-hailing companies price individual and pooled rides in a way that maximizes revenue while also encouraging riders to choose pooling to reduce vehicle miles traveled and hence the environmental footprint of urban transportation? 2. How should prices for individual and pooled rides be updated if automated vehicles and other automotive technologies reduce the cost of providing ride-hailing trips in the coming years?" (p.905)	Choice Model	• When driving costs decrease, the ride-hailing platform gains from widening the price gap between individual and pooled rides. • This pricing approach benefits both the ride-hailing platform and cities by reducing overall vehicle miles traveled.

(continued)

Number	Author (s)	Publication Year	Journal	Approach	Research Question(s)	Method	Insights
73	Wang et al.	2023	Transportation Science	Analytical modeling	What is the exact method to solve the first-mile ride-hailing problem?	Set-partitioning	• The proposed BPC algorithm is capable of solving optimality-modified Solomon benchmark instances with up to 100 riders, as well as real-world instances with up to 290 riders.
74	Zeng & He	2023	Decision Sciences	Analytical modeling	1. "What is the conflict between the financial objective of the sharing economy firm and the welfare of the affected community (i.e., all riders and all individual suppliers)? 2. How can we mitigate such conflict with regulatory interventions?" (p.515)	Game-theoretic Model	• As prices rise, demand initially increases because the perceived convenience for riders outweighs the price but eventually decreases as the price effect surpasses the convenience, leading to a "backward-bending" demand curve. • The financial goals of sharing economy firms do not always align with the well-being of the communities they impact. • Regulating the sharing economy by setting upper limits on price surges can help reconcile the financial interests of the sharing economy firm with the welfare of the affected community.
75	Zhang et al.	2023	Management Science	Analytical modeling	How can scalable algorithms be developed to support dial-a-ride routing with capacitated vehicles, time windows, and vehicle–rider coordination?	Multiple Stop Optimization	• Computational results demonstrate that this algorithm surpasses state-of-the-art benchmarks, delivering significantly better solutions in shorter computational times and supporting real-time operations in very large-scale systems. • Practically, the primary benefits of vehicle-rider coordination come from thoroughly reoptimizing "upstream" operations rather than just adjusting "downstream" stopping locations. • Vehicle-rider coordination results in mutually beneficial outcomes: increased profits, improved rider service, and a reduced environmental footprint.
76	Zhao et al.	2023	International Journal of Production Economics	Analytical modeling	1. "What are the effects of riders' green preference and subsidy preference on the optimal decisions and competitive equilibrium of ride-hailing platforms? 2. In the competitive equilibrium state, how should the government decide the optimal subsidy, and what would happen to the decisions of the two platforms?" (p.2)	Game-theoretic Model	• Riders' preferences for green practices and subsidies are more advantageous for ride-hailing platforms that operate their own new energy vehicles (NEVs) compared to those that use a franchised model with driver-owned vehicles. • An increase in total government investment in subsidies will lower both the optimal riding price and the fleet size for both types of ride-hailing platforms. • Riders' green preferences and government subsidies will both support the objective of achieving a carbon peak.

(continued)

Number	Author (s)	Publication Year	Journal	Approach	Research Question(s)	Method	Insights
77	Arora et al.	2024	Manufacturing & Service Operations Management	Empirical	"How can the government reduce the number of on-demand cabs on the road and, therefore, their GHG emissions by promoting pooled transportation such as shuttle services?" (p.594)	Choice Model	• Reducing walking distance by 20% can capture 40% of the benefits typically associated with congestion surcharge policies. It can also cut up to 4.8 thousand tonnes of greenhouse gas emissions, translating to savings of over a million dollars annually. • The government can implement policies to reduce walking distances by adding additional stops to existing shuttle routes. • By adjusting operational factors like service features in pooled transportation, cities can achieve significant congestion reduction benefits at essentially no cost, making green transport policies much more efficient compared to congestion surcharge approaches.
78	Fan et al.	2024	European Journal of Operational Research	Hybrid	What is the optimal fleet size of conventional taxis and automated taxis, which leads to the maximum profit of a ride-hailing platform at each stage of a mixed automated and non-automated driving network with the expansion of Avs-only zones?	Choice Model and Secondary Data Collection	• As the AVs-only zone expands, the fleet size of automated taxis grows in a nonlinear manner, while the fleet size of conventional taxis declines as demand shifts from human-driven to automated vehicles. • Decisions regarding fleet size are significantly influenced by the cost structure of the fleet, the locations, and the distribution of parking depots. • Initially, the presence of an AVs-only zone may cause detours for human-driven vehicles, but as the zone's size increases, it offers substantial benefits by alleviating congestion.
79	Haferkamp et al.	2024	Transportation Science	Analytical modeling	How do repositioning heatmaps impact driver availability, cancellation rate, and drivers' earning opportunities?	Stochastic Dynamic Programming	• Well-designed repositioning heatmaps can significantly cut down on service cancellations, thereby reducing revenue loss for both the ride-hailing platform and drivers. • Sharing heatmaps with drivers enhances their average earnings and stabilizes income fluctuations across the driver pool. • These heatmaps contribute to a more equitable and efficient distribution of service coverage throughout the city. • Offering repositioning heatmaps to new and less experienced drivers can simplify their integration into the system and create a more even playing field.

(continued)

Number	Author (s)	Publication Year	Journal	Approach	Research Question(s)	Method	Insights
80	Hu et al.	2024	Omega	Analytical modeling	1. "How does the ride-hailing platform set the service prices for each region and the cross-region in each period? 2. Can surge pricing and bonus incentive balance the supply and the demand, and benefit the ride-hailing platform? What are the impacts of the cross-regional demand on the performances of the two strategies? 3. Which strategy is better, from the perspective of the ride-hailing platform profit and the social welfare? 4. Under information asymmetry, will the ride-hailing platform share real information? How does surge pricing affect the credibility of shared information?" (p.2)	Game-theoretic Model	• To address surges in demand and supply shortages in a particular area, the ride-hailing platform can implement surge pricing or offer bonus incentives in neighboring regions before demand peaks, helping to balance supply and demand. • Surge pricing is advantageous for the ride-hailing platform when experiencing significant surge demand or when cross-regional demand is minimal. • Cross-regional demand enhances the effectiveness of bonus incentives but diminishes the effectiveness of surge pricing. • The ride-hailing platform favors using bonus incentives over surge pricing when only a few drivers are needed to relocate. • Sharing information with drivers can also promote their relocation, though its impact is limited, and only a certain proportion of drivers will move. • There is a risk that the ride-hailing platform might share misleading information, leading drivers to doubt the reliability of the information provided.
81	Krishnaprasad	2024	Journal of the Operational Research Society	Analytical modeling	What is the optimal preferential policy for ride-hailing platforms with dual capacities?	Linear Programming	• The Contingency Capacity Policy, which prioritizes self-schedulers in demand allocation, is the most benevolent of the three policies and achieves optimal profits for asset-light ride-hailing platforms (those with fewer full-time employees). • Managers of asset-light ride-hailing platforms can capitalize on the altruistic aspect of this policy to attract more self-schedulers, thereby gaining a substantial competitive edge.
82	Liu et al.	2024	Transportation Science	Hybrid	1. How do we estimate the congestion effect caused by ride-hailing pick-ups/drop-offs from observed traffic data? 2. How do we manage ride-hailing pick-ups/drop-offs to minimize the citywide total travel time based on the differences in heterogeneous congestion effects among regions?	Double and Separated Machine Learning and Secondary Data Collection	• Adding 100 ride-hailing pick-ups or drop-offs in a region could decrease traffic speed by 3.70 mph on weekdays and 4.54 mph on weekends. • Redirecting trips involving ride-hailing pick-ups or drop-offs from curb space could lower the overall system-wide travel time by 2.44% in Midtown and 2.12% in Central Park on weekdays.

(continued)

Number	Author (s)	Publication Year	Journal	Approach	Research Question(s)	Method	Insights
83	Lyu et al.	2024	Manufacturing & Service Operations Management	Analytical modeling	"How should one incorporate multiple objectives, including ride-hailing platform revenue, pick-up time, and ride service quality, in the design of the dispatch algorithm to minimizes the ℓ_p-norm–based distance function between the attained performance metrics and the target performances?" (p. 502)	Multi-objective Optimization	• They provide a compromise solution to the multi-objective stochastic optimization problem. • Under specific conditions, their proposed compromise matching policy offers better outcomes for riders, drivers, and the ride-hailing platform compared to other widely used matching policies.
84	Nie et al.	2024	Omega	Analytical modeling	1. "How do the pricing strategy and the collected information volume of the ride-hailing platform change with the implementation of privacy regulations? 2. How does privacy regulation affect riders' surplus, drivers' income, and the ride-hailing platforms' profits? 3. Under what conditions should privacy regulations be enforced?" (p.2)	Game-theoretic Model	• With the enforcement of privacy regulations, ride-hailing platforms are more likely to adopt partial-coverage pricing strategies rather than full-coverage ones. • When advertising does not significantly disturb riders, privacy regulations shift the decision-making authority regarding information from the ride-hailing platform to the riders, leveraging their self-interest to mitigate the negative effects of information collection. • Effective privacy regulation enhances information security but can reduce the benefits for stakeholders (riders, drivers, and platforms). Thus, privacy regulation involves a trade-off between economic benefits and information security.
85	Qiu et al.	2024	Production and Operations Management	Empirical	What is the impact of ride-hailing services on hate crimes?	Difference-in-differences	• Since the introduction of ride-hailing services, there has been a significant reduction in hate crimes, including a 5.75% decrease in racial hate crimes. • The most plausible explanation for this decline is the increased interaction between diverse groups facilitated by ride-hailing services. • These services foster positive environments and interactions that promote mutual understanding among different groups.

(continued)

Number	Author (s)	Publication Year	Journal	Approach	Research Question(s)	Method	Insights
86	Wang et al. (a)	2024	Operations Research	Analytical modeling	What is the optimal supply-demand matching considering abandonment and cancellations?	Fluid Model	• They achieve precise performance assessments and derive a clear optimality condition, leading to the proposal of a policy that adjusts to fluctuating demand. • As the policy becomes increasingly aggressive (i.e., by enlarging the matching radius to accelerate the process), the number of matches rises. This results in fewer idle drivers and waiting riders (and, thus, fewer abandonments). However, this approach compromises match quality (measured by pickup distance), leading to more cancellations.
87	Wang et al. (b)	2024	International Journal of Production Economics	Analytical modeling	1. "How should the ride-hailing platform adjust price and wage decisions based on market conditions under different service modes? 2. Which kind of ride-hailing mode should be recommended under what conditions? 3. How will the ride-hailing platform choose pricing strategies to adapt to a diverse market environment under Hybrid mode?" (p.3)	Linear Programming	• The ride-hailing platform's pricing strategies and service targets are shaped by both demand-side and supply-side factors. The choice between a deterministic or probabilistic approach depends on the riders' base valuation level and its variability. • Adding a bundled option does not always lead to an increase in the ride-hailing platform's profit.

Appendix B.

Numerical Analysis

Table 3-A-1.Sensitivity analysis with respect to the proportion of drivers in Zone A with $c = 0.3$

(*Data corresponds to Figure 3-1*)

	Model 1		**Model 2**		**Model 3**		**Model 4**		**Model 5**		**Model 6**		**Model 7**		**Model 8**	
α	Maximum matching efficiency	Optimal surge multiplier	Maximum matching efficiency	Optimal surge multiplier	Maximum matching efficiency	Optimal surge multiplier	Maximum matching efficiency	Optimal surge multiplier	Maximum matching efficiency	Optimal surge multiplier	Maximum matching efficiency	Optimal surge multiplier	Maximum matching efficiency	Optimal surge multiplier	Maximum matching efficiency	Optimal surge multiplier
0.45	1	1.923	1	1.923	1	1.755	1	1.755	1	1.498	1	1.498	1	1.494	1	1.494
0.5	1	2.075	1	2.075	1	1.755	1	1.755	1	1.567	1	1.567	1	1.494	1	1.494
0.55	1	2.211	1	2.211	1	1.755	1	1.755	1	1.647	1	1.647	1	1.494	1	1.494
0.6	1	2.335	1	2.335	1	1.755	1	1.755	1	1.756	1	1.756	1	1.494	1	1.494
0.65	1	2.447	1	2.447	1	1.755	1	1.755	1	1.864	1	1.864	1	1.494	1	1.494
0.7	1	2.549	1	2.549	1	1.755	1	1.755	1	1.970	1	1.970	1	1.494	1	1.494
0.75	1	2.643	1	2.643	1	1.755	1	1.755	1	2.072	1	2.072	1	1.494	1	1.494
0.8	1	2.729	1	2.729	1	1.755	1	1.755	1	2.170	1	2.170	1	1.494	1	1.494
0.85	1	2.809	1	2.809	1	1.755	1	1.755	1	2.262	1	2.262	1	1.494	1	1.494
0.9	1	2.882	1	2.882	1	1.755	1	1.755	1	2.348	1	2.348	1	1.494	1	1.494
0.95	1	2.951	1	2.951	1	1.755	1	1.755	1	2.427	1	2.427	1	1.494	1	1.494
0.99	1	3.002	1	3.002	1	1.755	1	1.755	1	2.483	1	2.483	1	1.494	1	1.494

$\rho = 0.4$	$c = 0.3$	$\eta = 1.2$	$p = 0.81$	$\theta = 0.75$	$n = 100$	$m_{max} = 5$	$Z = 2$	$\lambda = 1$

Table 3-A-2. Sensitivity analysis with respect to the proportion of drivers in Zone A with $c = 0.01$

(*Data corresponds to Figure 3-2*)

	Model 1		**Model 2**		**Model 3**		**Model 4**		**Model 5**		**Model 6**		**Model 7**		**Model 8**	
α	Maximum matching efficiency	Optimal surge multiplier	Maximum matching efficiency	Optimal surge multiplier	Maximum matching efficiency	Optimal surge multiplier	Maximum matching efficiency	Optimal surge multiplier	Maximum matching efficiency	Optimal surge multiplier	Maximum matching efficiency	Optimal surge multiplier	Maximum matching efficiency	Optimal surge multiplier	Maximum matching efficiency	Optimal surge multiplier
0.45	1	1.023	1	1.023	1	1.555	1	1.555	1	1.282	1	1.282	1	1.494	1	1.494
0.5	1	1.075	1	1.075	1	1.555	1	1.555	1	1.375	1	1.375	1	1.494	1	1.494
0.55	1	1.211	1	1.211	1	1.555	1	1.555	1	1.472	1	1.472	1	1.494	1	1.494
0.6	1	1.335	1	1.335	1	1.555	1	1.555	1	1.564	1	1.564	1	1.494	1	1.494
0.65	1	1.447	1	1.447	1	1.555	1	1.555	1	1.644	1	1.644	1	1.494	1	1.494
0.7	1	1.449	1	1.449	1	1.555	1	1.555	1	1.801	1	1.801	1	1.494	1	1.494
0.75	1	1.449	1	1.449	1	1.555	1	1.555	1	1.985	1	1.985	1	1.494	1	1.494

0.8	1	1.449	1	1.449	1	1.555	1	1.555	1	2.107	1	2.107	1	1.494	1	1.494
0.85	1	1.494	1	1.494	1	1.555	1	1.555	1	2.235	1	2.235	1	1.494	1	1.494
0.9	1	1.494	1	1.494	1	1.555	1	1.555	1	2.348	1	2.348	1	1.494	1	1.494
0.95	1	1.494	1	1.494	1	1.555	1	1.555	1	2.476	1	2.476	1	1.494	1	1.494
0.99	1	1.494	1	1.494	1	1.555	1	1.555	1	2.483	1	2.483	1	1.494	1	1.494

$\rho = 0.4$	$c = 0.01$	$\eta = 1.2$	$p = 0.81$	$\theta = 0.75$	$n = 100$	$m_{max} = 5$	$Z = 2$	$\lambda = 1$

Table 3-A-3. Sensitivity analysis with respect to the proportion of ride requests in Zone A

(*Data corresponds to Figure 3-3*)

	Model 1		Model 2		Model 3		Model 4		Model 5		Model 6		Model 7		Model 8	
ρ	Maximum matching efficiency	Optimal surge multiplier	Maximum matching efficiency	Optimal surge multiplier	Maximum matching efficiency	Optimal surge multiplier	Maximum matching efficiency	Optimal surge multiplier	Maximum matching efficiency	Optimal surge multiplier	Maximum matching efficiency	Optimal surge multiplier	Maximum matching efficiency	Optimal surge multiplier	Maximum matching efficiency	Optimal surge multiplier
0.95	1	0	1	0	1	0	1	0	1	0.499	1	0.499	1	0.506	1	0.506
0.9	1	0	1	0	1	0	1	0	1	0.487	1	0.487	1	0.506	1	0.506
0.85	1	0	1	0	1	0	1	0	1	0.455	1	0.455	1	0.506	1	0.506
0.8	1	0	1	0	1	0.003	1	0.003	1	0.422	1	0.422	1	0.506	1	0.506
0.75	1	0	1	0	1	0.040	1	0.040	1	0.389	1	0.389	1	0.506	1	0.506
0.7	1	0.013	1	0.013	1	0.081	1	0.081	1	0.355	1	0.355	1	0.506	1	0.506
0.65	1	0.040	1	0.040	1	0.124	1	0.124	1	0.320	1	0.320	1	0.506	1	0.506
0.6	1	0.069	1	0.069	1	0.172	1	0.172	1	0.286	1	0.286	1	0.506	1	0.506
0.55	1	0.099	1	0.099	1	0.223	1	0.223	1	0.250	1	0.250	1	0.506	1	0.506
0.5	1	0.131	1	0.131	1	0.279	1	0.279	1	0.214	1	0.214	1	0.506	1	0.506
0.45	1	0.165	1	0.165	1	0.341	1	0.341	1	0.176	1	0.176	1	0.506	1	0.506
0.35	1	0.201	1	0.201	1	0.409	1	0.409	1	0.138	1	0.138	1	0.506	1	0.506
0.3	1	0.239	1	0.239	1	0.484	1	0.484	1	0.099	1	0.099	1	0.506	1	0.506
0.25	1	0.279	1	0.279	1	0.567	1	0.567	1	0.090	1	0.090	1	0.506	1	0.506
0.2	1	2.212	1	2.212	1	2.159	1	2.159	1	1.094	1	1.094	1	1.494	1	1.494
0.15	1	2.532	1	2.532	1	2.333	1	2.333	1	1.056	1	1.056	1	1.494	1	1.494
0.1	1	2.921	1	2.921	1	2.532	1	2.532	1	1.025	1	1.025	1	1.494	1	1.494
0.05	1	3.408	1	3.408	1	2.762	1	2.762	1	1.011	1	1.011	1	1.494	1	1.494
0.01	1	3.893	1	3.893	1	2.974	1	2.974	1	1.001	1	1.001	1	1.494	1	1.494

$\alpha = 0.2$	$c = 0.3$	$\eta = 0.699$	$p = 0.81$	$\theta = 0.75$	$n = 100$	$m_{max} = 5$	$Z = 2$	$\lambda = 1$

Table 3-A-4. Sensitivity analysis with respect to the average ride distance in Zone B relative to Zone A

(*Data corresponds to Figure 3-4*)

	Model 1		Model 2		Model 3		Model 4		Model 5		Model 6		Model 7		Model 8	
λ	Maximum matching efficiency	Optimal surge multiplier	Maximum matching efficiency	Optimal surge multiplier	Maximum matching efficiency	Optimal surge multiplier	Maximum matching efficiency	Optimal surge multiplier	Maximum matching efficiency	Optimal surge multiplier	Maximum matching efficiency	Optimal surge multiplier	Maximum matching efficiency	Optimal surge multiplier	Maximum matching efficiency	Optimal surge multiplier
0.1	1	1.616	1	5	1	1.079	1	5	1	0.877	1	5	1	0.747	1	5
1	1	1.616	1	3.233	1	1.079	1	2.159	1	0.877	1	1.755	1	0.747	1	1.494
1.5	1	1.616	1	2.155	1	1.079	1	1.439	1	0.877	1	1.170	1	0.747	1	0.996
2	1	1.616	1	1.616	1	1.079	1	1.079	1	0.877	1	0.877	1	0.747	1	0.747
2.5	1	1.616	1	1.293	1	1.079	1	0.863	1	0.877	1	0.702	1	0.747	1	0.598
3.5	1	1.616	1	0.924	1	1.079	1	0.617	1	0.877	1	0.501	1	0.747	1	0.427
3.9	1	1.616	1	0.829	1	1.079	1	0.553	1	0.877	1	0.450	1	0.747	1	0.383

$\alpha = 0.9$	$\rho = 0.2$	$c = 0.3$	$\eta = 0.669$	$p = 0.81$	$\theta = 0.75$	$n = 100$	$m_{max} = 5$	$Z = 4$

Table 3-A-5. Sensitivity analysis with respect to supply-demand imbalance

(*Data corresponds to Figure 3-5*)

		Model 1		Model 2		Model 3		Model 4		Model 5		Model 6		Model 7		Model 8	
α	$\lvert\rho - \alpha\rvert$	Maximum matching efficiency	Optimal surge multiplier	Maximum matching efficiency	Optimal surge multiplier	Maximum matching efficiency	Optimal surge multiplier	Maximum matching efficiency	Optimal surge multiplier	Maximum matching efficiency	Optimal surge multiplier	Maximum matching efficiency	Optimal surge multiplier	Maximum matching efficiency	Optimal surge multiplier	Maximum matching efficiency	Optimal surge multiplier
0.2	0	1	1.753	1	1.753	1	3.014	1	3.014	1	1.092	1	1.092	1	1.494	1	1.494
0.25	0.05	1	1.010	1	1.010	1	2.159	1	2.159	1	1.092	1	1.092	1	1.494	1	1.494
0.3	0.1	1	1.091	1	1.091	1	2.159	1	2.159	1	1.124	1	1.124	1	1.494	1	1.494
0.35	0.15	1	1.387	1	1.387	1	2.159	1	2.159	1	1.162	1	1.162	1	1.494	1	1.494
0.4	0.2	1	1.972	1	1.972	1	2.159	1	2.159	1	1.469	1	1.469	1	1.494	1	1.494
0.45	0.25	1	2.053	1	2.053	1	2.159	1	2.159	1	1.525	1	1.525	1	1.494	1	1.494
0.5	0.3	1	2.156	1	2.156	1	2.159	1	2.159	1	1.576	1	1.576	1	1.494	1	1.494
0.55	0.35	1	2.484	1	2.484	1	2.159	1	2.159	1	1.622	1	1.622	1	1.494	1	1.494
0.6	0.4	1	2.691	1	2.691	1	2.159	1	2.159	1	1.664	1	1.664	1	1.494	1	1.494
0.65	0.45	1	2.989	1	2.989	1	2.159	1	2.159	1	1.700	1	1.700	1	1.494	1	1.494
0.7	0.5	1	3.049	1	3.049	1	2.159	1	2.159	1	1.731	1	1.731	1	1.494	1	1.494
0.75	0.55	1	3.102	1	3.102	1	2.159	1	2.159	1	1.753	1	1.753	1	1.494	1	1.494
0.8	0.6	1	3.150	1	3.150	1	2.159	1	2.159	1	1.827	1	1.827	1	1.494	1	1.494
0.85	0.65	1	3.194	1	3.194	1	2.159	1	2.159	1	1.906	1	1.906	1	1.494	1	1.494
0.9	0.7	1	3.233	1	3.233	1	2.159	1	2.159	1	1.997	1	1.997	1	1.494	1	1.494
0.95	0.75	1	3.268	1	3.268	1	2.159	1	2.159	1	2.127	1	2.127	1	1.494	1	1.494
0.99	0.79	1	3.295	1	3.295	1	2.159	1	2.159	1	2.146	1	2.146	1	1.494	1	1.494

$\rho = 0.2$	$c = 0.3$	$\eta = 1.2$	$p = 0.81$	$\theta = 0.75$	$n = 100$	$m_{max} = 5$	$Z = 2$

Table 3-A-6. Sensitivity analysis with respect to the cost of driver relocation with $\rho = 0.4$ and $\alpha = 0.95$

(*Data corresponds to Figure 3-6(a)*)

	Model 1		**Model 2**		**Model 3**		**Model 4**		**Model 5**		**Model 6**		**Model 7**		**Model 8**	
c	Maximum matching efficiency	Optimal surge multiplier	Maximum matching efficiency	Optimal surge multiplier	Maximum matching efficiency	Optimal surge multiplier	Maximum matching efficiency	Optimal surge multiplier	Maximum matching efficiency	Optimal surge multiplier	Maximum matching efficiency	Optimal surge multiplier	Maximum matching efficiency	Optimal surge multiplier	Maximum matching efficiency	Optimal surge multiplier
0.01	1	1.757	1	1.757	1	1.071	1	1.071	1	1.506	1	1.506	1	1.016	1	1.016
0.05	1	1.888	1	1.888	1	1.098	1	1.098	1	1.604	1	1.604	1	1.082	1	1.082
0.1	1	2.052	1	2.052	1	1.180	1	1.180	1	1.726	1	1.726	1	1.165	1	1.165
0.15	1	2.215	1	2.215	1	1.248	1	1.248	1	1.848	1	1.848	1	1.247	1	1.247
0.2	1	2.379	1	2.379	1	1.374	1	1.374	1	1.970	1	1.970	1	1.329	1	1.329
0.25	1	2.542	1	2.542	1	1.506	1	1.506	1	2.093	1	2.093	1	1.412	1	1.412
0.3	1	2.706	1	2.706	1	1.639	1	1.639	1	2.215	1	2.215	1	1.494	1	1.494
0.35	1	2.870	1	2.870	1	1.771	1	1.771	1	2.337	1	2.337	1	1.576	1	1.576
0.4	1	3.033	1	3.033	1	1.903	1	1.903	1	2.459	1	2.459	1	1.658	1	1.658
0.45	1	3.197	1	3.197	1	2.035	1	2.035	1	2.581	1	2.581	1	1.741	1	1.741
0.5	1	3.361	1	3.361	1	2.168	1	2.168	1	2.703	1	2.703	1	1.823	1	1.823
0.55	1	3.524	1	3.524	1	2.300	1	2.300	1	2.826	1	2.826	1	1.905	1	1.905
0.6	1	3.688	1	3.688	1	2.432	1	2.432	1	2.949	1	2.949	1	1.988	1	1.988

$p = 0.81$	$\theta = 0.75$	$\eta = 0.699$	$n = 100$	$m_{max} = 5$	$Z = 2$	$\lambda = 1$

Table 3-A-7. Sensitivity analysis with respect to the cost of driver relocation with $\rho = 0.95$ and $\alpha = 0.4$

(*Data corresponds to Figure 3-6(b)*)

	Model 1		**Model 2**		**Model 3**		**Model 4**		**Model 5**		**Model 6**		**Model 7**		**Model 8**	
c	Maximum matching efficiency	Optimal surge multiplier	Maximum matching efficiency	Optimal surge multiplier	Maximum matching efficiency	Optimal surge multiplier	Maximum matching efficiency	Optimal surge multiplier	Maximum matching efficiency	Optimal surge multiplier	Maximum matching efficiency	Optimal surge multiplier	Maximum matching efficiency	Optimal surge multiplier	Maximum matching efficiency	Optimal surge multiplier
0.01	1	0.391	1	0.391	1	0.498	1	0.498	1	0.996	1	0.996	1	0.984	1	0.984
0.05	1	0.323	1	0.323	1	0.430	1	0.430	1	0.978	1	0.978	1	0.918	1	0.918
0.1	1	0.238	1	0.238	1	0.345	1	0.345	1	0.952	1	0.952	1	0.835	1	0.835
0.15	1	0.154	1	0.154	1	0.260	1	0.260	1	0.855	1	0.855	1	0.753	1	0.753
0.2	1	0.069	1	0.069	1	0.175	1	0.175	1	0.759	1	0.759	1	0.671	1	0.671
0.25	0.97	0	0.97	0	0.98	0	0.98	0	1	0.662	1	0.662	1	0.588	1	0.588
0.3	0.81	0	0.81	0	0.85	0	0.85	0	1	0.566	1	0.566	1	0.506	1	0.506
0.35	0.65	0	0.65	0	0.72	0	0.72	0	1	0.469	1	0.469	1	0.424	1	0.424
0.4	0.51	0	0.51	0	0.59	0	0.59	0	1	0.372	1	0.372	1	0.342	1	0.342

0.45	0.45	2.081	0.45	2.081	0.46	0	0.46	0	1	0.276	1	0.276	1	0.259	1	0.259
0.5	0.45	2.201	0.45	2.201	0.45	2.525	0.45	2.525	1	0.179	1	0.179	1	0.177	1	0.177
0.55	0.45	2.321	0.45	2.321	0.45	2.657	0.45	2.657	1	0.100	1	0.100	1	0.095	1	0.095
0.6	0.45	2.441	0.45	2.441	0.45	2.789	0.45	2.789	1	0.013	1	0.013	1	0.012	1	0.012

$p = 0.81$	$\theta = 0.75$	$\eta = 0.699$	$n = 100$	$m_{max} = 5$	$Z = 2$	$\lambda = 1$

Table 3-A-8. Sensitivity analysis with respect to drivers' aversion toward regret

(*Data corresponds to Figure 3-7*)

	Model 1		**Model 2**		**Model 3**		**Model 4**		**Model 5**		**Model 6**		**Model 7**		**Model 8**	
η	Maximum matching efficiency	Optimal surge multiplier	Maximum matching efficiency	Optimal surge multiplier	Maximum matching efficiency	Optimal surge multiplier	Maximum matching efficiency	Optimal surge multiplier	Maximum matching efficiency	Optimal surge multiplier	Maximum matching efficiency	Optimal surge multiplier	Maximum matching efficiency	Optimal surge multiplier	Maximum matching efficiency	Optimal surge multiplier
0.00001	1	2.228	1	2.228	1	1.420	1	1.420	1	1.849	1	1.849	1	1.494	1	1.494
0.0001	1	2.228	1	2.228	1	1.420	1	1.420	1	1.849	1	1.849	1	1.494	1	1.494
0.001	1	2.229	1	2.229	1	1.420	1	1.420	1	1.850	1	1.850	1	1.494	1	1.494
0.01	1	2.234	1	2.234	1	1.423	1	1.423	1	1.853	1	1.853	1	1.494	1	1.494
0.1	1	2.286	1	2.286	1	1.456	1	1.456	1	1.884	1	1.884	1	1.494	1	1.494
1	1	2.727	1	2.727	1	1.712	1	1.712	1	2.195	1	2.195	1	1.494	1	1.494
10	1	4.274	1	4.274	1	2.394	1	2.394	1	4.901	1	4.901	1	1.494	1	1.494
100	1	5	1	5	1	2.690	1	2.690	1	5	1	5	1	1.494	1	1.494

$\alpha = 0.85$	$\rho = 0.4$	$c = 0.3$	$p = 0.81$	$\theta = 0.75$	$n = 100$	$m_{max} = 5$	$Z = 2$	$\lambda = 1$

Table 3-A-9. Optimal surge multiplier when maximizing profit vs. matching efficiency

(Data corresponds to Figure 3-8)

	Model 1		**Model 2**		**Model 3**		**Model 4**		**Model 5**		**Model 6**		**Model 7**		**Model 8**	
m_{max}	Optimal surge multiplier when maximizing matching efficiency	Optimal surge multiplier when maximizing profit	Optimal surge multiplier when maximizing matching efficiency	Optimal surge multiplier when maximizing profit	Optimal surge multiplier when maximizing matching efficiency	Optimal surge multiplier when maximizing profit	Optimal surge multiplier when maximizing matching efficiency	Optimal surge multiplier when maximizing profit	Optimal surge multiplier when maximizing matching efficiency	Optimal surge multiplier when maximizing profit	Optimal surge multiplier when maximizing matching efficiency	Optimal surge multiplier when maximizing profit	Optimal surge multiplier when maximizing matching efficiency	Optimal surge multiplier when maximizing profit	Optimal surge multiplier when maximizing matching efficiency	Optimal surge multiplier when maximizing profit
100	2.809	100	2.809	100	1.755	100	1.755	100	2.262	100	2.262	100	1.494	98.764	1.494	98.764
50	2.809	50	2.809	50	1.755	50	1.755	50	2.262	49.068	2.262	49.068	1.494	46.467	1.494	46.467
25	2.809	25	2.809	25	1.755	23.366	1.755	23.366	2.262	21.068	2.262	21.068	1.494	15.199	1.494	15.199
15	2.809	15	2.809	15	1.755	13.908	1.755	13.908	2.262	14.088	2.262	14.088	1.494	10.579	1.494	10.579

10	2.809	10	2.809	10	1.755	8.326	1.755	8.326	2.262	7.424	2.262	7.424	1.494	6.554	1.494	6.554
5	2.809	5	2.809	5	1.755	3.850	1.755	3.850	2.262	5	2.262	5	1.494	1.494	1.494	1.494
2	1.921	2	1.921	2	1.639	2	1.639	2	1.645	2	1.645	2	1.494	1.494	1.494	1.494
1.5	1.5	1.5	1.5	1.5	1.5	1.5	1.5	1.5	1.5	1.5	1.5	1.5	1.494	1.494	1.494	1.494

$\alpha = 0.85$	$\rho = 0.4$	$c = 0.3$	$\eta = 1.2$	$p = 0.81$	$\theta = 0.75$	$n = 100$	$Z = 2$	$\lambda = 1$

Proof of Theorem 1

From (9), the expected regret-aversion utility of a driver who is initially located in Zone A and relocates to Zone B or stays in Zone A is,

$\mathbb{E}_{\rho,\alpha,\lambda}\left[u_{A,A}(\eta|m)\right]$

$$
\begin{aligned}
&= \mathbb{E}_{\rho,\alpha,\lambda}\left[p\theta.\min\left\{1, \frac{\rho}{(1-\gamma_A)\alpha + \gamma_B(1-\alpha)}\right\}\right.\\
&\qquad \left. - \eta(mp\lambda\theta - c)\left(1 - \min\left\{1, \frac{\rho}{(1-\gamma_A)\alpha + \gamma_B(1-\alpha)}\right\}\right)\right]\\
&= \int_0^Z \left(\int_0^1 \left(\int_0^{(1-\gamma_A)\alpha+\gamma_B(1-\alpha)} \left(p\theta \frac{\rho}{(1-\gamma_A)\alpha + \gamma_B(1-\alpha)}\right.\right.\right.\\
&\qquad \left. - \eta(mp\lambda\theta - c)\left(1 - \frac{\rho}{(1-\gamma_A)\alpha + \gamma_B(1-\alpha)}\right)\right) d\rho\\
&\qquad \left.\left. + \int_{(1-\gamma_A)\alpha+\gamma_B(1-\alpha)}^1 p\theta\, d\rho\right) d\alpha\right)\frac{1}{Z}d\lambda\\
&= p\theta - \frac{1}{4}\left(p\theta + \eta\left(mp\frac{Z}{2}\theta - c\right)\right)(1 - \gamma_A + \gamma_B).
\end{aligned}
$$

$\mathbb{E}_{\rho,\alpha,\lambda}\left[u_{A,B}(\eta|m)\right]$

$$= \mathbb{E}_{\rho,\alpha,\lambda}\left[(mp\lambda\theta - c).\min\left\{1, \frac{1-\rho}{(1-\gamma_B)(1-\alpha)+\gamma_A\alpha}\right\}\right.$$

$$\left. - \big(c + \eta(p\theta + c)\big).\left(1 - \min\left\{1, \frac{1-\rho}{(1-\gamma_B)(1-\alpha)+\gamma_A\alpha}\right\}\right)\right]$$

$$= \int_0^Z \left(\int_0^1 \left(\int_0^{1-(1-\gamma_B)(1-\alpha)-\gamma_A\alpha} (mp\lambda\theta - c)\, d\rho\right.\right.$$

$$+ \int_{1-(1-\gamma_B)(1-\alpha)-\gamma_A\alpha}^1 \left((mp\lambda\theta - c)\frac{1-\rho}{(1-\gamma_B)(1-\alpha)+\gamma_A\alpha}\right.$$

$$\left.\left.\left. - \big(c + \eta(p\theta + c)\big)\left(1 - \frac{1-\rho}{(1-\gamma_B)(1-\alpha)+\gamma_A\alpha}\right)\right) d\rho\right) d\alpha\right)\frac{1}{Z} d\lambda$$

$$= mp\frac{Z}{2}\theta\frac{3+\gamma_B-\gamma_A}{4} - c - \eta(p\theta + c)\frac{1-\gamma_B+\gamma_A}{4}.$$

Similarly, from (10), the expected regret-aversion utility of a driver who is initially located in Zone B and relocates to Zone A or stays in Zone B is, respectively,

$$\mathbb{E}_{\rho,\alpha,\lambda}\left[u_{B,A}(\eta|m)\right]$$

$$= \mathbb{E}_{\rho,\alpha,\lambda}\left[(p\theta - c).\min\left\{1, \frac{\rho}{(1-\gamma_A)\alpha+\gamma_B(1-\alpha)}\right\}\right.$$

$$\left. - \big(c + \eta(mp\lambda\theta + c)\big)\left(1 - \min\left\{1, \frac{\rho}{(1-\gamma_A)\alpha+\gamma_B(1-\alpha)}\right\}\right)\right]$$

$$= \int_0^Z \left(\int_0^1 \left(\int_0^{(1-\gamma_A)\alpha+\gamma_B(1-\alpha)} \left((p\theta - c)\frac{\rho}{(1-\gamma_A)\alpha+\gamma_B(1-\alpha)}\right.\right.\right.$$

$$\left. - \big(c + \eta(mp\lambda\theta + c)\big)\left(1 - \frac{\rho}{(1-\gamma_A)\alpha+\gamma_B(1-\alpha)}\right)\right) d\rho$$

$$\left.\left. + \int_{(1-\gamma_A)\alpha+\gamma_B(1-\alpha)}^1 (p\theta - c)\, d\rho\right) d\alpha\right)\frac{1}{Z} d\lambda$$

$$= p\theta - c - \frac{1}{4}\left(p\theta + \eta\left(mp\frac{Z}{2}\theta + c\right)\right)(1-\gamma_A+\gamma_B).$$

$$\mathbb{E}_{\rho,\alpha,\lambda}\left[u_{B,B}(\eta|m)\right]$$

$$= \mathbb{E}_{\rho,\alpha,\lambda}\left[mp\lambda\theta.\min\left\{1,\frac{1-\rho}{(1-\gamma_B)(1-\alpha)+\gamma_A\alpha}\right\}\right.$$

$$\left.-\eta(p\theta-c).\left(1-\min\left\{1,\frac{1-\rho}{(1-\gamma_B)(1-\alpha)+\gamma_A\alpha}\right\}\right)\right]$$

$$= \int_0^Z\left(\int_0^1\left(\int_0^{1-(1-\gamma_B)(1-\alpha)-\gamma_A\alpha}(mp\lambda\theta)\,d\rho\right.\right.$$

$$+\int_{1-(1-\gamma_B)(1-\alpha)-\gamma_A\alpha}^{1}\left(mp\lambda\theta\frac{1-\rho}{(1-\gamma_B)(1-\alpha)+\gamma_A\alpha}\right.$$

$$\left.\left.\left.-\eta(p\theta-c)\left(1-\frac{1-\rho}{(1-\gamma_B)(1-\alpha)+\gamma_A\alpha}\right)\right)d\rho\right)d\alpha\right)\frac{1}{Z}d\lambda$$

$$= mp\frac{Z}{2}\theta-\left(mp\frac{Z}{2}\theta+\eta(p\theta-c)\right)\frac{1+\gamma_A-\gamma_B}{4}.$$

We separate the proof into multiple cases.

1. When $\gamma_A = 0$ and $\gamma_B = 0$, no drivers relocate from their original zone. For this to occur, the utility of staying in Zone A must exceed the utility of moving to Zone B for drivers who are initially located in Zone A, and the utility of staying in Zone B must exceed the utility of moving to Zone A for drivers who are initially located in Zone B. To find the range of m where no drivers relocate from their original zone, we evaluate $\mathbb{E}_{\rho,\alpha,\lambda}[u_{A,A}(\eta|m)] \geq \mathbb{E}_{\rho,\alpha,\lambda}[u_{A,B}(\eta|m)]$ and $\mathbb{E}_{\rho,\alpha,\lambda}[u_{B,B}(\eta|m)] \geq \mathbb{E}_{\rho,\alpha,\lambda}[u_{B,A}(\eta|m)]$ for $\gamma_A = 0$ and $\gamma_B = 0$. Re-arranging $\mathbb{E}_{\rho,\alpha,\lambda}[u_{A,A}(\eta|m)] \geq \mathbb{E}_{\rho,\alpha,\lambda}[u_{A,B}(\eta|m)]$ gives $m \leq \frac{2}{Z}\left(1+\frac{c(4+2\eta)}{p\theta(3+\eta)}\right)$ and re-arranging $\mathbb{E}_{\rho,\alpha,\lambda}[u_{B,B}(\eta|m)] \geq \mathbb{E}_{\rho,\alpha,\lambda}[u_{B,A}(\eta|m)]$ gives $m \geq \frac{2}{Z}\left(1-\frac{c(4+2\eta)}{p\theta(3+\eta)}\right)$. Thus, no drivers relocate from their original zone if $\frac{2}{Z}\left(1-\frac{c(4+2\eta)}{p\theta(3+\eta)}\right) \leq m \leq \frac{2}{Z}\left(1+\frac{c(4+2\eta)}{p\theta(3+\eta)}\right)$ as $\frac{2}{Z}\left(1+\frac{c(4+2\eta)}{p\theta(3+\eta)}\right)-\frac{2}{Z}\left(1-\frac{c(4+2\eta)}{p\theta(3+\eta)}\right)=\frac{16c+8c\eta}{3pZ\theta+pZ\eta\theta}$ is always non-negative.
2. When $\gamma_A = 1$ and $\gamma_B = 0$, only drivers who are initially located in Zone A relocate to Zone B, but drivers in Zone B remain in their original zone. For this to occur, the utility of moving to Zone B must exceed the utility of staying in Zone A for drivers who are initially located in Zone A, and the utility of staying in Zone B must exceed the utility of

moving to Zone A for drivers who are initially located in Zone B. To find the range of m, we evaluate $\mathbb{E}_{\rho,\alpha,\lambda}[u_{A,A}(\eta|m)] \leq \mathbb{E}_{\rho,\alpha,\lambda}[u_{A,B}(\eta|m)]$ and $\mathbb{E}_{\rho,\alpha,\lambda}[u_{B,B}(\eta|m)] \geq \mathbb{E}_{\rho,\alpha,\lambda}[u_{B,A}(\eta|m)]$ for $\gamma_A = 1$ and $\gamma_B = 0$. Re-arranging $\mathbb{E}_{\rho,\alpha,\lambda}[u_{A,A}(\eta|m)] \leq \mathbb{E}_{\rho,\alpha,\lambda}[u_{A,B}(\eta|m)]$ gives $m \geq \frac{2}{Z}\left(1 + \frac{c}{p\theta}\right)(2+\eta)$ and re-arranging $\mathbb{E}_{\rho,\alpha,\lambda}[u_{B,B}(\eta|m)] \geq \mathbb{E}_{\rho,\alpha,\lambda}[u_{B,A}(\eta|m)]$ gives $m \geq \frac{2}{Z}\left(1 - \frac{c}{p\theta}\right)(2+\eta)$. Because $\frac{2}{Z}\left(1 + \frac{c}{p\theta}\right)(2+\eta) \geq \frac{2}{Z}\left(1 - \frac{c}{p\theta}\right)(2+\eta)$, drivers from Zone A will relocate from their original zone and drivers from Zone B will remain in Zone B when $m \geq \frac{2}{Z}\left(1 + \frac{c}{p\theta}\right)(2+\eta)$. Furthermore, when $\mathbb{E}_{\rho,\alpha,\lambda}[u_{A,B}(\eta|m)] \geq 0$, $m \geq \frac{2}{Z}\left(\frac{c}{p\theta}(2+\eta) + \eta\right)$, which is less than $\frac{2}{Z}\left(1 + \frac{c}{p\theta}\right)(2+\eta)$, implying that the utility associated with drivers from Zone A relocating to Zone B will be positive when the threshold is reached.

3. When $\gamma_A = 0$ and $\gamma_B = 1$, only drivers who are initially located in Zone B relocate to Zone A, but drivers in Zone A remain in their original zone. For this to occur, the utility of staying in Zone A must exceed the utility of moving to Zone B for drivers who are initially located in Zone A, and the utility of moving to Zone A must exceed the utility of staying in Zone B for drivers who are initially located in Zone B. To find the range of m, we evaluate $\mathbb{E}_{\rho,\alpha,\lambda}[u_{A,A}(\eta|m)] \geq \mathbb{E}_{\rho,\alpha,\lambda}[u_{A,B}(\eta|m)]$ and $\mathbb{E}_{\rho,\alpha,\lambda}[u_{B,B}(\eta|m)] \leq \mathbb{E}_{\rho,\alpha,\lambda}[u_{B,A}(\eta|m)]$ for $\gamma_A = 0$ and $\gamma_B = 1$. Re-arranging $\mathbb{E}_{\rho,\alpha,\lambda}[u_{A,A}(\eta|m)] \geq \mathbb{E}_{\rho,\alpha,\lambda}[u_{A,B}(\eta|m)]$ gives $m \leq \frac{2}{Z}\left(\frac{1}{2+\eta} + \frac{c}{p\theta}\right)$ and re-arranging $\mathbb{E}_{\rho,\alpha,\lambda}[u_{B,B}(\eta|m)] \leq \mathbb{E}_{\rho,\alpha,\lambda}[u_{B,A}(\eta|m)]$ gives $m \leq \frac{2}{Z}\left(\frac{1}{2+\eta} - \frac{c}{p\theta}\right)$. Because $\frac{2}{Z}\left(\frac{1}{2+\eta} - \frac{c}{p\theta}\right) \leq \frac{2}{Z}\left(\frac{1}{2+\eta} + \frac{c}{p\theta}\right)$, drivers from Zone B will relocate from their original zone and drivers from Zone A will remain in Zone A when $m \leq \frac{2}{Z}\left(\frac{1}{2+\eta} - \frac{c}{p\theta}\right)$. Furthermore, when $\mathbb{E}_{\rho,\alpha,\lambda}[u_{B,A}(\eta|m)] \geq 0$, $m \leq \frac{2}{Z}\frac{2+\eta}{\eta}\left(\frac{1}{2+\eta} - \frac{c}{p\theta}\right)$. Thus, if $\frac{1}{2+\eta} - \frac{c}{p\theta} \leq 0$, there is no m where this occurs. However, when $\frac{1}{2+\eta} - \frac{c}{p\theta} > 0$, then $\frac{2}{Z}\frac{2+\eta}{\eta}\left(\frac{1}{2+\eta} - \frac{c}{p\theta}\right) > \frac{2}{Z}\left(\frac{1}{2+\eta} - \frac{c}{p\theta}\right)$, which implies that the utility associated with relocating will be positive when the threshold is reached.
4. When $\gamma_A = 1$ and $\gamma_B = 1$, all drivers will relocate from their original zones. For this to occur, the utility of moving to Zone B must exceed the utility of staying in Zone A for

drivers who are initially located in Zone A, and the utility of moving to Zone A must exceed the utility of staying in Zone B for drivers who are initially located in Zone B. To find the range of m, we evaluate $\mathbb{E}_{\rho,\alpha,\lambda}\left[u_{A,A}(\eta|m)\right] \leq \mathbb{E}_{\rho,\alpha,\lambda}\left[u_{A,B}(\eta|m)\right]$ and $\mathbb{E}_{\rho,\alpha,\lambda}\left[u_{B,B}(\eta|m)\right] \leq \mathbb{E}_{\rho,\alpha,\lambda}\left[u_{B,A}(\eta|m)\right]$ for $\gamma_A = 1$ and $\gamma_B = 1$. Re-arranging $\mathbb{E}_{\rho,\alpha,\lambda}\left[u_{A,A}(\eta|m)\right] \leq \mathbb{E}_{\rho,\alpha,\lambda}\left[u_{A,B}(\eta|m)\right]$ gives $m \geq \frac{2}{Z}\left(1 + \frac{c(4+2\eta)}{p\theta(3+\eta)}\right)$ while re-arranging $\mathbb{E}_{\rho,\alpha,\lambda}\left[u_{B,B}(\eta|m)\right] \leq \mathbb{E}_{\rho,\alpha,\lambda}\left[u_{B,A}(\eta|m)\right]$ gives $m \leq \frac{2}{Z}\left(1 - \frac{c(4+2\eta)}{p\theta(3+\eta)}\right)$. Since $\frac{2}{Z}\left(1 + \frac{c(4+2\eta)}{p\theta(3+\eta)}\right) \geq \frac{2}{Z}\left(1 - \frac{c(4+2\eta)}{p\theta(3+\eta)}\right)$, the interval is non-overlapping. Thus, we have a contradiction, i.e., there does not exist a surge multiplier m where all drivers will relocate from their original zones.

5. When $0 < \gamma_A < 1$ and $0 < \gamma_B < 1$, only some of the drivers in Zone A will relocate from their original zones. We need to find the equilibrium points γ_A^* and γ_B^* where drivers in Zone A become indifferent between staying in Zone A and relocating to Zone B and drivers in Zone B become indifferent between staying in Zone B and relocating to Zone A. To find these points, we solve a linear system with two variables (γ_A, γ_B) and two equations $\mathbb{E}_{\rho,\alpha,\lambda}\left[u_{A,A}(\eta|m)\right] = \mathbb{E}_{\rho,\alpha,\lambda}\left[u_{A,B}(\eta|m)\right]$ and $\mathbb{E}_{\rho,\alpha,\lambda}\left[u_{B,B}(\eta|m)\right] = \mathbb{E}_{\rho,\alpha,\lambda}\left[u_{B,A}(\eta|m)\right]$. Because the lines governing this linear system are parallel and never intersect, we obtain no solution. This implies that there is no equilibrium solution for this case.

6. When $\gamma_A = 1$ and $0 < \gamma_B < 1$, all drivers who are initially located in Zone A will relocate from their original zone, but only some of the drivers in Zone B will relocate to Zone A. To determine the optimal proportion γ_B^*, we find an equilibrium point where drivers in Zone B become indifferent between staying in Zone B and relocating to Zone A. Thus, we evaluate $\mathbb{E}_{\rho,\alpha,\lambda}\left[u_{B,B}(\eta|m)\right] = \mathbb{E}_{\rho,\alpha,\lambda}\left[u_{B,A}(\eta|m)\right]$ for $\gamma_A = 1$ which gives:

$$p\theta - c - \frac{1}{4}\left(p\theta + \eta\left(mp\frac{Z}{2}\theta + c\right)\right)\gamma_B = mp\frac{Z}{2}\theta - \frac{1}{4}\left(mp\frac{Z}{2}\theta + \eta(p\theta - c)\right)(2 - \gamma_B).$$

Solving for γ_B, it follows that $\gamma_B^* = \frac{(p\theta - c)(4+2\eta) - 2mp\frac{Z}{2}\theta}{(1+\eta)\left(p\theta + mp\frac{Z}{2}\theta\right)}$. For this case to occur, the utility of moving to Zone B must also exceed the utility of staying in Zone A for drivers who are initially in Zone A. Thus, we evaluate $\mathbb{E}_{\rho,\alpha,\lambda}\left[u_{A,A}(\eta|m)\right] \leq \mathbb{E}_{\rho,\alpha,\lambda}\left[u_{A,B}(\eta|m)\right]$ for $\gamma_B^* =$

$\frac{(p\theta-c)(4+2\eta)-2mp\frac{Z}{2}\theta}{(1+\eta)\left(p\theta+mp\frac{Z}{2}\theta\right)}$ and $\gamma_A = 1$, which yields a contradiction as the equation reduces to $c(2+\eta) < 0$ and all parameters are non-negative. Consequently, it follows that there is no equilibrium solution where all drivers in Zone A relocate to Zone B and some of the drivers in Zone B relocate to Zone A.

7. When $0 < \gamma_A < 1$ and $\gamma_B = 1$, all drivers who are initially located in Zone B will relocate from their original zone, but only some of the drivers in Zone A will relocate to Zone B. To determine the optimal proportion γ_A^*, we find an equilibrium point where drivers in Zone A become indifferent between staying in Zone A and relocating to Zone B. Thus, we evaluate $\mathbb{E}_{\rho,\alpha,\lambda}\left[u_{A,A}(\eta|m)\right] = \mathbb{E}_{\rho,\alpha,\lambda}\left[u_{A,B}(\eta|m)\right]$ for $\gamma_B = 1$ which gives:

$$p\theta - \frac{1}{4}\left(p\theta + \eta\left(mp\frac{Z}{2}\theta - c\right)\right)(2-\gamma_A) = mp\frac{Z}{2}\theta\left(\frac{4-\gamma_A}{4}\right) - c - \eta(p\theta + c)\frac{\gamma_A}{4}. \qquad \text{(A1)}$$

Solving (A1) for γ_A, it follows that $\gamma_A^* = \frac{\left(mp\frac{Z}{2}\theta-c\right)(4+2\eta)-2p\theta}{\left(mp\frac{Z}{2}\theta+p\theta\right)(1+\eta)}$. For this case to occur, the utility of moving to Zone A must also exceed the utility of staying in Zone B for drivers who are initially in Zone B. Thus, we evaluate $\mathbb{E}_{\rho,\alpha,\lambda}\left[u_{B,B}(\eta|m)\right] \leq \mathbb{E}_{\rho,\alpha,\lambda}\left[u_{B,A}(\eta|m)\right]$ for $\gamma_A^* = \frac{\left(mp\frac{Z}{2}\theta-c\right)(4+2\eta)-2p\theta}{\left(mp\frac{Z}{2}\theta+p\theta\right)(1+\eta)}$ and $\gamma_B = 1$, which yields a contradiction because, again, the equation reduces to $c(2+\eta) < 0$ and all parameters are non-negative. Consequently, it follows that there is no equilibrium solution where all drivers in Zone B relocate to Zone A and some of the drivers in Zone A relocate to Zone B.

8. When $\gamma_A = 0$ and $0 < \gamma_B < 1$, all drivers who are initially located in Zone A will stay in their original zone, but only some of the drivers in Zone B will relocate to Zone A. For this to occur, the utility of staying in Zone A must exceed the utility of moving to Zone B for drivers who are initially located in Zone A. To determine the optimal proportion γ_B^*, we find an equilibrium point where drivers in Zone B become indifferent between staying in Zone B and relocating to Zone A. Thus, we evaluate $\mathbb{E}_{\rho,\alpha,\lambda}\left[u_{B,B}(\eta|m)\right] = \mathbb{E}_{\rho,\alpha,\lambda}\left[u_{B,A}(\eta|m)\right]$ for $\gamma_A = 0$ which gives:

$$p\theta - c - \frac{1}{4}\left(p\theta + \eta\left(mp\frac{Z}{2}\theta + c\right)\right)(1+\gamma_B) = mp\frac{Z}{2}\theta - \frac{1}{4}\left(mp\frac{Z}{2}\theta + \eta(p\theta - c)\right)(1-\gamma_B).$$

(A2)

Solving (A2) for γ_B, it follows that $\gamma_B^* = \frac{p\theta(3+\eta)(2-mZ)-4c(2+\eta)}{p\theta(1+\eta)(mZ+2)}$. The range at which the equilibrium solution is valid can be calculated by finding the value of the surge multiplier m in the limit where $\gamma_A = 0$ and either $\gamma_B^* \to 0$ or $\gamma_B^* \to 1$. The respective equations are given by $\frac{p\theta(3+\eta)(2-mZ)-4c(2+\eta)}{p\theta(1+\eta)(mZ+2)} = 0$ and $\frac{p\theta(3+\eta)(2-mZ)-4c(2+\eta)}{p\theta(1+\eta)(mZ+2)} = 1$. Solving for m gives $\frac{2}{Z}\left(1-\frac{c(4+2\eta)}{p\theta(3+\eta)}\right)$ and $\frac{2}{Z}\left(\frac{1}{2+\eta}-\frac{c}{p\theta}\right)$, respectively, which are the thresholds derived in cases 1 and 3.

9. When $0 < \gamma_A < 1$ and $\gamma_B = 0$, only some of the drivers in Zone A will relocate to Zone B while all drivers who are initially located in Zone B will stay in their original zone. To determine the optimal proportion γ_A^*, we find an equilibrium point where drivers in Zone A become indifferent between staying in Zone A and relocating to Zone B. Thus, we evaluate $\mathbb{E}_{\rho,\alpha,\lambda}\left[u_{A,A}(\eta|m)\right] = \mathbb{E}_{\rho,\alpha,\lambda}\left[u_{A,B}(\eta|m)\right]$ for $\gamma_B = 0$ which gives:

$$p\theta - \frac{1}{4}\left(p\theta + \eta\left(mp\frac{Z}{2}\theta - c\right)\right)(1-\gamma_A) = mp\frac{Z}{2}\theta\left(\frac{3-\gamma_A}{4}\right) - c - \eta(p\theta + c)\frac{1+\gamma_A}{4}. \quad \text{(A3)}$$

Setting $\gamma_B = 0$, re-arranging and solving for γ_A in (A3), we obtain $\gamma_A^* = \frac{(3+\eta)\left(mp\frac{Z}{2}\theta - p\theta\right)-c(4+2\eta)}{(1+\eta)\left(p\theta+mp\frac{Z}{2}\theta\right)}$. The range at which the equilibrium solution is valid can be calculated by finding the value of the surge multiplier m in the limit when $\gamma_B = 0$ and either $\gamma_A^* \to 0$ or $\gamma_A^* \to 1$. The respective equations are given by $\frac{(3+\eta)\left(mp\frac{Z}{2}\theta - p\theta\right)-c(4+2\eta)}{(1+\eta)\left(p\theta+mp\frac{Z}{2}\theta\right)} = 0$ and $\frac{(3+\eta)\left(mp\frac{Z}{2}\theta - p\theta\right)-c(4+2\eta)}{(1+\eta)\left(p\theta+mp\frac{Z}{2}\theta\right)} = 1$. Solving for m gives $\frac{2}{Z}\left(1+\frac{c(4+2\eta)}{p\theta(3+\eta)}\right)$ and $\frac{2}{Z}\left(1+\frac{c}{p\theta}\right)(2+\eta)$, respectively, which are the thresholds derived in cases 1 and 2.

A summary of the cases appears in Table 3-A-10.

Table 3-A-10. Result summary for Theorem 1

Case	% of drivers γ_A^* initially located in Zone A relocating to Zone B	% of drivers γ_B^* initially located in Zone B relocating to Zone A	Range for the surge multiplier m
3	0	1	$0 \le m \le \frac{2}{Z}\left(\frac{1}{2+\eta}-\frac{c}{p\theta}\right)$
8	0	$0 < \gamma_B < 1$	$\frac{2}{Z}\left(\frac{1}{2+\eta}-\frac{c}{p\theta}\right) \le m \le \frac{2}{Z}\left(1-\frac{c(4+2\eta)}{p\theta(3+\eta)}\right)$

		$\gamma_B^* = \frac{p\theta(3+\eta)(2-mZ)-4c(2+\eta)}{p\theta(1+\eta)(mZ+2)}$	
1	0	0	$\frac{2}{Z}\left(1-\frac{c(4+2\eta)}{p\theta(3+\eta)}\right) \leq m \leq \frac{2}{Z}\left(1+\frac{c(4+2\eta)}{p\theta(3+\eta)}\right)$
9	$0 < \gamma_A < 1$ $\gamma_A^* = \frac{(3+\eta)\left(mp\frac{Z}{2}\theta - p\theta\right) - c(4+2\eta)}{(1+\eta)\left(p\theta + mp\frac{Z}{2}\theta\right)}$	0	$\frac{2}{Z}\left(1+\frac{c(4+2\eta)}{p\theta(3+\eta)}\right) \leq m \leq \frac{2}{Z}\left(1+\frac{c}{p\theta}\right)(2+\eta)$
2	1	0	$\frac{2}{Z}\left(1+\frac{c}{p\theta}\right)(2+\eta) \leq m \leq m_{max}$
7	$0 < \gamma_A < 1$	1	No equilibrium
5	$0 < \gamma_A < 1$	$0 < \gamma_B < 1$	
4	1	1	
6	1	$0 < \gamma_B < 1$	

Proof of Theorem 2

From (9) and (10), the expected regret-aversion utility of a driver who is initially located in Zone A and relocates to Zone B or stays in Zone A, and the expected regret-aversion utility of a driver who is initially located in Zone B and relocates to Zone A or stays in Zone B, depend on multiple cases. Following Theorem 1, we separate the proof into cases.

1. When $\gamma_A = 0$ and $\gamma_B = 0$, we have $\frac{\rho}{(1-\gamma_A)\alpha + \gamma_B(1-\alpha)} = \frac{\rho}{\alpha}$. Thus, $\frac{\rho}{(1-\gamma_A)\alpha + \gamma_B(1-\alpha)} \leq 1$ implies $\alpha \geq \rho$. Thus,

$$
\begin{aligned}
&\mathbb{E}_{\alpha,\lambda}\left[u_{A,A}(\eta|m,\rho)\right] \\
&\quad = \mathbb{E}_{\alpha,\lambda}\left[p\theta.\min\left\{1, \frac{\rho}{(1-\gamma_A)\alpha + \gamma_B(1-\alpha)}\right\}\right. \\
&\quad \left. - \eta(mp\lambda\theta - c)\left(1 - \min\left\{1, \frac{\rho}{(1-\gamma_A)\alpha + \gamma_B(1-\alpha)}\right\}\right)\right] \\
&\quad = \int_0^Z \left(\int_0^\rho p\theta \, d\alpha + \int_\rho^1 \left(\left(p\theta + \eta(mp\lambda\theta - c)\right)\frac{\rho}{\alpha} - \eta(mp\lambda\theta - c)\right) d\alpha\right)\frac{1}{Z} d\lambda \\
&\quad = p\theta\rho - \rho\log[\rho]\left(p\theta + \eta\left(mp\frac{Z}{2}\theta - c\right)\right) - \eta\left(mp\frac{Z}{2}\theta - c\right)(1-\rho).
\end{aligned}
$$

Similarly, when $\gamma_A = 0$ and $\gamma_B = 0$, $\frac{1-\rho}{(1-\gamma_B)(1-\alpha) + \gamma_A\alpha} \leq 1$ implies $\alpha \leq \rho$. Thus,

$$\mathbb{E}_{\alpha,\lambda}\left[u_{A,B}(\eta|m,\rho)\right]$$

$$= \mathbb{E}_{\alpha,\lambda}\Bigg[(mp\lambda\theta - c).\min\left\{1, \frac{1-\rho}{(1-\gamma_B)(1-\alpha)+\gamma_A\alpha}\right\}$$

$$- \big(c + \eta(p\theta + c)\big)\left(1 - \min\left\{1, \frac{1-\rho}{(1-\gamma_B)(1-\alpha)+\gamma_A\alpha}\right\}\right)\Bigg]$$

$$= \int_0^Z \left(\int_0^\rho \left(\big(mp\lambda\theta + \eta(p\theta + c)\big)\frac{1-\rho}{1-\alpha} - \big(c + \eta(p\theta + c)\big)\right) d\alpha\right.$$

$$\left. + \int_\rho^1 (mp\lambda\theta - c)\, d\alpha\right)\frac{1}{Z}\, d\lambda$$

$$= -(1-\rho)\log[1-\rho]\left(mp\frac{Z}{2}\theta + \eta(p\theta + c)\right)$$

$$- \rho\left(mp\frac{Z}{2}\theta + \eta(p\theta + c)\right) + \left(mp\frac{Z}{2}\theta - c\right).$$

$$\mathbb{E}_{\alpha,\lambda}\left[u_{B,A}(\eta|m,\rho)\right]$$

$$= \mathbb{E}_{\alpha,\lambda}\Bigg[(p\theta - c).\min\left\{1, \frac{\rho}{(1-\gamma_A)\alpha+\gamma_B(1-\alpha)}\right\}$$

$$- \big(c + \eta(mp\lambda\theta + c)\big)\left(1 - \min\left\{1, \frac{\rho}{(1-\gamma_A)\alpha+\gamma_B(1-\alpha)}\right\}\right)\Bigg]$$

$$= \int_0^Z \left(\int_0^\rho (p\theta - c)\, d\alpha\right.$$

$$\left. + \int_\rho^1 \left(\big(p\theta + \eta(mp\lambda\theta + c)\big)\frac{\rho}{\alpha} - \big(c + \eta(mp\lambda\theta + c)\big)\right) d\alpha\right)\frac{1}{Z}\, d\lambda$$

$$= p\theta\rho - c - \rho\log[\rho]\left(p\theta + \eta\left(mp\frac{Z}{2}\theta + c\right)\right) - \eta\left(mp\frac{Z}{2}\theta + c\right)(1-\rho).$$

$$\mathbb{E}_{\alpha,\lambda}\left[u_{B,B}(\eta|m,\rho)\right]$$

$$= \mathbb{E}_{\alpha,\lambda}\left[mp\lambda\theta.\min\left\{1,\frac{1-\rho}{(1-\gamma_B)(1-\alpha)+\gamma_A\alpha}\right\}\right.$$

$$\left.-\eta(p\theta-c)\left(1-\min\left\{1,\frac{1-\rho}{(1-\gamma_B)(1-\alpha)+\gamma_A\alpha}\right\}\right)\right]$$

$$= \int_0^Z\left(\int_0^\rho\left(\left(mp\lambda\theta+\eta(p\theta-c)\right)\frac{1-\rho}{1-\alpha}-\eta(p\theta-c)\right)d\alpha\right.$$

$$\left.+\int_\rho^1 mp\lambda\theta\, d\alpha\right)\frac{1}{Z}d\lambda$$

$$= -(1-\rho)\log[1-\rho]\left(mp\frac{Z}{2}\theta+\eta(p\theta-c)\right)$$

$$-\rho\left(mp\frac{Z}{2}\theta+\eta(p\theta-c)\right)+mp\frac{Z}{2}\theta.$$

When $\gamma_A = 0$ and $\gamma_B = 0$, no drivers relocate from their original zone. For this to occur, the utility of staying in Zone A must exceed the utility of moving to Zone B for drivers who are initially located in Zone A, and the utility of staying in Zone B must exceed the utility of moving to Zone A for drivers who are initially located in Zone B. To find the range of m where no drivers relocate from their original zone, we evaluate $\mathbb{E}_{\alpha,\lambda}\left[u_{A,A}(\eta|m,\rho)\right] > \mathbb{E}_{\alpha,\lambda}\left[u_{A,B}(\eta|m,\rho)\right]$ and $\mathbb{E}_{\alpha,\lambda}\left[u_{B,B}(\eta|m,\rho)\right] > \mathbb{E}_{\alpha,\lambda}\left[u_{B,A}(\eta|m,\rho)\right]$ for $\gamma_A = 0$ and $\gamma_B = 0$.

$\mathbb{E}_{\alpha,\lambda}\left[u_{A,A}(\eta|m,\rho)\right] > \mathbb{E}_{\alpha,\lambda}\left[u_{A,B}(\eta|m,\rho)\right]$ gives us, $p\theta\rho-\rho\log[\rho]\left(p\theta+\eta\left(mp\frac{Z}{2}\theta-c\right)\right)-\eta\left(mp\frac{Z}{2}\theta-c\right)(1-\rho) > -(1-\rho)\log[1-\rho]\left(mp\frac{Z}{2}\theta+\eta(p\theta+c)\right)-\rho\left(mp\frac{Z}{2}\theta+\eta(p\theta+c)\right)+\left(mp\frac{Z}{2}\theta-c\right)$, which implies $m < m_U := \frac{\frac{1+\eta}{1-\rho}(c+p\theta\rho)+\eta(c+p\theta)\log[1-\rho]+\frac{\rho}{1-\rho}(c\eta-p\theta)\log[\rho]}{\frac{1}{2}pZ\theta\left((1+\eta)-\log[1-\rho]+\eta\frac{\rho}{1-\rho}\log[\rho]\right)}$. Note that $(1+\eta)-\log[1-\rho]+\eta\frac{\rho}{1-\rho}\log[\rho] > 0$ for $\eta \geq 0$ and $\rho \in (0,1)$ because,

$$(1+\eta)-\log[1-\rho]+\eta\frac{\rho}{1-\rho}\log[\rho] \geq (1+\eta)+\eta\frac{\rho}{1-\rho}\text{Log}[\rho]$$

$$= 1 + \eta\left(1 + \frac{\rho}{1-\rho}\text{Log}[\rho]\right)$$

$$\geq 1 + \eta\left(1 + \frac{\rho}{1-\rho}\left(1 - \frac{1}{\rho}\right)\right)$$

$$\geq 1,$$

as $\frac{\rho}{1-\rho} \geq 0$ and $\log[\rho] \geq 1 - \frac{1}{\rho}$ for all $\rho > 0$.

Second, $\mathbb{E}_{\alpha,\lambda}\left[u_{B,B}(\eta|m,\rho)\right] > \mathbb{E}_{\alpha,\lambda}\left[u_{B,A}(\eta|m,\rho)\right]$ gives us $-(1-\rho)\log[1-\rho]\left(mp\frac{Z}{2}\theta + \eta(p\theta - c)\right) - \rho\left(mp\frac{Z}{2}\theta + \eta(p\theta - c)\right) + mp\frac{Z}{2}\theta > p\theta\rho - c - \rho\log[\rho]\left(p\theta + \eta\left(mp\frac{Z}{2}\theta + c\right)\right) - \eta\left(mp\frac{Z}{2}\theta + c\right)(1-\rho)$, which implies $m > m_L := \frac{\frac{1+\eta}{1-\rho}(p\theta\rho - c) + \eta(p\theta - c)\log[1-\rho] - \frac{\rho}{1-\rho}(c\eta + p\theta)\log[\rho]}{\frac{1}{2}pZ\theta\left((1+\eta) - \log[1-\rho] + \frac{\rho}{1-\rho}\eta\log[\rho]\right)}$. Note that $(1+\eta) - \log[1-\rho] + \frac{\rho}{1-\rho}\eta\log[\rho] > 0$ for $\eta \geq 0$ and $\rho \in (0,1)$ as shown before.

Finally, we have $m_U - m_L = \frac{\frac{1+\eta}{1-\rho}(c + p\theta\rho) + \eta(c + p\theta)\log[1-\rho] + \frac{\rho}{1-\rho}(c\eta - p\theta)\log[\rho]}{\frac{1}{2}pZ\theta\left((1+\eta) - \log[1-\rho] + \eta\frac{\rho}{1-\rho}\log[\rho]\right)} - \frac{\frac{1+\eta}{1-\rho}(p\theta\rho - c) + \eta(p\theta - c)\log[1-\rho] - \frac{\rho}{1-\rho}(c\eta + p\theta)\log[\rho]}{\frac{1}{2}pZ\theta\left((1+\eta) - \log[1-\rho] + \frac{\rho}{1-\rho}\eta\log[\rho]\right)} = \frac{4c}{pZ\theta}\left(\frac{\frac{1+\eta}{1-\rho} + \eta\frac{\rho}{1-\rho}\log[\rho] + \eta\log[1-\rho]}{(1+\eta) - \log[1-\rho] + \frac{\rho}{1-\rho}\eta\log[\rho]}\right)$. Note that $m_U - m_L \geq 0$ because

$$\frac{1+\eta}{1-\rho} + \eta\frac{\rho}{1-\rho}\log[\rho] + \eta\log[1-\rho] \geq \frac{1+\eta}{1-\rho} + \eta\frac{\rho}{1-\rho}\log[\rho]$$

$$= \frac{1}{1-\rho}[1 + \eta(1 + \rho\log[\rho])]$$

$$\geq 1 + \eta(1 + \rho\log[\rho])$$

$$\geq 1 + \eta\left(1 + \rho\left(1 - \frac{1}{\rho}\right)\right)$$

$$\geq 1.$$

Thus, no drivers relocate from their original zone when $m \in \left[\frac{\frac{1+\eta}{1-\rho}(p\theta\rho - c) + \eta(p\theta - c)\log[1-\rho] - \frac{\rho}{1-\rho}(c\eta + p\theta)\log[\rho]}{\frac{1}{2}pZ\theta\left((1+\eta) - \log[1-\rho] + \frac{\rho}{1-\rho}\eta\log[\rho]\right)}, \frac{\frac{1+\eta}{1-\rho}(c + p\theta\rho) + \eta(c + p\theta)\log[1-\rho] + \frac{\rho}{1-\rho}(c\eta - p\theta)\log[\rho]}{\frac{1}{2}pZ\theta\left((1+\eta) - \log[1-\rho] + \eta\frac{\rho}{1-\rho}\log[\rho]\right)}\right]$.

2. When $\gamma_A = 1$ and $\gamma_B = 1$, we have $\frac{\rho}{(1-\gamma_A)\alpha+\gamma_B(1-\alpha)} = \frac{\rho}{1-\alpha}$. Thus, $\frac{\rho}{(1-\gamma_A)\alpha+\gamma_B(1-\alpha)} \leq 1$ implies $\alpha \leq 1-\rho$. Then,

$$\mathbb{E}_{\alpha,\lambda}\left[u_{A,A}(\eta|m,\rho)\right]$$

$$= \mathbb{E}_{\alpha,\lambda}\left[p\theta.\min\left\{1,\frac{\rho}{(1-\gamma_A)\alpha+\gamma_B(1-\alpha)}\right\}\right.$$

$$\left.-\eta(mp\lambda\theta-c)\left(1-\min\left\{1,\frac{\rho}{(1-\gamma_A)\alpha+\gamma_B(1-\alpha)}\right\}\right)\right]$$

$$= \int_0^Z\left(\int_{1-\rho}^1 p\theta\, d\alpha\right.$$

$$\left.+\int_0^{1-\rho}\left(\big(p\theta+\eta(mp\lambda\theta-c)\big)\frac{\rho}{1-\alpha}-\eta(mp\lambda\theta-c)\right)d\alpha\right)\frac{1}{Z}d\lambda$$

$$= p\theta\rho-\rho\log[\rho]\left(p\theta+\eta\left(mp\frac{Z}{2}\theta-c\right)\right)-\eta\left(mp\frac{Z}{2}\theta-c\right)(1-\rho).$$

Similarly, when $\gamma_A = 1$ and $\gamma_B = 1$, $\frac{1-\rho}{(1-\gamma_B)(1-\alpha)+\gamma_A\alpha} \leq 1$ implies $\alpha \geq 1-\rho$. Thus,

$$\mathbb{E}_{\alpha,\lambda}\left[u_{A,B}(\eta|m,\rho)\right]$$

$$= \left[\mathbb{E}_{\alpha,\lambda}\left((mp\lambda\theta-c).\min\left\{1,\frac{1-\rho}{(1-\gamma_B)(1-\alpha)+\gamma_A\alpha}\right\}\right.\right.$$

$$\left.\left.-\big(c+\eta(p\theta+c)\big)\left(1-\min\left\{1,\frac{1-\rho}{(1-\gamma_B)(1-\alpha)+\gamma_A\alpha}\right\}\right)\right)\right]$$

$$= \int_0^Z\left(\int_{1-\rho}^1\left(\big(mp\lambda\theta+\eta(p\theta+c)\big)\frac{1-\rho}{\alpha}-\big(c+\eta(p\theta+c)\big)\right)d\alpha\right.$$

$$\left.+\int_0^{1-\rho}(mp\lambda\theta-c)\,d\alpha\right)\frac{1}{Z}d\lambda$$

$$= -(1-\rho)\log[1-\rho]\left(mp\frac{Z}{2}\theta+\eta(p\theta+c)\right)$$

$$-\rho\left(mp\frac{Z}{2}\theta+\eta(p\theta+c)\right)+\left(mp\frac{Z}{2}\theta-c\right).$$

$\mathbb{E}_{\alpha,\lambda}\left[u_{B,A}(\eta|m,\rho)\right]$ and $\mathbb{E}_{\alpha,\lambda}\left[u_{B,B}(\eta|m,\rho)\right]$ also gives the same results as case 1. To find the range of m, we evaluate $\mathbb{E}_{\alpha,\lambda}\left[u_{A,A}(\eta|m,\rho)\right] < \mathbb{E}_{\alpha,\lambda}\left[u_{A,B}(\eta|m,\rho)\right]$ and $\mathbb{E}_{\alpha,\lambda}\left[u_{B,B}(\eta|m,\rho)\right] < \mathbb{E}_{\alpha,\lambda}\left[u_{B,A}(\eta|m,\rho)\right]$ for $\gamma_A = 1$ and $\gamma_B = 1$. Re-arranging $\mathbb{E}_{\alpha,\lambda}\left[u_{A,A}(\eta|m,\rho)\right] < \mathbb{E}_{\alpha,\lambda}\left[u_{A,B}(\eta|m,\rho)\right]$ gives $m > \frac{\frac{1+\eta}{1-\rho}(c+p\theta\rho)+\eta(c+p\theta)\log[1-\rho]+\frac{\rho}{1-\rho}(c\eta-p\theta)\log[\rho]}{\frac{1}{2}pZ\theta\left((1+\eta)-\log[1-\rho]+\eta\frac{\rho}{1-\rho}\log[\rho]\right)}$ while re-arranging $\mathbb{E}_{\alpha,\lambda}\left[u_{B,B}(\eta|m,\rho)\right] <$ $\mathbb{E}_{\alpha,\lambda}\left[u_{B,A}(\eta|m,\rho)\right]$ gives $m < \frac{\frac{1+\eta}{1-\rho}(p\theta\rho-c)+\eta(p\theta-c)\log[1-\rho]-\frac{\rho}{1-\rho}(c\eta+p\theta)\log[\rho]}{\frac{1}{2}pZ\theta\left((1+\eta)-\log[1-\rho]+\frac{\rho}{1-\rho}\eta\log[\rho]\right)}$. Since

$$\frac{\frac{1+\eta}{1-\rho}(c+p\theta\rho)+\eta(c+p\theta)\log[1-\rho]+\frac{\rho}{1-\rho}(c\eta-p\theta)\log[\rho]}{\frac{1}{2}pZ\theta\left((1+\eta)-\log[1-\rho]+\eta\frac{\rho}{1-\rho}\log[\rho]\right)} \geq \frac{\frac{1+\eta}{1-\rho}(p\theta\rho-c)+\eta(p\theta-c)\log[1-\rho]-\frac{\rho}{1-\rho}(c\eta+p\theta)\log[\rho]}{\frac{1}{2}pZ\theta\left((1+\eta)-\log[1-\rho]+\frac{\rho}{1-\rho}\eta\log[\rho]\right)},$$

the interval is non-overlapping. Thus, we have a contradiction, i.e., there does not exist a surge multiplier m where all drivers will relocate from their original zones.

3. When $\gamma_A = 1$ and $\gamma_B = 0$, we have $\lim \frac{\rho}{(1-\gamma_A)\alpha+\gamma_B(1-\alpha)} \to \infty$. Thus, $\min\left\{1, \frac{\rho}{(1-\gamma_A)\alpha+\gamma_B(1-\alpha)}\right\} = 1$ for any $\alpha \in (0,1)$. Then,

$$\mathbb{E}_{\alpha,\lambda}\left[u_{A,A}(\eta|m,\rho)\right]$$
$$= \mathbb{E}_{\alpha,\lambda}\left[p\theta.\min\left\{1, \frac{\rho}{(1-\gamma_A)\alpha+\gamma_B(1-\alpha)}\right\} - \eta(mp\lambda\theta - c)\left(1-\min\left\{1, \frac{\rho}{(1-\gamma_A)\alpha+\gamma_B(1-\alpha)}\right\}\right)\right]$$
$$= \int_0^Z \left(\int_0^1 p\theta\, d\alpha\right)\frac{1}{Z}d\lambda = p\theta.$$

Similarly, when $\gamma_A = 1$ and $\gamma_B = 0$, $\frac{1-\rho}{(1-\gamma_B)(1-\alpha)+\gamma_A\alpha} \leq 1$ implies $1-\rho < 1$ which holds for any $\alpha \in (0,1)$. Thus,

$$\mathbb{E}_{\alpha,\lambda}\left[u_{A,B}(\eta|m,\rho)\right]$$

$$= \mathbb{E}_{\alpha,\lambda}\left[(mp\lambda\theta - c).\min\left\{1, \frac{1-\rho}{(1-\gamma_B)(1-\alpha)+\gamma_A\alpha}\right\}\right.$$

$$\left. - \left(c + \eta(p\theta + c)\right)\left(1 - \min\left\{1, \frac{1-\rho}{(1-\gamma_B)(1-\alpha)+\gamma_A\alpha}\right\}\right)\right]$$

$$= \int_0^Z \left(\int_0^1 \left(\left(mp\lambda\theta + \eta(p\theta + c)\right)(1-\rho) - \left(c + \eta(p\theta + c)\right)\right) d\alpha\right)\frac{1}{Z}d\lambda$$

$$= \left(mp\frac{Z}{2}\theta + \eta(p\theta + c)\right)(1-\rho) - \left(c + \eta(p\theta + c)\right).$$

Similarly,

$$\mathbb{E}_{\alpha,\lambda}\left[u_{B,A}(\eta|m,\rho)\right]$$

$$= \mathbb{E}_{\alpha,\lambda}\left[(p\theta - c).\min\left\{1, \frac{\rho}{(1-\gamma_A)\alpha+\gamma_B(1-\alpha)}\right\}\right.$$

$$\left. - \left(c + \eta(mp\lambda\theta + c)\right)\left(1 - \min\left\{1, \frac{\rho}{(1-\gamma_A)\alpha+\gamma_B(1-\alpha)}\right\}\right)\right]$$

$$= \int_0^Z \left(\int_0^1 (p\theta - c)\, d\alpha\right)\frac{1}{Z}d\lambda = p\theta - c.$$

$$\mathbb{E}_{\alpha,\lambda}\left[u_{B,B}(\eta|m,\rho)\right]$$

$$= \mathbb{E}_{\alpha,\lambda}\left[mp\lambda\theta.\min\left\{1, \frac{1-\rho}{(1-\gamma_B)(1-\alpha)+\gamma_A\alpha}\right\}\right.$$

$$\left. - \eta(p\theta - c)\left(1 - \min\left\{1, \frac{1-\rho}{(1-\gamma_B)(1-\alpha)+\gamma_A\alpha}\right\}\right)\right]$$

$$= \int_0^Z \left(\int_0^1 \left(\left(mp\lambda\theta + \eta(p\theta - c)\right)(1-\rho) - \eta(p\theta - c)\right) d\alpha\right)\frac{1}{Z}d\lambda$$

$$= \left(mp\frac{Z}{2}\theta + \eta(p\theta - c)\right)(1-\rho) - \eta(p\theta - c).$$

Re-arranging $\mathbb{E}_{\alpha,\lambda}\left[u_{A,A}(\eta|m,\rho)\right] < \mathbb{E}_{\alpha,\lambda}\left[u_{A,B}(\eta|m,\rho)\right]$ gives $m > \frac{2}{Z}\left(1 + \frac{c}{p\theta}\right)\left(\frac{1+\eta\rho}{1-\rho}\right)$ and re-arranging $\mathbb{E}_{\alpha,\lambda}\left[u_{B,B}(\eta|m,\rho)\right] > \mathbb{E}_{\alpha,\lambda}\left[u_{B,A}(\eta|m,\rho)\right]$ gives $m > \frac{2}{Z}\left(1 - \frac{c}{p\theta}\right)\left(\frac{1+\eta\rho}{1-\rho}\right)$. Because $\frac{2}{Z}\left(1 + \frac{c}{p\theta}\right)\left(\frac{1+\eta\rho}{1-\rho}\right) \geq \frac{2}{Z}\left(1 - \frac{c}{p\theta}\right)\left(\frac{1+\eta\rho}{1-\rho}\right)$, drivers from Zone A will relocate from their original zone and drivers from Zone B will remain in Zone B when $m \geq \frac{2}{Z}\left(1+\frac{c}{p\theta}\right)\left(\frac{1+\eta\rho}{1-\rho}\right)$.

4. When $\gamma_A = 0$ and $\gamma_B = 1$, we have $\frac{\rho}{(1-\gamma_A)\alpha+\gamma_B(1-\alpha)} \leq 1$ implies $\rho < 1$, which holds for any $\alpha \in (0,1)$. Thus, $\min\left\{1, \frac{\rho}{(1-\gamma_A)\alpha+\gamma_B(1-\alpha)}\right\} = \rho$ for any $\alpha \in (0,1)$. Then,

$$\mathbb{E}_{\alpha,\lambda}\left[u_{A,A}(\eta|m,\rho)\right]$$

$$= \mathbb{E}_{\alpha,\lambda}\left[p\theta.\min\left\{1, \frac{\rho}{(1-\gamma_A)\alpha+\gamma_B(1-\alpha)}\right\}\right.$$

$$\left.- \eta(mp\lambda\theta - c)\left(1-\min\left\{1, \frac{\rho}{(1-\gamma_A)\alpha+\gamma_B(1-\alpha)}\right\}\right)\right]$$

$$= \int_0^Z \left(\int_0^1 \left(\left(p\theta + \eta(mp\lambda\theta - c)\right)\rho - \eta(mp\lambda\theta - c)\right) d\alpha\right)\frac{1}{Z}d\lambda$$

$$= \left(p\theta + \eta\left(mp\frac{Z}{2}\theta - c\right)\right)\rho - \eta\left(mp\frac{Z}{2}\theta - c\right).$$

Similarly, when $\gamma_A = 0$ and $\gamma_B = 1$, $\lim \frac{1-\rho}{(1-\gamma_B)(1-\alpha)+\gamma_A\alpha} \to \infty$. Thus, $\min\left\{1, \frac{1-\rho}{(1-\gamma_B)(1-\alpha)+\gamma_A\alpha}\right\} = 1$ for any $\alpha \in (0,1)$. Then,

$$\mathbb{E}_{\alpha,\lambda}\left[u_{A,B}(\eta|m,\rho)\right]$$

$$= \mathbb{E}_{\alpha,\lambda}\left[(mp\lambda\theta - c).\min\left\{1, \frac{1-\rho}{(1-\gamma_B)(1-\alpha)+\gamma_A\alpha}\right\}\right.$$

$$\left.- \left(c + \eta(p\theta + c)\right)\left(1-\min\left\{1, \frac{1-\rho}{(1-\gamma_B)(1-\alpha)+\gamma_A\alpha}\right\}\right)\right]$$

$$= \int_0^Z \left(\int_0^1 (mp\lambda\theta - c)\, d\alpha\right)\frac{1}{Z}d\lambda = mp\frac{Z}{2}\theta - c.$$

Similarly,

$$\mathbb{E}_{\alpha,\lambda}\left[u_{B,A}(\eta|m,\rho)\right]$$

$$= \mathbb{E}_{\alpha,\lambda}\left[(p\theta - c).\min\left\{1, \frac{\rho}{(1-\gamma_A)\alpha + \gamma_B(1-\alpha)}\right\}\right.$$

$$\left. - \left(c + \eta(mp\lambda\theta + c)\right)\left(1 - \min\left\{1, \frac{\rho}{(1-\gamma_A)\alpha + \gamma_B(1-\alpha)}\right\}\right)\right]$$

$$= \int_0^Z \left(\int_0^1 \left(\left(p\theta + \eta(mp\lambda\theta + c)\right)\rho - \left(c + \eta(mp\lambda\theta + c)\right)\right) d\alpha\right)\frac{1}{Z}d\lambda$$

$$= \left(p\theta + \eta\left(mp\frac{Z}{2}\theta + c\right)\right)\rho - \left(c + \eta\left(mp\frac{Z}{2}\theta + c\right)\right).$$

$$\mathbb{E}_{\alpha,\lambda}\left[u_{B,B}(\eta|m,\rho)\right]$$

$$= \mathbb{E}_{\alpha,\lambda}\left[mp\lambda\theta.\min\left\{1, \frac{1-\rho}{(1-\gamma_B)(1-\alpha) + \gamma_A\alpha}\right\}\right.$$

$$\left. - \eta(p\theta - c)\left(1 - \min\left\{1, \frac{1-\rho}{(1-\gamma_B)(1-\alpha) + \gamma_A\alpha}\right\}\right)\right]$$

$$= \int_0^Z \left(\int_0^1 (mp\lambda\theta)\, d\alpha\right)\frac{1}{Z}d\lambda = mp\frac{Z}{2}\theta.$$

Re-arranging $\mathbb{E}_{\alpha,\lambda}\left[u_{A,A}(\eta|m,\rho)\right] > \mathbb{E}_{\alpha,\lambda}\left[u_{A,B}(\eta|m,\rho)\right]$ gives $m < \frac{2}{Z}\left(\frac{\rho}{1-\eta\rho+\eta} + \frac{c}{p\theta}\right)$ and re-arranging $\mathbb{E}_{\alpha,\lambda}\left[u_{B,B}(\eta|m,\rho)\right] < \mathbb{E}_{\alpha,\lambda}\left[u_{B,A}(\eta|m,\rho)\right]$ gives $m < \frac{2}{Z}\left(\frac{\rho}{1-\eta\rho+\eta} - \frac{c}{p\theta}\right)$. Because $\frac{2}{Z}\left(\frac{\rho}{1-\eta\rho+\eta} + \frac{c}{p\theta}\right) \geq \frac{2}{Z}\left(\frac{\rho}{1-\eta\rho+\eta} - \frac{c}{p\theta}\right)$, drivers from Zone B will relocate from their original zone and drivers from Zone A will remain in Zone A when $m \leq \frac{2}{Z}\left(\frac{\rho}{1-\eta\rho+\eta} - \frac{c}{p\theta}\right)$.

5. When $\gamma_A = 0$ and $0 \leq \gamma_B \leq 1$, we have $1 - \gamma_A - \gamma_B \geq 0$. Thus, we can simplify $\frac{\rho}{(1-\gamma_A)\alpha+\gamma_B(1-\alpha)} \leq 1$ as $\rho \leq (1-\gamma_A)\alpha + \gamma_B(1-\alpha)$ and $\rho - \gamma_B \leq (1 - \gamma_A - \gamma_B)\alpha$. Thus, $\frac{\rho}{(1-\gamma_A)\alpha+\gamma_B(1-\alpha)} \leq 1$ implies $\alpha \geq \max\left\{0, \frac{\rho-\gamma_B}{1-\gamma_A-\gamma_B}\right\}$ when $1 - \gamma_A - \gamma_B \geq 0$, and, as a results, $\alpha \geq \max\left\{0, \frac{\rho-\gamma_B}{1-\gamma_B}\right\}$ when $\gamma_A = 0$ and $0 < \gamma_B < 1$. Similarly, $\frac{1-\rho}{(1-\gamma_B)(1-\alpha)+\gamma_A\alpha} \leq 1$ implies $\alpha \leq \max\left\{0, \frac{\rho-\gamma_B}{1-\gamma_B}\right\}$. Thus,

5.1. When $\rho - \gamma_B \geq 0$, we have

$$\mathbb{E}_{\alpha,\lambda}\left[u_{A,A}(\eta|m,\rho)\right]$$

$$= \mathbb{E}_{\alpha,\lambda}\left[p\theta.\min\left\{1,\frac{\rho}{(1-\gamma_A)\alpha+\gamma_B(1-\alpha)}\right\}\right.$$

$$\left.-\eta(mp\lambda\theta-c)\left(1-\min\left\{1,\frac{\rho}{(1-\gamma_A)\alpha+\gamma_B(1-\alpha)}\right\}\right)\right]$$

$$= \int_0^Z\left(\int_0^{\frac{\rho-\gamma_B}{1-\gamma_B}} p\theta\,d\alpha\right.$$

$$+\int_{\frac{\rho-\gamma_B}{1-\gamma_B}}^{1}\left(\left(p\theta+\eta(mp\lambda\theta-c)\right)\frac{\rho}{\alpha(1-\gamma_B)+\gamma_B}\right.$$

$$\left.\left.-\eta(mp\lambda\theta-c)\right)d\alpha\right)\frac{1}{Z}d\lambda$$

$$= p\theta\frac{\rho-\gamma_B}{1-\gamma_B}-\frac{\rho}{1-\gamma_B}\log[\rho]\left(p\theta+\eta\left(mp\frac{Z}{2}\theta-c\right)\right)$$

$$-\eta\left(mp\frac{Z}{2}\theta-c\right)\left(1-\frac{\rho-\gamma_B}{1-\gamma_B}\right).$$

$$\mathbb{E}_{\alpha,\lambda}\left[u_{A,B}(\eta|m,\rho)\right]$$

$$= \mathbb{E}_{\alpha,\lambda}\left[(mp\lambda\theta-c).\min\left\{1,\frac{1-\rho}{(1-\gamma_B)(1-\alpha)+\gamma_A\alpha}\right\}\right.$$

$$\left.-\left(c+\eta(p\theta+c)\right)\left(1-\min\left\{1,\frac{1-\rho}{(1-\gamma_B)(1-\alpha)+\gamma_A\alpha}\right\}\right)\right]$$

$$= \int_0^Z\left(\int_0^{\frac{\rho-\gamma_B}{1-\gamma_B}}\left(\left(mp\lambda\theta+\eta(p\theta+c)\right)\frac{1-\rho}{(1-\gamma_B)(1-\alpha)}\right.\right.$$

$$\left.\left.-\left(c+\eta(p\theta+c)\right)\right)d\alpha+\int_{\frac{\rho-\gamma_B}{1-\gamma_B}}^{1}(mp\lambda\theta-c)\,d\alpha\right)\frac{1}{Z}d\lambda$$

$$= -\left(\frac{1-\rho}{1-\gamma_B}\right)\log\left[\frac{1-\rho}{1-\gamma_B}\right]\left(mp\frac{Z}{2}\theta+\eta(p\theta+c)\right)$$

$$-\frac{\rho-\gamma_B}{1-\gamma_B}\left(mp\frac{Z}{2}\theta+\eta(p\theta+c)\right)+\left(mp\frac{Z}{2}\theta-c\right).$$

$$\mathbb{E}_{\alpha,\lambda}[u_{B,A}(\eta|m,\rho)]$$

$$= \mathbb{E}_{\alpha,\lambda}\left[(p\theta - c).\min\left\{1, \frac{\rho}{(1-\gamma_A)\alpha + \gamma_B(1-\alpha)}\right\}\right.$$

$$\left. - \big(c + \eta(mp\lambda\theta + c)\big)\left(1 - \min\left\{1, \frac{\rho}{(1-\gamma_A)\alpha + \gamma_B(1-\alpha)}\right\}\right)\right]$$

$$= \int_0^Z \left(\int_0^{\frac{\rho-\gamma_B}{1-\gamma_B}} (p\theta - c)\, d\alpha\right.$$

$$+ \int_{\frac{\rho-\gamma_B}{1-\gamma_B}}^1 \left(\big(p\theta + \eta(mp\lambda\theta + c)\big)\frac{\rho}{\alpha(1-\gamma_B) + \gamma_B}\right.$$

$$\left.\left. - \big(c + \eta(mp\lambda\theta + c)\big)\right) d\alpha\right)\frac{1}{Z}\, d\lambda$$

$$= (p\theta - c)\frac{\rho - \gamma_B}{1 - \gamma_B} - \frac{\rho}{1 - \gamma_B}\log[\rho]\left(p\theta + \eta\left(mp\frac{Z}{2}\theta + c\right)\right)$$

$$- \left(c + \eta\left(mp\frac{Z}{2}\theta + c\right)\right)\left(1 - \frac{\rho - \gamma_B}{1 - \gamma_B}\right).$$

$$\mathbb{E}_{\alpha,\lambda}[u_{B,B}(\eta|m,\rho)]$$

$$= \mathbb{E}_{\alpha,\lambda}\left[mp\lambda\theta.\min\left\{1, \frac{1-\rho}{(1-\gamma_B)(1-\alpha) + \gamma_A\alpha}\right\}\right.$$

$$\left. - \eta(p\theta - c)\left(1 - \min\left\{1, \frac{1-\rho}{(1-\gamma_B)(1-\alpha) + \gamma_A\alpha}\right\}\right)\right]$$

$$= \int_0^Z \left(\int_0^{\frac{\rho-\gamma_B}{1-\gamma_B}} \left(\big(mp\lambda\theta + \eta(p\theta - c)\big)\frac{1-\rho}{(1-\gamma_B)(1-\alpha)} - \eta(p\theta - c)\right) d\alpha\right.$$

$$\left. + \int_{\frac{\rho-\gamma_B}{1-\gamma_B}}^1 mp\lambda\theta\, d\alpha\right)\frac{1}{Z}\, d\lambda$$

$$= -\left(\frac{1-\rho}{1-\gamma_B}\right)\log\left[\frac{1-\rho}{1-\gamma_B}\right]\left(mp\frac{Z}{2}\theta + \eta(p\theta - c)\right)$$

$$- \frac{\rho - \gamma_B}{1 - \gamma_B}\left(mp\frac{Z}{2}\theta + \eta(p\theta - c)\right) + mp\frac{Z}{2}\theta.$$

To determine the optimal proportion γ_B^*, we find an equilibrium point where drivers in Zone B become indifferent between staying in Zone B and relocating to Zone A. Thus, we evaluate $\mathbb{E}_{\alpha,\lambda}[u_{B,B}(\eta|m,\rho)] = \mathbb{E}_{\alpha,\lambda}[u_{B,A}(\eta|m,\rho)]$ for $\gamma_A = 0$ which gives:

$$-\left(\frac{1-\rho}{1-\gamma_B}\right)\log\left[\frac{1-\rho}{1-\gamma_B}\right]\left(mp\frac{Z}{2}\theta + \eta(p\theta - c)\right) - \frac{\rho-\gamma_B}{1-\gamma_B}\left(mp\frac{Z}{2}\theta + \eta(p\theta - c)\right) + mp\frac{Z}{2}\theta = (p\theta - c)\frac{\rho-\gamma_B}{1-\gamma_B} - \frac{\rho}{1-\gamma_B}\log[\rho]\left(p\theta + \eta\left(mp\frac{Z}{2}\theta + c\right)\right) - \left(c + \eta\left(mp\frac{Z}{2}\theta + c\right)\right)\left(1 - \frac{\rho-\gamma_B}{1-\gamma_B}\right).$$

Since $1 - \gamma_B \geq 0$, $-(1-\rho)\log\left[\frac{1-\rho}{1-\gamma_B}\right]\left(mp\frac{Z}{2}\theta + \eta(p\theta - c)\right) - (\rho - \gamma_B)\left(mp\frac{Z}{2}\theta + \eta(p\theta - c)\right) + (1 - \gamma_B)mp\frac{Z}{2}\theta = (p\theta - c)(\rho - \gamma_B) - \rho\log[\rho]\left(p\theta + \eta\left(mp\frac{Z}{2}\theta + c\right)\right) - \left(c + \eta\left(mp\frac{Z}{2}\theta + c\right)\right)(1-\rho)$.

Solving for γ_B, it follows that $A\log[1-\gamma_B] + B(1-\gamma_B) - C = 0$ where $A = -(1-\rho)\left(mp\frac{Z}{2}\theta + \eta(p\theta - c)\right)$, $B = (\eta+1)(p\theta - c)$ and $C = -(1-\rho)\log[1-\rho]\left(mp\frac{Z}{2}\theta + \eta(p\theta - c)\right) - \rho(p\theta - c) + \rho\log[\rho]\left(p\theta + \eta\left(mp\frac{Z}{2}\theta + c\right)\right) + \left(c + \eta\left(mp\frac{Z}{2}\theta + c\right)\right)(1-\rho) - \rho\left(mp\frac{Z}{2}\theta + \eta(p\theta - c)\right) + mp\frac{Z}{2}\theta + (\eta+1)(p\theta - c)$.

Then,

$$A\log[1-\gamma_B] + B(1-\gamma_B) - C = 0 \text{ is equivalent to } \log[1-\gamma_B] + \frac{B}{A}(1-\gamma_B)\log[e] - \frac{C}{A} = 0.$$

Defining $h(m) = \frac{A}{B}$ and $j(m) = \frac{C}{A}$, $\log\left[(1-\gamma_B)e^{\frac{1}{h(m)}(1-\gamma_B)}\right] = j(m)$ or $\frac{1}{h(m)}(1-\gamma_B)e^{\frac{1}{h(m)}(1-\gamma_B)} = \frac{1}{h(m)}e^{j(m)}$. Substituting $z = \frac{1}{h(m)}(1-\gamma_B)$ gives $ze^z = \frac{1}{h(m)}e^{j(m)}$, and $z = W\left(\frac{1}{h(m)}e^{j(m)}\right)$, where W is the Lambert W function. Thus, substituting z, we obtain

$$\frac{1}{h(m)}(1-\gamma_B) = W\left(\frac{1}{h(m)}e^{j(m)}\right) \text{ and } \gamma_B^* = 1 - h(m)W\left(\frac{1}{h(m)}e^{j(m)}\right).$$

The range at which the equilibrium solution is valid can be calculated by finding the value of the surge multiplier m in the limit where $\gamma_A = 0$ and either $\gamma_B^* \to 0$ or $\gamma_B^* \to 1$. The respective equations are given by $h(m)W\left(\frac{1}{h(m)}e^{j(m)}\right) = 1$ and $h(m)W\left(\frac{1}{h(m)}e^{j(m)}\right) = 0$. Solving $h(m)W\left(\frac{1}{h(m)}e^{j(m)}\right) = 1$ gives $W\left(\frac{1}{h(m)}e^{j(m)}\right) = \frac{1}{h(m)}$ and thus, $\frac{1}{h(m)}e^{j(m)} = \frac{1}{h(m)}e^{\frac{1}{h(m)}}$ or

$$-(1-\rho)\log[1-\rho]\left(mp\frac{Z}{2}\theta + \eta(p\theta - c)\right) - \rho(p\theta - c) + \rho\log[\rho]\left(p\theta + \eta\left(mp\frac{Z}{2}\theta + c\right)\right) + \left(c + \eta\left(mp\frac{Z}{2}\theta + c\right)\right)(1-\rho) - \rho\left(mp\frac{Z}{2}\theta + \eta(p\theta - c)\right) + mp\frac{Z}{2}\theta + (\eta+1)(p\theta - c) = (\eta+1)(p\theta - c).$$

Solving for m gives $\frac{\frac{1+\eta}{1-\rho}(p\theta\rho - c) + \eta(p\theta - c)\log[1-\rho] - \frac{\rho}{1-\rho}(c\eta + p\theta)\log[\rho]}{\frac{1}{2}pZ\theta\left((1+\eta) - \log[1-\rho] + \frac{\rho}{1-\rho}\eta\log[\rho]\right)}$. Solving $h(m)W\left(\frac{1}{h(m)}e^{j(m)}\right) = 0$ gives $h(m) = 0$ or $W\left(\frac{1}{h(m)}e^{j(m)}\right) = 0$, which gives $-(1-\rho)\left(mp\frac{Z}{2}\theta + \eta(p\theta - c)\right) = 0$ or $\frac{1}{h(m)}e^{j(m)} = 0$, implying that $(\eta+1)(p\theta - c) = 0$. There is no root for m for these equations.

5.2.When $\rho - \gamma_B \leq 0$, $\frac{\rho}{(1-\gamma_A)\alpha + \gamma_B(1-\alpha)} \leq 1$ implies $\alpha \geq \max\left\{0, \frac{\rho - \gamma_B}{1-\gamma_A - \gamma_B}\right\} = 0$ when $1 - \gamma_A - \gamma_B \geq 0$, and, as a results, $\alpha > 0$ when $\gamma_A = 0$ and $0 < \gamma_B < 1$. Similarly, $\frac{1-\rho}{(1-\gamma_B)(1-\alpha) + \gamma_A\alpha} \leq 1$ implies $\alpha < 0$. Then,

$$\mathbb{E}_{\alpha,\lambda}\left[u_{A,A}(\eta|m,\rho)\right]$$

$$= \mathbb{E}_{\alpha,\lambda}\left[p\theta.\min\left\{1, \frac{\rho}{(1-\gamma_A)\alpha+\gamma_B(1-\alpha)}\right\}\right.$$

$$\left. -\eta(mp\lambda\theta-c)\left(1-\min\left\{1, \frac{\rho}{(1-\gamma_A)\alpha+\gamma_B(1-\alpha)}\right\}\right)\right]$$

$$= \int_0^Z\left(\int_0^1\left(\big(p\theta+\eta(mp\lambda\theta-c)\big)\frac{\rho}{\alpha(1-\gamma_B)+\gamma_B}\right.\right.$$

$$\left.\left. -\eta(mp\lambda\theta-c)\right)d\alpha\right)\frac{1}{Z}d\lambda$$

$$= -\frac{\rho}{1-\ \gamma_B}\log[\gamma_B]\left(p\theta+\eta\left(mp\frac{Z}{2}\theta-c\right)\right)-\eta\left(mp\frac{Z}{2}\theta-c\right).$$

$$\mathbb{E}_{\alpha,\lambda}\left[u_{A,B}(\eta|m,\rho)\right]$$

$$= \mathbb{E}_{\alpha,\lambda}\left[(mp\lambda\theta-c).\min\left\{1, \frac{1-\rho}{(1-\gamma_B)(1-\alpha)+\gamma_A\alpha}\right\}\right.$$

$$\left. -\big(c+\eta(p\theta+c)\big)\left(1-\min\left\{1, \frac{1-\rho}{(1-\gamma_B)(1-\alpha)+\gamma_A\alpha}\right\}\right)\right]$$

$$= \int_0^Z\left(\int_0^1(mp\lambda\theta-c)\,d\alpha\right)\frac{1}{Z}d\lambda = mp\frac{Z}{2}\theta-c.$$

$$\mathbb{E}_{\alpha,\lambda}\left[u_{B,A}(\eta|m,\rho)\right]$$

$$= \mathbb{E}_{\alpha,\lambda}\left[(p\theta-c).\min\left\{1, \frac{\rho}{(1-\gamma_A)\alpha+\gamma_B(1-\alpha)}\right\}\right.$$

$$\left. -\big(c+\eta(mp\lambda\theta+c)\big)\left(1-\min\left\{1, \frac{\rho}{(1-\gamma_A)\alpha+\gamma_B(1-\alpha)}\right\}\right)\right]$$

$$= \int_0^Z\left(\int_0^1\left(\big(p\theta+\eta(mp\lambda\theta+c)\big)\frac{\rho}{\alpha(1-\gamma_B)+\gamma_B}\right.\right.$$

$$\left.\left. -\big(c+\eta(mp\lambda\theta+c)\big)\right)d\alpha\right)\frac{1}{Z}d\lambda$$

$$= \frac{\rho}{\gamma_B-1}\log[\gamma_B]\left(p\theta+\eta\left(mp\frac{Z}{2}\theta+c\right)\right)-\left(c+\eta\left(mp\frac{Z}{2}\theta+c\right)\right).$$

$$\mathbb{E}_{\alpha,\lambda}[u_{B,B}(\eta|m,\rho)]$$

$$= \mathbb{E}_{\alpha,\lambda}\left[mp\lambda\theta.\min\left\{1, \frac{1-\rho}{(1-\gamma_B)(1-\alpha)+\gamma_A\alpha}\right\}\right.$$

$$\left. -\eta(p\theta - c)\left(1-\min\left\{1, \frac{1-\rho}{(1-\gamma_B)(1-\alpha)+\gamma_A\alpha}\right\}\right)\right]$$

$$= \int_0^Z \left(\int_0^1 mp\lambda\theta \, d\alpha\right)\frac{1}{Z}d\lambda = mp\frac{Z}{2}\theta.$$

To determine the optimal proportion γ_B^*, we find an equilibrium point where drivers in Zone B become indifferent between staying in Zone B and relocating to Zone A. Thus, we evaluate $\mathbb{E}_{\alpha,\lambda}[u_{B,B}(\eta|m,\rho)] = \mathbb{E}_{\alpha,\lambda}[u_{B,A}(\eta|m,\rho)]$ for $\gamma_A = 0$, which gives $-\frac{\rho}{1-\gamma_B}\log[\gamma_B]\left(p\theta+\eta\left(mp\frac{Z}{2}\theta+c\right)\right)-\left(c+\eta\left(mp\frac{Z}{2}\theta+c\right)\right) = mp\frac{Z}{2}\theta$. Since $1-\gamma_B \geq 0$,

$-\rho\log[\gamma_B]\left(p\theta+\eta\left(mp\frac{Z}{2}\theta+c\right)\right)-(1-\gamma_B)\left(c+\eta\left(mp\frac{Z}{2}\theta+c\right)\right) = (1-\gamma_B)mp\frac{Z}{2}\theta$ or

$-\rho\log[\gamma_B]\left(p\theta+\eta\left(mp\frac{Z}{2}\theta+c\right)\right)+\gamma_B(\eta+1)\left(mp\frac{Z}{2}\theta+c\right)-(\eta+1)\left(mp\frac{Z}{2}\theta+c\right) = 0.$

Solving for γ_B, it follows that $A\log[\gamma_B]+B\gamma_B-B=0$ where $A = -\rho\left(p\theta+\eta\left(mp\frac{Z}{2}\theta+c\right)\right)$ and $B = (\eta+1)\left(mp\frac{Z}{2}\theta+c\right)$. Now, $A\log[\gamma_B]+B\gamma_B-B=0$ is equivalent to $\log[\gamma_B]+\frac{B}{A}\gamma_B\log[e]-\frac{B}{A}=0$. We define $l(m)=\frac{B}{A}$, and thus $\log\left[\gamma_B e^{\gamma_B l(m)}\right] = l(m)$ or $l(m)\gamma_B e^{\gamma_B l(m)} = l(m)e^{l(m)}$. Substituting $z = l(m)\gamma_B$ gives $ze^z = l(m)e^{l(m)}$ and $z = W\left(l(m)e^{l(m)}\right)$, where W is the Lambert W function. From the definition of Lamber function, $W\left(l(m)e^{l(m)}\right) = l(m)$. Thus, substituting z, we get $l(m)\gamma_B = l(m)$ and $\gamma_B^* = 1$. The range at which the equilibrium solution is valid can be calculated by finding the value of the surge multiplier m in the limit where $\gamma_A = 0$ and $\gamma_B^* \to 1$. Solving for $\gamma_B^* \to 1$, we have

$$\lim_{\gamma_B^*\to 1}\left[\mathbb{E}_{\alpha,\lambda}[u_{B,A}(\eta|m,\rho)] - \mathbb{E}_{\alpha,\lambda}[u_{B,B}(\eta|m,\rho)]\right] = 0$$

$$\lim_{\gamma_B^*\to 1}\left[\frac{\rho}{\gamma_B - 1}\log[\gamma_B]\left(p\theta + \eta\left(mp\frac{Z}{2}\theta + c\right)\right) - \left(c + \eta\left(mp\frac{Z}{2}\theta + c\right)\right) - mp\frac{Z}{2}\theta\right] = 0$$

$$-\left(c + \eta\left(mp\frac{Z}{2}\theta + c\right)\right) - mp\frac{Z}{2}\theta + \lim_{\gamma_B^*\to 1}\left[\frac{\rho}{\gamma_B - 1}\log[\gamma_B]\left(p\theta + \eta\left(mp\frac{Z}{2}\theta + c\right)\right)\right] = 0$$

$$-\left(c + \eta\left(mp\frac{Z}{2}\theta + c\right)\right) - mp\frac{Z}{2}\theta + \rho\left(p\theta + \eta\left(mp\frac{Z}{2}\theta + c\right)\right) = 0,$$

Solving for m gives $m = \frac{2}{Z}\left(\frac{\rho}{1-\eta\rho+\eta} - \frac{c}{p\theta}\right)$.

6. When $\gamma_B = 0$ and $0 \leq \gamma_A \leq 1$, first we assume that $\frac{\rho}{(1-\gamma_A)\alpha} \leq 1$. This occurs when $\alpha \geq \frac{\rho}{1-\gamma_A}$. Thus, $\frac{\rho}{(1-\gamma_A)\alpha+\gamma_B(1-\alpha)} \leq 1$ implies $\frac{\rho}{(1-\gamma_A)\alpha} \leq 1$ and $\min\left\{1, \frac{\rho}{(1-\gamma_A)\alpha}\right\} = \frac{\rho}{(1-\gamma_A)\alpha}$. Now. suppose that $\frac{1-\rho}{1-\alpha(1-\gamma_A)} \leq 1$ implies $\alpha \leq \frac{\rho}{1-\gamma_A}$. Then, $\frac{1-\rho}{(1-\gamma_B)(1-\alpha)+\gamma_A\alpha} \leq 1$ and $\min\left\{1, \frac{1-\rho}{(1-\alpha)+\gamma_A\alpha}\right\} = \frac{1-\rho}{1-\alpha(1-\gamma_A)}$.

6.1. When $\rho \geq 1 - \gamma_A$, then $\frac{\rho}{(1-\gamma_A)\alpha+\gamma_B(1-\alpha)} \geq 1$ and $\frac{1-\rho}{(1-\gamma_B)(1-\alpha)+\gamma_A\alpha} \leq 1$ for any $\alpha \in (0,1)$. Hence,

$$\begin{aligned}
&\mathbb{E}_{\alpha,\lambda}[u_{A,A}(\eta|m,\rho)] \\
&\quad = \mathbb{E}_{\alpha,\lambda}\left[p\theta.\min\left\{1, \frac{\rho}{(1-\gamma_A)\alpha + \gamma_B(1-\alpha)}\right\}\right. \\
&\quad \left. - \eta(mp\lambda\theta - c)\left(1 - \min\left\{1, \frac{\rho}{(1-\gamma_A)\alpha + \gamma_B(1-\alpha)}\right\}\right)\right] \\
&\quad = \int_0^Z \left(\int_0^1 p\theta\, d\alpha\right)\frac{1}{Z}d\lambda = p\theta.
\end{aligned}$$

$$\mathbb{E}_{\alpha,\lambda}\left[u_{A,B}(\eta|m,\rho)\right]$$

$$= \mathbb{E}_{\alpha,\lambda}\left[(mp\lambda\theta - c).\min\left\{1, \frac{1-\rho}{(1-\gamma_B)(1-\alpha)+\gamma_A\alpha}\right\}\right.$$

$$\left. - \big(c + \eta(p\theta + c)\big)\left(1 - \min\left\{1, \frac{1-\rho}{(1-\gamma_B)(1-\alpha)+\gamma_A\alpha}\right\}\right)\right]$$

$$= \int_0^Z \left(\int_0^1 \left(\big(mp\lambda\theta + \eta(p\theta + c)\big)\frac{1-\rho}{1-\alpha(1-\gamma_A)}\right.\right.$$

$$\left.\left. - \big(c + \eta(p\theta + c)\big)\right) d\alpha\right)\frac{1}{Z}d\lambda$$

$$= \left(\frac{1-\rho}{\gamma_A - 1}\right)\log[\gamma_A]\left(mp\frac{Z}{2}\theta + \eta(p\theta + c)\right) - \big(c + \eta(p\theta + c)\big).$$

$$\mathbb{E}_{\alpha,\lambda}\left[u_{B,A}(\eta|m,\rho)\right]$$

$$= \mathbb{E}_{\alpha,\lambda}\left[(p\theta - c).\min\left\{1, \frac{\rho}{(1-\gamma_A)\alpha+\gamma_B(1-\alpha)}\right\}\right.$$

$$\left. - \big(c + \eta(mp\lambda\theta + c)\big)\left(1 - \min\left\{1, \frac{\rho}{(1-\gamma_A)\alpha+\gamma_B(1-\alpha)}\right\}\right)\right]$$

$$= \int_0^Z \left(\int_0^1 (p\theta - c)\, d\alpha\right)\frac{1}{Z}d\lambda = p\theta - c.$$

$$\mathbb{E}_{\alpha,\lambda}\left[u_{B,B}(\eta|m,\rho)\right]$$

$$= \mathbb{E}_{\alpha,\lambda}\left[mp\lambda\theta.\min\left\{1, \frac{1-\rho}{(1-\gamma_B)(1-\alpha)+\gamma_A\alpha}\right\}\right.$$

$$\left. - \eta(p\theta - c)\left(1 - \min\left\{1, \frac{1-\rho}{(1-\gamma_B)(1-\alpha)+\gamma_A\alpha}\right\}\right)\right]$$

$$= \int_0^Z \left(\int_0^1 \left(\big(mp\lambda\theta + \eta(p\theta - c)\big)\frac{1-\rho}{1-\alpha(1-\gamma_A)} - \eta(p\theta - c)\right) d\alpha\right)\frac{1}{Z}d\lambda$$

$$= -\left(\frac{1-\rho}{1-\gamma_A}\right)\log[\gamma_A]\left(mp\frac{Z}{2}\theta + \eta(p\theta - c)\right) - \eta(p\theta - c).$$

To determine the optimal proportion γ_A^*, we find an equilibrium point where drivers in Zone A become indifferent between staying in Zone A and relocating to Zone B. Thus, we evaluate $\mathbb{E}_{\alpha,\lambda}\left[u_{A,A}(\eta|m,\rho)\right] = \mathbb{E}_{\alpha,\lambda}\left[u_{A,B}(\eta|m,\rho)\right]$ for $\gamma_B = 0$ which gives $p\theta = -\left(\frac{1-\rho}{1-\gamma_A}\right)\log[\gamma_A]\left(mp\frac{Z}{2}\theta + \eta(p\theta + c)\right) - \big(c + \eta(p\theta + c)\big)$. Since $1 - \gamma_A \geq 0$,

$$(1 - \gamma_A)p\theta = -(1-\rho)\log[\gamma_A]\left(mp\frac{Z}{2}\theta + \eta(p\theta + c)\right) - (1 - \gamma_A)\big(c + \eta(p\theta + c)\big).$$

Solving for γ_A, it follows that $A\log[\gamma_A] + B\gamma_A - B = 0$ where $A = -(1-\rho)\left(mp\frac{Z}{2}\theta + \eta(p\theta + c)\right)$ and $B = (1+\eta)(p\theta + c)$. Thus, $A\log[\gamma_A] + B\gamma_A - B = 0$ or $\log[\gamma_A] + \frac{B}{A}\gamma_A \log[e] - \frac{B}{A} = 0$. We define $k(m) = \frac{B}{A}$, thus $\log\left[\gamma_A e^{k(m)\gamma_A}\right] = k(m)$ or $k(m)\gamma_A e^{k(m)\gamma_A} = k(m)e^{k(m)}$. Substituting $z = k(m)\gamma_A$ gives $ze^z = k(m)e^{k(m)}$ and $z = W\left(k(m)e^{k(m)}\right)$, where W is the Lambert W function. Thus, substituting z, we obtain $k(m)\gamma_A = W\left(k(m)e^{k(m)}\right) = k(m)$ and $\gamma_A^* = 1$. The range at which the equilibrium solution is valid can be calculated by finding the value of the surge multiplier m in the limit where $\gamma_B = 0$ and $\gamma_A^* \to 1$. Solving for $\gamma_A^* \to 1$ yields

$$\lim_{\gamma_A^* \to 1}\left[\mathbb{E}_{\alpha,\lambda}\left[u_{A,A}(\eta|m,\rho)\right] - \mathbb{E}_{\alpha,\lambda}\left[u_{A,B}(\eta|m,\rho)\right]\right] = 0$$

$$\lim_{\gamma_A^* \to 1}\left[\left(\frac{1-\rho}{\gamma_A - 1}\right)\log[\gamma_A]\left(mp\frac{Z}{2}\theta + \eta(p\theta + c)\right) - \left(c + \eta(p\theta + c)\right) - p\theta\right] = 0$$

$$-\left(c + \eta(p\theta + c)\right) - p\theta + \lim_{\gamma_A^* \to 1}\left[\left(\frac{1-\rho}{\gamma_A - 1}\right)\log[\gamma_A]\left(mp\frac{Z}{2}\theta + \eta(p\theta + c)\right)\right] = 0$$

$$-\left(c + \eta(p\theta + c)\right) - p\theta + (1-\rho)\left(mp\frac{Z}{2}\theta + \eta(p\theta + c)\right) = 0.$$

Solving for m gives $m = \frac{2}{Z}\left(1 + \frac{c}{p\theta}\right)\left(\frac{1+\eta\rho}{1-\rho}\right)$.

6.2. When $\rho < 1 - \gamma_A$, then $\frac{\rho}{(1-\gamma_A)\alpha + \gamma_B(1-\alpha)} \leq 1$ and $\frac{1-\rho}{(1-\gamma_B)(1-\alpha) + \gamma_A\alpha} \geq 1$ for $\alpha \geq \frac{\rho}{1-\gamma_A}$, and $\frac{\rho}{(1-\gamma_A)\alpha + \gamma_B(1-\alpha)} \geq 1$ and $\frac{1-\rho}{(1-\gamma_B)(1-\alpha) + \gamma_A\alpha} \leq 1$ for $\alpha \leq \frac{\rho}{1-\gamma_A}$,

$$\mathbb{E}_{\alpha,\lambda}\left[u_{A,A}(\eta|m,\rho)\right]$$

$$= \mathbb{E}_{\alpha,\lambda}\left[p\theta.\min\left\{1,\frac{\rho}{(1-\gamma_A)\alpha+\gamma_B(1-\alpha)}\right\}\right.$$

$$\left.-\eta(mp\lambda\theta-c)\left(1-\min\left\{1,\frac{\rho}{(1-\gamma_A)\alpha+\gamma_B(1-\alpha)}\right\}\right)\right]$$

$$= \int_0^Z\left(\int_0^{\frac{\rho}{1-\gamma_A}} p\theta\, d\alpha\right.$$

$$\left.+\int_{\frac{\rho}{1-\gamma_A}}^1\left(\left(p\theta+\eta(mp\lambda\theta-c)\right)\frac{\rho}{\alpha(1-\gamma_A)}-\eta(mp\lambda\theta-c)\right)d\alpha\right)\frac{1}{Z}d\lambda$$

$$= p\theta\frac{\rho}{1-\gamma_A}-\frac{\rho}{1-\gamma_A}\log\left[\frac{\rho}{1-\gamma_A}\right]\left(p\theta+\eta\left(mp\frac{Z}{2}\theta-c\right)\right)$$

$$-\eta\left(mp\frac{Z}{2}\theta-c\right)\left(1-\frac{\rho}{1-\gamma_A}\right).$$

$$\mathbb{E}_{\alpha,\lambda}\left[u_{A,B}(\eta|m,\rho)\right]$$

$$= \mathbb{E}_{\alpha,\lambda}\left[(mp\lambda\theta-c).\min\left\{1,\frac{1-\rho}{(1-\gamma_B)(1-\alpha)+\gamma_A\alpha}\right\}\right.$$

$$\left.-\left(c+\eta(p\theta+c)\right)\left(1-\min\left\{1,\frac{1-\rho}{(1-\gamma_B)(1-\alpha)+\gamma_A\alpha}\right\}\right)\right]$$

$$= \int_0^Z\left(\int_0^{\frac{\rho}{1-\gamma_A}}\left(\left(mp\lambda\theta+\eta(p\theta+c)\right)\frac{1-\rho}{1-\alpha(1-\gamma_A)}\right.\right.$$

$$\left.\left.-\left(c+\eta(p\theta+c)\right)\right)d\alpha+\int_{\frac{\rho}{1-\gamma_A}}^1(mp\lambda\theta-c)\,d\alpha\right)\frac{1}{Z}d\lambda$$

$$= -\left(\frac{1-\rho}{1-\gamma_A}\right)\log[1-\rho]\left(mp\frac{Z}{2}\theta+\eta(p\theta+c)\right)$$

$$-\frac{\rho}{1-\gamma_A}\left(mp\frac{Z}{2}\theta+\eta(p\theta+c)\right)+\left(mp\frac{Z}{2}\theta-c\right).$$

$$\mathbb{E}_{\alpha,\lambda}\left[u_{B,A}(\eta|m,\rho)\right]$$

$$= \mathbb{E}_{\alpha,\lambda}\Bigg[(p\theta - c).\min\left\{1, \frac{\rho}{(1-\gamma_A)\alpha + \gamma_B(1-\alpha)}\right\}$$

$$-\big(c + \eta(mp\lambda\theta + c)\big)\left(1 - \min\left\{1, \frac{\rho}{(1-\gamma_A)\alpha + \gamma_B(1-\alpha)}\right\}\right)\Bigg]$$

$$= \int_0^Z \Bigg(\int_0^{\frac{\rho}{1-\gamma_A}} (p\theta - c)\, d\alpha$$

$$+ \int_{\frac{\rho}{1-\gamma_A}}^1 \bigg(\big(p\theta + \eta(mp\lambda\theta + c)\big)\frac{\rho}{\alpha(1-\gamma_A)}$$

$$-\big(c + \eta(mp\lambda\theta + c)\big)\bigg)\, d\alpha\Bigg)\frac{1}{Z}\, d\lambda$$

$$= (p\theta - c)\frac{\rho}{1-\gamma_A} - \frac{\rho}{1-\gamma_A}\log\left[\frac{\rho}{1-\gamma_A}\right]\left(p\theta + \eta\left(mp\frac{Z}{2}\theta + c\right)\right)$$

$$-\left(c + \eta\left(mp\frac{Z}{2}\theta + c\right)\right)\left(1 - \frac{\rho}{1-\gamma_A}\right).$$

$$\mathbb{E}_{\alpha,\lambda}\left[u_{B,B}(\eta|m,\rho)\right]$$

$$= \mathbb{E}_{\alpha,\lambda}\Bigg[mp\lambda\theta.\min\left\{1, \frac{1-\rho}{(1-\gamma_B)(1-\alpha) + \gamma_A\alpha}\right\}$$

$$-\eta(p\theta - c)\left(1 - \min\left\{1, \frac{1-\rho}{(1-\gamma_B)(1-\alpha) + \gamma_A\alpha}\right\}\right)\Bigg]$$

$$= \int_0^Z \Bigg(\int_0^{\frac{\rho}{1-\gamma_A}} \bigg(\big(mp\lambda\theta + \eta(p\theta - c)\big)\frac{1-\rho}{1-\alpha(1-\gamma_A)}$$

$$-\eta(p\theta - c)\bigg)\, d\alpha + \int_{\frac{\rho}{1-\gamma_A}}^1 mp\lambda\theta\, d\alpha\Bigg)\frac{1}{Z}\, d\lambda$$

$$= -\left(\frac{1-\rho}{1-\gamma_A}\right)\log[1-\rho]\left(mp\frac{Z}{2}\theta + \eta(p\theta - c)\right)$$

$$-\frac{\rho}{1-\gamma_A}\left(mp\frac{Z}{2}\theta + \eta(p\theta - c)\right) + mp\frac{Z}{2}\theta.$$

To determine the optimal proportion γ_A^*, we find an equilibrium point where drivers in Zone A become indifferent between staying in Zone A and relocating to Zone B. Thus, we evaluate $\mathbb{E}_{\alpha,\lambda}\left[u_{A,A}(\eta|m,\rho)\right] = \mathbb{E}_{\alpha,\lambda}\left[u_{A,B}(\eta|m,\rho)\right]$ for $\gamma_B = 0$ which gives $p\theta \frac{\rho}{1-\gamma_A} - \frac{\rho}{1-\gamma_A}\log\left[\frac{\rho}{1-\gamma_A}\right]\left(p\theta + \eta\left(mp\frac{Z}{2}\theta - c\right)\right) - \eta\left(mp\frac{Z}{2}\theta - c\right)\left(1 - \frac{\rho}{1-\gamma_A}\right) = -\left(\frac{1-\rho}{1-\gamma_A}\right)\log[1-\rho]\left(mp\frac{Z}{2}\theta + \eta(p\theta + c)\right) - \frac{\rho}{1-\gamma_A}\left(mp\frac{Z}{2}\theta + \eta(p\theta + c)\right) + \left(mp\frac{Z}{2}\theta - c\right)$. Since $1 - \gamma_A \geq 0$, $p\theta\rho - \rho\log\left[\frac{\rho}{1-\gamma_A}\right]\left(p\theta + \eta\left(mp\frac{Z}{2}\theta - c\right)\right) - \eta\left(mp\frac{Z}{2}\theta - c\right)(1 - \gamma_A - \rho) = -(1-\rho)\log[1-\rho]\left(mp\frac{Z}{2}\theta + \eta(p\theta + c)\right) - \rho\left(mp\frac{Z}{2}\theta + \eta(p\theta + c)\right) + (1 - \gamma_A)\left(mp\frac{Z}{2}\theta - c\right)$. Solving for γ_A, it follows that $A\log[1-\gamma_A] + B(1-\gamma_A) - C = 0$ where $A = -\rho\left(p\theta + \eta\left(mp\frac{Z}{2}\theta - c\right)\right)$, $B = (1+\eta)\left(mp\frac{Z}{2}\theta - c\right)$ and $C = p\theta\rho - \rho\log[\rho]\left(p\theta + \eta\left(mp\frac{Z}{2}\theta - c\right)\right) + \rho\eta\left(mp\frac{Z}{2}\theta - c\right) + (1-\rho)\log[1-\rho]\left(mp\frac{Z}{2}\theta + \eta(p\theta + c)\right) + \rho\left(mp\frac{Z}{2}\theta + \eta(p\theta + c)\right)$. Thus, $A\log[1-\gamma_A] + B(1-\gamma_A) - C = 0$ or $\log[1-\gamma_A] + \frac{B}{A}(1 - \gamma_A)\log[e] - \frac{C}{A} = 0$. Defining $f(m) = \frac{A}{B}$ and $g(m) = \frac{C}{A}$ give $\log\left[(1-\gamma_A)e^{\frac{1}{f(m)}(1-\gamma_A)}\right] = g(m)$ or $\frac{1}{f(m)}(1-\gamma_A)e^{\frac{1}{f(m)}(1-\gamma_A)} = \frac{1}{f(m)}e^{g(m)}$. Substituting $z = \frac{1}{f(m)}(1-\gamma_A)$ gives $ze^z = \frac{1}{f(m)}e^{g(m)}$ and $z = W\left(\frac{1}{f(m)}e^{g(m)}\right)$, where W is the Lambert W function. Thus, substituting z, we obtain $\frac{1}{f(m)}(1-\gamma_A) = W\left(\frac{1}{f(m)}e^{g(m)}\right)$ and $\gamma_A^* = 1 - f(m)W\left(\frac{1}{f(m)}e^{g(m)}\right)$. The range at which the equilibrium solution is valid can be calculated by finding the value of the surge multiplier m in the limit where $\gamma_B = 0$ and either $\gamma_A^* \to 0$ or $\gamma_A^* \to 1$. The respective equations are given by $f(m)W\left(\frac{1}{f(m)}e^{g(m)}\right) = 1$ and $f(m)W\left(\frac{1}{f(m)}e^{g(m)}\right) = 0$. Solving $f(m)W\left(\frac{1}{f(m)}e^{g(m)}\right) = 1$ gives $W\left(\frac{1}{f(m)}e^{g(m)}\right) = \frac{1}{f(m)}$ and $\frac{1}{f(m)}e^{g(m)} = \frac{1}{f(m)}e^{\frac{1}{f(m)}}$. That is,

$$p\theta\rho - \rho\log[\rho]\left(p\theta + \eta\left(mp\frac{Z}{2}\theta - c\right)\right) + \rho\eta\left(mp\frac{Z}{2}\theta - c\right) + (1-\rho)\log[1 - \rho]\left(mp\frac{Z}{2}\theta + \eta(p\theta + c)\right) + \rho\left(mp\frac{Z}{2}\theta + \eta(p\theta + c)\right) = (1+\eta)\left(mp\frac{Z}{2}\theta - c\right).$$

Solving for m gives $\frac{\frac{1+\eta}{1-\rho}(c+p\theta\rho)+\eta(c+p\theta)\log[1-\rho]+\frac{\rho}{1-\rho}(c\eta-p\theta)\log[\rho]}{\frac{1}{2}pZ\theta\left((1+\eta)-\log[1-\rho]+\eta\frac{\rho}{1-\rho}\log[\rho]\right)}$. Solving $f(m)W\left(\frac{1}{f(m)}e^{g(m)}\right) = 0$ gives $f(m) = 0$ or $W\left(\frac{1}{f(m)}e^{g(m)}\right) = 0$ and none of which has a root for m.

A summary of the cases appears in Table 3-A-11.

Table 3-A-11. Result summary for Theorem 2

Case	% of drivers γ_A^* initially located in Zone A relocating to Zone B	% of drivers γ_B^* initially located in Zone B relocating to Zone A	Range for the surge multiplier m
4	0	1	$0 \le m \le \frac{2}{Z}\left(\frac{\rho}{1-\eta\rho+\eta} - \frac{c}{p\theta}\right)$
5.2	0	1 when $\rho - \gamma_B < 0$.	$0 \le m \le \frac{\frac{1+\eta}{1-\rho}(p\theta\rho - c) + \eta(p\theta - c)\log[1-\rho] - \frac{\rho}{1-\rho}(c\eta + p\theta)\log[\rho]}{\frac{1}{2}pZ\theta\left((1+\eta) - \log[1-\rho] + \frac{\rho}{1-\rho}\eta\log[\rho]\right)}$
5.1	0	$0 < \gamma_B < 1$ $1 - h(m)W\left(\frac{1}{h(m)}e^{j(m)}\right)$ [5] when $\rho - \gamma_B \ge 0$	$\frac{2}{Z}\left(\frac{\rho}{1-\eta\rho+\eta} - \frac{c}{p\theta}\right) \le m \le \frac{\frac{1+\eta}{1-\rho}(p\theta\rho - c) + \eta(p\theta - c)\log[1-\rho] - \frac{\rho}{1-\rho}(c\eta + p\theta)\log[\rho]}{\frac{1}{2}pZ\theta\left((1+\eta) - \log[1-\rho] + \frac{\rho}{1-\rho}\eta\log[\rho]\right)}$
1	0	0	$\frac{\frac{1+\eta}{1-\rho}(p\theta\rho - c) + \eta(p\theta - c)\log[1-\rho] - \frac{\rho}{1-\rho}(c\eta + p\theta)\log[\rho]}{\frac{1}{2}pZ\theta\left((1+\eta) - \log[1-\rho] + \frac{\rho}{1-\rho}\eta\log[\rho]\right)} \le m \le \frac{\frac{1+\eta}{1-\rho}(c + p\theta\rho) + \eta(c + p\theta)\log[1-\rho] + \frac{\rho}{1-\rho}(c\eta - p\theta)\log[\rho]}{\frac{1}{2}pZ\theta\left((1+\eta) - \log[1-\rho] + \eta\frac{\rho}{1-\rho}\log[\rho]\right)}$
6.2	$0 < \gamma_A < 1$ $1 - f(m)W\left(\frac{1}{f(m)}e^{g(m)}\right)$ [6] when $\rho \le 1 - \gamma_A$	0	$\frac{\frac{1+\eta}{1-\rho}(c + p\theta\rho) + \eta(c + p\theta)\log[1-\rho] + \frac{\rho}{1-\rho}(c\eta - p\theta)\log[\rho]}{\frac{1}{2}pZ\theta\left((1+\eta) - \log[1-\rho] + \eta\frac{\rho}{1-\rho}\log[\rho]\right)} \le m \le \frac{2}{Z}\left(1 + \frac{c}{p\theta}\right)\left(\frac{1+\eta\rho}{1-\rho}\right)$
6.1	1 when $\rho > 1 - \gamma_A$.	0	$\frac{\frac{1+\eta}{1-\rho}(c + p\theta\rho) + \eta(c + p\theta)\log[1-\rho] + \frac{\rho}{1-\rho}(c\eta - p\theta)\log[\rho]}{\frac{1}{2}pZ\theta\left((1+\eta) - \log[1-\rho] + \eta\frac{\rho}{1-\rho}\log[\rho]\right)} \le m \le m_{max}$

5 $h(m) = \frac{-(1-\rho)\left(mp\frac{Z}{2}\theta+\eta(p\theta-c)\right)}{(\eta+1)(p\theta-c)}$ and $j(m) = \frac{1}{-(1-\rho)\left(mp\frac{Z}{2}\theta+\eta(p\theta-c)\right)}\left(-(1-\rho)\log[1-\rho]\left(mp\frac{Z}{2}\theta + \eta(p\theta - c)\right) - \rho(p\theta - c) + \rho\log[\rho]\left(p\theta + \eta\left(mp\frac{Z}{2}\theta + c\right)\right) + \left(c + \eta\left(mp\frac{Z}{2}\theta + c\right)\right)(1-\rho) - \rho\left(mp\frac{Z}{2}\theta + \eta(p\theta - c)\right) + mp\frac{Z}{2}\theta + (\eta+1)(p\theta - c)\right)$.

6 $f(m) = \frac{-\rho\left(p\theta+\eta\left(mp\frac{Z}{2}\theta-c\right)\right)}{(1+\eta)\left(mp\frac{Z}{2}\theta-c\right)}$ and $g(m) = \frac{1}{-\rho\left(p\theta+\eta\left(mp\frac{Z}{2}\theta-c\right)\right)}\left(p\theta\rho - \rho\log[\rho]\left(p\theta + \eta\left(mp\frac{Z}{2}\theta - c\right)\right) + \rho\eta\left(mp\frac{Z}{2}\theta - c\right) + (1-\rho)\log[1-\rho]\left(mp\frac{Z}{2}\theta + \eta(p\theta + c)\right) + \rho\left(mp\frac{Z}{2}\theta + \eta(p\theta + c)\right)\right)$.

3	1	0	$\frac{2}{Z}\left(1+\frac{c}{p\theta}\right)\left(\frac{1+\eta\rho}{1-\rho}\right) \le m \le m_{max}$
	$0<\gamma_A<1$	1	No equilibrium
	$0<\gamma_A<1$	$0<\gamma_B<1$	
2	1	1	
	1	$0<\gamma_B<1$	

Proof of Theorem 3

From (9) and (10), the expected regret-aversion utility of a driver who is initially located in Zone A and relocates to Zone B or stays in Zone A, and the expected regret-aversion utility of a driver who is initially located in Zone B and relocates to Zone A or stays in Zone B, depend again on multiple cases. Following Theorem 2, no surge multiplier m exists where $\gamma_A = 1$ and $\gamma_B = 1$, $0 < \gamma_A < 1$ and $0 < \gamma_B < 1$, $0 < \gamma_A < 1$ and $\gamma_B = 1$, or $\gamma_A = 1$ and $0 < \gamma_B < 1$, which implies $1 - \gamma_A - \gamma_B \ge 0$. Thus, we can simplify $\frac{\rho}{(1-\gamma_A)\alpha+\gamma_B(1-\alpha)} \le 1$ as $\rho \le (1-\gamma_A)\alpha + \gamma_B(1-\alpha)$ and $\rho - \gamma_B \le (1-\gamma_A-\gamma_B)\alpha$. Thus, $\frac{\rho}{(1-\gamma_A)\alpha+\gamma_B(1-\alpha)} \le 1$ implies $\alpha \ge \max\left\{0, \frac{\rho-\gamma_B}{1-\gamma_A-\gamma_B}\right\}$ when $1-\gamma_A-\gamma_B \ge 0$. Similarly, $\frac{1-\rho}{(1-\gamma_B)(1-\alpha)+\gamma_A\alpha} \le 1$ implies $\alpha \le \max\left\{0, \frac{\rho-\gamma_B}{1-\gamma_A-\gamma_B}\right\}$. Thus, we analyze two subcases for each of the cases.

1. When $\gamma_A = 0$ and $\gamma_B = 0$:

   1.1. When $\alpha \ge \max\left\{0, \frac{\rho-\gamma_B}{1-\gamma_A-\gamma_B}\right\}$, or equivalently, $\alpha \ge \rho$, we have $\frac{\rho}{(1-\gamma_A)\alpha+\gamma_B(1-\alpha)} \le 1$ and $\frac{1-\rho}{(1-\gamma_B)(1-\alpha)+\gamma_A\alpha} \ge 1$.

$$\mathbb{E}_\lambda\left[u_{A,A}(\eta|m,\rho,\alpha)\right]$$
$$= \mathbb{E}_\lambda\left[p\theta.\min\left\{1, \frac{\rho}{(1-\gamma_A)\alpha+\gamma_B(1-\alpha)}\right\} - \eta(mp\lambda\theta - c)\left(1-\min\left\{1, \frac{\rho}{(1-\gamma_A)\alpha+\gamma_B(1-\alpha)}\right\}\right)\right]$$
$$= \int_0^Z \left(\left(p\theta + \eta(mp\lambda\theta - c)\right)\frac{\rho}{\alpha} - \eta(mp\lambda\theta - c)\right)\frac{1}{Z}d\lambda$$
$$= \left(p\theta + \eta\left(mp\frac{Z}{2}\theta - c\right)\right)\frac{\rho}{\alpha} - \eta\left(mp\frac{Z}{2}\theta - c\right).$$

$$\mathbb{E}_\lambda\big[u_{A,B}(\eta|m,\rho,\alpha)\big]$$

$$= \mathbb{E}_\lambda\Bigg[(mp\lambda\theta - c).\min\left\{1,\frac{1-\rho}{(1-\gamma_B)(1-\alpha)+\gamma_A\alpha}\right\}$$

$$-\big(c+\eta(p\theta+c)\big)\left(1-\min\left\{1,\frac{1-\rho}{(1-\gamma_B)(1-\alpha)+\gamma_A\alpha}\right\}\right)\Bigg]$$

$$= \int_0^Z (mp\lambda\theta - c)\frac{1}{Z}d\lambda = mp\frac{Z}{2}\theta - c.$$

$$\mathbb{E}_\lambda\big[u_{B,A}(\eta|m,\rho,\alpha)\big]$$

$$= \mathbb{E}_\lambda\Bigg[(p\theta - c).\min\left\{1,\frac{\rho}{(1-\gamma_A)\alpha+\gamma_B(1-\alpha)}\right\}$$

$$-\big(c+\eta(mp\lambda\theta+c)\big)\left(1-\min\left\{1,\frac{\rho}{(1-\gamma_A)\alpha+\gamma_B(1-\alpha)}\right\}\right)\Bigg]$$

$$= \int_0^Z \left(\big(p\theta+\eta(mp\lambda\theta+c)\big)\frac{\rho}{\alpha} - \big(c+\eta(mp\lambda\theta+c)\big)\right)\frac{1}{Z}d\lambda$$

$$= \left(p\theta+\eta\left(mp\frac{Z}{2}\theta+c\right)\right)\frac{\rho}{\alpha} - \left(c+\eta\left(mp\frac{Z}{2}\theta+c\right)\right).$$

$$\mathbb{E}_\lambda\big[u_{B,B}(\eta|m,\rho,\alpha)\big]$$

$$= \mathbb{E}_\lambda\Bigg[mp\lambda\theta.\min\left\{1,\frac{1-\rho}{(1-\gamma_B)(1-\alpha)+\gamma_A\alpha}\right\}$$

$$-\eta(p\theta-c)\left(1-\min\left\{1,\frac{1-\rho}{(1-\gamma_B)(1-\alpha)+\gamma_A\alpha}\right\}\right)\Bigg]$$

$$= \int_0^Z (mp\lambda\theta)\frac{1}{Z}d\lambda = mp\frac{Z}{2}\theta.$$

When $\gamma_A = 0$ and $\gamma_B = 0$, no drivers relocate from their original zone. For this to occur, the utility of staying in Zone A must exceed the utility of moving to Zone B for drivers who are initially located in Zone A, and the utility of staying in Zone B must exceed the utility of moving to Zone A for drivers who are initially located in Zone B. To find the range of m where no drivers relocate from their original zone, we evaluate $\mathbb{E}_\lambda\big[u_{A,A}(\eta|m,\rho,\alpha)\big] > \mathbb{E}_\lambda\big[u_{A,B}(\eta|m,\rho,\alpha)\big]$ and $\mathbb{E}_\lambda\big[u_{B,B}(\eta|m,\rho,\alpha)\big] > \mathbb{E}_\lambda\big[u_{B,A}(\eta|m,\rho,\alpha)\big]$ for $\gamma_A = 0$ and $\gamma_B = 0$. Then,

$\mathbb{E}_{\lambda}[u_{A,A}(\eta|m,\rho,\alpha)] > \mathbb{E}_{\lambda}[u_{A,B}(\eta|m,\rho,\alpha)]$ gives us $\left(p\theta + \eta\left(mp\frac{Z}{2}\theta - c\right)\right)\frac{\rho}{\alpha} - \eta\left(mp\frac{Z}{2}\theta - c\right) > mp\frac{Z}{2}\theta - c$, which implies $m < m_U := \frac{2}{Z}\left(\frac{\rho}{\alpha+\eta(\alpha-\rho)} + \frac{c}{p\theta}\right)$. Note that $\frac{\rho}{\alpha+\eta(\alpha-\rho)} > 0$ for $\eta \geq 0$ and $\rho \in (0,1)$ because $\alpha \geq \rho$. Second, $\mathbb{E}_{\lambda}[u_{B,B}(\eta|m,\rho,\alpha)] > \mathbb{E}_{\lambda}[u_{B,A}(\eta|m,\rho,\alpha)]$ gives us $mp\frac{Z}{2}\theta > \left(p\theta + \eta\left(mp\frac{Z}{2}\theta + c\right)\right)\frac{\rho}{\alpha} - \left(c + \eta\left(mp\frac{Z}{2}\theta + c\right)\right)$, which implies $m > m_L := \frac{2}{Z}\left(\frac{\rho}{\alpha+\eta(\alpha-\rho)} - \frac{c}{p\theta}\right)$. Finally, we have $m_U - m_L = \frac{2}{Z}\left(\left(\frac{\rho}{\alpha+\eta(\alpha-\rho)} + \frac{c}{p\theta}\right) - \left(\frac{\rho}{\alpha+\eta(\alpha-\rho)} - \frac{c}{p\theta}\right)\right) = \frac{4c}{pZ\theta} \geq 0$. Thus, when $\alpha \geq \rho$, no drivers relocate from their original zone when $m \in \left[\frac{2}{Z}\left(\frac{\rho}{\alpha+\eta(\alpha-\rho)} - \frac{c}{p\theta}\right), \frac{2}{Z}\left(\frac{\rho}{\alpha+\eta(\alpha-\rho)} + \frac{c}{p\theta}\right)\right]$.

1.2. When $\alpha \leq \max\left\{0, \frac{\rho-\gamma_B}{1-\gamma_A-\gamma_B}\right\}$ or, equivalently, $\alpha \leq \rho$, we have $\frac{\rho}{(1-\gamma_A)\alpha+\gamma_B(1-\alpha)} \geq 1$ and $\frac{1-\rho}{(1-\gamma_B)(1-\alpha)+\gamma_A\alpha} \leq 1$. Then,

$$\mathbb{E}_{\lambda}[u_{A,A}(\eta|m,\rho,\alpha)]$$

$$= \mathbb{E}_{\lambda}\left[p\theta.\min\left\{1, \frac{\rho}{(1-\gamma_A)\alpha+\gamma_B(1-\alpha)}\right\} - \eta(mp\lambda\theta - c)\left(1 - \min\left\{1, \frac{\rho}{(1-\gamma_A)\alpha+\gamma_B(1-\alpha)}\right\}\right)\right] = \int_0^Z (p\theta)\frac{1}{Z}d\lambda$$

$$= p\theta.$$

$$\mathbb{E}_{\lambda}[u_{A,B}(\eta|m,\rho,\alpha)]$$

$$= \mathbb{E}_{\lambda}\left[(mp\lambda\theta - c).\min\left\{1, \frac{1-\rho}{(1-\gamma_B)(1-\alpha)+\gamma_A\alpha}\right\} - \left(c + \eta(p\theta + c)\right)\left(1 - \min\left\{1, \frac{1-\rho}{(1-\gamma_B)(1-\alpha)+\gamma_A\alpha}\right\}\right)\right]$$

$$= \int_0^Z \left(\left(mp\lambda\theta + \eta(p\theta + c)\right)\frac{1-\rho}{1-\alpha} - \left(c + \eta(p\theta + c)\right)\right)\frac{1}{Z}d\lambda$$

$$= \left(mp\frac{Z}{2}\theta + \eta(p\theta + c)\right)\frac{1-\rho}{1-\alpha} - \left(c + \eta(p\theta + c)\right).$$

$\mathbb{E}_\lambda\left[u_{B,A}(\eta|m,\rho,\alpha)\right]$

$$= \mathbb{E}_\lambda\left[(p\theta - c).\min\left\{1, \frac{\rho}{(1-\gamma_A)\alpha + \gamma_B(1-\alpha)}\right\}\right.$$

$$\left.- \big(c + \eta(mp\lambda\theta + c)\big)\left(1 - \min\left\{1, \frac{\rho}{(1-\gamma_A)\alpha + \gamma_B(1-\alpha)}\right\}\right)\right]$$

$$= \int_0^Z (p\theta - c)\frac{1}{Z}d\lambda = p\theta - c.$$

$\mathbb{E}_\lambda\left[u_{B,B}(\eta|m,\rho,\alpha)\right]$

$$= \mathbb{E}_\lambda\left[mp\lambda\theta.\min\left\{1, \frac{1-\rho}{(1-\gamma_B)(1-\alpha) + \gamma_A\alpha}\right\}\right.$$

$$\left.- \eta(p\theta - c)\left(1 - \min\left\{1, \frac{1-\rho}{(1-\gamma_B)(1-\alpha) + \gamma_A\alpha}\right\}\right)\right]$$

$$= \int_0^Z \left(\big(mp\lambda\theta + \eta(p\theta - c)\big)\frac{1-\rho}{1-\alpha} - \eta(p\theta - c)\right)\frac{1}{Z}d\lambda$$

$$= \left(mp\frac{Z}{2}\theta + \eta(p\theta - c)\right)\frac{1-\rho}{1-\alpha} - \eta(p\theta - c).$$

To find the range of m where no drivers relocate from their original zone, we evaluate $\mathbb{E}_\lambda\left[u_{A,A}(\eta|m,\rho,\alpha)\right] > \mathbb{E}_\lambda\left[u_{A,B}(\eta|m,\rho,\alpha)\right]$ and $\mathbb{E}_\lambda\left[u_{B,B}(\eta|m,\rho,\alpha)\right] > \mathbb{E}_\lambda\left[u_{B,A}(\eta|m,\rho,\alpha)\right]$ for $\gamma_A = 0$ and $\gamma_B = 0$. $\mathbb{E}_\lambda\left[u_{A,A}(\eta|m,\rho,\alpha)\right] > \mathbb{E}_\lambda\left[u_{A,B}(\eta|m,\rho,\alpha)\right]$ gives us $p\theta > \left(mp\frac{Z}{2}\theta + \eta(p\theta + c)\right)\frac{1-\rho}{1-\alpha} - \big(c + \eta(p\theta + c)\big)$, which implies $m < m_U := \frac{2}{Z}\left(1 + \frac{c}{p\theta}\right)\left(\frac{1-\alpha+\eta(\rho-\alpha)}{1-\rho}\right)$. Note that $\frac{\rho-\alpha}{1-\alpha} > 0$ for $\rho \in (0,1)$ because $\alpha \le \rho$. Second, $\mathbb{E}_\lambda\left[u_{B,B}(\eta|m,\rho,\alpha)\right] > \mathbb{E}_\lambda\left[u_{B,A}(\eta|m,\rho,\alpha)\right]$ gives us $\left(mp\frac{Z}{2}\theta + \eta(p\theta - c)\right)\frac{1-\rho}{1-\alpha} - \eta(p\theta - c) > p\theta - c$, which implies $m > m_L := \frac{2}{Z}\left(1 - \frac{c}{p\theta}\right)\left(\frac{1-\alpha+\eta(\rho-\alpha)}{1-\rho}\right)$. Finally, we have $m_U - m_L = \frac{2}{Z}\left(\frac{1-\alpha+\eta(\rho-\alpha)}{1-\rho}\right)\left(\frac{c}{p\theta} - \left(-\frac{c}{p\theta}\right)\right) \ge 0$. Thus, when $\alpha \le \rho$, no drivers relocate from their original zone when $m \in \left[\frac{2}{Z}\left(1 - \frac{c}{p\theta}\right)\left(\frac{1-\alpha+\eta(\rho-\alpha)}{1-\rho}\right), \frac{2}{Z}\left(1 + \frac{c}{p\theta}\right)\left(\frac{1-\alpha+\eta(\rho-\alpha)}{1-\rho}\right)\right]$.

2. When $\gamma_A = 1$ and $\gamma_B = 0$:

   2.1. $\alpha \ge \max\left\{0, \frac{\rho-\gamma_B}{1-\gamma_A-\gamma_B}\right\}$ implies $\alpha = 1$ which cannot happen since $\alpha \in (0,1)$.

2.2.When $\alpha \leq \max\left\{0, \frac{\rho-\gamma_B}{1-\gamma_A-\gamma_B}\right\}$ or, equivalently, $\alpha \leq \infty$, we have

$\min\left\{1, \frac{\rho}{(1-\gamma_A)\alpha+\gamma_B(1-\alpha)}\right\} = 1$ and $\min\left\{1, \frac{1-\rho}{(1-\gamma_B)(1-\alpha)+\gamma_A\alpha}\right\} = \frac{1-\rho}{(1-\gamma_B)(1-\alpha)+\gamma_A\alpha}$ for any $\alpha \in (0,1)$. Then,

$$\mathbb{E}_\lambda\left[u_{A,A}(\eta|m,\rho,\alpha)\right]$$

$$= \mathbb{E}_\lambda\left[p\theta.\min\left\{1, \frac{\rho}{(1-\gamma_A)\alpha+\gamma_B(1-\alpha)}\right\}\right.$$

$$\left.-\eta(mp\lambda\theta-c)\left(1-\min\left\{1, \frac{\rho}{(1-\gamma_A)\alpha+\gamma_B(1-\alpha)}\right\}\right)\right] = \int_0^Z (p\theta)\frac{1}{Z}d\lambda$$

$$= p\theta.$$

$$\mathbb{E}_\lambda\left[u_{A,A}(\eta|m,\rho,\alpha)\right]$$

$$= \mathbb{E}_\lambda\left[(mp\lambda\theta-c).\min\left\{1, \frac{1-\rho}{(1-\gamma_B)(1-\alpha)+\gamma_A\alpha}\right\}\right.$$

$$\left.-\big(c+\eta(p\theta+c)\big)\left(1-\min\left\{1, \frac{1-\rho}{(1-\gamma_B)(1-\alpha)+\gamma_A\alpha}\right\}\right)\right]$$

$$= \int_0^Z \Big(\big(mp\lambda\theta+\eta(p\theta+c)\big)(1-\rho)-\big(c+\eta(p\theta+c)\big)\Big)\frac{1}{Z}d\lambda$$

$$= \left(mp\frac{Z}{2}\theta+\eta(p\theta+c)\right)(1-\rho)-\big(c+\eta(p\theta+c)\big).$$

Similarly,

$$\mathbb{E}_\lambda\left[u_{B,A}(\eta|m,\rho,\alpha)\right]$$

$$= \mathbb{E}_\lambda\left[(p\theta-c).\min\left\{1, \frac{\rho}{(1-\gamma_A)\alpha+\gamma_B(1-\alpha)}\right\}\right.$$

$$\left.-\big(c+\eta(mp\lambda\theta+c)\big)\left(1-\min\left\{1, \frac{\rho}{(1-\gamma_A)\alpha+\gamma_B(1-\alpha)}\right\}\right)\right]$$

$$= \int_0^Z (p\theta-c)\frac{1}{Z}d\lambda = p\theta-c.$$

$\mathbb{E}_\lambda\left[u_{B,B}(\eta|m,\rho,\alpha)\right]$

$$= \mathbb{E}_\lambda\left[mp\lambda\theta.\min\left\{1,\frac{1-\rho}{(1-\gamma_B)(1-\alpha)+\gamma_A\alpha}\right\}\right.$$

$$\left.-\eta(p\theta-c)\left(1-\min\left\{1,\frac{1-\rho}{(1-\gamma_B)(1-\alpha)+\gamma_A\alpha}\right\}\right)\right]$$

$$= \int_0^Z \left(\left(mp\lambda\theta+\eta(p\theta-c)\right)(1-\rho)-\eta(p\theta-c)\right)\frac{1}{Z}d\lambda$$

$$= \left(mp\frac{Z}{2}\theta+\eta(p\theta-c)\right)(1-\rho)-\eta(p\theta-c).$$

Re-arranging $\mathbb{E}_\lambda\left[u_{A,A}(\eta|m,\rho,\alpha)\right] < \mathbb{E}_\lambda\left[u_{A,B}(\eta|m,\rho,\alpha)\right]$ gives $m > \frac{2}{Z}\left(1+\frac{c}{p\theta}\right)\left(\frac{1+\eta\rho}{1-\rho}\right)$ and re-arranging $\mathbb{E}_\lambda\left[u_{B,B}(\eta|m,\rho,\alpha)\right] > \mathbb{E}_\lambda\left[u_{B,A}(\eta|m,\rho,\alpha)\right]$ gives $m > \frac{2}{Z}\left(1-\frac{c}{p\theta}\right)\left(\frac{1+\eta\rho}{1-\rho}\right)$. Because $\frac{2}{Z}\left(1+\frac{c}{p\theta}\right)\left(\frac{1+\eta\rho}{1-\rho}\right) \geq \frac{2}{Z}\left(1-\frac{c}{p\theta}\right)\left(\frac{1+\eta\rho}{1-\rho}\right)$, drivers from Zone A will relocate from their original zone and drivers from Zone B will remain in Zone B when $m \geq \frac{2}{Z}\left(1+\frac{c}{p\theta}\right)\left(\frac{1+\eta\rho}{1-\rho}\right)$.

3. When $\gamma_A = 0$ and $\gamma_B = 1$:

   3.1. When $\alpha \geq \max\left(0,\frac{\rho-\gamma_B}{1-\gamma_A-\gamma_B}\right)$ or, equivalently, $\alpha > 0$, we have $\min\left\{1,\frac{\rho}{(1-\gamma_A)\alpha+\gamma_B(1-\alpha)}\right\} = \frac{\rho}{(1-\gamma_A)\alpha+\gamma_B(1-\alpha)} = \rho$ and $\min\left\{1,\frac{1-\rho}{(1-\gamma_B)(1-\alpha)+\gamma_A\alpha}\right\} = 1$ for any $\alpha \in (0,1)$. Thus, $\mathbb{E}_\lambda\left[u_{A,A}(\eta|m,\rho,\alpha)\right]$, $\mathbb{E}_\lambda\left[u_{A,B}(\eta|m,\rho,\alpha)\right]$, $\mathbb{E}_\lambda\left[u_{B,A}(\eta|m,\rho,\alpha)\right]$ and $\mathbb{E}_\lambda\left[u_{B,B}(\eta|m,\rho,\alpha)\right]$ are identical to Case 4 of Theorem 2. Re-arranging $\mathbb{E}_\lambda\left[u_{A,A}(\eta|m,\rho,\alpha)\right] > \mathbb{E}_\lambda\left[u_{A,B}(\eta|m,\rho,\alpha)\right]$ gives $m < \frac{2}{Z}\left(\frac{\rho}{1-\eta\rho+\eta}+\frac{c}{p\theta}\right)$ and re-arranging $\mathbb{E}_\lambda\left[u_{B,B}(\eta|m,\rho,\alpha)\right] < \mathbb{E}_\lambda\left[u_{B,A}(\eta|m,\rho,\alpha)\right]$ gives $m < \frac{2}{Z}\left(\frac{\rho}{1-\eta\rho+\eta}-\frac{c}{p\theta}\right)$. Because $\frac{2}{Z}\left(\frac{\rho}{1-\eta\rho+\eta}+\frac{c}{p\theta}\right) \geq \frac{2}{Z}\left(\frac{\rho}{1-\eta\rho+\eta}-\frac{c}{p\theta}\right)$, drivers from Zone B will relocate from their original zone and drivers from Zone A will remain in Zone A when $m \leq \frac{2}{Z}\left(\frac{\rho}{1-\eta\rho+\eta}-\frac{c}{p\theta}\right)$.

   3.2. When $\alpha \leq \max\left\{0,\frac{\rho-\gamma_B}{1-\gamma_A-\gamma_B}\right\}$, it implies $\alpha = 0$ which cannot happen since $\alpha \in (0,1)$.

4. When $\gamma_A = 0$ and $0 < \gamma_B < 1$:

4.1. When $\alpha \geq \max\left\{0, \frac{\rho-\gamma_B}{1-\gamma_A-\gamma_B}\right\}$ or, equivalently, $\alpha \geq \max\left\{0, \frac{\rho-\gamma_B}{1-\gamma_B}\right\}$, we have $\frac{\rho}{(1-\gamma_A)\alpha+\gamma_B(1-\alpha)} \leq 1$ and $\frac{1-\rho}{(1-\gamma_B)(1-\alpha)+\gamma_A\alpha} \geq 1$. Thus,

$$
\begin{aligned}
&\mathbb{E}_\lambda\left[u_{A,A}(\eta|m,\rho,\alpha)\right] \\
&\quad = \mathbb{E}_\lambda\left[p\theta.\min\left\{1, \frac{\rho}{(1-\gamma_A)\alpha+\gamma_B(1-\alpha)}\right\}\right. \\
&\quad \left. - \eta(mp\lambda\theta - c)\left(1-\min\left\{1, \frac{\rho}{(1-\gamma_A)\alpha+\gamma_B(1-\alpha)}\right\}\right)\right] \\
&\quad = \int_0^Z \left(\left(p\theta + \eta(mp\lambda\theta - c)\right)\frac{\rho}{\alpha(1-\gamma_B)+\gamma_B} - \eta(mp\lambda\theta - c)\right)\frac{1}{Z}d\lambda \\
&\quad = \left(p\theta + \eta\left(mp\frac{Z}{2}\theta - c\right)\right)\frac{\rho}{\alpha(1-\gamma_B)+\gamma_B} - \eta\left(mp\frac{Z}{2}\theta - c\right).
\end{aligned}
$$

$$
\begin{aligned}
&\mathbb{E}_\lambda\left[u_{A,B}(\eta|m,\rho,\alpha)\right] \\
&\quad = \mathbb{E}_\lambda\left[(mp\lambda\theta - c).\min\left\{1, \frac{1-\rho}{(1-\gamma_B)(1-\alpha)+\gamma_A\alpha}\right\}\right. \\
&\quad \left. - \left(c + \eta(p\theta + c)\right)\left(1-\min\left\{1, \frac{1-\rho}{(1-\gamma_B)(1-\alpha)+\gamma_A\alpha}\right\}\right)\right] \\
&\quad = \int_0^Z (mp\lambda\theta - c)\frac{1}{Z}d\lambda = mp\frac{Z}{2}\theta - c.
\end{aligned}
$$

$$
\begin{aligned}
&\mathbb{E}_\lambda\left[u_{B,A}(\eta|m,\rho,\alpha)\right] \\
&\quad = \mathbb{E}_\lambda\left[(p\theta - c).\min\left\{1, \frac{\rho}{(1-\gamma_A)\alpha+\gamma_B(1-\alpha)}\right\}\right. \\
&\quad \left. - \left(c + \eta(mp\lambda\theta + c)\right)\left(1-\min\left\{1, \frac{\rho}{(1-\gamma_A)\alpha+\gamma_B(1-\alpha)}\right\}\right)\right] \\
&\quad = \int_0^Z \left(\left(p\theta + \eta(mp\lambda\theta + c)\right)\frac{\rho}{\alpha(1-\gamma_B)+\gamma_B}\right. \\
&\quad \left. - \left(c + \eta(mp\lambda\theta + c)\right)\right)\frac{1}{Z}d\lambda \\
&\quad = \left(p\theta + \eta\left(mp\frac{Z}{2}\theta + c\right)\right)\frac{\rho}{\alpha(1-\gamma_B)+\gamma_B} - \left(c + \eta\left(mp\frac{Z}{2}\theta + c\right)\right).
\end{aligned}
$$

$\mathbb{E}_\lambda\left[u_{B,B}(\eta|m,\rho,\alpha)\right]$

$$= \mathbb{E}_\lambda\left[mp\lambda\theta.\min\left\{1,\frac{1-\rho}{(1-\gamma_B)(1-\alpha)+\gamma_A\alpha}\right\}\right.$$

$$\left. -\eta(p\theta-c)\left(1-\min\left\{1,\frac{1-\rho}{(1-\gamma_B)(1-\alpha)+\gamma_A\alpha}\right\}\right)\right]$$

$$= \int_0^Z (mp\lambda\theta)\frac{1}{Z}d\lambda = mp\frac{Z}{2}\theta.$$

To determine the optimal proportion γ_B^*, we find an equilibrium point where drivers in Zone B become indifferent between staying in Zone B and relocating to Zone A. Thus, we evaluate $\mathbb{E}_\lambda\left[u_{B,B}(\eta|m,\rho,\alpha)\right] = \mathbb{E}_\lambda\left[u_{B,A}(\eta|m,\rho,\alpha)\right]$ for $\gamma_A = 0$, which gives $mp\frac{Z}{2}\theta = \left(p\theta+\eta\left(mp\frac{Z}{2}\theta+c\right)\right)\frac{\rho}{\alpha(1-\gamma_B)+\gamma_B} - \left(c+\eta\left(mp\frac{Z}{2}\theta+c\right)\right)$. Solving for γ_B, it follows that $\gamma_B^* = \frac{\rho p\theta+\left(mp\frac{Z}{2}\theta+c\right)(\eta(\rho-\alpha)-\alpha)}{\left(mp\frac{Z}{2}\theta+c\right)(1-\alpha)\,(1+\eta)}$. The range at which the equilibrium solution is valid can be calculated by finding the value of the surge multiplier m in the limit where $\gamma_A = 0$ and either $\gamma_B^* \to 0$ or $\gamma_B^* \to 1$. The respective equations are given by $\frac{\rho p\theta+\left(mp\frac{Z}{2}\theta+c\right)(\eta(\rho-\alpha)-\alpha)}{\left(mp\frac{Z}{2}\theta+c\right)(1-\alpha)\,(1+\eta)} = 0$ and $\frac{\rho p\theta+\left(mp\frac{Z}{2}\theta+c\right)(\eta(\rho-\alpha)-\alpha)}{\left(mp\frac{Z}{2}\theta+c\right)(1-\alpha)\,(1+\eta)} = 1$ which gives $m = \frac{2}{Z}\left(\frac{\rho}{1-\eta\rho+\eta} - \frac{c}{p\theta}\right)$ and $m = \frac{2}{Z}\left(\frac{\rho}{\alpha+\eta(\alpha-\rho)} - \frac{c}{p\theta}\right)$.

4.2.When $\alpha \le \max\left\{0,\frac{\rho-\gamma_B}{1-\gamma_A-\gamma_B}\right\}$, or equivalently $\alpha \le \max\left\{0,\frac{\rho-\gamma_B}{1-\gamma_B}\right\}$, we have $\frac{\rho}{(1-\gamma_A)\alpha+\gamma_B(1-\alpha)} \ge 1$ and $\frac{1-\rho}{(1-\gamma_B)(1-\alpha)+\gamma_A\alpha} \le 1$. Thus,

$\mathbb{E}_\lambda\left[u_{A,A}(\eta|m,\rho,\alpha)\right]$

$$= \mathbb{E}_\lambda\left[p\theta.\min\left\{1,\frac{\rho}{(1-\gamma_A)\alpha+\gamma_B(1-\alpha)}\right\}\right.$$

$$\left. -\eta(mp\lambda\theta-c)\left(1-\min\left\{1,\frac{\rho}{(1-\gamma_A)\alpha+\gamma_B(1-\alpha)}\right\}\right)\right] = \int_0^Z (p\theta)\frac{1}{Z}d\lambda$$

$$= p\theta.$$

$$\mathbb{E}_\lambda\left[u_{A,B}(\eta|m,\rho,\alpha)\right]$$

$$= \mathbb{E}_\lambda\left[(mp\lambda\theta - c).\min\left\{1, \frac{1-\rho}{(1-\gamma_B)(1-\alpha)+\gamma_A\alpha}\right\}\right.$$

$$\left. - \big(c+\eta(p\theta+c)\big)\left(1-\min\left\{1, \frac{1-\rho}{(1-\gamma_B)(1-\alpha)+\gamma_A\alpha}\right\}\right)\right]$$

$$= \int_0^Z \left(\big(mp\lambda\theta+\eta(p\theta+c)\big)\frac{1-\rho}{(1-\gamma_B)(1-\alpha)} - \big(c+\eta(p\theta+c)\big)\right)\frac{1}{Z}d\lambda$$

$$= \left(mp\frac{Z}{2}\theta+\eta(p\theta+c)\right)\frac{1-\rho}{(1-\gamma_B)(1-\alpha)} - \big(c+\eta(p\theta+c)\big).$$

$$\mathbb{E}_\lambda\left[u_{B,A}(\eta|m,\rho,\alpha)\right]$$

$$= \mathbb{E}_\lambda\left[(p\theta - c).\min\left\{1, \frac{\rho}{(1-\gamma_A)\alpha+\gamma_B(1-\alpha)}\right\}\right.$$

$$\left. - \big(c+\eta(mp\lambda\theta+c)\big)\left(1-\min\left\{1, \frac{\rho}{(1-\gamma_A)\alpha+\gamma_B(1-\alpha)}\right\}\right)\right]$$

$$= \int_0^Z (p\theta-c)\frac{1}{Z}d\lambda = p\theta - c.$$

$$\mathbb{E}_\lambda\left[u_{B,B}(\eta|m,\rho,\alpha)\right]$$

$$= \mathbb{E}_\lambda\left[mp\lambda\theta.\min\left\{1, \frac{1-\rho}{(1-\gamma_B)(1-\alpha)+\gamma_A\alpha}\right\}\right.$$

$$\left. - \eta(p\theta-c)\left(1-\min\left\{1, \frac{1-\rho}{(1-\gamma_B)(1-\alpha)+\gamma_A\alpha}\right\}\right)\right]$$

$$= \int_0^Z \left(\big(mp\lambda\theta+\eta(p\theta-c)\big)\frac{1-\rho}{(1-\gamma_B)(1-\alpha)} - \eta(p\theta-c)\right)\frac{1}{Z}d\lambda$$

$$= \left(mp\frac{Z}{2}\theta+\eta(p\theta-c)\right)\frac{1-\rho}{(1-\gamma_B)(1-\alpha)} - \eta(p\theta-c).$$

To determine the optimal proportion γ_B^*, we find an equilibrium point where drivers in Zone B become indifferent between staying in Zone B and relocating to Zone A. Thus, we evaluate $\mathbb{E}_\lambda\left[u_{B,B}(\eta|m,\rho,\alpha)\right] = \mathbb{E}_\lambda\left[u_{B,A}(\eta|m,\rho,\alpha)\right]$ for $\gamma_A = 0$, which gives $\left(mp\frac{Z}{2}\theta+\eta(p\theta-c)\right)\frac{1-\rho}{(1-\gamma_B)(1-\alpha)} - \eta(p\theta-c) = p\theta - c$. Solving for γ_B, it follows that $\gamma_B^* = 1 - \frac{\left(mp\frac{Z}{2}\theta+\eta(p\theta-c)\right)(1-\rho)}{(p\theta-c)(1-\alpha)\,(1+\eta)}$. The range at which the equilibrium solution is valid can be calculated by finding the value of the surge multiplier m in the limit where $\gamma_A = 0$

and either $\gamma_B^* \to 0$ or $\gamma_B^* \to 1$. The respective equations are given by $1 - \frac{\left(mp\frac{Z}{2}\theta+\eta(p\theta-c)\right)(1-\rho)}{(p\theta-c)(1-\alpha)\,(1+\eta)} = 0$ and $1 - \frac{\left(mp\frac{Z}{2}\theta+\eta(p\theta-c)\right)(1-\rho)}{(p\theta-c)(1-\alpha)\,(1+\eta)} = 1$. The first equation gives $m = \frac{2}{Z}\left(1-\frac{c}{p\theta}\right)\frac{1-\alpha+\eta(\rho-\alpha)}{1-\rho}$ and the second equation gives $m = \frac{-2\eta}{Z}\left(1-\frac{c}{p\theta}\right) < 0$, which is infeasible because $\mathbb{E}_\lambda\left[u_{B,A}(\eta|m,\rho,\alpha)\right] = p\theta - c \geq 0$ from Assumption 3. Thus, $m \leq \frac{2}{Z}\left(1-\frac{c}{p\theta}\right)\frac{1-\alpha+\eta(\rho-\alpha)}{1-\rho}$ holds. To find the lower bound, we have $\gamma_B^* = 1 - \frac{\left(mp\frac{Z}{2}\theta+\eta(p\theta-c)\right)(1-\rho)}{(p\theta-c)(1-\alpha)\,(1+\eta)}$ and $\alpha \leq \frac{\rho-\gamma_B}{1-\gamma_B}$. Thus, $\gamma_B^* \leq \frac{\rho-\alpha}{1-\alpha}$. Solving $1 - \frac{\left(mp\frac{Z}{2}\theta+\eta(p\theta-c)\right)(1-\rho)}{(p\theta-c)(1-\alpha)\,(1+\eta)} \leq \frac{\rho-\alpha}{1-\alpha}$ gives $m \geq \frac{2}{Z}\left(1-\frac{c}{p\theta}\right)$. Hence, the range for m is $\frac{2}{Z}\left(1-\frac{c}{p\theta}\right) \leq m \leq \frac{2}{Z}\left(1-\frac{c}{p\theta}\right)\frac{1-\alpha+\eta(\rho-\alpha)}{1-\rho}$.

5. When $\gamma_B = 0$ and $0 < \gamma_A < 1$:

5.1. When $\alpha \geq \max\left\{0, \frac{\rho-\gamma_B}{1-\gamma_A-\gamma_B}\right\}$ or, equivalently, $\alpha \geq \max\left\{0, \frac{\rho}{1-\gamma_A}\right\}$, we have $\frac{\rho}{(1-\gamma_A)\alpha+\gamma_B(1-\alpha)} \leq 1$ and $\frac{1-\rho}{(1-\gamma_B)(1-\alpha)+\gamma_A\alpha} \geq 1$. Then,

$$\begin{aligned}
&\mathbb{E}_\lambda\left[u_{A,A}(\eta|m,\rho,\alpha)\right] \\
&\quad = \mathbb{E}_\lambda\left[p\theta.\min\left\{1, \frac{\rho}{(1-\gamma_A)\alpha+\gamma_B(1-\alpha)}\right\}\right. \\
&\quad \left. - \eta(mp\lambda\theta - c)\left(1-\min\left\{1, \frac{\rho}{(1-\gamma_A)\alpha+\gamma_B(1-\alpha)}\right\}\right)\right] \\
&\quad = \int_0^Z \left(\left(p\theta + \eta(mp\lambda\theta - c)\right)\frac{\rho}{\alpha(1-\gamma_A)} - \eta(mp\lambda\theta - c)\right)\frac{1}{Z}d\lambda \\
&\quad = \left(p\theta + \eta\left(mp\frac{Z}{2}\theta - c\right)\right)\frac{\rho}{\alpha(1-\gamma_A)} - \eta\left(mp\frac{Z}{2}\theta - c\right).
\end{aligned}$$

$$\begin{aligned}
&\mathbb{E}_\lambda\left[u_{A,B}(\eta|m,\rho,\alpha)\right] \\
&\quad = \mathbb{E}_\lambda\left[(mp\lambda\theta - c).\min\left\{1, \frac{1-\rho}{(1-\gamma_B)(1-\alpha)+\gamma_A\alpha}\right\}\right. \\
&\quad \left. - \left(c + \eta(p\theta + c)\right)\left(1-\min\left\{1, \frac{1-\rho}{(1-\gamma_B)(1-\alpha)+\gamma_A\alpha}\right\}\right)\right] \\
&\quad = \int_0^Z (mp\lambda\theta - c)\frac{1}{Z}d\lambda = mp\frac{Z}{2}\theta - c.
\end{aligned}$$

$$\mathbb{E}_\lambda\left[u_{B,A}(\eta|m,\rho,\alpha)\right]$$

$$= \mathbb{E}_\lambda\left[(p\theta - c).\min\left\{1, \frac{\rho}{(1-\gamma_A)\alpha + \gamma_B(1-\alpha)}\right\}\right.$$

$$\left. - \big(c + \eta(mp\lambda\theta + c)\big)\left(1 - \min\left\{1, \frac{\rho}{(1-\gamma_A)\alpha + \gamma_B(1-\alpha)}\right\}\right)\right]$$

$$= \int_0^Z \left(\big(p\theta + \eta(mp\lambda\theta + c)\big)\frac{\rho}{\alpha(1-\gamma_A)} - \big(c + \eta(mp\lambda\theta + c)\big)\right)\frac{1}{Z}d\lambda$$

$$= \left(p\theta + \eta\left(mp\frac{Z}{2}\theta + c\right)\right)\frac{\rho}{\alpha(1-\gamma_A)} - \left(c + \eta\left(mp\frac{Z}{2}\theta + c\right)\right).$$

$$\mathbb{E}_\lambda\left[u_{B,B}(\eta|m,\rho,\alpha)\right]$$

$$= \mathbb{E}_\lambda\left[mp\lambda\theta.\min\left\{1, \frac{1-\rho}{(1-\gamma_B)(1-\alpha) + \gamma_A\alpha}\right\}\right.$$

$$\left. - \eta(p\theta - c)\left(1 - \min\left\{1, \frac{1-\rho}{(1-\gamma_B)(1-\alpha) + \gamma_A\alpha}\right\}\right)\right]$$

$$= \int_0^Z (mp\lambda\theta)\frac{1}{Z}d\lambda = mp\frac{Z}{2}\theta.$$

To determine the optimal proportion γ_A^*, we find an equilibrium point where drivers in Zone A become indifferent between staying in Zone A and relocating to Zone B. Thus, we evaluate $\mathbb{E}_\lambda\left[u_{A,A}(\eta|m,\rho,\alpha)\right] = \mathbb{E}_\lambda\left[u_{A,B}(\eta|m,\rho,\alpha)\right]$ for $\gamma_B = 0$, which gives $\left(p\theta + \eta\left(mp\frac{Z}{2}\theta - c\right)\right)\frac{\rho}{\alpha(1-\gamma_A)} - \eta\left(mp\frac{Z}{2}\theta - c\right) = mp\frac{Z}{2}\theta - c$ and thus $\gamma_A^* = 1 - \frac{\rho\left(p\theta+\eta\left(mp\frac{Z}{2}\theta-c\right)\right)}{\alpha(1+\eta)\left(mp\frac{Z}{2}\theta-c\right)}$. The range at which the equilibrium solution is valid can be calculated by finding the value of the surge multiplier m in the limit where $\gamma_B = 0$ and either $\gamma_A^* \to 1$ or $\gamma_A^* \to 0$. The respective equations are given by $1 - \frac{\rho\left(p\theta+\eta\left(mp\frac{Z}{2}\theta-c\right)\right)}{\alpha(1+\eta)\left(mp\frac{Z}{2}\theta-c\right)} = 1$ and $1 - \frac{\rho\left(p\theta+\eta\left(mp\frac{Z}{2}\theta-c\right)\right)}{\alpha(1+\eta)\left(mp\frac{Z}{2}\theta-c\right)} = 0$. Solving for m gives no feasible solution for the first equation because $p\theta > 0$ and $mp\frac{Z}{2}\theta - c \geq 0$ from Assumption 2, but it gives $m = \frac{2}{Z}\left(\frac{\rho}{\alpha+\eta(\alpha-\rho)} + \frac{c}{p\theta}\right)$ for the second equation, which is the lower bound of the range for m.

The upper bound comes from $\alpha \geq \max\left(0, \frac{\rho}{1-\gamma_A}\right)$ as follows: $\gamma_A^* = 1 - \frac{\rho\left(p\theta+\eta\left(mp\frac{Z}{2}\theta-c\right)\right)}{\alpha(1+\eta)\left(mp\frac{Z}{2}\theta-c\right)} \leq 1 - \frac{\rho}{\alpha}$, which gives $m \leq \frac{2}{Z}\left(1+\frac{c}{p\theta}\right)$. Note that $\frac{\rho}{\alpha+\eta(\alpha-\rho)} \leq 1$ since $\alpha \geq \frac{\rho}{1-\gamma_A}$. Thus, $\frac{2}{Z}\left(\frac{\rho}{\alpha+\eta(\alpha-\rho)}+\frac{c}{p\theta}\right) \leq m \leq \frac{2}{Z}\left(1+\frac{c}{p\theta}\right)$.

5.2.When $\alpha \leq \max\left\{0, \frac{\rho-\gamma_B}{1-\gamma_A-\gamma_B}\right\}$ or, equivalently, $\alpha \leq \max\left\{0, \frac{\rho}{1-\gamma_A}\right\}$, we have $\frac{\rho}{(1-\gamma_A)\alpha+\gamma_B(1-\alpha)} \geq 1$ and $\frac{1-\rho}{(1-\gamma_B)(1-\alpha)+\gamma_A\alpha} \leq 1$. Then,

$$\begin{aligned}
&\mathbb{E}_\lambda\left[u_{A,A}(\eta|m,\rho,\alpha)\right] \\
&\quad = \mathbb{E}_\lambda\left[p\theta.\min\left\{1, \frac{\rho}{(1-\gamma_A)\alpha+\gamma_B(1-\alpha)}\right\}\right. \\
&\quad \left. -\eta(mp\lambda\theta-c)\left(1-\min\left\{1, \frac{\rho}{(1-\gamma_A)\alpha+\gamma_B(1-\alpha)}\right\}\right)\right] \\
&\quad = \int_0^Z (p\theta)\frac{1}{Z}d\lambda = p\theta.
\end{aligned}$$

$$\begin{aligned}
&\mathbb{E}_\lambda\left[u_{A,B}(\eta|m,\rho,\alpha)\right] \\
&\quad = \mathbb{E}_\lambda\left[(mp\lambda\theta-c).\min\left\{1, \frac{1-\rho}{(1-\gamma_B)(1-\alpha)+\gamma_A\alpha}\right\}\right. \\
&\quad \left. -\left(c+\eta(p\theta+c)\right)\left(1-\min\left\{1, \frac{1-\rho}{(1-\gamma_B)(1-\alpha)+\gamma_A\alpha}\right\}\right)\right] \\
&\quad = \int_0^Z \left(\left(mp\lambda\theta+\eta(p\theta+c)\right)\frac{1-\rho}{1-\alpha(1-\gamma_A)} - \left(c+\eta(p\theta+c)\right)\right)\frac{1}{Z}d\lambda \\
&\quad = \left(mp\frac{Z}{2}\theta+\eta(p\theta+c)\right)\frac{1-\rho}{1-\alpha(1-\gamma_A)} - \left(c+\eta(p\theta+c)\right).
\end{aligned}$$

$$\begin{aligned}
&\mathbb{E}_\lambda\left[u_{B,A}(\eta|m,\rho,\alpha)\right] \\
&\quad = \mathbb{E}_\lambda\left[(p\theta-c).\min\left\{1, \frac{\rho}{(1-\gamma_A)\alpha+\gamma_B(1-\alpha)}\right\}\right. \\
&\quad \left. -\left(c+\eta(mp\lambda\theta+c)\right)\left(1-\min\left\{1, \frac{\rho}{(1-\gamma_A)\alpha+\gamma_B(1-\alpha)}\right\}\right)\right] \\
&\quad = \int_0^Z (p\theta-c)\frac{1}{Z}d\lambda = p\theta-c.
\end{aligned}$$

$$\mathbb{E}_\lambda[u_{B,B}(\eta|m,\rho,\alpha)]$$

$$= \mathbb{E}_\lambda\left[mp\lambda\theta.\min\left\{1,\frac{1-\rho}{(1-\gamma_B)(1-\alpha)+\gamma_A\alpha}\right\}\right.$$

$$\left.-\eta(p\theta-c)\left(1-\min\left\{1,\frac{1-\rho}{(1-\gamma_B)(1-\alpha)+\gamma_A\alpha}\right\}\right)\right]$$

$$= \int_0^Z\left(\left(mp\lambda\theta+\eta(p\theta-c)\right)\frac{1-\rho}{1-\alpha(1-\gamma_A)}-\eta(p\theta-c)\right)\frac{1}{Z}d\lambda$$

$$= \left(mp\frac{Z}{2}\theta+\eta(p\theta-c)\right)\frac{1-\rho}{1-\alpha(1-\gamma_A)}-\eta(p\theta-c).$$

To determine the optimal proportion γ_A^*, we find an equilibrium point where drivers in Zone A become indifferent between staying in Zone A and relocating to Zone B. Thus, we evaluate $\mathbb{E}_\lambda[u_{A,A}(\eta|m,\rho,\alpha)] = \mathbb{E}_\lambda[u_{A,B}(\eta|m,\rho,\alpha)]$ for $\gamma_B = 0$, which gives $p\theta = \left(mp\frac{Z}{2}\theta+\eta(p\theta+c)\right)\frac{1-\rho}{1-\alpha(1-\gamma_A)}-\left(c+\eta(p\theta+c)\right)$. Therefore, $\gamma_A^* = \frac{(1-\rho)mp\frac{Z}{2}\theta-(p\theta+c)(1-\alpha+\eta(\rho-\alpha))}{\alpha(p\theta+c)(1+\eta)}$. The range at which the equilibrium solution is feasible can be calculated by finding the value of the surge multiplier m in the limit where $\gamma_B = 0$ and either $\gamma_A^* \to 1$ or $\gamma_A^* \to 0$. The respective equations are given by $\frac{(1-\rho)mp\frac{Z}{2}\theta-(p\theta+c)(1-\alpha+\eta(\rho-\alpha))}{\alpha(p\theta+c)(1+\eta)} = 1$ and $\frac{(1-\rho)mp\frac{Z}{2}\theta-(p\theta+c)(1-\alpha+\eta(\rho-\alpha))}{\alpha(p\theta+c)(1+\eta)} = 0$. Solving for m gives $m = \frac{2}{Z}\left(1+\frac{c}{p\theta}\right)\left(\frac{1+\eta\rho}{1-\rho}\right)$ and $m = \frac{2}{Z}\left(1+\frac{c}{p\theta}\right)\frac{1-\alpha+\eta(\rho-\alpha)}{1-\rho}$.

A summary of the cases appears in Tables 3-A-12 and 3-A-13.

Table 3-A-12. Result summary for Theorem 3 when $\alpha \geq max\left\{0,\frac{\rho-\gamma_B^*}{1-\gamma_A^*-\gamma_B^*}\right\}$

Case	% of drivers γ_A^* initially located in Zone A relocating to Zone B	% of drivers γ_B^* initially located in Zone B relocating to Zone A	Range for the surge multiplier m
3	0	1	$0 \leq m \leq \frac{2}{Z}\left(\frac{\rho}{1-\eta\rho+\eta}-\frac{c}{p\theta}\right)$
4	0	$0 < \gamma_B < 1$ $\gamma_B^* = \frac{\rho p\theta+\left(mp\frac{Z}{2}\theta+c\right)(\eta(\rho-\alpha)-\alpha)}{\left(mp\frac{Z}{2}\theta+c\right)(1-\alpha)(1+\eta)}$	$\frac{2}{Z}\left(\frac{\rho}{1-\eta\rho+\eta}-\frac{c}{p\theta}\right) \leq m \leq \frac{2}{Z}\left(\frac{\rho}{\alpha+\eta(\alpha-\rho)}-\frac{c}{p\theta}\right)$
1	0	0	$\frac{2}{Z}\left(\frac{\rho}{\alpha+\eta(\alpha-\rho)}-\frac{c}{p\theta}\right) \leq m \leq \frac{2}{Z}\left(\frac{\rho}{\alpha+\eta(\alpha-\rho)}+\frac{c}{p\theta}\right)$
5	$0 < \gamma_A < 1$	0	$\frac{2}{Z}\left(\frac{\rho}{\alpha+\eta(\alpha-\rho)}+\frac{c}{p\theta}\right) \leq m \leq \frac{2}{Z}\left(1+\frac{c}{p\theta}\right)$

	$\gamma_A^* = 1 - \frac{\rho\left(p\theta + \eta\left(mp\frac{Z}{2}\theta - c\right)\right)}{\alpha(1+\eta)\left(mp\frac{Z}{2}\theta - c\right)}$		
2	1	0	No equilibrium
	$0 < \gamma_A < 1$	1	No equilibrium
	$0 < \gamma_A < 1$	$0 < \gamma_B < 1$	
	1	1	
	1	$0 < \gamma_B < 1$	

Table 3-A-13. Result summary for Theorem 3 when $\alpha \leq max\left\{0, \frac{\rho - \gamma_B^*}{1 - \gamma_A^* - \gamma_B^*}\right\}$

Case	**% of drivers γ_A^* initially located in Zone A relocating to Zone B**	**% of drivers γ_B^* initially located in Zone B relocating to Zone A**	**Range for the surge multiplier m**
3	0	1	No equilibrium
4	0	$0 < \gamma_B < 1$ $\gamma_B^* = 1 - \frac{\left(mp\frac{Z}{2}\theta + \eta(p\theta - c)\right)(1-\rho)}{(p\theta - c)(1-\alpha)(1+\eta)}$	$\frac{2}{Z}\left(1 - \frac{c}{p\theta}\right) \leq m \leq \frac{2}{Z}\left(1 - \frac{c}{p\theta}\right)\frac{1 - \alpha + \eta(\rho - \alpha)}{1 - \rho}$
1	0	0	$\frac{2}{Z}\left(1 - \frac{c}{p\theta}\right)\left(\frac{1 - \alpha + \eta(\rho - \alpha)}{1 - \rho}\right) \leq m \leq \frac{2}{Z}\left(1 + \frac{c}{p\theta}\right)\left(\frac{1 - \alpha + \eta(\rho - \alpha)}{1 - \rho}\right)$
5	$0 < \gamma_A < 1$ $\gamma_A^* = \frac{(1-\rho)mp\frac{Z}{2}\theta - (p\theta + c)\left(1 - \alpha + \eta(\rho - \alpha)\right)}{\alpha(p\theta + c)(1+\eta)}$	0	$\frac{2}{Z}\left(1 + \frac{c}{p\theta}\right)\frac{1 - \alpha + \eta(\rho - \alpha)}{1 - \rho} \leq m \leq \frac{2}{Z}\left(1 + \frac{c}{p\theta}\right)\left(\frac{1 + \eta\rho}{1 - \rho}\right)$
2	1	0	$\frac{2}{Z}\left(1 + \frac{c}{p\theta}\right)\left(\frac{1 + \eta\rho}{1 - \rho}\right) \leq m \leq m_{max}$
	$0 < \gamma_A < 1$	1	No equilibrium
	$0 < \gamma_A < 1$	$0 < \gamma_B < 1$	
	1	1	
	1	$0 < \gamma_B < 1$	

Proof of Theorem 4

Matching efficiency for Models 1–4

The optimal surge multiplier and maximum matching efficiency for Models 1–4 are similar except for λ replacing $\frac{Z}{2}$ in Models 2 and 4 while γ_A^* and γ_B^* are multiplied by $\frac{1+\alpha+\alpha\eta}{(3+\eta)(1-\alpha)}$ in Models 3 and 4. The optimal values depend on the regions for m described in Theorem 1. We first simplify the matching efficiency function as follows:

$$\widehat{M}^* = \frac{\min\{S_A^1, D_A\} + \min\{S_B^1, D_B\}}{n}$$
$$= \frac{\min\{(1-\gamma_A^*)\alpha n + \gamma_B^*(1-\alpha)n, \rho n\} + \min\{(1-\gamma_B^*)(1-\alpha)n + \gamma_A^*\alpha n, (1-\rho)n\}}{n}$$
$$= \frac{1}{n}\left(\frac{1}{2}(S_A^1 + D_A) - \frac{1}{2}|S_A^1 - D_A| + \frac{1}{2}(S_B^1 + D_B) - \frac{1}{2}|S_B^1 - D_B|\right)$$
$$= \frac{1}{2n}\Big(\big((1-\gamma_A^*)\alpha n + \gamma_B^*(1-\alpha)n + \rho n\big) - |(1-\gamma_A^*)\alpha n + \gamma_B^*(1-\alpha)n - \rho n|$$
$$+ \big((1-\gamma_B^*)(1-\alpha)n + \gamma_A^*\alpha n + (1-\rho)n\big) - |(1-\gamma_B^*)(1-\alpha)n + \gamma_A^*\alpha n - (1-\rho)n|\Big)$$
$$= 1 - |\rho - \alpha(1-\gamma_A^*) - (1-\alpha)\gamma_B^*|. \tag{A4}$$

From Theorem 1 and Table 3-A-10, which describes the optimal γ_A^* and γ_B^* for Model 1, five regions must be examined for m.

Region 1. When $\gamma_A^* = 0, \gamma_B^* = 1$, and $m \le \frac{2}{Z}\left(\frac{1}{2+\eta} - \frac{c}{p\theta}\right)$, the platform's matching efficiency is $\widehat{M}^* = 1 - |-1+\rho| = \rho$ since $0 < \rho < 1$. Hence, the matching efficiency is not a function of m and the surge multiplier that maximizes the platform's matching efficiency is any $m \ge 0$ where $m \in \left[0, \frac{2}{Z}\left(\frac{1}{2+\eta} - \frac{c}{p\theta}\right)\right]$. Note that for the upper bound of the interval to be greater than the lower bound, it requires $\frac{c}{p\theta} \le \frac{1}{2+\eta}$.

Region 2. We have that $\gamma_A^* = 0$ and $\gamma_B^* = \frac{p\theta(3+\eta)(2-mZ)-4c(2+\eta)}{p\theta(1+\eta)(mZ+2)}$ within this region and $\frac{2}{Z}\left(\frac{1}{2+\eta} - \frac{c}{p\theta}\right) \le m \le \frac{2}{Z}\left(1 - \frac{c(4+2\eta)}{p\theta(3+\eta)}\right)$. Thus, the matching efficiency is given by $\widehat{M}^* = 1 - \left|\rho - \alpha - \frac{(1-\alpha)(-4c(2+\eta)+p\theta(2-mZ)(3+\eta))}{p\theta(2+mZ)(1+\eta)}\right|$. Assuming that $\rho - \alpha - \frac{(1-\alpha)(-4c(2+\eta)+p\theta(2-mZ)(3+\eta))}{p\theta(2+mZ)(1+\eta)} \ne 0$, the first-order derivative with respect to m is either $\frac{\partial \widehat{M}^*}{\partial m} = \frac{-4Z(1-\alpha)(p\theta(3+\eta)-c(2+\eta))}{p\theta(1+\eta)(2+mZ)^2}$ or $\frac{\partial \widehat{M}^*}{\partial m} = \frac{-4Z(1-\alpha)(-p\theta(3+\eta)+c(2+\eta))}{p\theta(1+\eta)(2+mZ)^2}$, and the second-order derivative is, respectively, $\frac{\partial^2 \widehat{M}^*}{\partial m^2} = \frac{8Z^2(1-\alpha)(p\theta(3+\eta)-c(2+\eta))}{p\theta(1+\eta)(2+mZ)^3}$ or $\frac{\partial^2 \widehat{M}^*}{\partial m^2} = \frac{8Z^2(1-\alpha)(-p\theta(3+\eta)+c(2+\eta))}{p\theta(1+\eta)(2+mZ)^3}$. Since $\frac{c}{p\theta} \le 1$ from Assumption 3, depending on the magnitude of $\frac{c}{p\theta}$, we have three cases:

i. Case 1: $\frac{1}{2+\eta} \leq \frac{3+\eta}{2(2+\eta)} \leq \frac{c}{p\theta} \leq \frac{3+\eta}{2+\eta}$

The lower and upper bounds of the surge multiplier range are both negative. Thus, there is no nonnegative surge multiplier in this region that maximizes the matching efficiency.

ii. Case 2: $\frac{1}{2+\eta} \leq \frac{c}{p\theta} \leq \frac{3+\eta}{2(2+\eta)} \leq \frac{3+\eta}{2+\eta}$

In this case, the upper bound is positive and the lower bound is negative. Depending on the sign of $\left|\rho - \alpha - \frac{(1-\alpha)(-4c(2+\eta)+p\theta(2-mZ)(3+\eta))}{p\theta(2+mZ)(1+\eta)}\right|$, the matching efficiency has regions that are either decreasing and convex or increasing and concave. However, the lower bound of the surge multiplier range is negative in this case, which implies that the lowest feasible surge multiplier must occur at $m = 0$; this gives $\widehat{M}^* = 1 - \left|\rho - \alpha - \frac{(1-\alpha)(-2c(2+\eta)+p\theta(3+\eta))}{p\theta(1+\eta)}\right|$, which we define as M_0. Alternatively, at the upper bound of the surge multiplier interval, $m = \frac{2}{Z}\left(1 - \frac{c(4+2\eta)}{p\theta(3+\eta)}\right) > 0$ which gives $\widehat{M}^* = 1 - |\rho - \alpha|$. Because we assume $\frac{c}{p\theta} \leq \frac{3+\eta}{2(2+\eta)}$, it follows that $\frac{(1-\alpha)(-2c(2+\eta)+p\theta(3+\eta))}{p\theta(1+\eta)} \geq 0$, which implies that if $\alpha \leq \rho$, $m^* = 0$ and $\widehat{M}^* = M_0$. Otherwise, if $\alpha \geq \rho$, $m^* = \frac{2}{Z}\left(1 - \frac{c(4+2\eta)}{p\theta(3+\eta)}\right)$ and $\widehat{M}^* = 1 - |\rho - \alpha|$.

iii. Case 3: $\frac{c}{p\theta} \leq \frac{1}{2+\eta} \leq \frac{3+\eta}{2(2+\eta)} \leq \frac{3+\eta}{2+\eta}$

In this case, the lower and upper bounds are both positive. Depending on the sign of $\left|\rho - \alpha - \frac{(1-\alpha)(-4c(2+\eta)+p\theta(2-mZ)(3+\eta))}{p\theta(2+mZ)(1+\eta)}\right|$, the matching efficiency has regions that are decreasing and convex or increasing and concave, which means that the optimal surge multiplier value is either the lower or upper bound of this region. At the lower bound, $m = \frac{2}{Z}\left(\frac{1}{2+\eta} - \frac{c}{p\theta}\right) > 0$ and the matching efficiency is $\widehat{M}^* = \rho$. At the upper bound, $m = \frac{2}{Z}\left(1 - \frac{c(4+2\eta)}{p\theta(3+\eta)}\right) > 0$ and the matching efficiency is $\widehat{M}^* = 1 - |\rho - \alpha|$.

Note that a critical point also exists when $\left|\rho - \alpha - \frac{(1-\alpha)(-4c(2+\eta)+p\theta(2-mZ)(3+\eta))}{p\theta(2+mZ)(1+\eta)}\right| = 0$ because it marks the boundary between the two continuous regions. Solving for the optimal surge multiplier gives $m^+ = -\frac{4c(1-\alpha)(2+\eta)+2p\theta(-3+2\alpha-\eta(1-\rho)+\rho)}{pZ\theta(3+\eta-2\alpha(2+\eta)+\rho+\eta\rho)}$ and $\widehat{M}^* = 1$. First notice that for some $\epsilon \geq 0$, $\lim_{\alpha \to \rho - \frac{(3+\eta)}{2(2+\eta)}\epsilon} \left(\frac{2}{Z}\left(1 - \frac{c(4+2\eta)}{p\theta(3+\eta)}\right) - m^+\right) = \frac{2\epsilon(1+\eta)(-c(2+\eta)+p(3+\eta)\theta)}{pZ(2+\eta)(3+\eta)\theta(1+\epsilon-\rho)} \geq 0$ and $\lim_{\alpha \to \rho - \frac{(3+\eta)}{2(2+\eta)}\epsilon} \left(m^+ - \frac{2}{Z}\left(\frac{1}{2+\eta} - \frac{c}{p\theta}\right)\right) = \frac{2(1+\eta)(-c(2+\eta)+p(3+\eta)\theta)(1-\rho)}{pZ(2+\eta)(3+\eta)\theta(1+\epsilon-\rho)} \geq 0$ since $\frac{c}{p\theta} \leq \frac{3+\eta}{2+\eta}$ from Assumption 3. This implies that for $\frac{2}{Z}\left(1 - \frac{c(4+2\eta)}{p\theta(3+\eta)}\right) \geq m^+ \geq \frac{2}{Z}\left(\frac{1}{2+\eta} - \frac{c}{p\theta}\right) \geq 0$ or $\frac{2}{Z}\left(1 - \frac{c(4+2\eta)}{p\theta(3+\eta)}\right) \geq m^+ \geq 0 \geq \frac{2}{Z}\left(\frac{1}{2+\eta} - \frac{c}{p\theta}\right)$, we must have $\alpha \leq \rho$ and $\widehat{M}^* = 1$. If $\frac{2}{Z}\left(1 - \frac{c(4+2\eta)}{p\theta(3+\eta)}\right) \geq 0 \geq m^+ \geq \frac{2}{Z}\left(\frac{1}{2+\eta} - \frac{c}{p\theta}\right)$, it follows that $m^* = 0$ and $\widehat{M}^* = M_0$. Otherwise, when $\alpha \geq \rho$, it follows that $m^+ \geq \frac{2}{Z}\left(1 - \frac{c(4+2\eta)}{p\theta(3+\eta)}\right)$, which means that $m^* = \frac{2}{Z}\left(1 - \frac{c(4+2\eta)}{p\theta(3+\eta)}\right)$ and $\widehat{M}^* = 1 - |\rho - \alpha|$. This holds because $1 - |\rho - \alpha| = 1 - (\alpha - \rho) = \rho + 1 - \alpha > \rho$.

Region 3. When $\gamma_A^* = 0, \gamma_B^* = 0$, and $\frac{2}{Z}\left(1 - \frac{c(4+2\eta)}{p\theta(3+\eta)}\right) \leq m \leq \frac{2}{Z}\left(1 + \frac{c(4+2\eta)}{p\theta(3+\eta)}\right)$, the platform's matching efficiency is either $\widehat{M}^* = 1 - (\rho - \alpha)$ or $\widehat{M}^* = 1 - (\alpha - \rho)$. This is equivalent to $\widehat{M}^* = 1 - |\rho - \alpha|$, which is not a function of m. Thus, the surge multiplier that maximizes the platform's matching efficiency is any $m \geq 0$ where $m \in \left[\frac{2}{Z}\left(1 - \frac{c(4+2\eta)}{p\theta(3+\eta)}\right), \frac{2}{Z}\left(1 + \frac{c(4+2\eta)}{p\theta(3+\eta)}\right)\right]$.

Region 4. We have that $\gamma_A^* = \frac{(3+\eta)\left(mp\frac{Z}{2}\theta - p\theta\right) - c(4+2\eta)}{(1+\eta)\left(p\theta + mp\frac{Z}{2}\theta\right)}$ and $\gamma_B^* = 0$ within the range $\frac{2}{Z}\left(1 + \frac{c(4+2\eta)}{p\theta(3+\eta)}\right) \leq m \leq \frac{2}{Z}\left(1 + \frac{c}{p\theta}\right)(2+\eta)$, and the matching efficiency is given by $\widehat{M}^* = 1 - \left|\rho - \frac{4c\alpha(2+\eta)+2p\theta\alpha(4-mZ+2\eta)}{p\theta(2+mZ)(1+\eta)}\right|$. Assuming that $\rho - \frac{4c\alpha(2+\eta)+2p\theta\alpha(4-mZ+2\eta)}{p\theta(2+mZ)(1+\eta)} \neq 0$, the first-order derivative is either $\frac{\partial \widehat{M}^*}{\partial m} = \frac{-4Z\alpha\left(p\theta(3+\eta)+c(2+\eta)\right)}{p\theta(1+\eta)(2+mZ)^2}$ or $\frac{\partial \widehat{M}^*}{\partial m} = \frac{4Z\alpha\left(p\theta(3+\eta)+c(2+\eta)\right)}{p\theta(1+\eta)(2+mZ)^2}$, and the second-order derivative is, respectively, $\frac{\partial^2 \widehat{M}^*}{\partial m^2} = \frac{8Z^2\alpha\left(p\theta(3+\eta)+c(2+\eta)\right)}{p\theta(1+\eta)(2+mZ)^3}$ or $\frac{\partial^2 \widehat{M}^*}{\partial m^2} = \frac{-8Z^2\alpha\left(p\theta(3+\eta)+c(2+\eta)\right)}{p\theta(1+\eta)(2+mZ)^3}$. This implies that the matching efficiency has regions that are decreasing and convex or increasing and concave, which means that the optimal surge multiplier is either the lower or upper bound of this region. If $m = \frac{2}{Z}\left(1 + \frac{c(4+2\eta)}{p\theta(3+\eta)}\right)$, then $\widehat{M}^* = 1 - |\rho - \alpha|$ but if $m = \frac{2}{Z}\left(1 + \frac{c}{p\theta}\right)(2+\eta)$, then $\widehat{M}^* = 1 - \rho$.

Note that a critical point also exists when $\left|\rho - \frac{4c\alpha(2+\eta)+2p\theta\alpha(4-mZ+2\eta)}{p\theta(2+mZ)(1+\eta)}\right| = 0$ because it marks the boundary between the two continuous regions. Solving for the optimal surge multiplier gives $m = \frac{4\alpha(2+\eta)(c+p\theta)-2p(1+\eta)\theta\rho}{pZ\theta(2\alpha+\rho+\eta\rho)}$ and $\widehat{M}^* = 1$. However, notice that $\frac{2}{Z}\left(1+\frac{c}{p\theta}\right)(2+\eta) - \frac{4\alpha(2+\eta)(c+p\theta)-2p(1+\eta)\theta\rho}{pZ\theta(2\alpha+\rho+\eta\rho)} = \frac{2(1+\eta)(c(2+\eta)+p(3+\eta)\theta)\rho}{pZ\theta(2\alpha+\rho+\eta\rho)} \geq 0$ for all feasible parameter values but $\frac{4\alpha(2+\eta)(c+p\theta)-2p(1+\eta)\theta\rho}{pZ\theta(2\alpha+\rho+\eta\rho)} - \frac{2}{Z}\left(1+\frac{c(4+2\eta)}{p\theta(3+\eta)}\right) = \frac{4(1+\eta)\left(c(2+\eta)+p\theta(3+\eta)\right)}{pZ(3+\eta)\theta(2\alpha+\rho+\eta\rho)}(\alpha-\rho)$, which depends on whether $\alpha \geq \rho$. Thus, $m = \frac{4\alpha(2+\eta)(c+p\theta)-2p(1+\eta)\theta\rho}{pZ\theta(2\alpha+\rho+\eta\rho)}$ is always less than the upper bound of the region but may or may not be greater than the lower bound. As a consequence, if $\alpha \geq \rho$ then $m^* = \frac{4\alpha(2+\eta)(c+p\theta)-2p(1+\eta)\theta\rho}{pZ\theta(2\alpha+\rho+\eta\rho)}$ and $\widehat{M}^* = 1$ or else, $m^* = \frac{2}{Z}\left(1+\frac{c(4+2\eta)}{p\theta(3+\eta)}\right)$ and $\widehat{M}^* = 1 - |\rho - \alpha|$ because when $\alpha < \rho$, $1 - |\rho - \alpha| = 1 - \rho + \alpha > 1 - \rho$.

Region 5. When $\gamma_A^* = 1$, $\gamma_B^* = 0$, and $m \geq \frac{2}{Z}\left(1+\frac{c}{p\theta}\right)(2+\eta)$, the platform's matching efficiency is $\widehat{M}^* = 1 - |\rho| = 1 - \rho$, which is not a function of m. Thus, the surge multiplier that maximizes the platform's matching efficiency is any $m \in \left[\frac{2}{Z}\left(1+\frac{c}{p\theta}\right)(2+\eta), m_{max}\right]$.

Matching efficiency for Models 5–6

The optimal surge multiplier and maximum matching efficiency for Models 5 and 6 are similar except for λ replacing $\frac{Z}{2}$ for Model 6 and depend on the regions for m described in Theorem 2. The matching efficiency function is from (A4). From Theorem 2 and Table 3-A-11, which describes the optimal γ_A^* and γ_B^* for Model 5, five regions must be considered for m.

Region 1. When $\gamma_A^* = 0$, $\gamma_B^* = 1$, and $0 \leq m \leq \frac{2}{Z}\left(\frac{\rho}{1-\eta\rho+\eta} - \frac{c}{p\theta}\right)$, the platform's matching efficiency is $\widehat{M}^* = 1 - |-1+\rho| = \rho$ as $0 < \rho < 1$. Thus, the surge multiplier that maximizes the platform's matching efficiency is any $m \in \left[0, \frac{2}{Z}\left(\frac{\rho}{1-\eta\rho+\eta} - \frac{c}{p\theta}\right)\right]$.

Region 2.1. When $\gamma_A^* = 0$, $\gamma_B^* = 1$, and $\frac{2}{Z}\left(\frac{\rho}{1-\eta\rho+\eta} - \frac{c}{p\theta}\right) \leq m \leq \frac{\frac{1+\eta}{1-\rho}(p\theta\rho - c) + \eta(p\theta - c)\log[1-\rho] - \frac{\rho}{1-\rho}(c\eta + p\theta)\log[\rho]}{\frac{1}{2}pZ\theta\left((1+\eta) - \log[1-\rho] + \frac{\rho}{1-\rho}\eta\log[\rho]\right)}$, the platform's matching efficiency is $\widehat{M}^* = 1 - |-1+\rho| = \rho$ as $0 < \rho < 1$. Thus, the surge multiplier that maximizes the platform's matching efficiency is any $m \geq 0$ where $m \in \left[\frac{2}{Z}\left(\frac{\rho}{1-\eta\rho+\eta} - \frac{c}{p\theta}\right), \frac{\frac{1+\eta}{1-\rho}(p\theta\rho - c) + \eta(p\theta - c)\log[1-\rho] - \frac{\rho}{1-\rho}(c\eta + p\theta)\log[\rho]}{\frac{1}{2}pZ\theta\left((1+\eta) - \log[1-\rho] + \frac{\rho}{1-\rho}\eta\log[\rho]\right)}\right]$.

Region 2.2. When $\gamma_A^* = 0$, $\gamma_B^* = 1 - h(m)$[7] $W\left(\frac{1}{h(m)}e^{j(m)}\right)$[8], and $\frac{2}{Z}\left(\frac{\rho}{1-\eta\rho+\eta} - \frac{c}{p\theta}\right) \leq m \leq \frac{\frac{1+\eta}{1-\rho}(p\theta\rho - c) + \eta(p\theta - c)\log[1-\rho] - \frac{\rho}{1-\rho}(c\eta + p\theta)\log[\rho]}{\frac{1}{2}pZ\theta\left((1+\eta) - \log[1-\rho] + \frac{\rho}{1-\rho}\eta\log[\rho]\right)}$, assuming $\rho - \gamma_B \geq 0$, the platform's matching efficiency is $\widehat{M}^* = 1 - \left|1 - \rho - (1-\alpha)h(m)W\left(\frac{1}{h(m)}e^{j(m)}\right)\right|$. First assume that $\left|1 - \rho - (1-\alpha)h(m)W\left(\frac{1}{h(m)}e^{j(m)}\right)\right| \neq 0$. The first-order derivative is $\frac{\partial \widehat{M}^*}{\partial m} = \pm \frac{(1-\alpha)W\left(\frac{1}{h\,(m)}e^{j\,(m)}\right)}{1+W\left(\frac{1}{h\,(m)}e^{j\,(m)}\right)}\left(W\left(\frac{1}{h\,(m)}e^{j\,(m)}\right)h'(m) + h\,(m)j'(m)\right)$. We must evaluate all points at which the first-order derivative is either zero or undefined. Four such cases exist:

i. Case 1: $W\left(\frac{1}{h\,(m)}e^{j\,(m)}\right) = 0$. There is no m that satisfies this condition.

ii. Case 2: $W\left(\frac{1}{h\,(m)}e^{j\,(m)}\right) = -1$. No closed-form expression exists but there is an analytic solution where m^{++} solves the following equation: $j(m^{++}) - \log[-h(m^{++})] = -1$. Analyzing the matching efficiency, we obtain $\widehat{M}^* = 1 - |1 - \rho + (1-\alpha)h(m^{++})|$. The validity of this solution depends on whether $h(m) < 0$, which does not always hold.

---

[7] $h(m) = \frac{-(1-\rho)\left(mp\frac{Z}{2}\theta + \eta(p\theta - c)\right)}{(\eta+1)(p\theta - c)}$,

[8] $j(m) = \frac{-(1-\rho)\log[1-\rho]\left(mp\frac{Z}{2}\theta + \eta(p\theta-c)\right) - \rho(p\theta - c) + \rho\log[\rho]\left(p\theta + \eta\left(mp\frac{Z}{2}\theta + c\right)\right) + \left(c + \eta\left(mp\frac{Z}{2}\theta + c\right)\right)(1-\rho) - \rho\left(mp\frac{Z}{2}\theta + \eta(p\theta - c)\right) + mp\frac{Z}{2}\theta + (\eta+1)(p\theta - c)}{-(1-\rho)\left(mp\frac{Z}{2}\theta + \eta(p\theta - c)\right)}$

iii. Case 3: $W\left(\frac{1}{h\,(m)}e^{j\,(m)}\right)h'(m)+h\,(m)j'(m)=0$. The left-hand-side of this equation is independent of m, which implies there is no root. However, this does indicate that we must evaluate the endpoints of the interval $\frac{2}{Z}\left(\frac{\rho}{1-\eta\rho+\eta}-\frac{c}{p\theta}\right)$ and $\frac{\frac{1+\eta}{1-\rho}(p\theta\rho-c)+\eta(p\theta-c)\log[1-\rho]-\frac{\rho}{1-\rho}(c\eta+p\theta)\log[\rho]}{\frac{1}{2}pZ\theta\left((1+\eta)-\log[1-\rho]+\frac{\rho}{1-\rho}\eta\log[\rho]\right)}$ as there may exist parameter values where the first-order derivative is strictly positive/negative.

iv. Case 4: There exist certain cases where $m=0$. When this occurs, we define $M_0=1-\left|1-\rho-(1-\alpha)h(0)W\left(\frac{1}{h(0)}e^{j(0)}\right)\right|$.

Finally, we must also evaluate the critical point implied by $1-\rho-(1-\alpha)h(m)W\left(\frac{1}{h(m)}e^{j(m)}\right)=0$ or $W\left(\frac{1}{h(m)}e^{j(m)}\right)=\frac{1-\rho}{(1-\alpha)h(m)}$. Re-arranging and simplifying, we obtain $m^{+}=\frac{\frac{1+\eta}{1-\alpha}(p\alpha\theta-c)+\eta(p\theta-c)\log[1-\alpha]-\frac{\rho}{1-\rho}(c\eta+p\theta)\log[\rho]}{\frac{1}{2}pZ\theta\left((1+\eta)-\log[1-\alpha]+\frac{\rho}{1-\rho}\eta\log[\rho]\right)}$ and $\widehat{M}^{*}=1$.

To characterize the extreme points, first notice that $m^{+}\geq\frac{2}{Z}\left(\frac{\rho}{1-\eta\rho+\eta}-\frac{c}{p\theta}\right)$ for all feasible α. Thus, if $\rho\geq\alpha$ and $\frac{\frac{1+\eta}{1-\rho}(p\theta\rho-c)+\eta(p\theta-c)\log[1-\rho]-\frac{\rho}{1-\rho}(c\eta+p\theta)\log[\rho]}{\frac{1}{2}pZ\theta\left((1+\eta)-\log[1-\rho]+\frac{\rho}{1-\rho}\eta\log[\rho]\right)}\geq 0>m^{+}$, then $m^{*}=0$ and $\widehat{M}^{*}=M_0$ because $M_0<\widehat{M}^{*}=1$ occurs at a negative value and is decreasing (by definition) as we move away from that point. Otherwise, if $\rho\geq\alpha$ and $\frac{\frac{1+\eta}{1-\rho}(p\theta\rho-c)+\eta(p\theta-c)\log[1-\rho]-\frac{\rho}{1-\rho}(c\eta+p\theta)\log[\rho]}{\frac{1}{2}pZ\theta\left((1+\eta)-\log[1-\rho]+\frac{\rho}{1-\rho}\eta\log[\rho]\right)}>m^{+}\geq 0$, then $m^{*}=m^{+}$ and $\widehat{M}^{*}=1$ as this is the maximum matching efficiency that can be obtained. Finally, since $\frac{\frac{1+\eta}{1-\rho}(p\theta\rho-c)+\eta(p\theta-c)\log[1-\rho]-\frac{\rho}{1-\rho}(c\eta+p\theta)\log[\rho]}{\frac{1}{2}pZ\theta\left((1+\eta)-\log[1-\rho]+\frac{\rho}{1-\rho}\eta\log[\rho]\right)}\rightarrow m^{+}$ in the limit as $\alpha\rightarrow\rho$, then $m^{*}=$

$\frac{\frac{1+\eta}{1-\rho}(p\theta\rho-c)+\eta(p\theta-c)\log[1-\rho]-\frac{\rho}{1-\rho}(c\eta+p\theta)\log[\rho]}{\frac{1}{2}pZ\theta\left((1+\eta)-\log[1-\rho]+\frac{\rho}{1-\rho}\eta\log[\rho]\right)}$ when $\rho \leq \alpha$ as we have that $m^{+} >$ $\frac{\frac{1+\eta}{1-\rho}(p\theta\rho-c)+\eta(p\theta-c)\log[1-\rho]-\frac{\rho}{1-\rho}(c\eta+p\theta)\log[\rho]}{\frac{1}{2}pZ\theta\left((1+\eta)-\log[1-\rho]+\frac{\rho}{1-\rho}\eta\log[\rho]\right)} \geq \frac{2}{Z}\left(\frac{\rho}{1-\eta\rho+\eta}-\frac{c}{p\theta}\right)$.

Region 3. When $\gamma_A^* = 0$ and $\gamma_B^* = 0$ and $\frac{\frac{1+\eta}{1-\rho}(p\theta\rho-c)+\eta(p\theta-c)\log[1-\rho]-\frac{\rho}{1-\rho}(c\eta+p\theta)\log[\rho]}{\frac{1}{2}pZ\theta\left((1+\eta)-\log[1-\rho]+\frac{\rho}{1-\rho}\eta\log[\rho]\right)} \leq m \leq$ $\frac{\frac{1+\eta}{1-\rho}(c+p\theta\rho)+\eta(c+p\theta)\log[1-\rho]+\frac{\rho}{1-\rho}(c\eta-p\theta)\log[\rho]}{\frac{1}{2}pZ\theta\left((1+\eta)-\log[1-\rho]+\eta\frac{\rho}{1-\rho}\log[\rho]\right)}$, the platform's matching efficiency is $\widehat{M}^* = 1 + |\rho-\alpha|$. Thus, the surge multiplier that maximizes the platform's matching efficiency is any $m \in \left[\frac{\frac{1+\eta}{1-\rho}(p\theta\rho-c)+\eta(p\theta-c)\log[1-\rho]-\frac{\rho}{1-\rho}(c\eta+p\theta)\log[\rho]}{\frac{1}{2}pZ\theta\left((1+\eta)-\log[1-\rho]+\frac{\rho}{1-\rho}\eta\log[\rho]\right)}, \frac{\frac{1+\eta}{1-\rho}(c+p\theta\rho)+\eta(c+p\theta)\log[1-\rho]+\frac{\rho}{1-\rho}(c\eta-p\theta)\log[\rho]}{\frac{1}{2}pZ\theta\left((1+\eta)-\log[1-\rho]+\eta\frac{\rho}{1-\rho}\log[\rho]\right)}\right]$.

Region 4.1. When $\gamma_A^* = 1 - f(m)$[9] $W\left(\frac{1}{f(m)}e^{g(m)}\right)$[10], $\gamma_B^* = 0$, and $\frac{\frac{1+\eta}{1-\rho}(c+p\theta\rho)+\eta(c+p\theta)\log[1-\rho]+\frac{\rho}{1-\rho}(c\eta-p\theta)\log[\rho]}{\frac{1}{2}pZ\theta\left((1+\eta)-\log[1-\rho]+\eta\frac{\rho}{1-\rho}\log[\rho]\right)} \leq m \leq \frac{2}{Z}\left(1+\frac{c}{p\theta}\right)\left(\frac{1+\eta\rho}{1-\rho}\right)$, assuming $\rho \leq 1-\gamma_A$, the platform's matching efficiency is $\widehat{M}^* = 1 - \left|\rho - \alpha f(m) W\left(\frac{1}{f(m)}e^{g(m)}\right)\right|$. First assume that $\left|\rho - \alpha f(m) W\left(\frac{1}{f(m)}e^{g(m)}\right)\right| \neq 0$. The first-order derivative is $\frac{\partial \widehat{M}^*}{\partial m} =$ $\pm\frac{\alpha W\left(\frac{1}{f(m)}e^{g(m)}\right)}{1+W\left(\frac{1}{f(m)}e^{g(m)}\right)}\left(W\left(\frac{1}{f(m)}e^{g(m)}\right)f'(m)+f(m)g'(m)\right)\right)$. Note that we must evaluate all points at which the first-order derivative is either 0 or undefined. Thus, three cases exist:

i. Case 1: $W\left(\frac{1}{f(m)}e^{g(m)}\right) = 0$. This implies that $m = \frac{2c}{pZ\theta}$ and $\widehat{M}^* = 1 - |\rho|$.
ii. Case 2: $W\left(\frac{1}{f(m)}e^{g(m)}\right) = -1$. No closed-form expression exists but there is an analytic solution where m^{++} solves the following equation: $g(m^{++}) - \log[-f(m^{++})] = -1$.

[9] $f(m) = \frac{-\rho\left(p\theta+\eta\left(mp\frac{Z}{2}\theta-c\right)\right)}{(1+\eta)\left(mp\frac{Z}{2}\theta-c\right)}$

[10] $g(m) = \frac{p\theta\rho-\rho\log[\rho]\left(p\theta+\eta\left(mp\frac{Z}{2}\theta-c\right)\right)+\rho\eta\left(mp\frac{Z}{2}\theta-c\right)+(1-\rho)\log[1-\rho]\left(mp\frac{Z}{2}\theta+\eta(p\theta+c)\right)+\rho\left(mp\frac{Z}{2}\theta+\eta(p\theta+c)\right)}{-\rho\left(p\theta+\eta\left(mp\frac{Z}{2}\theta-c\right)\right)}$

Analyzing the matching efficiency, we obtain $\widehat{M}^* = 1 - |\rho + \alpha f(m^{++})|$, which is a valid solution since $f(m) < 0$ owing to Assumption 2.

iii. Case 3: $W\left(\frac{1}{f\,(m)} e^{g\,(m)}\right) f'(m) + f\,(m) g'(m) = 0$. The left-hand-side of this equation is independent of m, which implies that there is no root. However, this does indicate that we must evaluate the endpoints of the interval $\frac{\frac{1+\eta}{1-\rho}(c+p\theta\rho)+\eta(c+p\theta)\log[1-\rho]+\frac{\rho}{1-\rho}(c\eta-p\theta)\log[\rho]}{\frac{1}{2}pZ\theta\left((1+\eta)-\log[1-\rho]+\eta\frac{\rho}{1-\rho}\log[\rho]\right)}$ and $\frac{2}{Z}\left(1+\frac{c}{p\theta}\right)\left(\frac{1+\eta\rho}{1-\rho}\right)$ as there may exist parameter values where the first-order derivative is strictly positive/negative.

Finally, we must also evaluate the critical point implied by $\rho - \alpha f(m) W\left(\frac{1}{f(m)} e^{g(m)}\right) = 0$ or $W\left(\frac{1}{f(m)} e^{g(m)}\right) = \frac{\rho}{\alpha f(m)}$. Re-arranging and simplifying, we obtain $m^+ = \frac{\frac{1+\eta}{1-\alpha}(c+p\alpha\theta)+\frac{\alpha}{1-\alpha}\eta(c+p\theta)\left(\frac{1-\rho}{\rho}\right)\log[1-\rho]+\frac{\alpha}{1-\alpha}(c\eta-p\theta)\log[\alpha]}{\frac{1}{2}pZ\theta\left((1+\eta)+\frac{\alpha}{1-\alpha}\eta\log[\alpha]-\frac{\alpha}{1-\alpha}\left(\frac{1-\rho}{\rho}\right)\log[1-\rho]\right)}$ and in this case, $\widehat{M}^* = 1$.

To characterize the extreme points, notice that (i) $\frac{2}{Z}\left(1+\frac{c}{p\theta}\right)\left(\frac{1+\eta\rho}{1-\rho}\right) \geq m^+$ for all feasible α; and (ii) $m^+ \geq \frac{\frac{1+\eta}{1-\rho}(c+p\theta\rho)+\eta(c+p\theta)\log[1-\rho]+\frac{\rho}{1-\rho}(c\eta-p\theta)\log[\rho]}{\frac{1}{2}pZ\theta\left((1+\eta)-\log[1-\rho]+\eta\frac{\rho}{1-\rho}\log[\rho]\right)}$ for $\rho \leq \alpha$, with equality achieved in the limit as $\alpha \to \rho$. Thus, $m^* = m^+$ and $\widehat{M}^* = 1$ when $\rho \leq \alpha$ since $\frac{2}{Z}\left(1+\frac{c}{p\theta}\right)\left(\frac{1+\eta\rho}{1-\rho}\right) \geq m^+ \geq \frac{\frac{1+\eta}{1-\rho}(c+p\theta\rho)+\eta(c+p\theta)\log[1-\rho]+\frac{\rho}{1-\rho}(c\eta-p\theta)\log[\rho]}{\frac{1}{2}pZ\theta\left((1+\eta)-\log[1-\rho]+\eta\frac{\rho}{1-\rho}\log[\rho]\right)}$. However $m^* = \frac{\frac{1+\eta}{1-\rho}(c+p\theta\rho)+\eta(c+p\theta)\log[1-\rho]+\frac{\rho}{1-\rho}(c\eta-p\theta)\log[\rho]}{\frac{1}{2}pZ\theta\left((1+\eta)-\log[1-\rho]+\eta\frac{\rho}{1-\rho}\log[\rho]\right)}$ when $\rho \geq \alpha$ since $\frac{2}{Z}\left(1+\frac{c}{p\theta}\right)\left(\frac{1+\eta\rho}{1-\rho}\right) \geq \frac{\frac{1+\eta}{1-\rho}(c+p\theta\rho)+\eta(c+p\theta)\log[1-\rho]+\frac{\rho}{1-\rho}(c\eta-p\theta)\log[\rho]}{\frac{1}{2}pZ\theta\left((1+\eta)-\log[1-\rho]+\eta\frac{\rho}{1-\rho}\log[\rho]\right)} \geq m^+$ holds in this case.

Region 4.2. When $\gamma_A^* = 1, \gamma_B^* = 0$, and $\frac{\frac{1+\eta}{1-\rho}(c+p\theta\rho)+\eta(c+p\theta)\log[1-\rho]+\frac{\rho}{1-\rho}(c\eta-p\theta)\log[\rho]}{\frac{1}{2}pZ\theta\left((1+\eta)-\log[1-\rho]+\eta\frac{\rho}{1-\rho}\log[\rho]\right)} \leq m \leq$ $\frac{2}{Z}\left(1+\frac{c}{p\theta}\right)\left(\frac{1+\eta\rho}{1-\rho}\right)$, the platform's matching efficiency is $\widehat{M}^* = 1 - |\rho| = 1 - \rho$. Thus, the surge multiplier that maximizes matching efficiency is any $m \in$ $\left[\frac{\frac{1+\eta}{1-\rho}(c+p\theta\rho)+\eta(c+p\theta)\log[1-\rho]+\frac{\rho}{1-\rho}(c\eta-p\theta)\log[\rho]}{\frac{1}{2}pZ\theta\left((1+\eta)-\log[1-\rho]+\eta\frac{\rho}{1-\rho}\log[\rho]\right)} \leq m \leq \frac{2}{Z}\left(1+\frac{c}{p\theta}\right)\left(\frac{1+\eta\rho}{1-\rho}\right)\right]$.

Region 5. When $\gamma_A^* = 1, \gamma_B^* = 0$, and $m \geq \frac{2}{Z}\left(1+\frac{c}{p\theta}\right)\left(\frac{1+\eta\rho}{1-\rho}\right)$, the platform's matching efficiency is $\widehat{M}^* = 1 - |\rho| = 1 - \rho$. Thus, the surge multiplier that maximizes matching efficiency is any $m \in \left[\frac{2}{Z}\left(1+\frac{c}{p\theta}\right)\left(\frac{1+\eta\rho}{1-\rho}\right), m_{max}\right]$.

Matching efficiency for Models 7–8

The optimal surge multiplier and maximum matching efficiency for Models 7 and 8 are similar except for λ replacing $\frac{Z}{2}$ in Model 8 and depend on the regions for m described in Theorem 3. The matching efficiency function is from (A4). From Theorem 3 and Table 3-A-12 and 3-A-13, which describes the optimal γ_A^* and γ_B^* for Model 7, four regions exist for m when $\alpha \geq \max\left\{0, \frac{\rho-\gamma_B^*}{1-\gamma_A^*-\gamma_B^*}\right\}$ and also four regions when $\alpha \leq \max\left\{0, \frac{\rho-\gamma_B^*}{1-\gamma_A^*-\gamma_B^*}\right\}$ as follows.

1- When $\alpha \geq \max\left\{0, \frac{\rho-\gamma_B^*}{1-\gamma_A^*-\gamma_B^*}\right\}$:

Region 1. When $\gamma_A^* = 0, \gamma_B^* = 1$, and $0 \leq m \leq \frac{2}{Z}\left(\frac{\rho}{1-\eta\rho+\eta} - \frac{c}{p\theta}\right)$, the platform's matching efficiency is either $\widehat{M}^* = 1 - |-1+\rho|$ or $\widehat{M}^* = \rho$ which yield identical solutions. For the upper bound of the interval to be greater than the lower bound, it requires $\frac{c}{p\theta} \leq \frac{\rho}{1-\eta\rho+\eta}$. Under this condition, the surge multiplier that maximizes matching efficiency is any $m \in \left[0,\ \frac{2}{Z}\left(\frac{\rho}{1-\eta\rho+\eta} - \frac{c}{p\theta}\right)\right]$.

Region 2. When $\gamma_A^* = 0, \gamma_B^* = \frac{\rho p\theta + \left(mp\frac{Z}{2}\theta + c\right)(\eta(\rho-\alpha)-\alpha)}{\left(mp\frac{Z}{2}\theta + c\right)(1-\alpha)\,(1+\eta)}$, and $\frac{2}{Z}\left(\frac{\rho}{1-\eta\rho+\eta} - \frac{c}{p\theta}\right) \le m \le \frac{2}{Z}\left(\frac{\rho}{\alpha+\eta(\alpha-\rho)} - \frac{c}{p\theta}\right)$, the platform's matching efficiency is $\widehat{M}^* = 1 - \left|\frac{(2c+p(-2+mZ)\theta)\rho}{(1+\eta)(2c+mpZ\theta)}\right|$. We first note that $\frac{\rho}{1-\eta\rho+\eta} = \frac{\rho}{1+\eta(1-\rho)} \ge 0$ for any choice of ρ and η. Thus, for the upper bound of the interval to be greater than the lower bound, it must be that $\frac{2(1-\alpha)(1+\eta)\rho}{Z(1+\eta(1-\rho))(\alpha+\eta(\alpha-\rho))} \ge 0$ which holds if $\alpha \ge \frac{\eta}{1+\eta}\rho$ where $\frac{\eta}{1+\eta} \le 1$; we utilize this property in the rest of the proof of Region 2. Assuming $\frac{(2c+p(-2+mZ)\theta)\rho}{(1+\eta)(2c+mpZ\theta)} \ne 0$, the first-order derivative is either $\frac{\partial \widehat{M}^*}{\partial m} = \frac{-2p^2Z\theta^2\rho}{(1+\eta)(2c+mp\theta Z)^2}$ or $\frac{\partial \widehat{M}^*}{\partial m} = \frac{2p^2Z\theta^2\rho}{(1+\eta)(2c+mp\theta Z)^2}$, and the second-order derivative is, respectively, $\frac{\partial^2 \widehat{M}^*}{\partial m^2} = \frac{4p^3Z^2\theta^3\rho}{(1+\eta)(2c+mp\theta Z)^3}$ or $\frac{\partial^2 \widehat{M}^*}{\partial m^2} = \frac{-4p^3Z^2\theta^3\rho}{(1+\eta)(2c+mp\theta Z)^3}$. Depending on the magnitude of $\frac{c}{p\theta}$, we have three cases:

i. Case 1: $\frac{\rho}{1-\eta\rho+\eta} \le \frac{\rho}{\alpha+\eta(\alpha-\rho)} \le \frac{c}{p\theta}$

   The lower and upper bounds of the surge multiplier range are both negative. Thus, no surge multiplier exists in this region that maximizes matching efficiency.

ii. Case 2: $\frac{\rho}{1-\eta\rho+\eta} \le \frac{c}{p\theta} \le \frac{\rho}{\alpha+\eta(\alpha-\rho)}$

   The upper bound is positive and the lower bound is negative. Depending on the sign of $\left|\frac{(2c+p(-2+mZ)\theta)\rho}{(1+\eta)(2c+mpZ\theta)}\right|$, the matching efficiency function has regions where it is strictly decreasing and convex or increasing and concave. However, in this case, the lower bound of the surge multiplier range is negative, which implies that the smallest feasible surge multiplier occurs at $m = 0$; this gives $\widehat{M}^* = 1 - \left|\frac{(c-p\theta)\rho}{c(1+\eta)}\right|$, which we define as M_0. Alternatively, at the upper bound of the interval, $m = \frac{2}{Z}\left(\frac{\rho}{\alpha+\eta(\alpha-\rho)} - \frac{c}{p\theta}\right) > 0$, which yields $\widehat{M}^* = 1 - |\rho - \alpha|$.

iii. Case 3: $\frac{c}{p\theta} \le \frac{\rho}{1-\eta\rho+\eta} \le \frac{\rho}{\alpha+\eta(\alpha-\rho)}$

The lower and upper bounds are both positive. Depending on the sign of $\left|\frac{(2c+p(-2+mZ)\theta)\rho}{(1+\eta)(2c+mpZ\theta)}\right|$, the matching efficiency function has regions that are strictly decreasing and convex or increasing and concave, which means that the optimal surge multiplier is either the lower or upper bound of its interval. At the lower bound, $m = \frac{2}{Z}\left(\frac{\rho}{1-\eta\rho+\eta} - \frac{c}{p\theta}\right) > 0$ and the matching efficiency is $\widehat{M}^* = 1 - |-1+\rho| = \rho$. At the upper bound, $m = \frac{2}{Z}\left(\frac{\rho}{\alpha+\eta(\alpha-\rho)} - \frac{c}{p\theta}\right) > 0$ and the matching efficiency is $\widehat{M}^* = 1 - |\rho - \alpha|$. When $\alpha \geq \rho$, then $1 - |\rho - \alpha| = 1 - \alpha + \rho \geq \rho$ and the upper bound yields a higher matching efficiency.

Note that a critical point exists when $\left|\frac{(2c+p(-2+mZ)\theta)\rho}{(1+\eta)(2c+mpZ\theta)}\right| = 0$ since it marks the boundary between the two continuous regions. Solving for the optimal surge multiplier gives $m^+ = \frac{2(p\theta-c)}{pZ\theta}$ and $\widehat{M}^* = 1$. Notice that $m^+ - \frac{2}{Z}\left(\frac{\rho}{1-\eta\rho+\eta} - \frac{c}{p\theta}\right) \geq 0$ for all feasible parameter values since we assumed $\frac{1}{\alpha+\eta(\alpha-\rho)} \geq 0$. However, $\frac{2}{Z}\left(\frac{\rho}{\alpha+\eta(\alpha-\rho)} - \frac{c}{p\theta}\right) - m^+$ is positive only when $\frac{\rho-\alpha}{\alpha+\eta(\alpha-\rho)} \geq 0$. Thus, if $\alpha \geq \rho$, then $m^+ > \frac{2}{Z}\left(\frac{\rho}{\alpha+\eta(\alpha-\rho)} - \frac{c}{p\theta}\right)$ and m^+ is an invalid surge multiplier. If $\rho \geq \alpha$, then $\frac{2}{Z}\left(\frac{\rho}{\alpha+\eta(\alpha-\rho)} - \frac{c}{p\theta}\right) - m^+ \geq 0$ and m^+ is the optimal surge multiplier. Note that m^+ is a critical point and the matching efficiency function is continuous for all $m \neq m^+$. From the previous analysis of the first- and second-order derivatives, the matching efficiency is increasing and concave for $m < m^+$ and decreasing and convex for $m > m^+$.

Putting the cases together, if $\alpha \geq \rho$, then $m^+ \geq \frac{2}{Z}\left(\frac{\rho}{\alpha+\eta(\alpha-\rho)} - \frac{c}{p\theta}\right) \geq 0 \geq \frac{2}{Z}\left(\frac{\rho}{1-\eta\rho+\eta} - \frac{c}{p\theta}\right)$ or $m^+ \geq \frac{2}{Z}\left(\frac{\rho}{\alpha+\eta(\alpha-\rho)} - \frac{c}{p\theta}\right) \geq \frac{2}{Z}\left(\frac{\rho}{1-\eta\rho+\eta} - \frac{c}{p\theta}\right) \geq 0$. It then follows from Cases 2 and 3 that $\widehat{M}^* = 1 - (\alpha - \rho)$ and $m^* = \frac{2}{Z}\left(\frac{\rho}{\alpha+\eta(\alpha-\rho)} - \frac{c}{p\theta}\right)$, since the matching efficiency function is increasing and concave for $m < m^+$. If $\rho \geq \alpha$, then $0 \leq \frac{2}{Z}\left(\frac{\rho}{1-\eta\rho+\eta} - \frac{c}{p\theta}\right) \leq m^+ \leq \frac{2}{Z}\left(\frac{\rho}{\alpha+\eta(\alpha-\rho)} - \frac{c}{p\theta}\right)$ or $\frac{2}{Z}\left(\frac{\rho}{1-\eta\rho+\eta} - \frac{c}{p\theta}\right) \leq 0 \leq m^+ \leq \frac{2}{Z}\left(\frac{\rho}{\alpha+\eta(\alpha-\rho)} - \frac{c}{p\theta}\right)$ and it follows that $m^* = m^+$ because $\widehat{M}^* = 1$ (the maximum efficiency value). If $\rho \geq \alpha$ but $\frac{2}{Z}\left(\frac{\rho}{1-\eta\rho+\eta} - \frac{c}{p\theta}\right) \leq$

$m^+ \leq 0 \leq \frac{2}{Z}\left(\frac{\rho}{\alpha+\eta(\alpha-\rho)} - \frac{c}{p\theta}\right)$, then $m^* = 0$ and $\widehat{M}^* = M_0$ as the matching efficiency function is decreasing and convex for $m > m^+$.

Region 3. When $\gamma_A^* = 0, \gamma_B^* = 0$, and $\frac{2}{Z}\left(\frac{\rho}{\alpha+\eta(\alpha-\rho)} - \frac{c}{p\theta}\right) \leq m \leq \frac{2}{Z}\left(\frac{\rho}{\alpha+\eta(\alpha-\rho)} + \frac{c}{p\theta}\right)$, the platform's matching efficiency is $\widehat{M}^* = 1 - |\rho - \alpha|$. Thus, the surge multiplier that maximizes matching efficiency is any $m \in \left[\frac{2}{Z}\left(\frac{\rho}{\alpha+\eta(\alpha-\rho)} - \frac{c}{p\theta}\right), \frac{2}{Z}\left(\frac{\rho}{\alpha+\eta(\alpha-\rho)} + \frac{c}{p\theta}\right)\right]$.

Region 4. We have that $\gamma_A^* = 1 - \frac{\rho\left(p\theta+\eta\left(mp\frac{Z}{2}\theta-c\right)\right)}{\alpha(1+\eta)\left(mp\frac{Z}{2}\theta-c\right)}$ and $\gamma_B^* = 0$ within the range $\frac{2}{Z}\left(\frac{\rho}{\alpha+\eta(\alpha-\rho)} + \frac{c}{p\theta}\right) \leq m \leq \frac{2}{Z}\left(1 + \frac{c}{p\theta}\right)$, and the matching efficiency is given by $\widehat{M}^* = 1 - \left|\frac{(2c+p(2-mZ)\theta)\rho}{(1+\eta)(2c-mpZ\theta)}\right|$. Assuming $\frac{(2c+p(2-mZ)\theta)\rho}{(1+\eta)(2c-mpZ\theta)} \neq 0$, the first-order derivative is either $\frac{\partial \widehat{M}^*}{\partial m} = \frac{-2p^2Z\theta^2\rho}{(1+\eta)(2c-mp\theta Z)^2}$ or $\frac{\partial \widehat{M}^*}{\partial m} = \frac{2p^2Z\theta^2\rho}{(1+\eta)(2c-mp\theta Z)^2}$, and the second-order derivative is, respectively, $\frac{\partial^2 \widehat{M}^*}{\partial m^2} = \frac{4p^3Z^2\theta^3\rho}{(1+\eta)(mp\theta Z-2c)^3}$ or $\frac{\partial^2 \widehat{M}^*}{\partial m^2} = \frac{-4p^3Z^2\theta^3\rho}{(1+\eta)(mp\theta Z-2c)^3}$. This implies that the matching efficiency function has regions that are decreasing and convex or increasing and concave (by Assumption 2) and a valid surge multiplier is either the lower or upper bound of this region. Further, the critical point $\frac{(2c+p(2-mZ)\theta)\rho}{(1+\eta)(2c-mpZ\theta)} = 0$ is equal to the upper bound of the surge multiplier interval. Thus, $m^* = \frac{2}{Z}\left(1 + \frac{c}{p\theta}\right)$ with $\widehat{M}^* = 1$ since $1 - |\alpha - \rho|$ is the matching efficiency function at the lower bound of the surge interval. To ensure $\frac{2}{Z}\left(1 + \frac{c}{p\theta}\right) \geq \frac{2}{Z}\left(\frac{\rho}{\alpha+\eta(\alpha-\rho)} + \frac{c}{p\theta}\right)$, it follows that $\frac{2(1+\eta)(\alpha-\rho)}{Z(\alpha+\alpha\eta-\eta\rho)} \geq 0$ which requires $\alpha < \frac{\eta}{1+\eta}\rho$ (in which case both the numerator and denominator are negative) or $\alpha \geq \rho$ (in which case both the numerator and denominator are positive).

2- When $\alpha \leq \max\left\{0, \frac{\rho-\gamma_B^*}{1-\gamma_A^*-\gamma_B^*}\right\}$:

Region 1. When $\gamma_A^* = 0$, $\gamma_B^* = 1 - \frac{\left(mp\frac{Z}{2}\theta + \eta(p\theta - c)\right)(1-\rho)}{(p\theta - c)(1-\alpha)(1+\eta)}$, and $\frac{2}{Z}\left(1 - \frac{c}{p\theta}\right) \leq m \leq \frac{2}{Z}\left(1 - \frac{c}{p\theta}\right)\frac{1-\alpha+\eta(\rho-\alpha)}{1-\rho}$, the platform's matching efficiency is $\widehat{M}^* = 1 - \frac{1}{2}\left|\frac{(2c+p(-2+mZ)\theta)(-1+\rho)}{(1+\eta)(c-p\theta)}\right|$.

Assuming $\frac{(2c+p(-2+mZ)\theta)(-1+\rho)}{(1+\eta)(c-p\theta)} \neq 0$, the first-order derivative is either $\frac{\partial \widehat{M}^*}{\partial m} = \frac{-pZ\theta(1-\rho)}{2(1+\eta)(p\theta-c)}$ or $\frac{\partial \widehat{M}^*}{\partial m} = \frac{pZ\theta(1-\rho)}{2(1+\eta)(p\theta-c)}$. Thus, the matching efficiency function is linearly increasing or decreasing over the interval. If $m = \frac{2}{Z}\left(1 - \frac{c}{p\theta}\right)$, then $\widehat{M}^* = 1$ and if $m = \frac{2}{Z}\left(1 - \frac{c}{p\theta}\right)\frac{1-\alpha+\eta(\rho-\alpha)}{1-\rho}$, then $\widehat{M}^* = 1 - |\rho - \alpha|$. Note that the critical point is equal to the lower bound in this case. Since $1 - \frac{c}{p\theta} \geq 0$ from Assumption 3, two cases must be considered:

i. Case 1: $\frac{1-\alpha+\eta(\rho-\alpha)}{1-\rho} \geq 1$:

   The entire range yields nonnegative surge multiplier values. Given the analysis above, we have $m^* = \frac{2}{Z}\left(1 - \frac{c}{p\theta}\right)$ as $1 \geq 1 - |\rho - \alpha|$ and thus $\widehat{M}^* = 1$.

ii. Case 2: $\frac{1-\alpha+\eta(\rho-\alpha)}{1-\rho} \leq 1$:

   The lower surge multiplier is positive and exceeds the upper bound (which is negative if $\frac{1-\alpha+\eta(\rho-\alpha)}{1-\rho} \leq 0$). Consequently, this case is inadmissible.

Region 2. When $\gamma_A^* = 0$, $\gamma_B^* = 0$, and $\frac{2}{Z}\left(1 - \frac{c}{p\theta}\right)\left(\frac{1-\alpha+\eta(\rho-\alpha)}{1-\rho}\right) \leq m \leq \frac{2}{Z}\left(1 + \frac{c}{p\theta}\right)\left(\frac{1-\alpha+\eta(\rho-\alpha)}{1-\rho}\right)$, the platform's matching efficiency is $\widehat{M}^* = 1 - |\rho - \alpha|$, which is not a function of m. Thus, the surge multiplier that maximizes matching efficiency is any $m \geq 0$ where $m \in \left[\frac{2}{Z}\left(1 - \frac{c}{p\theta}\right)\left(\frac{1-\alpha+\eta(\rho-\alpha)}{1-\rho}\right), \frac{2}{Z}\left(1 + \frac{c}{p\theta}\right)\left(\frac{1-\alpha+\eta(\rho-\alpha)}{1-\rho}\right)\right]$. Note that for the upper bound of the interval to be greater than the lower bound, it requires $\frac{4c(1-\alpha-\alpha\eta+\eta\rho)}{pZ\theta(1-\rho)} \geq 0$, which implies $\alpha \leq \frac{1}{1+\eta} + \frac{\eta}{1+\eta}\rho$ where $\frac{1}{1+\eta} \leq 1$ and $\frac{\eta}{1+\eta} \leq 1$.

Region 3. We have that $\gamma_A^* = \frac{(1-\rho)mp\frac{Z}{2}\theta-(p\theta+c)(1-\alpha+\eta(\rho-\alpha))}{\alpha(p\theta+c)(1+\eta)}$ and $\gamma_B^* = 0$ within the range $\frac{2}{Z}\left(1+\frac{c}{p\theta}\right)\frac{1-\alpha+\eta(\rho-\alpha)}{1-\rho} \leq m \leq \frac{2}{Z}\left(1+\frac{c}{p\theta}\right)\left(\frac{1+\eta\rho}{1-\rho}\right)$ while the matching efficiency is given by $\widehat{M}^* = 1-\frac{1}{2}\left|\frac{(2c+p(2-mZ)\theta)(-1+\rho)}{(1+\eta)(c+p\theta)}\right|$. Assuming $\frac{(2c+p(2-mZ)\theta)(-1+\rho)}{(1+\eta)(c+p\theta)} \neq 0$, the first-order derivative is either $\frac{\partial\widehat{M}^*}{\partial m} = \frac{-(1-\rho)pZ\theta}{2(p\theta+c)(1+\eta)}$ or $\frac{\partial\widehat{M}^*}{\partial m} = \frac{(1-\rho)pZ\theta}{2(p\theta+c)(1+\eta)}$, which implies that the matching efficiency function is either linearly increasing or decreasing over the interval. Thus, a feasible surge multiplier must occur at the lower bound $m = \frac{2}{Z}\left(1+\frac{c}{p\theta}\right)\frac{1-\alpha+\eta(\rho-\alpha)}{1-\rho}$, which yields $\widehat{M}^* = 1-|\rho-\alpha|$, or at the upper bound $m = \frac{2}{Z}\left(1+\frac{c}{p\theta}\right)\left(\frac{1+\eta\rho}{1-\rho}\right)$, which gives $\widehat{M}^* = 1-|\rho| = 1-\rho$.

Note that $m^+ = \frac{2}{Z}\left(1+\frac{c}{p\theta}\right) \geq 0$ is a critical point that can be obtained by solving $\frac{(2c+p(2-mZ)\theta)(-1+\rho)}{(1+\eta)(c+p\theta)} = 0$ and gives $\widehat{M}^* = 1$. Further, $\frac{2}{Z}\left(1+\frac{c}{p\theta}\right)\left(\frac{1+\eta\rho}{1-\rho}\right) - m^+ \geq 0$ for all feasible parameter values and $m^+ - \frac{2}{Z}\left(1+\frac{c}{p\theta}\right)\frac{1-\alpha+\eta(\rho-\alpha)}{1-\rho} = \frac{2(1+\eta)(c+p\theta)(\alpha-\rho)}{pZ\theta(1-\rho)}$, which depends on whether $\alpha \geq \rho$, or not Thus, to obtain $\widehat{M}^* = 1$, $m^* = m^+$ and we must have $\alpha \geq \rho$. Otherwise, when $\alpha \leq \rho$, $m^* = \frac{2}{Z}\left(1+\frac{c}{p\theta}\right)\frac{1-\alpha+\eta(\rho-\alpha)}{1-\rho}$, which follows because $\widehat{M}^* = 1-|\rho-\alpha| = 1-\rho+\alpha > 1-\rho$. Finally, while $\frac{1-\alpha+\eta(\rho-\alpha)}{1-\rho} \leq 0$, it can only occur if $\alpha \geq \rho$ and $m^* = 0$, which yields $\widehat{M}^* = 1-\left(\frac{1-\rho}{1+\eta}\right) < 1$ (suboptimal).

Region 4. When $\gamma_A^* = 1$, $\gamma_B^* = 0$, and $m \geq \frac{2}{Z}\left(1+\frac{c}{p\theta}\right)\left(\frac{1+\eta\rho}{1-\rho}\right)$, the platform's matching efficiency is $\widehat{M}^* = 1-|\rho| = 1-\rho$, which is not a function of m. Thus, the surge multiplier that maximizes matching efficiency is any $m \in \left[\frac{2}{Z}\left(1+\frac{c}{p\theta}\right)\left(\frac{1+\eta\rho}{1-\rho}\right), m_{max}\right]$.

Proof of Theorem 5

Profit for Models 1–4

The optimal surge multiplier and maximum profit for Models 1–4 are similar except for λ replacing $\frac{Z}{2}$ in Models 2 and 4 while γ_A^* and γ_B^* are multiplied by $\frac{1+\alpha+\alpha\eta}{(3+\eta)(1-\alpha)}$ in Models 3 and 4. The optimal values depend on the regions for m described in Theorem 1. We first simplify the profit function as follows,

$$\widehat{\Pi}^* = p(1-\theta)\min\{S_A^1, D_A\} + mp\lambda(1-\theta)\min\{S_B^1, D_B\}$$

$$= \frac{1}{2}p(1-\theta)(S_A^1 + D_A - |S_A^1 - D_A|) + \frac{1}{2}mp\lambda(1-\theta)(S_B^1 + D_B - |S_B^1 - D_B|)$$

$$= \tfrac{1}{2}np(1-\theta)\Big(\big(\rho + \alpha(1-\gamma_A^*) + \gamma_B^*(1-\alpha)\big)(1-m\lambda) + 2m\lambda\Big) -$$
$$\tfrac{1}{2}np(1-\theta)(1+m\lambda)|\rho - \alpha(1-\gamma_A^*) - (1-\alpha)\gamma_B^*|.$$
(A5)

From Theorem 1 and Table 3-A-10, which describes the optimal γ_A^* and γ_B^* for Model 1, five regions for m exist.

Region 1. When $\gamma_A^* = 0$, $\gamma_B^* = 1$, and $m \le \frac{2}{Z}\left(\frac{1}{2+\eta} - \frac{c}{p\theta}\right)$, the platform's profit is $\widehat{\Pi}^* = \frac{1}{2}np(1-\theta)\big((\rho+1)(1-m\lambda) + 2m\lambda\big) - \frac{1}{2}np(1-\theta)(1+m\lambda)|\rho - 1| = np\rho(1-\theta)$ as $0 < \rho < 1$, which is not a function of m, and the surge multiplier that maximizes the platform's profit is any $m \ge 0$ where $m \in \left[0, \frac{2}{Z}\left(\frac{1}{2+\eta} - \frac{c}{p\theta}\right)\right]$. Note that for the upper bound of the interval to be greater than the lower bound, it must be that $\frac{c}{p\theta} \le \frac{1}{2+\eta}$.

Region 2. When $\gamma_A^* = 0$, $\gamma_B^* = \frac{p\theta(3+\eta)(2-mZ)-4c(2+\eta)}{p\theta(1+\eta)(mZ+2)}$, and $\frac{2}{Z}\left(\frac{1}{2+\eta} - \frac{c}{p\theta}\right) \le m \le \frac{2}{Z}\left(1 - \frac{c(4+2\eta)}{p\theta(3+\eta)}\right)$, the profit is $\widehat{\Pi}^* = \frac{1}{2}np(1-\theta)\left(2m\lambda - (-1+m\lambda)\left(\alpha + \rho - \frac{(1-\alpha)(4c(2+\eta)+p(-2+mZ)(3+\eta)\theta)}{p(2+mZ)(1+\eta)\theta}\right) - (1+m\lambda)\left|\alpha - \rho - \frac{(1-\alpha)(4c(2+\eta)+p(-2+mZ)(3+\eta)\theta)}{p(2+mZ)(1+\eta)\theta}\right|\right)$. Assuming $\alpha - \rho - \frac{(1-\alpha)(4c(2+\eta)+p(-2+mZ)(3+\eta)\theta)}{p(2+mZ)(1+\eta)\theta} \ne 0$, the first-order derivative is either $\frac{\partial\widehat{\Pi}^*}{\partial m} = \frac{n(-1+\theta)\left(4cZ(-1+\alpha)(2+\eta)+p\theta\left(-4Z(-1+\alpha)(3+\eta)-(2+mZ)^2(1+\eta)\lambda+(2+mZ)^2(1+\eta)\lambda\rho\right)\right)}{(2+mZ)^2(1+\eta)\theta}$ or $\frac{\partial\widehat{\Pi}^*}{\partial m} =$

$\frac{2n\lambda(-1+\alpha)(-1+\theta)\left(4c(2+\eta)+p\theta\left(-4+mZ(4+mZ)(2+\eta)\right)\right)}{(2+mZ)^2(1+\eta)\theta}$, and the analysis of the first-order conditions for optimality give either $\left\{m_1 \to \frac{2}{Z}\left(-1+\sqrt{\frac{Z(1-\alpha)\left(p\theta(3+\eta)-c(2+\eta)\right)}{p\theta\lambda(1-\rho)(1+\eta)}}\right), m_2 \to \frac{2}{Z}\left(-1-\sqrt{\frac{Z(1-\alpha)\left(p\theta(3+\eta)-c(2+\eta)\right)}{p\theta\lambda(1-\rho)(1+\eta)}}\right)\right\}$ or $\left\{m_3 \to \frac{2}{Z}\left(-1+\sqrt{\frac{\left(p\theta(3+\eta)-c(2+\eta)\right)}{p\theta(2+\eta)}}\right), m_4 \to \frac{2}{Z}\left(-1-\sqrt{\frac{\left(p\theta(3+\eta)-c(2+\eta)\right)}{p\theta(2+\eta)}}\right)\right\}$. Notice that m_2 and m_4 are negative and thus, infeasible. This implies that only m_1 and m_3 are viable. The second-order derivative is $\frac{\partial^2\hat{\Pi}^*}{\partial m^2} = \frac{8nZ^2(1-\alpha)(1-\theta)\left(p\theta(3+\eta)-c(2+\eta)\right)}{(1+\eta)\theta(mZ+2)^3}$ or $\frac{\partial^2\hat{\Pi}^*}{\partial m^2} = \frac{16nZ\lambda(1-\alpha)(1-\theta)\left(p\theta(3+\eta)-c(2+\eta)\right)}{(1+\eta)\theta(mZ+2)^3}$. Since $\frac{c}{p\theta} \leq 1$ from Assumption 3, depending on the magnitude of $\frac{c}{p\theta}$, we have three cases:

i. Case 1: $\frac{1}{2+\eta} \leq \frac{3+\eta}{2(2+\eta)} \leq \frac{c}{p\theta} \leq \frac{3+\eta}{2+\eta}$

   The lower and upper bounds of the surge multiplier range are both negative. Thus, no nonnegative surge multiplier exists in this region that maximizes profit.

ii. Case 2: $\frac{1}{2+\eta} \leq \frac{c}{p\theta} \leq \frac{3+\eta}{2(2+\eta)} \leq \frac{3+\eta}{2+\eta}$

   The upper bound is positive and the lower bound is negative. Although m_1 and m_3 can be positive, they are infeasible surge multipliers for two reasons. First, the second-order derivative at m_1 equals to $\frac{\partial^2\hat{\Pi}^*}{\partial m^2}(m \to m_1) = \frac{np^2Z(1+\eta)(1-\theta)\theta\lambda^2(1-\rho)}{\sqrt{p\theta Z\lambda(1-\alpha)(1+\eta)\left(p\theta(3+\eta)-c(2+\eta)\right)}} > 0$ and the second-order derivative at m_3 equals to $\frac{\partial^2\hat{\Pi}^*}{\partial m^2}(m \to m_3) = \frac{2np(2+\eta)Z(1-\alpha)(1-\theta)\sqrt{p\theta\lambda(2+\eta)\left(p\theta(3+\eta)-c(2+\eta)\right)}}{(1+\eta)\left(p\theta(3+\eta)-c(2+\eta)\right)} > 0$, which implies that m_1 and m_3 are local minima. Second, both second-order derivatives are positive, which implies that the profit functions are convex under these assumptions. Thus, the optimal surge multiplier value is either the lower or upper bound of this region. However, the lower bound of the surge multiplier range is negative, which means that the lowest feasible surge multiplier must occur at $m = 0$; this gives $\hat{\Pi}^* = \frac{1}{2}np(1-\theta)\left(\left(\alpha+\rho+\frac{(1-\alpha)\left(p\theta(3+\eta)-2c(2+\eta)\right)}{p(1+\eta)\theta}\right)-\right.$

$\left|\alpha - \rho + \frac{(1-\alpha)(p\theta(3+\eta)-2c(2+\eta))}{p(1+\eta)\theta}\right|\Big)$, which we define as Π_0. Alternatively, at the upper bound of the interval, $m = \frac{2}{Z}\left(1 - \frac{c(4+2\eta)}{p\theta(3+\eta)}\right) > 0$ and $\widehat{\Pi}^* = \frac{1}{2Z}n(1-\theta)\Big(\Big(4p\lambda + \frac{4c(2+\eta)\lambda(-2+\alpha+\rho)}{(3+\eta)\theta} + p(Z-2\lambda)(\alpha+\rho)\Big) - \left(p(Z+2\lambda) - \frac{4c(2+\eta)\lambda}{(3+\eta)\theta}\right)|\alpha-\rho|\Big)$, which we define as Π_2. Because we assume $\frac{c}{p\theta} \leq \frac{3+\eta}{2(2+\eta)}$, it follows that $\frac{(1-\alpha)(p\theta(3+\eta)-2c(2+\eta))}{p\theta(1+\eta)} \geq 0$. If $\alpha \geq \rho$, the difference between the profit functions is $\frac{2n(1-\alpha)(1-\theta)((p\theta 3+\eta)-2c(2+\eta))\lambda}{Z(3+\eta)\theta} \geq 0$, which implies $\widehat{\Pi}^* = \Pi_2$ as $\Pi_2 \geq \Pi_0$. Otherwise, if $\alpha \leq \rho$, we have $\widehat{\Pi}^* = \max\{\Pi_0, \Pi_2\}$.

iii. Case 3: $\frac{c}{p\theta} \leq \frac{1}{2+\eta} \leq \frac{3+\eta}{2(2+\eta)} \leq \frac{3+\eta}{2+\eta}$

For the same reasoning as in Case 3, the optimal surge multiplier value is either the lower or upper bound of this region. For the lower bound, $m = \frac{2}{Z}\left(\frac{1}{2+\eta} - \frac{c}{p\theta}\right) > 0$ and the profit is $\widehat{\Pi}^* = np(1-\theta)\rho$, which is independent of m. Since the difference between the profit functions is $\frac{2n(1-\alpha)(1-\theta)((p\theta 3+\eta)-2c(2+\eta))\lambda}{Z(3+\eta)\theta} \geq 0$, it implies that for this case, $\widehat{\Pi}^* = \Pi_2$.

Note that a critical point also exists when $\left|\alpha - \rho - \frac{(1-\alpha)(4c(2+\eta)+p(-2+mZ)(3+\eta)\theta)}{p(2+mZ)(1+\eta)\theta}\right| = 0$ since it marks the boundary between the two continuous regions. Solving for the optimal surge multiplier gives $m^+ = -\frac{4c(1-\alpha)(2+\eta)+2p\theta(-3+2\alpha-\eta(1-\rho)+\rho)}{pZ\theta(3+\eta-2\alpha(2+\eta)+\rho+\eta\rho)}$ and $\widehat{\Pi}^* = \frac{n(1-\theta)\left(-4c(-1+\alpha)(2+\eta)\lambda(-1+\rho)+p\theta\left(2\lambda(-1+\rho)(-3+2\alpha+\eta(-1+\rho)+\rho)+Z\rho(3+\eta-2\alpha(2+\eta)+\rho+\eta\rho)\right)\right)}{Z\theta(3+\eta-2\alpha(2+\eta)+\rho+\eta\rho)}$, which we define as Π_1. First notice that for some $\epsilon \geq 0$, $\lim_{\alpha \to \rho - \frac{(3+\eta)}{2(2+\eta)}\epsilon} \left(\frac{2}{Z}\left(1 - \frac{c(4+2\eta)}{p\theta(3+\eta)}\right) - m^+\right) = \frac{2\epsilon(1+\eta)(-c(2+\eta)+p\theta(3+\eta))}{pZ(2+\eta)(3+\eta)\theta(1+\epsilon-\rho)} \geq 0$ and $\lim_{\alpha \to \rho - \frac{(3+\eta)}{2(2+\eta)}\epsilon} \left(m^+ - \frac{2}{Z}\left(\frac{1}{2+\eta} - \frac{c}{p\theta}\right)\right) = \frac{2\epsilon(1+\eta)(-c(2+\eta)+p\theta(3+\eta))(1-\rho)}{pZ(2+\eta)(3+\eta)\theta(1+\epsilon-\rho)} \geq 0$ assuming $\frac{c}{p\theta} \leq \frac{3+\eta}{2+\eta}$ (which holds from Assumption 3). This implies that when $m^+ \leq \frac{2}{Z}\left(1 - \frac{c(4+2\eta)}{p\theta(3+\eta)}\right)$, $\alpha \leq \rho$. We also have that when $\alpha \leq \rho$ and $\frac{2}{Z}\left(\frac{1}{2+\eta} - \frac{c}{p\theta}\right) \geq 0$, $\Pi_1 - np(1-\theta)\rho \geq \frac{2np(1+\eta)(1-\theta)\lambda(1-\rho)^2}{Z(3+\eta-2\alpha(2+\eta)+\rho+\eta\rho)} \geq 0$. This is because the denominator $3+\eta-2\alpha(2+\eta)+\rho+\eta\rho=(3-4\alpha)+\eta(1-2\alpha)+\rho(1+\eta)$ is nonnegative for any choice of $\alpha \leq \rho$ and $\eta \geq 0$. Thus, the lower surge bound is never optimal.

Putting the cases together, when $\alpha \geq \rho$, $m^{+} \geq \frac{2}{Z}\left(1-\frac{c(4+2\eta)}{p\theta(3+\eta)}\right)$ and the optimal surge multiplier is $m^{*}=\frac{2}{Z}\left(1-\frac{c(4+2\eta)}{p\theta(3+\eta)}\right)$ where $\widehat{\Pi}^{*}=\Pi_2$. Alternatively, when $\alpha \leq \rho$ and the lower surge bound is negative, $\widehat{\Pi}^{*}=\max\{\Pi_0,\Pi_2\}$ and either $m^{*}=0$ or $m^{*}=\frac{2}{Z}\left(1-\frac{c(4+2\eta)}{p\theta(3+\eta)}\right)$. When $\alpha \leq \rho$ and the lower surge bound is positive, $\widehat{\Pi}^{*}=\max\{\Pi_1,\Pi_2\}$ and either $m^{*}=-\frac{4c(1-\alpha)(2+\eta)+2p\theta(-3+2\alpha-\eta(1-\rho)+\rho)}{pZ\theta(3+\eta-2\alpha(2+\eta)+\rho+\eta\rho)}$ or $m^{*}=\frac{2}{Z}\left(1-\frac{c(4+2\eta)}{p\theta(3+\eta)}\right)$.

Region 3. When $\gamma_A^{*}=0$, $\gamma_B^{*}=0$, and $\frac{2}{Z}\left(1-\frac{c(4+2\eta)}{p\theta(3+\eta)}\right) \leq m \leq \frac{2}{Z}\left(1+\frac{c(4+2\eta)}{p\theta(3+\eta)}\right)$, the platform's profit is $\widehat{\Pi}^{*}=\frac{1}{2}np(1-\theta)\big((\rho+\alpha)(1-m\lambda)+2m\lambda-(1+m\lambda)|\rho-\alpha|\big)$ which is either $\widehat{\Pi}^{*}=np(1-\theta)\big(\rho+m\lambda(1-\alpha)\big)$ or $\widehat{\Pi}^{*}=np(1-\theta)\big(\alpha+m\lambda(1-\rho)\big)$, both of which are linear increasing functions of m. Thus, the surge multiplier that maximizes profit is the upper bound of this region, which is $m^{*}=\frac{2}{Z}\left(1+\frac{c(4+2\eta)}{p\theta(3+\eta)}\right)$.

Region 4. When $\gamma_A^{*}=\frac{(3+\eta)\left(mp\frac{Z}{2}\theta-p\theta\right)-c(4+2\eta)}{(1+\eta)\left(p\theta+mp\frac{Z}{2}\theta\right)}$, $\gamma_B^{*}=0$, and $\frac{2}{Z}\left(1+\frac{c(4+2\eta)}{p\theta(3+\eta)}\right) \leq m \leq \frac{2}{Z}\left(1+\frac{c}{p\theta}\right)(2+\eta)$, the profit function is $\widehat{\Pi}^{*}=\frac{1}{2}np(1-\theta)\Big(2m\lambda-\frac{(-1+m\lambda)\left(4c\alpha(2+\eta)+p\theta(\alpha(8-2mZ+4\eta)+(2+mZ)(1+\eta)\rho)\right)}{p(2+mZ)(1+\eta)\theta}-(1+m\lambda)\left|\rho-\frac{2\alpha(2c(2+\eta)+p(4-mZ+2\eta)\theta)}{p(2+mZ)(1+\eta)\theta}\right|\Big)$.
Assuming that $\rho-\frac{2\alpha(2c(2+\eta)+p(4-mZ+2\eta)\theta)}{p(2+mZ)(1+\eta)\theta} \neq 0$, the first-order derivative is either $\frac{\partial\widehat{\Pi}^{*}}{\partial m}=\frac{n(-1+\theta)\left(4cZ\alpha(2+\eta)+p\theta\left(4Z\alpha(3+\eta)-(2+mZ)^2(1+\eta)\lambda+(2+mZ)^2(1+\eta)\lambda\rho\right)\right)}{(2+mZ)^2(1+\eta)\theta}$ or $\frac{\partial\widehat{\Pi}^{*}}{\partial m}=-\frac{n(-1+\theta)\left(-8c\alpha(2+\eta)+p\left(4+4\eta-8\alpha(2+\eta)+4mZ(1+2\alpha+\eta)+m^2Z^2(1+2\alpha+\eta)\right)\theta\right)\lambda}{(2+mZ)^2(1+\eta)\theta}$, and the analysis of the first order conditions for optimality gives either $\left\{m_1 \to \frac{-2}{Z}\left(1-\sqrt{\frac{Z\alpha\left(c(2+\eta)+p\theta(3+\eta)\right)}{p\theta\lambda(1-\rho)(1+\eta)}}\right), m_2 \to \frac{-2}{Z}\left(1+\sqrt{\frac{Z\alpha\left(c(2+\eta)+p\theta(3+\eta)\right)}{p\theta\lambda(1-\rho)(1+\eta)}}\right)\right\}$ or $\left\{m_3 \to \frac{-2}{Z}\left(1-\sqrt{\frac{2\alpha\left(c(2+\eta)+p\theta(3+\eta)\right)}{p\theta(1+2\alpha+\eta)}}\right), m_4 \to\right.$

$\frac{-2}{Z}\left(1+\sqrt{\frac{2\alpha\left(c(2+\eta)+p\theta(3+\eta)\right)}{p\theta(1+2\alpha+\eta)}}\right)\Bigg\}$. Notice that m_2 and m_4 are negative and thus, infeasible.

Although m_1 and m_3 can be positive, they are also infeasible surge multipliers for two reasons. First, the second-order derivative at m_1 equals to $\frac{\partial^2 \widehat{\Pi}^*}{\partial m^2}(m \to m_1) = \frac{np^2Z^2(1+\eta)(-1+\theta)^2\theta\lambda^2(-1+\rho)^2}{\sqrt{pZ^3\alpha(1+\eta)(-1+\theta)^2\theta(c(2+\eta)+p(3+\eta)\theta)\lambda(1-\rho)}} > 0$ and the second-order derivative at m_3 equals to $\frac{\partial^2 \widehat{\Pi}^*}{\partial m^2}(m \to m_3) = \frac{np^2Z^2(1+2\alpha+\eta)^2(-1+\theta)^2\theta\lambda}{\sqrt{2}(1+\eta)\sqrt{pZ^2\alpha(1+2\alpha+\eta)(-1+\theta)^2\theta(c(2+\eta)+p(3+\eta)\theta)}} > 0$, which implies that m_1 and m_3 are local minima. In addition, the second-order derivatives are $\frac{\partial^2 \widehat{\Pi}^*}{\partial m^2} = \frac{8nZ^2\alpha(1-\theta)(c(2+\eta)+p(3+\eta)\theta)}{(2+mZ)^3(1+\eta)\theta}$ or $\frac{\partial^2 \widehat{\Pi}^*}{\partial m^2} = \frac{16nZ\alpha(1-\theta)(c(2+\eta)+p(3+\eta)\theta)\lambda}{(2+mZ)^3(1+\eta)\theta}$, which are both positive and thus imply that the profit functions are convex. Thus, the optimal surge multiplier is either the lower or upper bound of its region. If $m = \frac{2}{Z}\left(1+\frac{c(4+2\eta)}{p\theta(3+\eta)}\right)$, then $\widehat{\Pi}^* = \frac{n(1-\theta)\left(4(2c(2+\eta)+p(3+\eta)\theta)\lambda+(p(3+\eta)\theta(Z-2\lambda)-4c(2+\eta)\lambda)(\alpha+\rho)-\left(4c(2+\eta)\lambda+p(3+\eta)\theta(Z+2\lambda)\right)|\alpha-\rho|\right)}{2Z(3+\eta)\theta}$, which we define as Π_1. If $m = \frac{2}{Z}\left(1+\frac{c}{p\theta}\right)(2+\eta)$, then $\widehat{\Pi}^* = \frac{2n(2+\eta)(1-\theta)(c+p\theta)\lambda(1-\rho)}{Z\theta}$, which we define as Π_2. Note that a critical point also exists when $\left|\rho - \frac{4c\alpha(2+\eta)+2p\theta\alpha(4-mZ+2\eta)}{p\theta(2+mZ)(1+\eta)}\right| = 0$ since it marks the boundary between the two continuous regions. Solving for the optimal surge multiplier gives $m^+ = \frac{4\alpha(2+\eta)(c+p\theta)-2p(1+\eta)\theta\rho}{pZ\theta(2\alpha+\rho+\eta\rho)}$ and $\widehat{\Pi}^* = \frac{n(1-\theta)\left(-4c\alpha(2+\eta)\lambda(-1+\rho)+p\theta\left((1+\eta)\rho(2\lambda(-1+\rho)+Z\rho)+\alpha(-4(2+\eta)\lambda(-1+\rho)+2Z\rho)\right)\right)}{Z\theta(2\alpha+\rho+\eta\rho)}$, which we define as Π_0. First, assume that $\rho \geq \alpha$, then $\widehat{\Pi}^* = \max\{\Pi_1, \Pi_2\}$ as $\frac{2}{Z}\left(1+\frac{c(4+2\eta)}{p\theta(3+\eta)}\right) - m^+ \geq \frac{4(1+\eta)(c(2+\eta)+p(3+\eta)\theta)(\rho-\alpha)}{pZ(3+\eta)\theta(2\alpha+\rho+\eta\rho)} \geq 0$, which implies that m^+ is an infeasible surge multiplier and $\frac{2}{Z}\left(1+\frac{c}{p\theta}\right)(2+\eta) - m^+ \geq 0$ for all parameters. Thus, $m^* = \frac{2}{Z}\left(1+\frac{c(4+2\eta)}{p\theta(3+\eta)}\right)$ or $m^* = \frac{2}{Z}\left(1+\frac{c}{p\theta}\right)(2+\eta)$. Alternatively, if $\alpha \geq \rho$, then $\widehat{\Pi}^* = \max\{\Pi_0, \Pi_2\}$ since $\Pi_0 \geq \Pi_1$ (which can be verified by re-arranging the respective profit functions) and $m^* = m^+$ or $m^* = \frac{2}{Z}\left(1+\frac{c}{p\theta}\right)(2+\eta)$.

Region 5. When $\gamma_A^* = 1, \gamma_B^* = 0$, and $m \geq \frac{2}{Z}\left(1 + \frac{c}{p\theta}\right)(2+\eta)$, the platform's profit is either $\widehat{\Pi}^* = np(1-\theta)(\rho + m\lambda)$ or $\widehat{\Pi}^* = np(1-\theta)m\lambda(1-\rho)$, which are linearly increasing function of m. Thus, the surge multiplier that maximizes profit is $m^* = m_{max}$ following Assumption 1.

Profit for Models 5–6

The optimal surge multiplier and maximum profit for Models 5 and 6 are similar except for λ replacing $\frac{Z}{2}$ in Model 6 and depend on the regions for m described in Theorem 2. The profit function is from (A5). From Theorem 2 and Table 3-A-11, which describes the optimal γ_A^* and γ_B^* for Model 5, five regions for m must be considered.

Region 1. When $\gamma_A^* = 0, \gamma_B^* = 1$, and $0 \leq m \leq \frac{2}{Z}\left(\frac{\rho}{1-\eta\rho+\eta} - \frac{c}{p\theta}\right)$, the platform's profit is $\widehat{\Pi}^* = \frac{1}{2}np(1-\theta)\left((\rho+1)(1-m\lambda)+2m\lambda\right) - \frac{1}{2}np(1-\theta)(1+m\lambda)|\rho-1| = np\rho(1-\theta)$ as $0 < \rho < 1$, which is not a function of m, and the surge multiplier that maximizes profit is any $m \geq 0$ where $m \in \left[0, \frac{2}{Z}\left(\frac{1}{2+\eta} - \frac{c}{p\theta}\right)\right]$.

Region 2.1. Similarly, when $\gamma_A^* = 0, \gamma_B^* = 1$, and $\frac{2}{Z}\left(\frac{\rho}{1-\eta\rho+\eta} - \frac{c}{p\theta}\right) \leq m \leq \frac{\frac{1+\eta}{1-\rho}(p\theta\rho-c)+\eta(p\theta-c)\log[1-\rho]-\frac{\rho}{1-\rho}(c\eta+p\theta)\log[\rho]}{\frac{1}{2}pZ\theta\left((1+\eta)-\log[1-\rho]+\frac{\rho}{1-\rho}\eta\log[\rho]\right)}$, the surge multiplier that maximizes the platform's profit is any $m \geq 0$ where $m \in \left[\frac{2}{Z}\left(\frac{\rho}{1-\eta\rho+\eta} - \frac{c}{p\theta}\right), \frac{\frac{1+\eta}{1-\rho}(p\theta\rho-c)+\eta(p\theta-c)\log[1-\rho]-\frac{\rho}{1-\rho}(c\eta+p\theta)\log[\rho]}{\frac{1}{2}pZ\theta\left((1+\eta)-\log[1-\rho]+\frac{\rho}{1-\rho}\eta\log[\rho]\right)}\right]$.

Region 2.2. When $\gamma_A^* = 0, \gamma_B^* = 1 - h(m)$[11] $W\left(\frac{1}{h(m)}e^{j(m)}\right)$[12], and $\frac{2}{Z}\left(\frac{\rho}{1-\eta\rho+\eta} - \frac{c}{p\theta}\right) \leq m \leq \frac{\frac{1+\eta}{1-\rho}(p\theta\rho-c)+\eta(p\theta-c)\log[1-\rho]-\frac{\rho}{1-\rho}(c\eta+p\theta)\log[\rho]}{\frac{1}{2}pZ\theta\left((1+\eta)-\log[1-\rho]+\frac{\rho}{1-\rho}\eta\log[\rho]\right)}$, assuming $\rho - \gamma_B \geq 0$, the platform's profit is $\widehat{\Pi}^* =$

---

[11] $h(m) = \frac{-(1-\rho)\left(mp\frac{Z}{2}\theta+\eta(p\theta-c)\right)}{(\eta+1)(p\theta-c)}$,

[12] $j(m) = \frac{-(1-\rho)\log[1-\rho]\left(mp\frac{Z}{2}\theta+\eta(p\theta-c)\right)-\rho(p\theta-c)+\rho\log[\rho]\left(p\theta+\eta\left(mp\frac{Z}{2}\theta+c\right)\right)+\left(c+\eta\left(mp\frac{Z}{2}\theta+c\right)\right)(1-\rho)-\rho\left(mp\frac{Z}{2}\theta+\eta(p\theta-c)\right)+mp\frac{Z}{2}\theta+(\eta+1)(p\theta-c)}{-(1-\rho)\left(mp\frac{Z}{2}\theta+\eta(p\theta-c)\right)}$

$\frac{1}{2}np(1-\theta)\left(1+m\lambda(1-\rho)+\rho-(1+m\lambda)\left|1-\rho-(1-\alpha)h(m)W\left(\frac{1}{h(m)}e^{j(m)}\right)\right|-\right.$ $\left.(1-\alpha)(1-m\lambda)h(m)W\left(\frac{1}{h(m)}e^{j(m)}\right)\right)$. First, assume $\left|1-\rho-(1-\alpha)h(m)W\left(\frac{1}{h(m)}e^{j(m)}\right)\right|\neq 0$, then the first-order derivative is either $\frac{\partial\widehat{\Pi}^*}{\partial m}=$ $\frac{-np(1-\theta)}{1+W\left(\frac{1}{h(m)}e^{j(m)}\right)}\left(-\lambda(1-\rho)+W\left(\frac{1}{h(m)}e^{j(m)}\right)\left(\lambda(-1+\rho)+(1-\alpha)W\left(\frac{1}{h(m)}e^{j(m)}\right)h'(m)+\right.\right.$ $\left.\left.(1-\alpha)\,h(m)\,j'(m)\right)\right)$ or $\frac{\partial\widehat{\Pi}^*}{\partial m}=\frac{np\lambda(1-\alpha)(1-\theta)W\left(\frac{1}{h(m)}e^{j(m)}\right)}{1+W\left(\frac{1}{h(m)}e^{j(m)}\right)}\left(mW\left(\frac{1}{h(m)}e^{j(m)}\right)h'(m)+\right.$ $\left.h(m)\left(1+W\left(\frac{1}{h(m)}e^{j(m)}\right)+mj'(m)\right)\right)$.

To evaluate all critical points, seven cases must be considered:

i. Case 1: $W\left(\frac{1}{h(m)}e^{j(m)}\right)=0$. No m satisfies this condition.

ii. Case 2: $W\left(\frac{1}{h(m)}e^{j(m)}\right)=-1$. No closed-form expression exists but there is an analytic solution where m^+ solves $j(m^+)-\log[-h(m^+)]=-1$. For the profit we obtain $\widehat{\Pi}^*=\frac{1}{2}np(1-\theta)\big(1+m^+\lambda(1-\rho)+\rho-(1+m^+\lambda)|1-\rho+(1-\alpha)h(m^+)|+(1-\alpha)(1-m^+\lambda)h(m^+)\big)$. The validity of this solution depends on whether $h(m)<0$ which does not always hold. Nevertheless, this Case 2 does factor into the optimal solution because the profit function is dominated by the profit function associated with Case 7.

iii. Case 3: $mW\left(\frac{e^{j(m)}}{h(m)}\right)h'(m)+h(m)(1+W\left(\frac{e^{j(m)}}{h(m)}\right)+mj'(m))=0$. Simplifying this expression, we obtain $m=\frac{\frac{1+\eta}{1-\rho}(p\theta\rho-c)+\eta(p\theta-c)\log[1-\rho]-\frac{\rho}{1-\rho}(c\eta+p\theta)\log[\rho]}{\frac{1}{2}pZ\theta\left((1+\eta)-\log[1-\rho]+\frac{\rho}{1-\rho}\eta\log[\rho]\right)}$, which is the upper bound of the interval for m. Due to the complexity of the closed-form expression, we denote the profit as Π_2.

iv. Case 4: $W\left(\frac{e^{j(m)}}{h(m)}\right)\left(-\lambda(1-\rho)+(1-\alpha)W\left(\frac{e^{j(m)}}{h(m)}\right)h'(m)+(1-\alpha)h(m)j'(m)\right)=$ $\lambda(1-\rho)$. Simplifying this expression, we again obtain $m = \frac{\frac{1+\eta}{1-\rho}(p\theta\rho-c)+\eta(p\theta-c)\log[1-\rho]-\frac{\rho}{1-\rho}(c\eta+p\theta)\log[\rho]}{\frac{1}{2}pZ\theta\left((1+\eta)-\log[1-\rho]+\frac{\rho}{1-\rho}\eta\log[\rho]\right)}$, which is the upper bound of the interval for m.

v. Case 5: Since the first-order derivative(s) may be monotonic, we also evaluate the lower bound of the surge multiplier interval, which is $m=\frac{2}{Z}\left(\frac{\rho}{1-\eta\rho+\eta}-\frac{c}{p\theta}\right)$. Due to the complexity of the closed-form expression, we denote the profit as Π_1.

vi. Case 6: It is possible that $\frac{2}{Z}\left(\frac{\rho}{1-\eta\rho+\eta}-\frac{c}{p\theta}\right)\leq 0$. In this case, a critical point is $m=0$. Due to the complexity of the closed-form expression, we denote the profit as Π_0.

vii. Case 7: We must also evaluate the critical point implied by $1-\rho-(1-\alpha)h(m)W\left(\frac{1}{h(m)}e^{j(m)}\right)=0$ or $W\left(\frac{1}{h(m)}e^{j(m)}\right)=\frac{1-\rho}{(1-\alpha)h(m)}$. Re-arranging and simplifying, we obtain $m^{++}=\frac{\frac{1+\eta}{1-\alpha}(p\alpha\theta-c)+\eta(p\theta-c)\log[1-\alpha]-\frac{\rho}{1-\rho}(c\eta+p\theta)\log[\rho]}{\frac{1}{2}p\,Z\,\theta\left((1+\eta)-\log[1-\alpha]+\frac{\rho}{1-\rho}\eta\log[\rho]\right)}$ and $\widehat{\Pi}^*=\frac{1}{2}np(1-\theta)\left(1+m^{++}\lambda(1-\rho)+\rho-(1-\alpha)(1-m^{++}\lambda)h(m^{++})W\left(\frac{1}{h(m^{++})}e^{j(m^{++})}\right)\right)$. Due to the complexity of the closed-form expression, we denote the profit as Π_+.

Notice that the profit values are either analytic or can be written in closed form. Nevertheless, they are tedious. Thus, we instead derive a process for producing optimal solutions:

1) If the lower bound on the surge multiplier is negative, then evaluate $\widehat{\Pi}^*=\max\{\Pi_0,\Pi_2\}$ if $m^{++}\leq 0$, otherwise $\widehat{\Pi}^*=\max\{\Pi_+,\Pi_2\}$.
2) If the lower bound on the surge multiplier is positive, then evaluate $\widehat{\Pi}^*=\max\{\Pi_1,\Pi_2\}$ if $m^{++}\leq 0$, otherwise $\widehat{\Pi}^*=\max\{\Pi_+,\Pi_2\}$.

Region 3. When $\gamma_A^* = 0$, $\gamma_B^* = 0$, and $\frac{\frac{1+\eta}{1-\rho}(p\theta\rho - c) + \eta(p\theta - c)\log[1-\rho] - \frac{\rho}{1-\rho}(c\eta + p\theta)\log[\rho]}{\frac{1}{2}pZ\theta\left((1+\eta) - \log[1-\rho] + \frac{\rho}{1-\rho}\eta\log[\rho]\right)} \leq m \leq \frac{\frac{1+\eta}{1-\rho}(c + p\theta\rho) + \eta(c + p\theta)\log[1-\rho] + \frac{\rho}{1-\rho}(c\eta - p\theta)\log[\rho]}{\frac{1}{2}pZ\theta\left((1+\eta) - \log[1-\rho] + \eta\frac{\rho}{1-\rho}\log[\rho]\right)}$, the profit is $\widehat{\Pi}^* = \frac{1}{2}np(1-\theta)\big((\rho+\alpha)(1-m\lambda) + 2m\lambda - (1+m\lambda)|\rho-\alpha|\big)$ or $\widehat{\Pi}^* = np(1-\theta)\big(\rho + m\lambda(1-\alpha)\big)$ or $\widehat{\Pi}^* = np(1-\theta)\big(\alpha + m\lambda(1-\rho)\big)$, both of which are linear increasing functions of m. Thus, the surge multiplier that maximize the platform's profit is the upper bound of its range, which is $m^* = \frac{\frac{1+\eta}{1-\rho}(c + p\theta\rho) + \eta(c + p\theta)\log[1-\rho] + \frac{\rho}{1-\rho}(c\eta - p\theta)\log[\rho]}{\frac{1}{2}pZ\theta\left((1+\eta) - \log[1-\rho] + \eta\frac{\rho}{1-\rho}\log[\rho]\right)}$.

Region 4.1. When $\gamma_A^* = 1 - f(m)$[13]$W\left(\frac{1}{f(m)}e^{g(m)}\right)$[14], $\gamma_B^* = 0$, and $\frac{\frac{1+\eta}{1-\rho}(c + p\theta\rho) + \eta(c + p\theta)\log[1-\rho] + \frac{\rho}{1-\rho}(c\eta - p\theta)\log[\rho]}{\frac{1}{2}pZ\theta\left((1+\eta) - \log[1-\rho] + \eta\frac{\rho}{1-\rho}\log[\rho]\right)} \leq m \leq \frac{2}{Z}\left(1 + \frac{c}{p\theta}\right)\left(\frac{1+\eta\rho}{1-\rho}\right)$, assuming $\rho \leq 1 - \gamma_A$, the platform's profit is $\widehat{\Pi}^* = \frac{1}{2}np(1-\theta)\left(m\lambda(2-\rho) + \rho - (1+m\lambda)\left|\rho - \alpha f(m)W\left(\frac{1}{f(m)}e^{g(m)}\right)\right| + \alpha(1-m\lambda)f(m)W\left(\frac{1}{f(m)}e^{g(m)}\right)\right)$. First, assume that $\left|\rho - \alpha f(m)W\left(\frac{1}{f(m)}e^{g(m)}\right)\right| \neq 0$ and thus first-order derivative is either $\frac{\partial\widehat{\Pi}^*}{\partial m} = \frac{np(1-\theta)\left(\lambda(1-\rho) + W\left(\frac{1}{f(m)}e^{g(m)}\right)\left(\lambda(1-\rho) + \alpha W\left(\frac{1}{f(m)}e^{g(m)}\right)f'(m) + \alpha f(m)g'(m)\right)\right)}{1 + W\left(\frac{1}{f(m)}e^{g(m)}\right)}$ or $\frac{\partial\widehat{\Pi}^*}{\partial m} = \frac{np(1-\theta)\lambda\left(1 - \alpha W^2\left(\frac{1}{f(m)}e^{g(m)}\right)\big(f(m) + mf'(m)\big) + W\left(\frac{1}{f(m)}e^{g(m)}\right)\Big(1 - f(m)\big(\alpha + m\alpha g'(m)\big)\Big)\right)}{1 + W\left(\frac{1}{f(m)}e^{g(m)}\right)}$.

To evaluate all critical points, five cases must be considered:

[13] $f(m) = \frac{-\rho\left(p\theta + \eta\left(mp\frac{Z}{2}\theta - c\right)\right)}{(1+\eta)\left(mp\frac{Z}{2}\theta - c\right)}$

[14] $g(m) = \frac{p\theta\rho - \rho\log[\rho]\left(p\theta + \eta\left(mp\frac{Z}{2}\theta - c\right)\right) + \rho\eta\left(mp\frac{Z}{2}\theta - c\right) + (1-\rho)\log[1-\rho]\left(mp\frac{Z}{2}\theta + \eta(p\theta + c)\right) + \rho\left(mp\frac{Z}{2}\theta + \eta(p\theta + c)\right)}{-\rho\left(p\theta + \eta\left(mp\frac{Z}{2}\theta - c\right)\right)}$

i. Case 1: $W\left(\frac{1}{f(m)}e^{g(m)}\right) = -1$. No closed-form expression exists but there is an analytic solution where m^+ solves $g(m^+) - \log[-f(m^+)] = -1$. For the profit we obtain $\widehat{\Pi}^* = np(1-\theta)\big(m^+\lambda + \rho - \alpha f(m^+)\big)$. The validity of this solution depends on whether $f(m) < 0$, which always holds from Assumption 2. Due to the complexity of the closed-form expression, we denote the profit as Π_{-1}.

ii. Case 2: $-\lambda(1-\rho)\left(1 + \frac{1}{W\left(\frac{1}{f(m)}e^{g(m)}\right)}\right) - \alpha W\left(\frac{1}{f(m)}e^{g(m)}\right) f'(m) = \alpha f(m) g'(m)$.

Simplifying this expression, we obtain $m = \frac{\frac{1+\eta}{1-\rho}(c+p\theta\rho)+\eta(c+p\theta)\log[1-\rho]+\frac{\rho}{1-\rho}(c\eta-p\theta)\log[\rho]}{\frac{1}{2}pZ\theta\left((1+\eta)-\log[1-\rho]+\eta\frac{\rho}{1-\rho}\log[\rho]\right)}$,

which is the lower bound of the surge multiplier interval. Due to the complexity of the closed-form expression, we denote the profit as Π_1.

iii. Case 3: $\alpha W^2\left(\frac{1}{f(m)}e^{g(m)}\right)\big(f(m) + mf'(m)\big) - W\left(\frac{1}{f(m)}e^{g(m)}\right)\Big(1 - f(m)\big(\alpha + m\alpha g'(m)\big)\Big) = 1$. Simplifying this expression, we again obtain $m = \frac{\frac{1+\eta}{1-\rho}(c+p\theta\rho)+\eta(c+p\theta)\log[1-\rho]+\frac{\rho}{1-\rho}(c\eta-p\theta)\log[\rho]}{\frac{1}{2}pZ\theta\left((1+\eta)-\log[1-\rho]+\eta\frac{\rho}{1-\rho}\log[\rho]\right)}$, which is the lower bound of the interval for m.

iv. Case 4: Since the first derivative(s) may be monotonic, we also evaluate the upper bound of the surge multiplier interval, which is $m = \frac{2}{Z}\left(1 + \frac{c}{p\theta}\right)\left(\frac{1+\eta\rho}{1-\rho}\right)$. Due to the complexity of the closed-form expression, we denote the profit as Π_2.

v. Case 5: We evaluate the critical point implied by $\rho - \alpha f(m) W\left(\frac{1}{f(m)}e^{g(m)}\right) = 0$ or $W\left(\frac{1}{f(m)}e^{g(m)}\right) = \frac{\rho}{\alpha f(m)}$. Re-arranging and simplifying, we obtain $m^{++} = \frac{\frac{1+\eta}{1-\alpha}(c+p\alpha\theta)+\frac{\alpha}{1-\alpha}\eta(c+p\theta)\left(\frac{1-\rho}{\rho}\right)\log[1-\rho]+\frac{\alpha}{1-\alpha}(c\eta-p\theta)\log[\alpha]}{\frac{1}{2}pZ\theta\left((1+\eta)+\frac{\alpha}{1-\alpha}\eta\log[\alpha]-\frac{\alpha}{1-\alpha}\left(\frac{1-\rho}{\rho}\right)\log[1-\rho]\right)}$ and $\widehat{\Pi}^* = \frac{1}{2}np(1-\theta)\left(m^{++}\lambda(2-\rho) + \rho + \alpha(1-m^{++}\lambda)f(m^{++})W\left(\frac{1}{f(m^{++})}e^{g(m^{++})}\right)\right)$. We denote the profit as $\Pi_0 = \frac{1}{2}np(1-\theta)(m^{++}\lambda - 1)(1-2\rho)$.

Region 4.2. When $\gamma_A^* = 1, \gamma_B^* = 0$, and $\frac{\frac{1+\eta}{1-\rho}(c+p\theta\rho)+\eta(c+p\theta)\log[1-\rho]+\frac{\rho}{1-\rho}(c\eta-p\theta)\log[\rho]}{\frac{1}{2}pZ\theta\left((1+\eta)-\log[1-\rho]+\eta\frac{\rho}{1-\rho}\log[\rho]\right)} \leq m \leq$ $\frac{2}{Z}\left(1+\frac{c}{p\theta}\right)\left(\frac{1+\eta\rho}{1-\rho}\right)$, the platform's profit is linear and increasing in m. Thus, surge multiplier that maximizes profit is the upper bound of this region, which is $m^* = \frac{2}{Z}\left(1+\frac{c}{p\theta}\right)\left(\frac{1+\eta\rho}{1-\rho}\right)$.

Region 5. When $\gamma_A^* = 1, \gamma_B^* = 0$, and $m \geq \frac{2}{Z}\left(1+\frac{c}{p\theta}\right)\left(\frac{1+\eta\rho}{1-\rho}\right)$, the platform's profit is either $\widehat{\Pi}^* = np(1-\theta)(\rho+m\lambda)$ or $\widehat{\Pi}^* = np(1-\theta)m\lambda(1-\rho)$, which are linearly increasing in m. Thus, the surge multiplier that maximizes profit is $m^* = m_{max}$ following Assumption 1.

Profit for Models 7–8

The optimal surge multiplier and maximum profit for Models 7 and 8 are similar except for λ replacing $\frac{Z}{2}$ in Model 8 and depend on the regions for m described in Theorem 3. The profit function is from (A5). From Theorem 3 and Table 3-A-12 and 3-A-13, which describes the optimal γ_A^* and γ_B^* for Model 7, four regions for m exist when $\alpha \geq \max\left\{0, \frac{\rho-\gamma_B^*}{1-\gamma_A^*-\gamma_B^*}\right\}$ and also four regions when $\alpha \leq \max\left\{0, \frac{\rho-\gamma_B^*}{1-\gamma_A^*-\gamma_B^*}\right\}$.

1- When $\alpha \geq \max\left\{0, \frac{\rho-\gamma_B^*}{1-\gamma_A^*-\gamma_B^*}\right\}$:

Region 1. When $\gamma_A^* = 0, \gamma_B^* = 1$, and $0 \leq m \leq \frac{2}{Z}\left(\frac{\rho}{1-\eta\rho+\eta} - \frac{c}{p\theta}\right)$, for the upper bound of the interval to be greater than the lower bound, it must be that $\frac{c}{p\theta} \leq \frac{\rho}{1-\eta\rho+\eta}$. Under this condition, the platform's profit is $\widehat{\Pi}^* = \frac{1}{2}np(1-\theta)\big((\rho+1)(1-m\lambda)+2m\lambda\big) - \frac{1}{2}np(1-\theta)(1+m\lambda)|\rho-1| = np\rho(1-\theta)$ as $0<\rho<1$, and the surge value that maximizes profit is any $m \in \left[0, \frac{2}{Z}\left(\frac{\rho}{1-\eta\rho+\eta} - \frac{c}{p\theta}\right)\right]$.

Region 2. When $\gamma_A^* = 0, \gamma_B^* = \frac{\rho p\theta+\left(mp\frac{Z}{2}\theta+c\right)(\eta(\rho-\alpha)-\alpha)}{\left(mp\frac{Z}{2}\theta+c\right)(1-\alpha)(1+\eta)}$, and $\frac{2}{Z}\left(\frac{\rho}{1-\eta\rho+\eta} - \frac{c}{p\theta}\right) \leq m \leq$ $\frac{2}{Z}\left(\frac{\rho}{\alpha+\eta(\alpha-\rho)} - \frac{c}{p\theta}\right)$, the platform's profit is $\widehat{\Pi}^* = \frac{1}{2}np(1-\theta)\Big(2m\lambda -$

$\frac{(c(2+4\eta)+p(2+mZ+2mZ\eta)\theta)(-1+m\lambda)\rho}{(1+\eta)(2c+mpZ\theta)} - (1+m\lambda)\left|\frac{(2c+p(-2+mZ)\theta)\rho}{(1+\eta)(2c+mpZ\theta)}\right|\Big)$. Assuming $\frac{(2c+p(-2+mZ)\theta)\rho}{(1+\eta)(2c+mpZ\theta)} \neq 0$, the first-order derivative is either $\frac{\partial \hat{\Pi}^*}{\partial m} = \frac{np(-1+\theta)\left(4c^2(1+\eta)\lambda(-1+\rho)+4cmpZ(1+\eta)\theta\lambda(-1+\rho)+p^2Z\theta^2\left(m^2Z(1+\eta)\lambda(-1+\rho)+2\rho\right)\right)}{(1+\eta)(2c+mpZ\theta)^2}$ or $\frac{\partial \hat{\Pi}^*}{\partial m} = \frac{np(-1+\theta)\lambda\left(4c^2(-1+\eta(-1+\rho))+m^2p^2Z^2\theta^2(-1+\eta(-1+\rho))+4cp\theta(mZ(-1+\eta(-1+\rho))+\rho)\right)}{(1+\eta)(2c+mpZ\theta)^2}$, and the analysis of the first-order conditions for optimality give, respectively, $\left\{m_1 \to \frac{-2c}{p\theta Z} + \sqrt{\frac{2\rho}{Z\lambda(1-\rho)(1+\eta)}}, m_2 \to \frac{-2c}{p\theta Z} - \sqrt{\frac{2\rho}{Z\lambda(1-\rho)(1+\eta)}}\right\}$ or $\left\{m_3 \to \frac{-2}{Z}\left(\frac{c}{p\theta} - \sqrt{\frac{c\rho}{p\theta(1+\eta-\eta\rho)}}\right), m_4 \to \frac{-2}{Z}\left(\frac{c}{p\theta} + \sqrt{\frac{c\rho}{p\theta(1+\eta-\eta\rho)}}\right)\right\}$. Notice that m_2 and m_4 are negative and thus, infeasible solutions. This implies that only m_1 and m_3 are viable. The second-order derivative is, respectively, $\frac{\partial^2 \hat{\Pi}^*}{\partial m^2} = \frac{4np^4Z^2(1-\theta)\theta^3\rho}{(1+\eta)(2c+mpZ\theta)^3}$ or $\frac{\partial^2 \hat{\Pi}^*}{\partial m^2} = \frac{8cnp^3Z(1-\theta)\theta^2\lambda\rho}{(1+\eta)(2c+mpZ\theta)^3}$. We first note that $\frac{\rho}{1-\eta\rho+\eta} = \frac{\rho}{1+\eta(1-\rho)} \geq 0$ for any choice of ρ and η. Thus, for the upper bound of the interval to be greater than the lower bound, it must be that $\frac{2(1-\alpha)(1+\eta)\rho}{Z(1+\eta(1-\rho))(\alpha+\eta(\alpha-\rho))} \geq 0$, which holds if $\alpha \geq \frac{\eta}{1+\eta}\rho$ where $\frac{\eta}{1+\eta} \leq 1$; we utilize this property in the rest of the proof of Region 2. Depending on the magnitude of $\frac{c}{p\theta}$, we have three cases:

i. Case 1: $\frac{\rho}{1-\eta\rho+\eta} \leq \frac{\rho}{\alpha+\eta(\alpha-\rho)} \leq \frac{c}{p\theta}$

The lower and upper bounds of the surge multiplier range are both negative. Thus, no nonnegative surge multiplier exists in this region that maximizes profit.

ii. Case 2: $\frac{\rho}{1-\eta\rho+\eta} \leq \frac{c}{p\theta} \leq \frac{\rho}{\alpha+\eta(\alpha-\rho)}$

The upper bound is positive and the lower bound is negative. Although m_1 and m_3 can be positive, they are not feasible surge multipliers for two reasons. First, the second-order derivative at m_1 equals to $\frac{\partial^2 \hat{\Pi}^*}{\partial m^2}(m \to m_1) = \frac{\sqrt{2}n\lambda(1-\rho)\sqrt{p^4Z^3(1+\eta)(-1+\theta)^2\theta^4\lambda(1-\rho)\rho}}{pZ\theta^2\rho} > 0$ and the second-order derivative at m_3 equals to $\frac{\partial^2 \hat{\Pi}^*}{\partial m^2}(m \to m_3) =$

$\frac{n\lambda(1+\eta-\eta\rho)\sqrt{cp^3Z^2(-1+\theta)^2\theta^3(1+\eta(1-\rho))\rho}}{c(1+\eta)\theta\rho} > 0$, which implies that m_1 or m_3 are local minima. Further, both second derivatives are positive, which means that the profit function is convex in these regions. Thus, optimal the surge multiplier value is either the lower or upper bound of this region. However, the lower bound of the surge multiplier range is negative in this case, which implies that the optimal surge multiplier may be at $m = 0$; this gives $\widehat{\Pi}^* = \frac{1}{2}np(1-\theta)\left(\frac{(c(1+2\eta)+p\theta)\rho}{c(1+\eta)} - \left|\frac{(c-p\theta)\rho}{c(1+\eta)}\right|\right)$, which we denote as Π_0. Alternatively, at the upper bound of the interval, $m = \frac{2}{Z}\left(\frac{\rho}{\alpha+\eta(\alpha-\rho)} - \frac{c}{p\theta}\right) > 0$, which gives $\widehat{\Pi}^* = -\frac{1}{2Z\theta(\alpha+\alpha\eta-\eta\rho)}n(-1+\theta)\big(2c\lambda(-2+\alpha+\rho)(\alpha+\alpha\eta-\eta\rho) + p\theta\big(-2\lambda\rho(-2+\alpha+\rho) + Z(\alpha+\rho)(\alpha+\alpha\eta-\eta\rho)\big) - (\alpha(1+\eta)(pZ\theta-2c\lambda) + 2c\eta\lambda\rho + p\theta(-Z\eta+2\lambda)\rho)|\alpha-\rho|\big)$, which we denote as Π_2. Notice that when $\alpha \geq \rho$, then $\Pi_2 - \Pi_0 = \Pi_2 - np(1-\theta)\rho = \frac{1}{Z}2n(1-\alpha)(1-\theta)\lambda p\left(\frac{\rho}{\alpha+\alpha\eta-\eta\rho} - \frac{c}{p\theta}\right) \geq 0$. When $\rho \geq \alpha$, $\widehat{\Pi}^* = \max\{\Pi_0, \Pi_2\}$.

iii. Case 3: $\frac{c}{p\theta} \leq \frac{\rho}{1-\eta\rho+\eta} \leq \frac{\rho}{\alpha+\eta(\alpha-\rho)}$

For the same reasoning as in Case 2, the optimal surge multiplier is either the lower or upper bound of this region. At the lower bound, $m = \frac{2}{Z}\left(\frac{\rho}{1-\eta\rho+\eta} - \frac{c}{p\theta}\right) > 0$ and the profit is $\widehat{\Pi}^* = np(1-\theta)\rho$. At the upper bound, $m = \frac{2}{Z}\left(\frac{\rho}{\alpha+\eta(\alpha-\rho)} - \frac{c}{p\theta}\right) > 0$ and the profit is Π_2 (see the previous case for the exact specification). It follows that when $\alpha \geq \rho$, then $\Pi_2 - np(1-\theta)\rho = \frac{1}{Z}2n(1-\alpha)(1-\theta)\lambda p\left(\frac{\rho}{\alpha+\alpha\eta-\eta\rho} - \frac{c}{p\theta}\right) \geq 0$ and the upper bound yields the highest profit.

Note that a critical point also exists when $\left|\frac{(2c+p(-2+mZ)\theta)\rho}{(1+\eta)(2c+mpZ\theta)}\right| = 0$ since it marks the boundary between the two continuous regions. Solving for the optimal surge multiplier gives $m^+ = \frac{2(p\theta-c)}{pZ\theta}$ and $\widehat{\Pi}^* = \frac{n(1-\theta)\big(2c\lambda(1-\rho)-p\theta(2\lambda(1-\rho)+Z\rho)\big)}{Z\theta}$, which we denote as Π_1. Notice that $m^+ - \frac{2}{Z}\left(\frac{\rho}{1-\eta\rho+\eta} - \frac{c}{p\theta}\right) \geq 0$ for all feasible parameter values since we assumed $\frac{1}{\alpha+\eta(\alpha-\rho)} \geq 0$.

However, $\frac{2}{Z}\left(\frac{\rho}{\alpha+\eta(\alpha-\rho)}-\frac{c}{p\theta}\right)-m^{+}$ is positive only when $\frac{\rho-\alpha}{\alpha+\eta(\alpha-\rho)}\geq 0$. Thus, if $\alpha\geq\rho$, then $m^{+}>\frac{2}{Z}\left(\frac{\rho}{\alpha+\eta(\alpha-\rho)}-\frac{c}{p\theta}\right)$ and m^{+} is not a valid surge multiplier. If $\rho\geq\alpha$, then $\frac{2}{Z}\left(\frac{\rho}{\alpha+\eta(\alpha-\rho)}-\frac{c}{p\theta}\right)-m^{+}\geq 0$ and provided $m^{+}\geq 0$ (which holds from Assumption 3), $\Pi_1\geq np(1-\theta)\rho$, which implies $\Pi_1\geq\Pi_0$.

Putting the cases together, when $\alpha\geq\rho$, $m^{+}\geq\frac{2}{Z}\left(\frac{\rho}{\alpha+\eta(\alpha-\rho)}-\frac{c}{p\theta}\right)\geq 0\geq\frac{2}{Z}\left(\frac{\rho}{1-\eta\rho+\eta}-\frac{c}{p\theta}\right)$ or $m^{+}\geq\frac{2}{Z}\left(\frac{\rho}{\alpha+\eta(\alpha-\rho)}-\frac{c}{p\theta}\right)\geq\frac{2}{Z}\left(\frac{\rho}{1-\eta\rho+\eta}-\frac{c}{p\theta}\right)\geq 0$ and it follows from Cases 2 and 3 that $\widehat{\Pi}^{*}=\Pi_2$ and $m^{*}=\frac{2}{Z}\left(\frac{\rho}{\alpha+\eta(\alpha-\rho)}-\frac{c}{p\theta}\right)$. Alternatively, when $\rho\geq\alpha$, $\frac{2}{Z}\left(\frac{\rho}{\alpha+\eta(\alpha-\rho)}-\frac{c}{p\theta}\right)\geq m^{+}\geq 0\geq\frac{2}{Z}\left(\frac{\rho}{1-\eta\rho+\eta}-\frac{c}{p\theta}\right)$ or $\frac{2}{Z}\left(\frac{\rho}{\alpha+\eta(\alpha-\rho)}-\frac{c}{p\theta}\right)\geq 0\geq m^{+}\geq\frac{2}{Z}\left(\frac{\rho}{1-\eta\rho+\eta}-\frac{c}{p\theta}\right)$. Thus, either $\widehat{\Pi}^{*}=\max\{\Pi_1,\Pi_2\}$ when $m^{+}\geq 0$, which implies that $m^{*}=m^{+}$or $m^{*}=\frac{2}{Z}\left(\frac{\rho}{\alpha+\eta(\alpha-\rho)}-\frac{c}{p\theta}\right)$, or $\widehat{\Pi}^{*}=\max\{\Pi_0,\Pi_2\}$, which implies that $m^{*}=0$ or $m^{*}=\frac{2}{Z}\left(\frac{\rho}{\alpha+\eta(\alpha-\rho)}-\frac{c}{p\theta}\right)$.

Region 3. When $\gamma_A^{*}=0,\gamma_B^{*}=0$, and $\frac{2}{Z}\left(\frac{\rho}{\alpha+\eta(\alpha-\rho)}-\frac{c}{p\theta}\right)\leq m\leq\frac{2}{Z}\left(\frac{\rho}{\alpha+\eta(\alpha-\rho)}+\frac{c}{p\theta}\right)$, the platform's profit is $\widehat{\Pi}^{*}=\frac{1}{2}np(1-\theta)\big((\rho+\alpha)(1-m\lambda)+2m\lambda-(1+m\lambda)|\rho-\alpha|\big)$, which is either $\widehat{\Pi}^{*}=np(1-\theta)\big(\rho+m\lambda(1-\alpha)\big)$ or $\widehat{\Pi}^{*}=np(1-\theta)\big(\alpha+m\lambda(1-\rho)\big)$, both of which are linearly increasing functions of m. Thus, the surge multiplier that maximizes profit is the upper bound of this range, which is $m^{*}=\frac{2}{Z}\left(\frac{\rho}{\alpha+\eta(\alpha-\rho)}+\frac{c}{p\theta}\right)$.

Region 4. When $\gamma_A^{*}=1-\frac{\rho\left(p\theta+\eta\left(mp\frac{Z}{2}\theta-c\right)\right)}{\alpha(1+\eta)\left(mp\frac{Z}{2}\theta-c\right)}$, $\gamma_B^{*}=0$, and $\frac{2}{Z}\left(\frac{\rho}{\alpha+\eta(\alpha-\rho)}+\frac{c}{p\theta}\right)\leq m\leq\frac{2}{Z}\left(1+\frac{c}{p\theta}\right)$, the profit is given by $\widehat{\Pi}^{*}=\frac{1}{2}np(1-\theta)\left(2m\lambda+\frac{\left(-2c(1+2\eta)+p\theta\left(2+mZ(2+\eta)\right)\right)(-1+m\lambda)\rho}{(1+\eta)(2c-mpZ\theta)}-(1+m\lambda)\left|\frac{(2c+p(2-mZ)\theta)\rho}{(1+\eta)(2c-mpZ\theta)}\right|\right)$. Assuming $\frac{(2c+p(2-mZ)\theta)\rho}{(1+\eta)(2c-mpZ\theta)}\neq 0$, the first-order derivative is either $\frac{\partial\widehat{\Pi}^{*}}{\partial m}=$

$\frac{np(-1+\theta)\left(4c^2(1+\eta)\lambda(-1+\rho)-4cmpZ(1+\eta)\theta\lambda(-1+\rho)+p^2Z\theta^2\left(m^2Z(1+\eta)\lambda(-1+\rho)+2\rho\right)\right)}{(1+\eta)(-2c+mpZ\theta)^2}$ or $\frac{\partial\hat{\Pi}^*}{\partial m} =$ $\frac{np(-1+\theta)\lambda\left(4c^2\left(-1+\eta(-1+\rho)\right)+m^2p^2Z^2\theta^2\left(-1+\eta(-1+\rho)\right)-4cp\theta\left(mZ\left(-1+\eta(-1+\rho)\right)+\rho\right)\right)}{(1+\eta)(-2c+mpZ\theta)^2}$, and the first-order conditions for optimality gives, respectively, $\left\{m_1 \to \frac{2c}{pZ\theta} - \sqrt{\frac{2\rho}{Z(1+\eta)\lambda(1-\rho)}}, m_2 \to \frac{2c}{pZ\theta} + \sqrt{\frac{2\rho}{Z(1+\eta)\lambda(1-\rho)}}\right\}$ or $\left\{m_3 \to \frac{2c}{pZ\theta} - 2\sqrt{\frac{c\rho}{-pZ^2\theta\left(1+\eta(1-\rho)\right)}}, m_4 \to \frac{2c}{pZ\theta} + 2\sqrt{\frac{c\rho}{-pZ^2\theta\left(1+\eta(1-\rho)\right)}}\right\}$. Notice that m_3 and m_4 are not real and thus, infeasible. Although m_1 and m_2 can be positive, only one is a valid surge multiplier. This is because the second-order derivative at m_1 equals $\frac{\partial^2\hat{\Pi}^*}{\partial m^2}(m \to m_1) = -\frac{\sqrt{2}np(1-\theta)\left(Z^3(1+\eta)\lambda(1-\rho)\rho\right)^{3/2}}{Z^4(1+\eta)\rho^2} < 0$ and the second-order derivative at m_2 equals $\frac{\partial^2\hat{\Pi}^*}{\partial m^2}(m \to m_2) = \frac{\sqrt{2}np(1-\theta)\lambda(1-\rho)\sqrt{Z^3(1+\eta)\lambda(1-\rho)\rho}}{Z\rho} > 0$, which implies that m_1 is a local maximum and m_2 is a local minimum. Second, one of the regions has $\frac{\partial^2\hat{\Pi}^*}{\partial m^2} = \frac{4np^4Z^2(1-\theta)\theta^3\rho}{(1+\eta)(mpZ\theta-2c)^3} > 0$ for any $m \geq 0$ that abides by Assumption 2, which implies that the profit function has regions of convexity. Thus, in addition to m_1, the surge multiplier values at the lower or upper bound of the interval are also candidate solutions. Finally, notice that the critical point $\frac{(2c+p(2-mZ)\theta)\rho}{(1+\eta)(2c-mpZ\theta)} = 0$ gives the same surge multiplier value as the upper bound of the interval. For clarity, define Π_0 and Π_2 as the profit functions associated with the lower and upper bounds of the surge multiplier interval, while Π_1 is the profit associated with the critical point m_1. We note that $\Pi_2 - \Pi_1 = \frac{np(1-\theta)}{Z^2(1+\eta)}\left(2Z(1+\eta)\lambda(1-\rho) + Z^2\rho + 2\sqrt{2(Z^3(1+\eta)\lambda(1-\rho)\rho)}\right) \geq 0$, which implies that m_1 is never optimal.

To ensure $\frac{2}{Z}\left(1 + \frac{c}{p\theta}\right) \geq \frac{2}{Z}\left(\frac{\rho}{\alpha+\eta(\alpha-\rho)} + \frac{c}{p\theta}\right)$, it follows that $\frac{2(1+\eta)(\alpha-\rho)}{Z(\alpha+\alpha\eta-\eta\rho)} \geq 0$, which requires $\alpha < \frac{\eta}{1+\eta}\rho$ (in which case both the numerator and denominator are negative) or $\alpha \geq \rho$ (in which case both the numerator and denominator are positive). Thus, first assume $\alpha \geq \rho$, then $\Pi_2 - \Pi_0 = \frac{2n(1-\theta)\lambda(\alpha-\rho)}{Z\theta(\alpha+\alpha\eta-\eta\rho)}\left(\alpha c + c\eta(\alpha-\rho) + p\theta + p\eta\theta(1-\rho)\right) \geq 0$. Conversely, assume $\rho \geq \alpha$, then $\Pi_2 - \Pi_0 = np(1-\theta)(\rho-\alpha)\left(1 - \frac{2(1+\eta)\lambda(1-\rho)}{Z(\alpha+\alpha\eta-\eta\rho)}\right) = p(1-\theta)\Bigg((\rho-\alpha) +$

$\left.\frac{2(\alpha-\rho)(1+\eta)\lambda(1-\rho)}{Z(\alpha+\alpha\eta-\eta\rho)}\right) \geq 0$ since $\frac{2(1+\eta)(\alpha-\rho)}{Z(\alpha+\alpha\eta-\eta\rho)} \geq 0$. Thus, $m^* = \frac{2}{Z}\left(1+\frac{c}{p\theta}\right)$ and $\widehat{\Pi}^* = \Pi_2 = \frac{n(1-\theta)\left(2c\lambda(1-\rho)+p\theta(2\lambda(1-\rho)+Z\rho)\right)}{Z\theta}$.

2- When $\alpha \leq \max\left\{0, \frac{\rho-\gamma_B^*}{1-\gamma_A^*-\gamma_B^*}\right\}$:

Region 1. When $\gamma_A^* = 0$, $\gamma_B^* = 1 - \frac{\left(mp\frac{Z}{2}\theta+\eta(p\theta-c)\right)(1-\rho)}{(p\theta-c)(1-\alpha)\,(1+\eta)}$, and $\frac{2}{Z}\left(1-\frac{c}{p\theta}\right) \leq m \leq \frac{2}{Z}\left(1-\frac{c}{p\theta}\right)\frac{1-\alpha+\eta(\rho-\alpha)}{1-\rho}$, the platform's profit is $\widehat{\Pi}^* = \frac{1}{4}np(1-\theta)\left(4m\lambda + \frac{(-1+m\lambda)\left(-2c(1+\rho+2\eta\rho)+p\theta\left(mZ(-1+\rho)+2(1+\rho+2\eta\rho)\right)\right)}{(1+\eta)(c-p\theta)} - (1+m\lambda)\left|\frac{(2c+p(-2+mZ)\theta)(-1+\rho)}{(1+\eta)(c-p\theta)}\right|\right)$.

Assuming $\frac{(2c+p(-2+mZ)\theta)(-1+\rho)}{(1+\eta)(c-p\theta)} \neq 0$, the first-order derivative is either $\frac{\partial\widehat{\Pi}^*}{\partial m} = \frac{np(1-\theta)\left(2c(1+\eta)\lambda+p\theta(Z-2(1+\eta)\lambda)\right)(1-\rho)}{2(1+\eta)(c-p\theta)}$ or $\frac{\partial\widehat{\Pi}^*}{\partial m} = \frac{np(1-\theta)(c\eta-p(mZ+\eta)\theta)\lambda(1-\rho)}{(1+\eta)(c-p\theta)}$. The former is independent of m and indicates that, depending on the parameter values, the profit function is linearly increasing or decreasing over the interval for m. The implication is that each of the endpoints represents a candidate solution for the optimal surge multiplier. The latter first-order derivative gives $m^+ = -\frac{\eta(p\theta-c)}{pZ\theta}$. The critical point, obtained by setting $\frac{(2c+p(-2+mZ)\theta)(-1+\rho)}{(1+\eta)(c-p\theta)} = 0$, gives the same surge multiplier value as the lower bound. Define Π_1 and Π_2 as the profit functions associated with the lower and upper surge bounds, respectively. Since $1-\frac{c}{p\theta} \geq 0$ from Assumption 3, two cases must be considered:

i. Case 1: $\frac{1-\alpha+\eta(\rho-\alpha)}{1-\rho} \geq 1$:

The entire range yields nonnegative surge multiplier values and both m^+ and $m=0$ are inadmissible solutions. If $\alpha \geq \rho$, then $\widehat{\Pi}^* = \Pi_1$ as $\Pi_1 - \Pi_2 = \frac{2n(1-\theta)}{Z\theta(1-\rho)}(p\theta-c)\lambda(\alpha-\rho)\left((1-\alpha)+\eta(1-\alpha)+(1-\rho)\right) \geq 0$, which contradicts the assumption that $\frac{1-\alpha+\eta(\rho-\alpha)}{1-\rho} \geq 1$. This implies $\rho \geq \alpha$ and thus, $\widehat{\Pi}^* = \max\{\Pi_1, \Pi_2\}$.

ii. Case 2: $\frac{1-\alpha+\eta(\rho-\alpha)}{1-\rho} \leq 1$:

In this case, the lower surge multiplier is positive and exceeds the upper bound (which is negative if $\frac{1-\alpha+\eta(\rho-\alpha)}{1-\rho} \leq 0$). Consequently, this case is inadmissible. This also implies that the critical point, $m^+ = -\frac{\eta(p\theta-c)}{pZ\theta}$, is never an optimal solution.

Region 2. When $\gamma_A^* = 0, \gamma_B^* = 0$, and $\frac{2}{Z}\left(1-\frac{c}{p\theta}\right)\left(\frac{1-\alpha+\eta(\rho-\alpha)}{1-\rho}\right) \leq m \leq \frac{2}{Z}\left(1+\frac{c}{p\theta}\right)\left(\frac{1-\alpha+\eta(\rho-\alpha)}{1-\rho}\right)$, the platform's profit is $\widehat{\Pi}^* = \frac{1}{2}np(1-\theta)\big((\rho+\alpha)(1-m\lambda)+2m\lambda-(1+m\lambda)|\rho-\alpha|\big)$, which is either $\widehat{\Pi}^* = np(1-\theta)\big(\rho+m\lambda(1-\alpha)\big)$ or $\widehat{\Pi}^* = np(1-\theta)\big(\alpha+m\lambda(1-\rho)\big)$, both of which are linear increasing functions of m. Thus, the surge multiplier that maximizes profit is the upper bound of this range, which is $m^* = \frac{2}{Z}\left(1+\frac{c}{p\theta}\right)\left(\frac{1-\alpha+\eta(\rho-\alpha)}{1-\rho}\right)$. Note that for the upper bound of the interval to be greater than the lower bound, it requires $\frac{4c(1-\alpha-\alpha\eta+\eta\rho)}{pZ\theta(1-\rho)} \geq 0$, which implies that $\alpha \leq \frac{1}{1+\eta}+\frac{\eta}{1+\eta}\rho$ where $\frac{1}{1+\eta} \leq 1$ and $\frac{\eta}{1+\eta} \leq 1$.

Region 3. When $\gamma_A^* = \frac{(1-\rho)mp\frac{Z}{2}\theta-(p\theta+c)\big(1-\alpha+\eta(\rho-\alpha)\big)}{\alpha(p\theta+c)(1+\eta)}, \gamma_B^* = 0$, and $\frac{2}{Z}\left(1+\frac{c}{p\theta}\right)\frac{1-\alpha+\eta(\rho-\alpha)}{1-\rho} \leq m \leq \frac{2}{Z}\left(1+\frac{c}{p\theta}\right)\left(\frac{1+\eta\rho}{1-\rho}\right)$, the profit is given by $\widehat{\Pi}^* = \frac{1}{2}np(1-\theta)\Bigg(2m\lambda - \frac{(-1+m\lambda)\big(2c(1+\rho+2\eta\rho)+p\theta\big(mZ(-1+\rho)+2(1+\rho+2\eta\rho)\big)\big)}{2(1+\eta)(c+p\theta)} - \frac{1}{2}(1+m\lambda)\left|\frac{(2c+p(2-mZ)\theta)(-1+\rho)}{(1+\eta)(c+p\theta)}\right|\Bigg)$.

Assuming $\frac{(2c+p(2-mZ)\theta)(-1+\rho)}{(1+\eta)(c+p\theta)} \neq 0$, the first-order derivative is either $\frac{\partial\widehat{\Pi}^*}{\partial m} = \frac{np(1-\theta)(-pZ\theta+2(1+\eta)(c+p\theta)\lambda)(1-\rho)}{2(1+\eta)(c+p\theta)}$ or $\frac{\partial\widehat{\Pi}^*}{\partial m} = \frac{np(1-\theta)(c\eta+p(mZ+\eta)\theta)\lambda(1-\rho)}{(1+\eta)(c+p\theta)}$. The former is not a function of m, which means that the profit function is linearly increasing/decreasing in this region; the lower or upper bound of the surge multiplier's interval are candidate solutions. The first-order condition for optimality for the latter derivative gives $m^+ = -\frac{\eta\,(c+p\theta)}{pZ\theta}$, which is negative, and thus, inadmissible. The second-order derivative is, respectively, $\frac{\partial^2\widehat{\Pi}^*}{\partial m^2} = 0$ or $\frac{\partial^2\widehat{\Pi}^*}{\partial m^2} = \frac{np^2Z(1-\theta)\theta\lambda(1-\rho)}{(1+\eta)(c+p\theta)} > 0$, which reinforces the notion that the lower and upper bound of the surge multiplier's interval are candidates. We denote Π_1 and Π_2 as the profit functions associated with the lower and upper surge bounds, respectively.

Note that $m^+ = \frac{2}{Z}\left(1 + \frac{c}{p\theta}\right) \geq 0$ is a critical point obtained by solving $\frac{(2c+p(2-mZ)\theta)(-1+\rho)}{(1+\eta)(c+p\theta)} = 0$ and yields a profit of $\Pi_0 = \frac{n(1-\theta)\left(2c\lambda(1-\rho)+p\theta(2\lambda(1-\rho)+Z\rho)\right)}{Z\theta}$. Further, $\frac{2}{Z}\left(1 + \frac{c}{p\theta}\right)\left(\frac{1+\eta\rho}{1-\rho}\right) - m^+ \geq 0$ for all feasible parameter values and $m^+ - \frac{2}{Z}\left(1 + \frac{c}{p\theta}\right)\frac{1-\alpha+\eta(\rho-\alpha)}{1-\rho} = \frac{2(1+\eta)(c+p\theta)(\alpha-\rho)}{pZ\theta(1-\rho)}$, which depends on whether $\alpha \geq \rho$. Because $\Pi_0 - \Pi_1 = \frac{2n(1-\theta)(c+p\theta)\lambda(\alpha-\rho)}{Z\theta(1-\rho)}\left((1-\alpha) + \eta(1-\alpha) + (1-\rho)\right)$, $\Pi_0 \geq \Pi_1$ when $\alpha \geq \rho$ and $\Pi_1 \geq \Pi_0$ when $\rho \geq \alpha$. Further, if $\frac{1-\alpha+\eta(\rho-\alpha)}{1-\rho} \leq 0$, then $\alpha \geq \rho$ and the lower bound of the range is negative, the upper bound is positive, and the profit is $np(1-\theta)\rho$. Nevertheless, $\Pi_0 - np(1-\theta)\rho \geq 0$, which means it can be ignored.

Note that $\frac{2}{Z}\left(1 + \frac{c}{p\theta}\right)\left(\frac{1+\eta\rho}{1-\rho}\right) \geq \frac{2}{Z}\left(1 + \frac{c}{p\theta}\right)\frac{1-\alpha+\eta(\rho-\alpha)}{1-\rho}$ holds for any choice of the parameters. Thus, first suppose $\alpha \geq \rho$. Then, from the above analysis, $\widehat{\Pi}^* = \max\{\Pi_0, \Pi_2\}$, which implies that the optimal surge multiplier is either $m^* = m^+$ or $m^* = \frac{2}{Z}\left(1 + \frac{c}{p\theta}\right)\left(\frac{1+\eta\rho}{1-\rho}\right)$.
Alternatively, if $\rho \geq \alpha$, then $\widehat{\Pi}^* = \max\{\Pi_1, \Pi_2\}$ and the optimal surge multiplier is either $m^* = \frac{2}{Z}\left(1 + \frac{c}{p\theta}\right)\frac{1-\alpha+\eta(\rho-\alpha)}{1-\rho}$ or $m^* = \frac{2}{Z}\left(1 + \frac{c}{p\theta}\right)\left(\frac{1+\eta\rho}{1-\rho}\right)$.

Region 4. When $\gamma_A^* = 1, \gamma_B^* = 0$, and $m \geq \frac{2}{Z}\left(1 + \frac{c}{p\theta}\right)\left(\frac{1+\eta\rho}{1-\rho}\right)$, the platform's profit is $\widehat{\Pi}^* = mnp(1-\theta)\lambda(1-\rho)$, which is linearly increasing in m. Thus, the surge multiplier that maximizes profit is $m^* = m_{max}$ following Assumption 1.